SBUF

PROJEKTNR. 13766

Tillämpningsmodellering av fuktfenomen i betong för modern uttorkningssimulering del 2

Slutrapport

Marcin Stelmarczyk och Hans Hedlund
Luleå Tekniska Universitet och Skanska Sverige AB

2024-03-18

LULEÅ UNIVERSITY OF TECHNOLOGY

SKANSKA

Förord

Projektet har genomförts vid Luleå Tekniska Universitet (LTU), institutionen för samhällsbyggnad och naturresurser, avdelningen för Byggkonstruktion och brand, Byggmaterial. Projektledare har varit Hans Hedlund och doktorand och rapportförfattare Marcin Stelmarczyk. Handledare har förutom Hans Hedlund (Skanska/LTU), varit Andrzej Cwirzen (LTU).

Stort tack till finansiärerna SBUF och Skanska som möjliggjorde detta projekt. Ett stort tack även till referensgruppen som följt, stöttat och engagerat sig i projektet. Era synpunkter och funderingar har varit mycket värdefulla.

Stockholm, Mars 2024

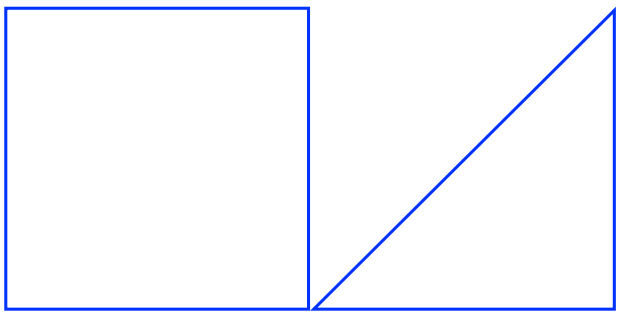

Sammanfattning

Denna rapport beskriver genomförande och resultat av SBUF-projektet som motsvarar den andra delen av forskningen bakom Dr Marcin Stelmarczyks avhandling ”Applied Modeling of Moisture Phenomena in Concrete”. I avhandlingen, som bifogas, presenteras en ny modell för hydratationsgrad och kemiskt bundet vatten. Hydratationsgraden beräknas direkt utan användning av mognadsålder och modellen för kemiskt bundet vatten tar hänsyn till temperaturens inverkan på hur mycket vatten som binds per mängd hydratiserat bindemedel. Vidare presenteras i avhandlingen två familjer av modeller, för sorption respektive transport av fukt. Bägge modellfamiljerna innehåller modellvarianter för isoterma, förenklade icke isoterma samt generaliserade icke isoterma förhållanden. En rad olika anpassningsmetoder för modellparametrar till mätdata redovisas också. Slutligen innehåller slutrapporten även slutsatser och rekommendationer för framtida projekt baserade på de presenterade forskningsresultaten.

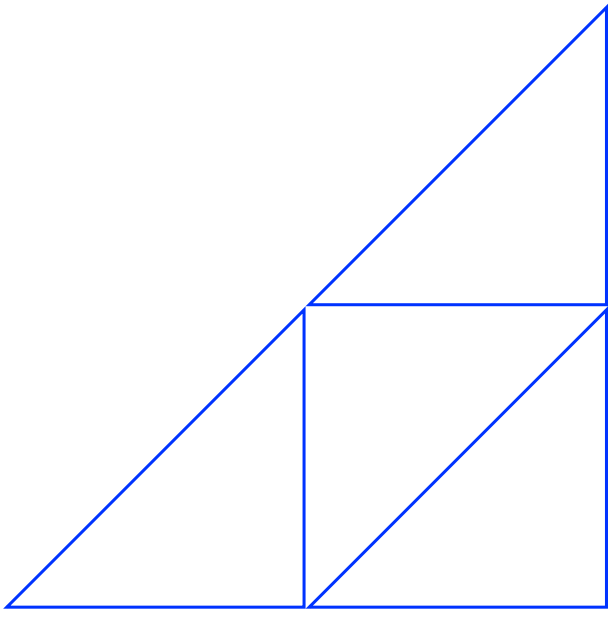

Innehåll

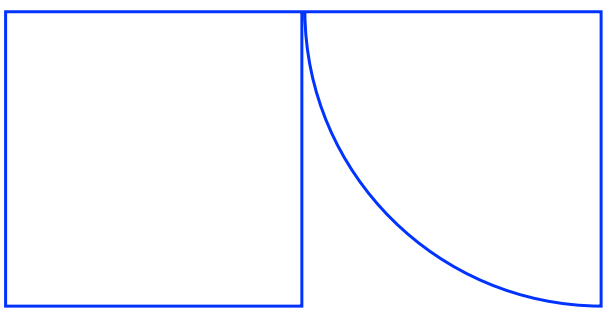

1 Inledning

Detta projekt är ett följdprojekt till SBUF 13140 *Tillämpningsmodellering av fuktfenomen i betong för modern uttorkningssimulering*, som i syfte att förse den tilltänkta utbyggnaden av mjukvaran Produktionsplanering Betong (PPB) i separata projekt, med reviderade materialmodeller för fuktfenomenologi i betong. Detta behov identifierades tidigt inom SBUF 13064 Förstudie Fukt PPB. Detta projekt är alltså en försättning på detta arbete och omfattar andra delen i samma doktorandprojekt.

Denna rapport redovisar projektetens genomförande och resultat.

1.1 Rapportens struktur

Denna rapport omfattar följande 5 kapitel:

- Inledning – detta kapitel.
- Projektets genomförande – här redovisas det arbetet som utfördes under projektet.
- Resultat – här redovisas en övergripande bild av resultaten.
- Slutsatser – här presenteras de slutsatser som går att dra av projektresultaten
- Rekommendationer avseende framtida projekt – här diskuteras framtida behov av vidare arbete inom samma och anslutande områden

Den innehåller även själva doktorsavhandlingen som bilaga 1.

2 Projektets genomförande

Forskningsarbetet inklusive framtagning och försvar av avhandling utfördes av doktoranden Marcin Stelmarczyk vid LTU under handledning av prof. Andrzej Ćwirzeń samt adj. prof. Hans Hedlund. Nyckeldelar av forskningen i doktorandprojektet hade redan utförts inom ramen av SBUF 13140. Planeringen av de återstående delarna inklusive färdigställande av avhandlingen ärvdes också från SBUF 13140. Därför begränsades projektstyrningen till doktorandens ledning från handledare samt att styrgruppen hölls löpande underrättad om projektets framskridande. Referensgruppen användes endast vid behov. Ett styrgruppsmöte ägde rum 2024-03-18 då styrgruppen bestämde att acceptera den försvarade avhandlingen, avsluta projektet samt godkänna denna slutrapport.

2.1 Samarbete med SBUF 13711

Samarbete med SBUF 13711 *Fuktomfördelning i golvsystem i Produktionsplanering Betong* har skett löpande under projekttiden. Detta projekt försåg 13711 med materialmodeller och beräkningsmetodik för implementation i PPB rörande fuktförhållanden i golvavjämning samt fuktutbyte med lim och ytskikt.

2.2 Spikning av avhandling

Avhandlingen spikades 2023-12-13.

2.3 Försvar av avhandling

Avhandlingen försvarades 2024-01-26 med deltagande:

- Opponent:
    - Prof. Klaas van Berugel, Faculty of Civil Engineering and Geosciences, Delft University of Technology
- Betygskommitté:
    - Prof. Barbara Klemczak, Faculty of Civil Engineering / Department of Structural Engineering, Politechnika Śląska
    - Assoc. Prof. Guang Ye, Faculty of Civil Engineering and Geosciences, Delft University of Technology
    - Assoc. Prof. Didier Snoeck, Building, Architecture and Town Planning (BATir) Department, Universite Libre de Bruxelles

3 Resultat

Avhandling innehåller nya och förbättrade modeller, baserade på tillämpad forskning som kombinerar numerisk modellering och materialforskning inom hydratation och kemisk bindning av vatten, sorption av fukt och transport av fukt i betong.

Den presenterade modellen för hydratation och kemisk bindning av vatten är baserad på generell modellering av kinetik och beräknar hydratationsgraden direkt utan användning av mognadsålder. Den hanterar beroenden av temperatur samt tillgänglighet av både bindemedel och vatten. Den modellerar även fördröjning av reaktionen i början av hydratationen samt möjliggör för linjärt temperaturberoende av hur mycket vatten som binds per mängd bindemedel, vilket hanterar korsningseffekter i utveckling av kemiskt bundet vatten som funktion av ålder mätt vid olika hydratationstemperaturer.

Inom sorption av fukt presenteras en familj av modeller. Dessa bygger på domänbaserad modellering kombinerad med explicit representation av koncentrationen av sorptionsenheter för varierande desorptions- och absorptionsvillkor i form av en matris av anpassningsbara värden. De föreslagna modellerna erbjuder en spline-liknande möjlighet att välja antalet anpassningsbara parametrar och därmed modellens precision. Två modellvarianter presenteras:

- en modell för isoterma förhållanden
- en modell för icke isoterma förhållanden

En uppsättning av metoder för anpassning av modellparametrar till uppmätta data föreslås för olika scenarier, även här för både isoterma och icke isoterma förhållanden. Deras egenskaper verifieras till viss grad matematiskt och deras modelleringsförmåga diskuteras.

Inom transport av fukt presenteras en familj av modeller, konceptuellt liknande de föreslagna modellerna för sorption. Dessa bygger också på domänbaserad modellering kombinerad med explicit representation av koncentrationen av bidrag till den totala transportenegenskapen för varierande desorptions- och absorptionsvillkor i form av en matris av anpassningsbara värden. De föreslagna modellerna erbjuder en spline-liknande möjlighet att välja antalet

anpassningsbara parametrar och därmed modellens precision. Tre modellvarianter presenteras:

- en modell för isoterma förhållanden
- en generaliserad modell för icke isoterma förhållanden
- en förenklad modell för icke isoterma förhållanden, där kapillärt undertryck antas dominera transporten

En uppsättning av metoder för anpassning av modellparametrar till uppmätta data föreslås för olika scenarier för samtliga tre modellversioner. Deras egenskaper verifieras till viss grad matematiskt och deras modelleringsförmåga diskuteras.

3.1 Industriell tillämpning

Ett flertal av de presenterade modellerna används redan i det branschgemensamma beräkningsverktyget Produktionsplanering Betong (PPB). Den första tillämpningen skedde inom ramen för SBUF 13197 *Utveckling av beräkning av uttorkning i programmet Produktionsplanering Betong*, där grundberäkning av uttorkning av betong implementerades i PPB och SBUF 13198 *Inmätning av Bascement för uttorkningsberäkning i Produktionsplanering Betong*, där materialegenskaper för betong med Bascement mättes in för vidare användning i PPB. Vidare tillämning har även skett inom SBUF 13711 *Fuktomfördelning i golvsystem i Produktionsplanering Betong*, där fuktberäkningen i PPB utökades till att omfatta även fuktsamverkan med golvavjämning samt pålimmat ytskikt.

4 Slutsatser

Den framlagda och vetenskapligt försvarade avhandlingen presenterar forskningsresultat som löser de formulerade forskningsproblemen. Nya och/eller reviderade modeller for hydratation och kemisk bindning av vatten, sorption och transport av fukt i betong görs tillgängliga för tillämpning inom modellering av dessa fenomen i betong.

Samverkan mellan dessa doktorandprojekt, dvs del 1 SBUF 13140 samt del 2 SBUF 13766, samt PPB:s utvecklingsprojekt SBUF 13197 & 13198 samt 13711 har möjliggjort en direkt industriell tillämpning av forskningsresultaten. Detta har skett i form av fuktsimulering och uttorkningsberäkning för betonggolv med eller utan golvavjämning och/eller pålimmat ytskikt.

De framlagda forskningsresultaten utgör vidare en grund för framtida forskning inom området, se gärna diskussion i kap. 5 i doktorsavhandlingen, bilaga 1.

5 Rekommendationer avseende framtida projekt

Detta projekt vill slutligen peka ut två områden där omedelbar framtida forskning är av intresse. Vidareutveckling av hydratationsmodellen samt dess koppling mot andra hydratationsrelaterade egenskaper som genererad värme och tryckhållfasthet är av primärt intresse. Detta dels för att säkerställa samma modelleringsbas för beräkning av dessa variabler

under en simulering och dels för att undersöka om den gemensamma grunden kan utnyttjas för förenklingar inom uppmätning av fuktrelaterade egenskaper. Det skall nämnas att detta område redan är adresserat inom ramen för det pågående projektet SBUF 14165 *Förenklad inmätning av värme- och fuktbeteende i betong för PPB*.

Det andra området av omedelbart intresse är sammankopplingen av presenterade modeller för sorption och transport med modellen för hydratation och kemisk bindning av vatten. Detta bör ske i syfte att återspegla dynamiken i porsystemets utveckling under tiden som betongen hydratiserar. Sorptions- och transportmodellerna är idag statiska och beskriver huvudsakligen egenskaper som baserar sig på mätningar på mogen betong, då dessa mätningar tar för lång tid att utföra för att man skall hinna utföra dem under pågående hydratation. Utveckling av den efterfrågade sammankopplingen av modellerna behöver därför basera sig på en mer avancerad teoretisk bild av porsystemets utveckling och ett fåtal egenskaper som går att mäta eller beräkna under pågående hydratation

Bilagor

1. *Applied Modeling of Moisture Phenomena in Concrete*, M. Stelmarczyk, doktorsavhandling 2023, LTU

Litteraturförteckning

SBUF 13064 *Förstudie och metodutveckling för implementering av fuktberäkningsmodul i datorprogrammet Produktionsplanering Betong, Slutrapport*, M. Stelmarczyk, H. Hedlund, P. Johansson, L.-O. Nilsson, M. Åhs, T. Rapp, 2015

SBUF 13140 *Tillämpningsmodellering av fuktfenomen i betong för modern uttorkningssimulering, Slutrapport*, M. Stelmarczyk, H. Hedlund, T. Rapp, 2019

SBUF 13197 & 13198 *Utveckling av beräkning av uttorkning i programmet Produktionsplanering Betong samt Inmätning av Bascement för uttorkningsberäkning i Produktionsplanering Betong, Slutrapport*, M. Stelmarczyk, T. Rapp, H. Hedlund, S. Carlström, 2019

SBUF 13710 & 13711 *Pedagogikrevidering och extern kommunikation avs. fukt i PPB samt Fuktomfördelning i golvsystem i Produktionsplanering Betong, Slutrapport*, M. Stelmarczyk, T. Rapp, H. Hedlund, 2020

DOCTORAL THESIS

Applied Modeling of Moisture Phenomena in Concrete

Marcin Stelmarczyk

Building Materials

LULEÅ UNIVERSITY OF TECHNOLOGY

LULEÅ UNIVERSITY OF TECHNOLOGY

DOCTORAL THESIS

Applied Modeling of Moisture Phenomena in Concrete

Marcin Stelmarczyk

Building Materials
Department of Civil, Environmental and Natural Resources Engineering
Luleå University of Technology
SE-97187 Luleå, Sweden

December 2023

Printed by Luleå University of Technology, 2023

ISSN 1402-1544

ISBN: 978-91-8048-428-2 (Print)

ISBN: 978-91-8048-429-9 (Electronic)

Luleå 2023

www.ltu.se

Academic thesis

For the Degree of Doctor of Philosophy in Building Materials, which by due of the Technical Faculty Board at Luleå University of Technology will be publicly defended in:

Room F1031, Luleå University of Technology
Friday, January 26th, 2024, 10:00

Faculty opponent:	Prof. Klaas van Breugel Faculty of Civil Engineering and Geosciences Delft University of Technology
Examining committee:	Prof. Barbara Klemczak Faculty of Civil Engineering / Department of Structural Engineering Politechnika Śląska
	Assoc. Prof. Guang Ye Faculty of Civil Engineering and Geosciences Delft University of Technology
	Assoc. Prof. Didier Snoeck Building, Architecture and Town Planning (BATir) Department Universite Libre de Bruxelles
Chairman:	Prof. Anders Lagerkvist Department of Civil, Environmental and Natural Resources Engineering Luleå University of Technology (LTU)
Principal supervisor:	Prof. Andrzej Ćwirzeń Department of Civil, Environmental and Natural Resources Engineering Luleå University of Technology (LTU)
Assistant supervisor:	Adj. Prof. Hans Hedlund Department of Civil, Environmental and Natural Resources Engineering Luleå University of Technology (LTU)

Preface

This work resulted in a more advanced applied modeling of moisture phenomenology in concrete, initialized by and later used in the Swedish construction industry. The research was carried out between 2016 and 2023, in parallel with industrial work, initially started at Division of Building Materials at Lund University and later finalized at Building Materials Group, Department of Civil, Environmental, and Natural Resources Engineering, Luleå University of Technology, Sweden. The research project was financed by the Development Fund of the Swedish Construction Industry (SBUF), Skanska Sverige AB and Luleå University of Technology. I would like to express my great appreciation and gratitude to the above mentioned organizations and companies for funding and making this work possible.

I would like to thank my supervisors:

- Prof. Lars Wadsö, my initial supervisor at Lund University
- Prof. Andrzej Ćwirzeń, my final supervisor at Luleå University of Technology
- Adj. Prof. Hans Hedlund, my later co-supervisor at Luleå University of Technology

for their guidance, support, patience, sharing of knowledge and experience and constructive questioning of what I was doing during this work and how I was expressing myself in this thesis.

I would also like to express my gratitude to all my colleagues at Lund University and Luleå University of Technology for interesting discussions and other various types of support during this work.

I would like to express my appreciation to my network in the construction industry for their support in general and specifically for helping me understand the application area and keeping at least one of my feet in contact with the ground.

Special acknowledgements are directed to former Prof. Jan-Erik Jonasson at Luleå University of Technology, without whose co-operation and efforts, dating as far as late 1980-ies, I would probably never perform any research nor development work connected to the construction industry and building materials at all.

Finally I would like to thank everybody involved in growing, harvesting, drying and all other steps in production and transport to Stockholm of Lung Ching, a Chinese, ecological, green tea. Without their efforts this thesis would most probably never have been finished.

Marcin Stelmarczyk

Tranholmen, December 2023

Abstract

This thesis contains new and improved calculation models, based on applied research merging numerical modeling and material research, in the areas of hydration and chemical binding of water, sorption of moisture and transport of moisture in concrete.

The proposed model for hydration and chemical binding of water is based on general kinetics modeling and calculates degree of hydration directly, without using of equivalent time of maturity. It handles dependencies on temperature as well as availability of binder and water. It models the dormant phase in the beginning of hydration. It allows also for linear variability with temperature of how much water is bounded per amount of binder, which models cross-over effects in development of chemical binding of water, measured at different temperatures.

In the area of moisture sorption a family of models is proposed, building on a domain-based approach combined with explicit modeling of sorption site concentration for various desorption and absorption conditions by a matrix of adaptable values. The proposed modeling idea offers a spline-like possibility of choosing the amount of adaptation parameters and the precision of the model. Two formulations of the sorption model are presented – for both isothermal and non-isothermal conditions. A selection of methods to adapt the parameters to measured data is proposed for various situations, also covering both isothermal and non-isothermal conditions. Their properties are to some degree mathematically verified and their performance is discussed.

In the area of moisture transport, a family of models is proposed, conceptually similar to the proposed sorption models. It also builds on a domain-based approach combined with explicit modeling of concentration of contributions to the overall transport, for various desorption and absorption conditions by a matrix of adaptable values. The proposed modeling idea offers a spline-like possibility of choosing the amount of adaptation parameters and the precision of the model. Three formulations of the transport model are presented – one for isothermal conditions, one generalized for non-isothermal conditions and one simplified for non-isothermal conditions where capillary suction is assumed to dominate transport phenomena. A selection of methods to adapt the parameters to measured data is proposed for various situations, covering all three proposed model versions. Their properties are to some degree mathematically verified and their performance is discussed.

Keywords: Concrete, Modeling degree of hydration, Modeling chemically bounded water, Modeling moisture sorption, Modeling moisture transport, Hysteresis

Sammanfattning

Denna avhandling innehåller nya och förbättrade modeller, baserade på tillämpad forskning som kombinerar numerisk modellering och materialforskning inom hydratation och kemisk bindning av vatten, sorption av fukt och transport av fukt i betong.

Den presenterade modellen för hydratation och kemisk bindning av vatten är baserad på generell modellering av kinetik och beräknar hydratationsgraden direkt utan användning av mognadsålder. Den hanterar beroenden av temperatur samt tillgänglighet av både bindemedel och vatten. Den modellerar även fördröjning av reaktionen i början av hydratationen samt möjliggör för linjärt temperaturberoende av hur mycket vatten som binds per mängd bindemedel, vilket hanterar korsningseffekter i utveckling av kemiskt bundet vatten som funktion av ålder mätt vid olika hydratationstemperaturer.

Inom sorption av fukt presenteras en familj av modeller. Dessa bygger på domänbaserad modellering kombinerad med explicit representation av koncentrationen av sorptionsenheter för varierande desorptions- och absorptionsvillkor i form av en matris av anpassningsbara värden. De föreslagna modellerna erbjuder en spline-liknande möjlighet att välja antalet anpassningsbara parametrar och därmed modellens precision. Två modellvarianter presenteras – en för isoterma och en för icke isoterma förhållanden. En uppsättning av metoder för anpassning av modellparametrar till uppmätta data föreslås för olika scenarier, även här för både isoterma och icke isoterma förhållanden. Deras egenskaper verifieras till viss grad matematiskt och deras modelleringsförmåga diskuteras.

Inom transport av fukt presenteras en familj av modeller, konceptuellt liknande de föreslagna modellerna för sorption. Dessa bygger också på domänbaserad modellering kombinerad med explicit representation av koncentrationen av bidrag till den totala transportenegenskapen för varierande desorptions- och absorptionsvillkor i form av en matris av anpassningsbara värden. De föreslagna modellerna erbjuder en spline-liknande möjlighet att välja antalet anpassningsbara parametrar och därmed modellens precision. Tre modellvarianter presenteras – en för isoterma förhållanden, en generaliserad för icke isoterma förhållanden samt en förenklad för icke isoterma förhållanden där kapillärt undertryck antas dominera transporten. En uppsättning av metoder för anpassning av modellparametrar till uppmätta data föreslås för olika scenarier för samtliga tre modellversioner. Deras egenskaper verifieras till viss grad matematiskt och deras modelleringsförmåga diskuteras.

Nyckelord: Betong, Modellering av hydratationsgrad, Modellering av kemiskt bundet vatten, Modellering av sorption av fukt, Modellering av transport av fukt, Hysteres

Contents

List of figures

List of tables

Notation

Scalar values use font with normal thickness. Vector values use bold font. If multiple explanations are given, see specification beside specific equation.

General variables:

$A_{i,j}(Step_x)$ – area of cross-section between the integration domain of step x in the history of meniscus curvature and the corresponding model matrix element for sorption or transport coefficients [1/m^2]

$A^k_{i,j}(Step_x)$ – area of cross-section between the integration domain of step x in the history of meniscus curvature and the corresponding model matrix element for permeability [1/m^2]

$A^\gamma_{i,j}(Step_x)$ – area of cross-section between the integration domain of step x in the history of meniscus curvature and the corresponding model matrix element for fraction of medium cross-section available for vapor diffusion [1/m^2]

a – adaptation parameter [-]

$B_{i,j}$ – coefficient of linearity for adaptation of model matrix elements for sorption or transport coefficients by linear regression [1/m^2]

$B^k_{i,j}$ – coefficient of linearity for adaptation of model matrix element for permeability [1/m^2]

$B^\gamma_{i,j}$ – coefficient of linearity for adaptation of model matrix element for fraction of medium cross-section available for vapor diffusion [1/m^2]

$b_{i,j}$ – coefficient used for substitution during adaptation of model matrix elements by linear regression, unit depending on use

b – adaptation parameter [-]

b_0 – adaptation parameter [h]

b_{adj} – adaptation parameter [h]

b_c – adaptation parameter [h]

b_{start} – adaptation parameter [h]

C – cement contents [kg/m^3]

c – heat capacitivity [J/kg K] or adaptation parameter [-]

$c(\varphi, T)$ – hydraulic curvature of meniscus [1/m], a function of relative humidity and temperature

c_a – hydraulic curvature of meniscus [1/m], a variable controlling absorption condition

c_d – hydraulic curvature of meniscus [1/m], a variable controlling desorption condition

c_i – relative concentrations of reactants or products of a chemical reaction [-]

$c_{i,j}$ – coefficient used for substitution during adaptation of model matrix elements by linear regression, unit depending on use

D_v – diffusivity of water vapor in air [m^2/s]

d – proportion of capillary pores filled with water [-]

E_a – activation energy [J/mol]

E_1 – heat of adsorption for the first layer [J/mol]
E_l – heat of liquefaction [J/mol]
$\boldsymbol{F}_g$ – gravity field [m/s^2]
$F_{g,z}$ – z-component of the gravity field [m/s^2]
$f(\dots)$ – a general function with indicated variable dependencies
$f(\varphi_d, \varphi_a)$ – concentration of sorption sites [kg/m^3]
$f_{ad}(\varphi, T)$ – adsorption modeling function describing the dependency on relative humidity and temperature [-]
f_{cc} – compressive strength [MPa]
$f_{cc,28d}$ – 28 days compressive strength [MPa]
$f_{cc,ref}$ – reference strength, without reduction due to high temperatures [MPa]
f^k – function of state variables or their gradients [kg/m^4 s] giving the transport contribution from capillary suction when multiplied with intrinsic permeability
f^γ – function of state variables or their gradients [kg/m^2 s] giving the transport contribution from vapor diffusion when multiplied with the cross-section factor for a medium
$\boldsymbol{g}$ – the field of moisture flow [kg/m^2 s]
$g_{x,m}$ – measured value of moisture flow [kg/m^2 s] in the x-direction
$g(x)$ – an example function of one variable
$Hist[X]$ – some kind of description of history of variable X
H_j – history j of hydraulic curvature
$h(x)$ – an example function of one variable
p – pressure in general or partial pressure of water vapor [Pa]
h_T – heat transfer coefficient [W/K m^2]
h_v – water vapor transfer coefficient [m/s]
L – length [m]
k – intrinsic permeability of a medium [m^2] or reaction kinetics parameter dependent on temperature [1/s]
k_m –value for intrinsic permeability of a medium [m^2] corresponding to a measurement of a transport coefficient
k_{offset} – offset value for intrinsic permeability of a medium [m^2]
k_r – rate parameter for reaction speed
L – length or characteristic linear dimension [m]
$m_{i,j}$ –model matrix element for sorption [kg/m] or transport coefficient [m^4/s]
$m_{i,j}^k$ –model matrix element for permeability [m^4]
$m_{i,j}^\gamma$ –model matrix element for fraction of medium cross-section available for vapor diffusion [-]
$\bar{p}$ – full set of model parameters being adapted
p_i – adaptation parameters in linear regression, unit depending on use
p_s – partial pressure of water vapor at saturation [Pa]
p_c – capillary pressure of water [Pa]
Q – volumetric flow rate [m^3/s]
Q_H – generated heat of hydration per volume [J/m^3]

$Q_{H,max}$ – generated heat at full hydration per amount of cement [J/kg]
$\boldsymbol{q}$ – flux field of a fluid [m/s]
R – the gas constant [J/K mol]
R_v – the gas constant for the water vapor [J/kg K]
Re – Reynold's number [-]
r – radius [m]
r_c – capillary radius [m]
r_h – hydraulic radius [m]
$\bar{r}$ – normalized neck radius of pores [-]
s – adaptation parameter [-]
T – absolute temperature [K]
T_{env} – temperature of environment [K]
T_{ref} – reference temperature [K]
$Temp_D$ – adaptation parameter [ºC]
t – time or age [s], other units can be used for specific equations, see explanation below resp. equation
t_1 – adaptation parameter [h]
t_2 – adaptation parameter [h]
t_e – equivalent time of maturity [h]
$time_D$ – adaptation parameter [h]
V_a – amount of adsorbed water [kg] or [m^3]
V_m – amount of water adsorbed in a filled monolayer [kg] or [m^3]
v – velocity field of a fluid [m/s]
w – water contents [kg/m^3]
w_a – amount of physically bounded water at absorption [kg/m^3]
w_{ad} – amount of adsorbed water [kg/m^3]
$w_{ad,1}$ – amount of water adsorbed in a filled monolayer [kg/m^3]
w_b – amount of blending water [kg/m^3]
w_{cc} – amount of capillary condensed water [kg/m^3]
w_d – amount of physically bounded water at desorption[kg/m^3]
$w_{m,j}$ – measured amount of physically bounded water [kg/m^3] corresponding to a hydraulic curvature history j
w_{Ph} - physically bounded water contents [kg/m^3]
$w_{Ph,iso}$ – physically bounded water contents in isothermal conditions [kg/m^3]
$w_{Ph,max}$ – physically bounded water contents at saturation [kg/m^3]
$w_{Ph,ni}$ – physically bounded water contents in non-isothermal conditions [kg/m^3]
$w_{Ph,stop}$ – physically bounded water contents limiting hydration [kg/m^3]
w_{Ch} – chemically bounded water contents [kg/m^3]
$w_{Ch,m}$ – measured chemically bounded water contents [kg/m^3]
$w_{Ch,ref}$ – adaptation parameter [kg/m^3]
x – adaptation parameter [-] or length coordinate [m]
$\bar{x}_i$ – Full set of environmental conditions defining measurement point i

z – length coordinate [m]
Z_T – heat resistance [K m^2/W]
Z_v – water vapor resistance [s/m]
α_C – hydration degree of cement [-]
$\alpha_{C,max}$ – maximum hydration degree of cement [-]
$\alpha_{C,H}$ – hydration degree of cement, based on generated heat of hydration [-]
$\alpha_{C,W}$ – hydration degree of cement, based on comparison of consumed water [-]
α_i – orders of dependency [-]
α_W –adjusted or water oriented degree of hydration [-]
β_{adj} – adjustment factor for water-oriented or adjusted degree of hydration [-]
β_i – factors influencing rate of hydration [-]
β_{start} – factor modeling an initial delay in hydration rate due to the dormant phase in reaction [-]
β_T – temperature factor [-]
β_w – moisture content factor [-]
β_α – hydration degree factor [-]
β_Δ – general speed factor [h]
β_φ – moisture content factor [-]
$\Gamma_{H,0}$ – part of boundary with no heat flow, i.e. adiabatic
$\Gamma_{H,C}$ – part of boundary with convective heat flow
$\Gamma_{H,F}$ – part of boundary with fixed temperature
$\Gamma_{M,0}$ – part of boundary with no moisture flow
$\Gamma_{M,C}$ – part of boundary with convective moisture flow
$\Gamma_{M,F}$ – part of boundary with fixed water vapor content
γ_{Temp} – temperature dependent reduction function for strength [-]
γ_{Time} – age dependent reduction function for strength [-]
γ_v – fraction of medium cross-section available for vapor diffusion [-]
$\gamma_{v,offset}$ – offset value for fraction of medium cross-section available for vapor diffusion [-]
ΔE – heat of sorption difference from the condensed liquid to the secondary sites [J/mol]
ΔE_0 – heat of sorption difference from the condensed liquid to the primary sites [J/mol]
ΔG – free energy of the secondary adsorbed molecules [J/mol]
ΔG_0 – free energy of the primary adsorbed molecules [J/mol]
$\Delta_{drop,28d}^{max}$ – adaptation parameter giving maximum relative reduction for strength at 28d, [-]
ΔS – entropy difference from the condensed liquid to the secondary sites [J/mol K]
ΔS_0 – entropy difference from the condensed liquid to the primary sites [J/mol K]
$\Delta t_{e,0}$ – start value of equivalent time of maturity, used to adjust for admixture effects [h]
δ_{drop} – current reduction factor for strength [-]
δ_{ref} – maximum reduction factor for strength [-]
δ_T – moisture transport coefficient for gradient in temperature [kg/K m s]

δ_v – moisture transport coefficient for gradient in water vapor contents [m^2/s]
$\delta_{v,iso}$ – moisture transport coefficient for gradient in water vapor contents in isothermal conditions [m^2/s]
$\delta_{v,iso,offset}$ – offset value for moisture transport coefficient for gradient in water vapor contents in isothermal conditions [m^2/s]
$\delta_{v,m}$ – measured value of moisture transport coefficient for gradient in water vapor contents [m^2/s]
ζ – proportion factor giving amount of water bounded by per amount of cement [kg/kg]
θ_{ref} – adaptation parameter that can be interpreted as activation temperature [K]
κ – thermal conductivity [W/m K]
κ_1 – adaptation parameter [-]
κ_2 – adaptation parameter [-]
κ_3 – adaptation parameter [-]
κ_c – adaptation parameter [-]
κ_{Temp} – adaptation parameter [-]
κ_{Time} – adaptation parameter [-]
κ_w – adaptation parameter [-]
λ_1 – adaptation parameter [-]
μ_D – dynamic viscosity [Pa s]
μ_K – kinematic viscosity [m^2/s]
υ – water vapor contents [kg/m^3]
υ_s – water vapor contents at saturation [kg/m^3]
ρ – density [kg/m^3]
ρ_w – density of water [kg/m^3]
$\bar{\rho}$ – normalized body radius of pores [-]
σ – surface tension [N/m]
τ_{start} – adaptation parameter [-]
φ – relative humidity [-]
φ_a – relative humidity variable controlling absorption condition [-]
φ_d – relative humidity variable controlling desorption condition [-]
φ_{stop} – relative humidity level limiting hydration, adaptation parameter [-]

1. Introduction

1.1 Background

While making concrete, at least three key functional components are mixed with each other. These are binder or binders, water and aggregate or aggregates. Simplifying the material interactions, the main function of aggregates is to fill majority of the space and the main function of binders and water is to react with each other, forming a solid that holds the aggregates together and fills the remaining space in between them. The chemical reaction between the binders and water is typically referred to as hydration. During it a part of the blending water, i.e. the initial amount of water, is chemically bounded to binders and forms a new solid. This is chemical binding of water. The resulting solid does not fill all the space between the aggregates. Some space remains and forms a system of pores of various sizes – the pore system. A part of the pore system is empty, i.e. it contains air. Another part is filled with the remaining water, that was not chemically bounded in the hydration of binders. This water is by multiple mechanisms physically bounded in the pore system of concrete and can by multiple mechanisms be transported within concrete as well as in and out of it.

The solid that is formed as a result of hydration of binders, contain salts that are partially dissolved in the water in the pore system. This raises the pH of the concrete to high levels of about 12 to 14, making it strongly alkalic. The hydroxide ions, dissolved in the water in the pore system, are mobile, can be transported to the surface of the concrete and can interact with any adjacent material. If concrete is used as a base for a floor, there are typically other materials on top of it, forming the surface of the floor. One example often used is a plastic carpet that is glued on top of the concrete floor. This creates a situation where hydroxide ions from the concrete can migrate to the glue and the plastic carpet and cause a chemical reaction referred to as alkalic hydrolysis with binders in the glue and softeners in the plastic carpet. Beside partial degradation of the glue and the surface layer, this unwanted reaction can produce so called volatile organic compounds (VOC), typically various alcohols, that can penetrate the surface layer, evaporate into the air in the space above the floor and make people there feels sick.

The transport of the hydroxide ions to the surface layer on top of the concrete is dependent on the availability of the medium in which the ions can move, i.e. on water. Thus, the amount of water in the pore system of concrete controls indirectly the intensity of possible degrading reaction with glue and surface layer. This amount of water is affected by various phenomena. The already mentioned blending water is a starting point. The hydration with its chemical binding of water contributes to so called self-desiccation and reduces it. Possible drying of the concrete by diffusion of water into the surrounding air reduces further the resulting amount. Use of water-based glues under the surface layer of the floor increases it. Use of self-leveling screed between the concrete and the surface layer of the floor with its drying procedure affects it as well. Finally, the pore system with its various pore shapes and sizes and connections between the pores affects also how the water behave in the concrete and how it can be utilized for the transport of the hydroxide ions.

The ability to predict and control behavior of moisture in concrete floors is therefore of value for avoiding the problems connected to the undesired alkalic hydrolysis in the surface layer of the floor. Simulation of construction performance requires models of material behavior in general, *van Breugel 2018*. In this particular case, simulation of moisture behavior of concrete requires adequate models for the contributing phenomena such as chemical binding of water, physical binding of water in the pore system of concrete, so called sorption, and transport of moisture in concrete. Providing such applied models for full-scale simulation of water behavior in concrete floor is the aim of this research.

1.2 Scope of the thesis

This work is a typical example of problem-solving research and addresses three connected research problems. All of them deal with proposing an applied model or models, describing the behavior of moisture in concrete. Each research problem targets one of the following three phenomenology areas:

1. Chemical binding of water including hydration causing it.
2. Sorption of moisture, i.e. physical binding of moisture in the pore system of concrete.
3. Transport of moisture

Each research problem is subject to various requirements. The research results presented in this thesis cover beside the proposed models also various levels of validation of their mathematical properties, direct or indirect connection to underlying physical phenomenology and modeling at a deeper level as well as a presentation of their use in practice by adaptation to measured properties from various scientific and industrial sources and comparison to other relevant models.

The scope of this research does not cover performing any measurements of material properties used for the proposed models. The work reuses, for model validation, material properties from existing sources.

For more specific formulation of the targeted research problems see section 1.8.

For the background to the research problems and an analysis explaining to why they are formulated as they are, see sections 1.4 to 1.7.

1.3 Structure of the thesis

The thesis is subdivided in the following chapters:

- Chapter 1 – an introduction, explaining background to this thesis, its scope and structure, analyzing the application area behind this research and specifying the targeted research questions.
- Chapter 2 – a literature study of the three phenomenological areas of this research, i.e. hydration and chemical binding of water, moisture sorption and moisture transport.
- Chapter 3 – proposed solutions for the research problems in all three phenomenological areas of this research including presenting of various levels of validation of the models.

- Chapter 4 - discussion of the presented word and conclusions that can be drawn on the basis of it.
- Chapter 5 - identification and discussion of desirable future research based on and complementing the presented work.

1.4 Moisture safety in concrete floors in Sweden

1.4.1 Drying requirement at equivalent depth

The key to understanding the approach of the construction industry in Sweden towards safe handling of concrete moisture in floor systems is the idea of so-called equivalent depth, *Nilsson 1979*. It is based on the observation that after drying, the concrete floor has a certain moisture contents profile. When a tight surface layer, carpet of some kind, is glued on the concrete, a redistribution of moisture will occur and the relative humidity of concrete in contact with the surface layer and/or the glue will after the redistribution be higher than initially. This will increase the transport of hydroxide ions from the concrete to the glue and the surface layer, increasing the risk of alkalic hydrolysis of binders in glue and/or softeners in the surface layer and connected emissions of volatile organic compounds (VOC), *Bornehag 1994* and *Alexandersson 2000*. In order to gain practical control of the highest relative humidity of concrete exposed to glue/surface layer and by that also control of the risk for hydrolysis, measuring of relative humidity prior to application of the surface layer is required, *RBK 2023*. The equivalent depth, at which the measurement is required, is defined so that the relative humidity measured there before redistribution shall be the same as the relative humidity measured under the surface layer after redistribution. The depth is chosen so that the moisture buffering capacity of the dryer concrete above the depth will balance out the excess moisture below, see Figure 1.1.

The standard equivalent depth is calculated and specified for a few of the most common structures and drying cases, *RBK 2023*. For the specific case, material properties used and chosen circumstances see *Nilsson 1979*.

The requirement for the maximum relative humidity, measured on the equivalent depth, indicating that the concrete is dry enough not to cause migration of hydroxide ions and hydrolysis in the glue/surface layer, is commonly based on a practical investigation *Wengholt Johnsson 1995*. A number of slabs were dried to various levels of relative humidity, the surface layer was applied and emissions of results of possible hydrolysis were measured. Other studies added further understanding how the emissions are affected by concrete moisture, *Sjöberg 2001*. This together resulted in today's default limit of 85% RF at 20 °C, *Svensk Byggtjänst 2018*, if not specified otherwise by the manufacturer of the glue or the surface layer. Some exceptions to that rule apply, e.g. regarding use of water-based glue directly on concrete with a low water-cement-ratio.

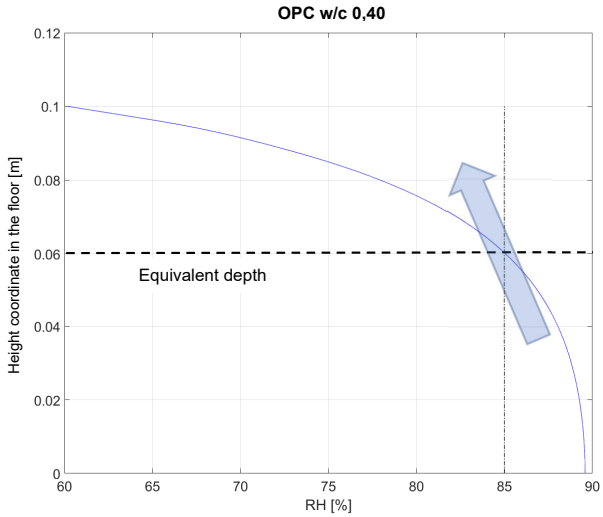

Figure 1.1, Moisture distribution in a slab after self-desiccation to approx. 90% RH and one-sided drying towards air with 60% RH. The dashed line indicates the equivalent depth. The blue arrow indicates the following redistribution of moisture in the slab after adding on top an impenetrable surface layer.

For more complex situations than covered by the precalculated equivalent depths, *RBK 2023* opens up for recalculation of the equivalent depth by a simulation of moisture redistribution for the specific case. This requires of course access to relevant material properties.

1.4.2 Existing simulation tool

During 1990-ties a software tool named TorkaS was developed for simulation of drying of concrete slabs. The tools was updated a few times since and has at the time of writing a version 3.2 that was released 2012, *Arfvidsson et al 1998-2012*.

The manual gives some theoretical background to how the tool calculate drying of concrete. However, the provided documentation is partial, sometimes ambiguous and not stringent enough to give what could be considered as a complete explanation to the performed simulation. On one hand, clear references to material properties and some models are given, e.g.

- General moisture modeling is based on Kirchoff's potential described in *Arfvidsson 1998*
- Transport properties are based on *Hedenblad 1993*
- Sorption properties are based on *Nilsson 2006* and their modeling is based on *Mjörnell 1994* and *Mjörnell 1997*

On the other hand, there are also parts of the documentation that are incomplete, e.g.

- Material data for and modeling of chemically bounded water is not explicitly described nor referenced to any external source. Only an indirect reference is given to modeling of hydration in *Mjörnell 1997* without further explanation to how it is used.

- A dependency of self-desiccation on the temperature is an early phase of hydration is observed in measured relative humidities in concrete samples on which the material data are based. It is then stated that the calculation of hydration in the software has been adjusted to take this into account but not based on any existing theory. There is no further explanation to how this is done.
- A calculation of the temperature of the concrete slab is implemented in the last version of the tool, however it assumes that the slab is thin enough to eliminate any temperature variation across it, i.e. the slab's temperature varies only with time and is constant in space.

More detailed analysis of how TorkaS is simulating the moisture state of concrete during hydration and later drying is not possible to do with respect to the incomplete available documentation. The following conclusions are the ones that can be drawn with reasonable certainty:

- Only desorption is considered. There is no attempt to model scanning.
- Transport properties are dependent on moisture state only, not on moisture history.
- Modeling of hydration and chemically bounded water is not possible to analyze. There is no complete modeling framework. Only most fundamental equations are presented. Statements are made regarding some dependencies without further references or unambiguous explicit documentation.
- Material data are based on measurements of fundamental properties of sorption transport (and probably chemical binding of water) from 1980-ties and early 1990-ties. The only modern data that influence the tool are measurements of relative humidity in various drying situations for concrete with new cements, i.e. measurements of the total result of the simulation.

1.4.3 Material development

Since the measurements of fundamental moisture properties for concrete such as transport or sorption behind the simulation tool described above, a significand development of the material has taken place in the Swedish construction industry. During 1990-ies the almost exclusively used binder was Ordinary Portland Cement (OPC). Since then until the start of this research work, a number of major changes in the composition of concrete has taken place, e.g.

- Routine use of 4-5% exchange of OPC for limestone filler in almost all cements.
- Introduction of Byggcement, CEM II/A-LL 42,5 R, an OPC with ~15% limestone filler
- Introduction of Bascement CEM II/A-V 52.5 N, an OPC with ~15% fly ash and 4% limestone filler

During the latter part of the same period of time, there has been an increasing amount of observations of problems connected to drying of concrete. The main two problems were

- Longer real drying times needed to fulfill a requirement of specific relative humidity on an equivalent depth of a slab, compared to predicted by simulation
- Lack of response in drying when additional measures, e.g. drying of surrounding air, were applied after the initially planned time point for screeding or gluing of a surface layer was missed.

This information has been available unofficially for a period of time. It has been investigated and documented in parallel with this work and presented officially in *Svensson Tengberg 2018*.

Based on the material development and the application problems observed, it was concluded that the material data, material models and the simulation method used in the existing tool might be in need of revision, renewal and/or further development.

1.4.4 Investigation of the needs

The situation resulted in a pre-study, done in co-operation between industry and academia, regarding development of a new simulation tool. It focused on the investigation of the situation and its aim was to reach conclusions regarding a new tool and what research and development efforts were necessary to deal with the, at time, present situation. It was executed during 2015 and published a report *Stelmarczyk et al 2015* at the end of that year. The pre-study investigated mainly the two areas:

- what was expected from a new tool for prediction of drying in concrete from the applicational point of view
- what the identified need of simulation implied in the areas of:
    - simulation methodology
    - used material models
    - used material data

The results of the first area are presented in detail in chapter 1.6. The second area was investigated only up to the point when conclusions were drawn about input to the following projects that addressed the necessary research and development. Regarding material data, conclusions were drawn, that formed input to the development project that performed measurements of material properties:

- New measurements of fundamental moisture properties, such as sorption, transport and chemical binding of water, have to be done. Measuring relative humidity only, in a number of cases, is not considered to be enough. Changes to the contents of concrete are suspected to affect the fundamental moisture properties largely enough to make the latest measurements of them inadequate for the application.
- Measurement of properties has to cover the entire sorption context and not only desorption, i.e. also absorption and scanning. Drying of concrete in practice is almost never performed without some additional wetting due to rain and there is also an interest in simulation of moisture redistribution in concrete due to screeding and gluing of surface layers.

The conclusions regarding simulation methodology and material modeling will be presented in the following sections, where they fit naturally into the context.

1.5 Context of this research

In Sweden there is a history of cooperation between the academia and industry resulting in development and use of software tools in order to simulate and predict behavior of concrete in production. When it comes to the temperature and strength development in concrete, this starts during 1980-ties with a simple text-based tool for MS-DOS compatible personal computers and continues with Hett5 released 1991, *Jonasson & Stelmarczyk 1991*, as the first Windows-based tool, Hett97 released 1997, *SBUF et al 1997,* and finally with Produktionsplanering Betong (PPB) released 2014, *Byggföretagen & SBUF 2013-2023*. For predicting early cracking the history starts during mid 1990-ties with Hett2DL & Tempstre and continues 1998 with ConTeSt, *JEJMS Concrete AB 1999*. For drying of concrete, a tool TorkaS was released in 1998, *Arfvidsson et al 1998-2012,* and PPB v 2.0, released 2018 as a result of this project.

Around 2014 a need for further developing the moisture simulation capability was loosely identified. The new tool for simulation of concrete behavior in production, PPB, was initially intended to cover all three simulation areas (temperature/strength, moisture and early cracking) and therefore a pre-study project was executed during 2015. After closer investigation, *Stelmarczyk et al 2015*, three work packages were started to cover the entire identified need:

- Work Package 1 – a research project with a goal of revision of material modeling in the area, in order to extend the simulation capacity to cover new materials, larger set of environmental circumstances and phenomenology. This work package resulted in this thesis.
- Work Package 2 – a development project with a goal of measuring various moisture and hydration properties of concrete with a selected, market dominating cement. This work package resulted in input to the other two work packages.
- Work Package 3 – a development project with a goal of implementing the simulation of moisture behavior in concrete as an extension of the existing tool PPB. This work package resulted in a new version of the simulation tool.

These work packages were executed more or less in parallel. The flow of the generated results is shown in Figure 1.2. There was also a considerable level of coordination in between.

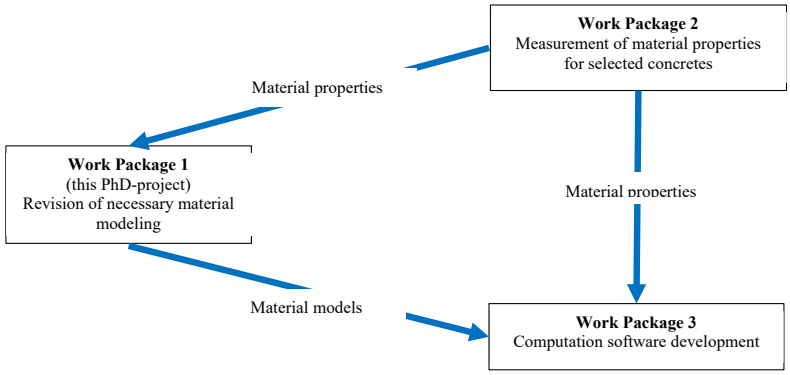

Figure 1.2, Collaboration between the three work packages.

1.6 Applied simulation need

To support adequate planning of effective and safe execution of concrete floor production, a simulation fool for predicting the moisture state of concrete is required. This section describes what was expected from a new such tool, as identified by the pre-study *Stelmarczyk et al 2015*. This tool shall mainly handle two different types of simulation goals/situations.

1.6.1 Drying of concrete

The key scenario is drying of concrete. This starts with casting of concrete into the formwork. It continues further through hydration of concrete and in later stages drying by diffusion or other moisture exchange with the environment. The goal here is to find out when the concrete will be dry enough to continue the construction of the floor system. Normally the drying criterion is a certain relative humidity at the so called equivalent depth, introduced in chapter 1.4.1. Still a simulation and presentation of the moisture state in the entire structure is of a great value for understanding of what is going on in the concrete and possible adjustment of material selection and/or drying method in order to achieve required drying results in required production time.

1.6.2 Moisture in entire floor systems

A complementary scenario for the simulation is drying of concrete extended further with simulation of later stages in the construction of the floor system, see e.g. in Figure 1.3.

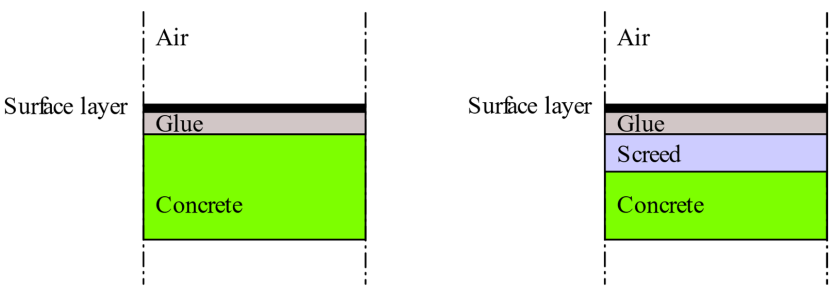

Figure 1.3, Two types of floor systems, with and without screed.

These stages typically consist of application of

- Primer (optional)
- Screed, including drying (optional)
- Surface layer with glue or without

Here, the goal is to simulate the entire redistribution of moisture, coming from various sources, such as concrete, primer, screed and glue. The key objective is to monitor the level of relative humidity in concrete and possible screed, that is in contact with glue/surface layer. Beside this, the moisture state in the entire floor system during the production stages is of interest, as in the drying case, for general understanding and a possibility of effective planning and adjusting material choices and working methodology.

1.6.3 Various geometrical cases

1.6.3.1 One-dimensional geometry

The most simplified case is the one-dimensional. This corresponds to a middle section of a large structure with constant thickness. Some typical variants of one-dimensional geometry are shown in Figure 1.4.

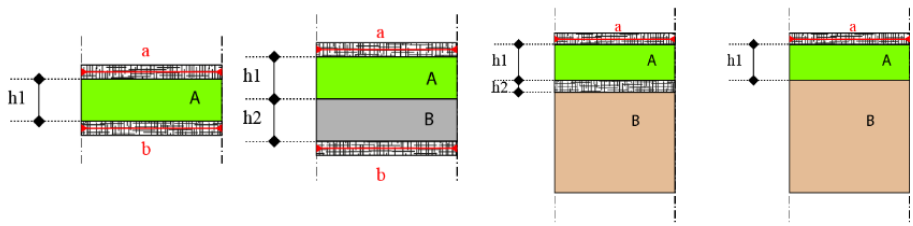

Figure 1.4, Examples of one-dimensional computation geometries: slab, slab on pre-casted concrete, slab on ground with and without insulation in between.

The simulation has to cope with variation of moisture state along the thickness dimension, the only space dimension, beside the time dependency. These cases are also easily extended to the later stages of floor production, while screed and surface layers normally cover the entire floor, i.e. do not affect the one-dimensionality of the moisture variation in space. The majority of applied moisture problems is well described by these cases.

1.6.3.2 Two-dimensional geometry

Some aspects of the moisture state of a concrete floor are not adequately described by the one-dimensional geometry. In Figure 1.5 some typical examples are shown.

In such cases a two-dimensional geometry of problem must be used. This does not make the conceptual problem more complex, regarding principal moisture interaction or modeling of material properties. However, it requires more advanced computation algorithms and typically more computation power and memory.

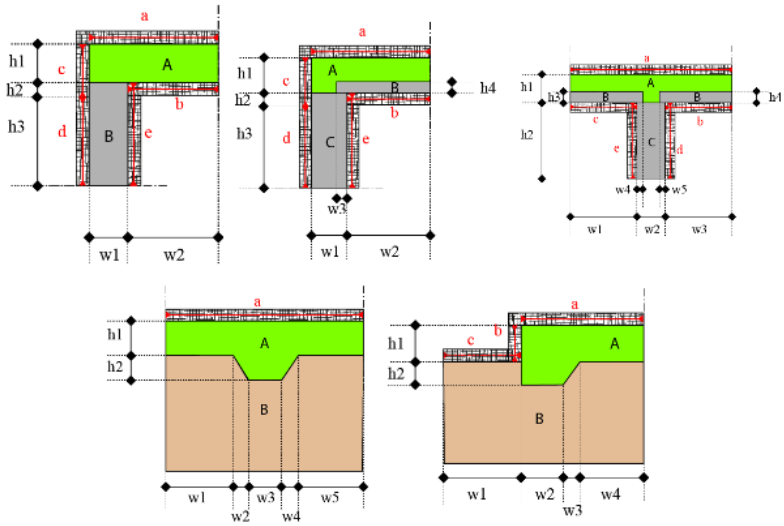

Figure 1.5, Examples of two-dimensional computation geometries.

1.6.4 Materials

When it comes to material behavior and properties in these simulations, the main focus is on concrete, initially hydrating and later just drying. However other materials, such as old concrete (non-hydrating), screed, floor surface etc. may be present in more advanced cases.

1.6.4.1 Concrete

Drying in concrete phenomenologically consists of both self-desiccation due to hydration of the binders and of possible diffusive drying, i.e. exchange of moisture with the surroundings. Simulation of this requires simulation of the hydration behavior of the concrete with its consumption of water (chemical binding of water) as well as both sorption and transport of water in concrete. One shall also observe that due to hydration and transition of concrete from a liquid to a solid state, there is a significant change in structure of the material resulting in dynamics of material properties for phenomena such as sorption and transport.

Simulation of old concrete (non-hydrating) allows a simplification of the above. No water consumption needs to be simulated because there is no hydration going on. Also, material properties regarding sorption and transport are normally assumed to be constant, despite some slow-rate changes occurring due to e.g. carbonation.

1.6.4.2 Screed

Screed is basically very similar in behavior to concrete. However, some aspects of its drying differ:

- High level of fluidity, required for achieving self-leveling properties, normally gives a low level of self-desiccation.
- Combined further with larger amounts of aluminate cements in the binder mixture it results in a very fast hydration process.

- Screed is applied in inhouse conditions, which gives a much more stable hydration process that for concrete, with much less varying hydration results.

These facts are usually used as reasons for simplifying of the modeling of screed behavior. The hydration process and the chemical binding of water is sometimes not simulated at all. A result of this process, constant sorption and transport properties for moisture and a starting relative humidity, are assumed as starting conditions for a simulation of moisture sorption and transport only. Sometimes a simple model for chemical binding of water is used. For details see *Anderberg & Wadsö 2007.*

1.6.4.3 Floor surface layers

The capabilities of storing moisture in floor surface layers, e.g. plastic carpets, are negligible in comparison to concrete or screed. What is of importance in the simulation is its transport properties. Therefore, this part of the floor is simulated as an infinitely thin insulation layer with a certain resistance to vapor transfer. This property is not necessarily constant. It may vary with relative humidity and/or temperature. Temperature variation is normally omitted in this simulation due to the fact that surface layers are applied and used in in-house conditions with low variation of temperature.

1.6.4.4 Glues and primers

To ensure the bond strength of connection between different layers of the floor system, glues and primers are used. These are typically various polymer dispersions with initially a high moisture content to ensure fluidity during application and an even distribution on a large floor surface.

They have naturally both sorption and transport properties for moisture. These change as a result of drying of these substances. Normally what matters is their high initial water content and simulation of these substances is mainly focused on the amount of moisture they add to the floor system. Later in the simulation, these layers are typically simulated in the same way as a floor surface layer, i.e. as infinitely thin layers with a certain resistance to vapor transfer.

1.6.5 Environment and execution of concrete works

1.6.5.1 Casting conditions

Simulation of hydration of concrete requires full understanding of the temperature during this process. The kinetics of the chemical reactions involved are typically temperature dependent. The reactions are exothermic, i.e. producing heat. There is heat exchange with surroundings such as, adjacent structure, formwork, possible insulation and/or covering etc. The weather conditions are also of importance, especially in Scandinavian climate when winter condition can affect uninsulated structures strongly.

1.6.5.2 Weather conditions during drying

During the hydration phase and thereafter, both heat and moisture exchange can take place between the structure and the surroundings. The temperature of the structure is initially a function of both hydration heat and the heat exchange with surroundings. After the hydration peak and some cooling, the temperature of the structure typically follows the average temperature of the surroundings, due to lack of heat of hydration. The moisture is exchanged

with surrounding air. There is a possibility of sucking in rainwater that can accumulate on the unprotected surface of the concrete.

1.6.5.3 Weather protection and inhouse conditions

Sooner or later in the process of floor production, some kind of weather protection will be installed and inhouse conditions will take place. In Sweden there are typically three possible stages of this applied on the construction sites:

- Weather proofing – roof above the structure and walls around, eliminating effects of rain and wind
- Drying conditions – artificially constructed conditions intended for creating a specific environment for diffusive drying of the concrete floor, typically a "tight house" reinforced with heaters and dehumidifiers resulting in stable increased temperature and removal of moisture from the ambient air, creating a significant gradient in water vapor contents between the air and the concrete
- Inhouse conditions – similar to drying conditions but based on the fact that the construction is entering its final stages of production, not specifically intended to reinforce drying process

The weather protection described above is affects typically the environmental conditions for the concrete floor by altering the outside weather, eliminating some of its elements and/or creating entirely controlled conditions.

1.6.6 Limitations

Planning of casting and drying of concrete is a typical task executed at offices or construction sites. This simulation will be performed by use of a MS Windows-based personal computer with a performance and capacity not exceeding a better office PC or a simpler workstation. The acceptable computation time for one simulation can typically be in a range up to several minutes but preferably not more.

Another practical limitation that exists but is a little difficult to estimate more precisely is the cost and time necessary to measure material properties necessary for a new concrete mixture. Full scale measurements of fundamental moisture properties such as sorption, transport and hydration with chemical binding of water take time and money. As already mentioned in section 1.4.4, a necessity of such measurements had been identified and a decision had been taken to perform them in a parallel work package. A summary of the measurement data, supported by the parallel work package 2 is given in section 1.7.3.4.2 and Table 1.1 The output of work package 2 will be used in this work as a source of data for validation of the proposed models as a complement to material data from other sources.

1.7 Analysis of the applied simulation problem

In order to satisfy the identified need for simulation of drying in concrete, the simulation problem will in this section be analyzed. Typical physical descriptions of the phenomena in question will be presented together with some basic considerations regarding modeling of material behavior as well as various boundary conditions. Finally some initial decisions

regarding the simulation method are presented. These are strongly influenced by the conclusions from the pre-study, *Stelmarczyk et al 2015*, regarding computation methodology:

- New computation approach has to be used, allowing more flexible modeling of properties. The use of Kirchioff's potential in the old calculation tool does not give the possibility of modeling scanning and dependency of sorption and transport properties on it.
- The moisture computation has to be combined with a heat simulation of concrete in order to correctly handle the hydration temperature and its impact on moisture properties.

It shall be understood that the analysis below is not regarded in this context as research. It simply does not contain new material enough. It is an application of existing knowledge and methodology in order to understand and identify what research is necessary in the area of material modeling in order to fulfill the requested requirements and simulation need. The identified research problems are presented in section 1.8 and the research challenge is addressed in chapters 2 and 3.

1.7.1 Core problem

The first question to be addressed is regarding the physical level of simulation. Earlier the material was treated as a continuum with the problem expressed as mass flow of water/moisture through it. There are possibilities to model this phenomenology on a deeper level. E.g. the mass flow can be subdivided in various phases of water and utilize more classical fluid mechanics in a more specific/localized description of a pore system, e.g. *Johannesson 2000b*. This level require however a lot of material data consisting of the geometry of the pore system and also raises some problems regarding adequate setting of boundary conditions for the flow simulation, as mentioned in the reference above. Finally, the cost of simulation below the level of continuum-based mass flow is not suitable for the intended computers and expected computation time, see section 1.6.6. The general conclusion is that the continuum level with the classical mass flow differential equation is appropriate for this problem. The main differences from the earlier approach are that the transport formulation has to be treated in a more general way and the entire mass flow equation has to be solved for a non-isothermal case.

Regarding simulation of temperature and hydration, a similar argumentation is adopted. There are possibilities to simulate hydration on a molecular level, e.g. *Lothenbach & Winnefeld 2006*. In order to be representative for the entire concrete floor, this approach is not practical on targeted computers. A similar continuum approach with the heat flow differential equation is much more appropriate, as long as it takes into account the spatial variation of temperature and hydration state, as required by the pre-study.

1.7.1.1 Moisture state and flow

Moisture state in a body is governed by the mass-balance equation. It is a differential equation that can be used to describe other substances as well. It requires balance between three fundamental phenomena: storage, flow and creation/consumption of a substance. Being a differential equation, it has to be fulfilled for entire space and time domain in question, i.e. for

the entire body of interest and during the entire time period of interest. There are various ways of expressing the mass balance equation, e.g. *Luikov 1980*. One typical way of expressing it is given in equ. (1.1).

$$\frac{\partial w_{Ph}}{\partial t} = -\nabla \cdot \boldsymbol{g} - \frac{\partial w_{Ch}}{\partial t} \tag{1.1}$$

where

w_{Ph} - is the moisture content of the material, i.e. physically bounded water, [kg/m^3]

w_{Ch} - is consumed moisture, i.e. chemically bounded water, [kg/m^3]

$\boldsymbol{g}$ – is the field of moisture flow, [kg/m^{2}s]

To the left of the equality sign the time derivative of storage is found. The right of the equation is a sum of the divergence, i.e. source density, of the flow field and the time derivative of the creation or consumption depending on the sign.

The creation/consumption term is probably easiest to evaluate. The only case of the problem described in section 1.6 implying some kind of creation or consumption of moisture by volume is chemical binding of water due to hydration in concrete. It will be explored further in section 1.7.3.1.2.

When it comes to transport and storage one normally describes them indirectly using some kind of potential describing the concentration or contents of the substance in question. For moisture one can choose in general between vapor content, moisture content, partial vapor pressure, relative humidity or, for porous materials with capillary condensation of water, capillary pressure. However, there are differences between them and choosing one or the other can have some consequences for the solving of the problem.

Choice of moisture contents is preferably avoided when more than one material can occur in the simulation. Moisture balance over a boundary between two materials implies equality for most potentials, except the moisture contents, due to its dependency on sorption properties of materials. Relation between vapor contents, partial vapor pressure and relative humidity is simply scaling by vapor contents at saturation or partial vapor pressure at saturation, *Arfvidsson et al 2017*, see equ. (1.2).

$$\varphi = \frac{\upsilon}{\upsilon_s} = \frac{p}{p_s} \tag{1.2}$$

where

φ - is the relative humidity, [-]

υ - is the vapor content, [kg/m^3]

υ_s - is the vapor content at saturation, [kg/m^3]

p - is the partial vapor pressure, [Pa]

p_s - is the partial vapor pressure at saturation, [Pa]

Connection to the capillary pressure is more complicated and under the common assumption that the wetting angle between water and inner surface if concrete porous structure is effectively zero, *Arfvidsson et al 2017*, is govern by equ. (1.3).

$$p_c = \rho_w R_v T \ln \varphi \tag{1.3}$$

where

p_c - is the capillary pressure, [Pa]

ρ_w - is the density of water, [kg/m^3]

R_v - is the gas constant for the water vapor, [J/kg K]

T - is the absolute temperature [K]

In an isothermal case this allows a relatively free choice of potential for the mass-balance equation. Due to the fact that most materials used as layers on the boundaries are described by a vapor resistance in terms of a difference in vapor contents, this potential is commonly used and gives the version of the mass-balance equation shown in equ. (1.4).

$$\frac{\partial w_{Ph}}{\partial v}\frac{\partial v}{\partial t} = -\nabla \cdot (\delta_v \nabla v) - \frac{\partial w_{Ch}}{\partial t} \tag{1.4}$$

where

δ_v - is the transport coefficient for vapor content, [m^2/s]

Here the storage term is now expressed as a product between a moisture capacity with respect to vapor contents $\frac{\partial w_{Ph}}{\partial v}$ and the time derivative of the vapor contents. The transport term is based on the expression of the transport field as proportional to the gradient of the vapor contents, most often with transport coefficient varying with vapor contents.

When the situation changes to non-isothermal, which is implied by the applied problem formulation, some complications occur. The moisture potential is suddenly not the only state variable. The is one more, independent from moisture – temperature. For the storage term, addition of another state variable results in equ. (1.5).

$$\frac{\partial}{\partial t} w_{Ph}(v, T) = \frac{\partial w_{Ph}}{\partial v}\frac{\partial v}{\partial t} + \frac{\partial w_{Ph}}{\partial T}\frac{\partial T}{\partial t} \tag{1.5}$$

This simply expresses that the moisture contents of a material is not only dependent on vapor contents but also on temperature, which is the case for porous materials due to both capillary condensation and adsorption as will be investigated in chapter 2.2. The time derivative of the moisture contents becomes a sum of a term due to change in vapor contents and a term due to change in temperature.

The flow term might also change due to the varying temperature. Here the main question is what gradient is really driving the flow. If it is the gradient of vapor content, there will be no

complications. If it is a gradient of another moisture potential or a combination, the translation between can get complicated due to the fact that the saturation conditions are temperature dependent. This will be further explored in chapter 3.4. Let for now just acknowledge the fact that transferring gradient between moisture potentials can result in a sum of a vapor contents gradient and a temperature gradient, each with a transport coefficient possible dependent on both vapor content and temperature.

This gives together the non-isothermal version of the mass-balance equation, see equ. (1.6).

$$\frac{\partial w_{Ph}}{\partial v}\frac{\partial v}{\partial t} + \frac{\partial w_{Ph}}{\partial T}\frac{\partial T}{\partial t} = -\nabla \cdot (\delta_v \nabla v + \delta_T \nabla T) - \frac{\partial w_{Ch}}{\partial t} \qquad (1.6)$$

where

δ_T - is the moisture transport coefficient for temperature gradient, [kg m/s K]

1.7.1.2 Heat state and flow

The differential equation governing heat state and flow is similar to the mass-balance equation. It is the heat equation. It balances in similar way storage, flow and creation/consumption, however not of a physical substance but of thermal energy, *Luikov 1980*. A typical form is shown in equ. (1.7).

$$\rho c \frac{\partial T}{\partial t} = -\nabla \cdot (\kappa \nabla T) - \frac{\partial Q_H}{\partial t} \qquad (1.7)$$

where

ρ - is the material density, [kg/m^3]

c - is the heat capacitivity, [J/kg K]

κ - is the heat conductivity, [W/m K]

Q_H - is the generated hydration heat per volume, [J/m^3]

There are some differences between this and the mass-balance equation for moisture. In the case of heat the temperature is the given potential for calculation. The storage is based on a heat capacity, that for the current applied problem is considered constant, i.e. not dependent on either temperature or moisture state. The transport may be driven by a both a temperature gradient and a moisture gradient. However the influence of the later one is typically considered as negligible, *Klemczak 2011*, so the transport description is reduced to being driven by the gradient of only temperature. It has been observed that the heat conductivity has a dependency on age/maturity for concrete, mainly connected to the change of state from liquid to solid and the connected chemical binding of water.

Regarding the creation/consumption term, a significant heat contribution during the early phase of concretes life is the hydration heat. Later on, phase change of water, between condensed state, adsorbed state, and/or vapor, might case a contribution depending on where the change takes place.

1.7.2 Boundary Conditions

1.7.2.1 No Flow

One of the simplest boundary conditions to handle is no flow at all. In the case of moisture, a sealed boundary is not unusual in this problem domain. A non-removable formwork for a slab is a typical example. For heat, the fully insulated conditions are normally not corresponding to a physical boundary, due to the fact that that high level of insulation is not a part of the applied problem. On the other hand, when only a part of a structure is studied, due to symmetries, the cross-section cut, ending such a part is chosen to be in a place where there is no flow, i.e. it has the very boundary condition in question. This can apply to both heat and moisture.

A typical way for expressing this type of boundary condition is requiring the flow field to be zero on that part of the boundary, see equ. (1.8) for the heat case and equ. (1.9) for moisture case.

$$\nabla T = 0 \; on \; \Gamma_{H,0} \tag{1.8}$$

$$\delta_v \nabla v + \delta_T \nabla T = 0 \; on \; \Gamma_{M,0} \tag{1.9}$$

where

$\Gamma_{H,0}$ - is the part of boundary where there is no heat flow

$\Gamma_{M,0}$ - is the part of boundary where there is no moisture flow

1.7.2.2 Convective Flow

Convective flow is probably the most commonly used boundary condition in the problem type. It describes interaction with a fixed value of the potential in question over one or a set of resistances. In the heat case the flow is driven by the temperature difference between the surrounding temperature and the boundary temperature with a heat transfer coefficient or a heat resistance, see equ. (1.10).

$$\kappa \nabla T = h_T (T_{env} - T) = \frac{1}{Z_T} (T_{env} - T) \; on \; \Gamma_{H,C} \tag{1.10}$$

where

$\Gamma_{H,C}$ - is the part of boundary where there is convective heat flow

T_{env} - is the temperature of the environment, [K]

h_T - is the heat transfer coefficient, [W/K m^2]

Z_T - is the heat resistance, [K m^2/W]

In the case of moisture, the flow is driven by the vapor contents difference between the surrounding air and the inner side of the boundary with a vapor transfer coefficient or a vapor resistance, see equ. (1.11).

$$\delta_v \nabla v + \delta_T \nabla T = h_v(v_{env} - v) = \frac{1}{Z_v}(v_{env} - v) on\ \Gamma_{M,C} \quad (1.11)$$

where

$\Gamma_{M,C}$ - is the part of boundary where there is convective moisture flow

υ_{env} - is the vapor content of the environment, [kg/m^3]

h_υ - is the vapor transfer coefficient, [m/s]

Z_υ - is the vapor resistance, [s/m]

An important aspect of the specification of the resistance is that resistances of multiple layers on the same boundary are additive, *Arfvidsson et al 2017*, see equ. (1.12). This applies to both vapor and heat.

$$Z_{Tot} = \sum Z_i \quad (1.12)$$

Z_{Tot} - is the total resistance

Z_i - is the resistance of layer i

When the boundary conditions are describing interaction with air, an important aspect of this interaction is movement of the air, i.e. wind impact. When the air is standing still, the heat or vapor exchange affects the layers of air closer to the boundary and changes their initial temperature of vapor contents. If the air is moving, more fresh air comes in contact with the boundary and the effect of changing the temperature or vapor content of the surrounding air is decreasing with the increasing wind velocity. In reality this affects T_s and/or υ_s, but this effect has been successfully modeled for both heat, *Jonasson & Stelmarczyk 1991*, and vapor, *Zhang 2014*, transfer by defining a transfer coefficient based on the wind velocity and adding it to the layer structure while keeping the surrounding temperature or vapor content constant.

1.7.2.3 Fixed Value

One possible boundary condition is a fixed value for the potential, temperature for heat, see equ. (1.13), and vapor contents for moisture, see equ. (1.14). This is a very special boundary condition, implying potentially unlimited flow of heat or vapor over the boundary, if needed to really hold the boundary level of the potential fixed. This corresponds to very few real situations and requires large reservoirs of heat or moisture to be in contact with the boundary.

$$T = T_{env}\ on\ \Gamma_{H,F} \quad (1.13)$$

$$v = v_{env}\ on\ \Gamma_{M,F} \quad (1.14)$$

where

$\Gamma_{H,F}$ - is the part of boundary where the temperature is fixed

$\Gamma_{M,F}$ - is the part of boundary where the vapor content is fixed

In the heat case, one example of such a case is the temperature deep enough in ground below a structure. In Sweden, the temperature at around 2 m depth or deeper is typically not affected by variations in weather, *Jonasson & Stelmarczyk 1991*, and if a heat simulation shall include ground under a slab, one way of simulating it may be to include 2 m of ground in the heat simulation and set the lower boundary condition as fixed temperature.

In the case of moisture, a good candidate for such a situation is direct suction of condensed water from the boundary surface, e.g. accumulated there after rainy weather.

1.7.3 Material Properties

In section 1.7.1 necessary, material related, properties were identified as significant parts of the differential equations describing the problem concerned. Some of them require little attention due to their simplicity and few dependencies, such as heat capacity and thermal conductivity, as stated before. Below, the investigation of the other, more complicated ones continue.

1.7.3.1 Hydration

Hydration is the most dynamic phase of a concrete's existence. Phase change from liquid to solid takes place due to a set of chemical reactions. This has consequences for almost all material properties.

1.7.3.1.1 Heat

The nature of the chemical reactions involved in hydration of cement is exothermic. The accumulated enthalpy of the reactions in question forms what is commonly named as heat of hydration. Handling of this in the heat equation requires expressing the phenomenon as amount of generated thermal energy per time and volume [J/m^{3}s]. This term will typically vary. Initially it will be low. It will then rise with the hydration intensity and later on decline when the hydration is over, see detailed discussion in chapter 2. This indicates that the temporary value of this term will typically depend not only on the momentaneous value of the temperature and vapor content but also on the hydration history, i.e. the history of both computation potentials, see equation (1.15).

$$\frac{\partial Q_H}{\partial t} = f(T, v, Hist[T], Hist[v]) \qquad (1.15)$$

where

f(, ...) – is a general function with indicated variable dependencies

Hist[X] – is some kind of description of history of X since casting

1.7.3.1.2 Chemical binding of water

Further insight in the nature of the chemical reactions involved in hydration of cement, reveals, as the word 'hydration' indicates, reaction with and binding of water to a resulting solid phase of the concrete. This will be referred to as chemical binding of water, as opposed to physical binding i.e. sorption. The required mathematical description of the phenomenon for handling in the mass-balance equation is similar to the case of hydration heat - a term representing amount of water being chemically bounded per time and volume [kg/m^{3}s]. This

term will also behave in a similar fashion to the hydration heat, see detailed discussion in chapter 2, and will depend on a history of temperature and moisture state in concrete, see equ. (1.16).

$$\frac{\partial w_{Ch}}{\partial t} = f(T, \upsilon, Hist[T], Hist[\upsilon]) \tag{1.16}$$

1.7.3.1.3 Compressive strength

Compressive strength of the concrete is not directly involved in the problem description and the governing differential equations. However, removal of formwork, sometimes including a considerable amount of thermal insulation, is often connected to achieving a certain level of strength in the structure. This implies that growth of compressive strength in some simulations will affect change of boundary conditions for both heat and moisture, indirectly affecting the problem in question.

The phenomenology of strength growth is connected to the hydration of the concrete. It is a result of the phase change and typically growths with varying speed during the hydration process. Of similar reason as for heat of hydration and chemical bounding of water, the value will depend on the history of temperature and moisture state, see equ. (1.17).

$$f_{cc} = f(T, \upsilon, Hist[T], Hist[\upsilon]) \tag{1.17}$$

where

f_{cc} – is compressive strength, [MPa]

1.7.3.2 Sorption

Reversible storing of moisture in a material is referred to as sorption. It is based on physical binding of water, which is a looser binding than chemical binding. Typical mechanisms for sorption in concrete are capillary condensation and adsorption, see detailed discussion in chapter 2.2. The moisture content is easily affected by the moisture potential and by the temperature. Due to some mechanisms there is also a memory effect involved - a hysteresis. Two states with different history can have different moisture content despite having the same temperature and vapor content. For a static pore system, this can be summarized mathematically in equ. (1.18).

$$w_{Ph} = f(T, \upsilon, Hist[T], Hist[\upsilon]) \tag{1.18}$$

In concrete, the pore system is not static. It changes rapidly during the first days of hydration. The rate of change decreases then, but there is evidence that the change continues for months ahead, *Olsson et al 2018*. This adds some type of age dependency and possibly also a dependency on the course of hydration. The pore systems may be different depending on how the hydration proceeded and not only to what age.

Beside this it is important to note that the mathematical expression of moisture contents is not enough. The main use in the differential equation of the storage description is in form of its partial derivatives with respect to vapor contents $\frac{\partial w_{Ph}}{\partial \upsilon}$ and temperature $\frac{\partial w_{Ph}}{\partial T}$.

1.7.3.3 Transport

Transport properties, especially during non-isothermal conditions require careful and detailed study, which is done in chapter 2.3. At this stage of investigation of the problem it is enough to observe that moisture can be transported both as vapor and in its condensed state. Due to the large difference in concentration [kg/m^3] of those two phases, the filling state of the pore system can rightfully be suspected to strongly influence the transport properties. This connects the transport properties to the entire sorption phenomenology. This should be no surprise due to the fact that both phenomena take place in the same pore system. This results in the same suspected dependencies for the transport coefficients, see equ. (1.19) and (1.20).

$$\delta_v = f(T, v, Hist[T], Hist[v]) \tag{1.19}$$

$$\delta_T = f(T, v, Hist[T], Hist[v]) \tag{1.20}$$

The dependency on age and course of hydration applies even here. Some simplification, compared to sorption, is that the values of the transport coefficients are used directly in the differential equation and no further differentiation is necessary.

1.7.3.4 Limitations of Measuring Material Properties

1.7.3.4.1 Physical Limitations

Measuring properties in a material that changes can be challenging. There are two techniques to deal with the change. Either the change is stopped, and the properties of the material frozen during the measurement or one has to perform the measurement quickly enough compared to the change rate of the material for the properties to be approximately constant during the measurement. Both techniques can sometimes be impossible to perform practically.

Measuring of concrete properties at early age, i.e. during hydration present this kind of challenge. Many methods for stopping hydration have been developed in order to make execution of slower measurements possible. Almost all of them involve removal of chemically unbounded water from concrete, *Zhang & Scherer 2011* and *Collier et al 2008*. This poses a problem for measurement of sorption and transport properties for moisture, where measurement methods require presence of chemically unbounded water in the measurement object.

An alternative to removing water has been developed by partial exchange of cement with similar size of particle inert to concrete constituents, *Termkhajornkit et al 2015*. Due to lack of proof that the sorption and transport properties in such a pore system remain unaffected compared to a similar hydration degree of real concrete, the method was rejected. In case of mixed binders, where the degrees of reactions or each binder are not following each other, the method is impractical, which added as an argument to the rejection decision.

As a consequence of above, there will be no knowledge of sorption and transport properties during approximately two first weeks of the hydration. This has to be considered during further modeling.

1.7.3.4.2 Practical Limitations

Another set of limitations for the modeling attempt is connected to practicalities of the measurement work package, providing the measured values as input for the modeling and this research. Table 1.1 gives an overview of the performed measurements and provided measurement.

Table 1.1 Overview of measurements and measurement conditions in parallel work package 2, intended to be targeted by the modeling in this research work.

Type of data / status	Curing conditions	Measurement conditions
Moisture transport		
Transport coefficients for vapor contents / Measured	Sealed curing at 20 ºC, ages 6 and 12 months	Connected RH-intervals forming an entire curve, at 20 ºC for both desorption and absorption
Moisture sorption		
Moisture contents / Measured	Sealed curing at 20 ºC, ages 6 and 12 months	RH-levels forming an entire curve, at 20 ºC for both desorption and absorption and some scanning under desorption
Moisture contents / Measured	Sealed curing at 20 ºC, ages 6 and 12 months	At capillary saturation
Hydration		
Chemically bounded water / Measured	Sealed curing at 5, 20, 35 and 50 ºC, various ages up to 6 months	Hydration stopped by fast drying to 11% RH at 20 ºC with following TGA analysis
Chemically bounded water / Measured	Curing at 5 and 20 ºC, at capillary saturation, various ages up to 6 months	Hydration stopped by fast drying to 11% RH at 20 ºC with following TGA analysis
Hydration heat / Measured	Sealed curing at semi-adiabatic conditions	Semi-adiabatic calorimetry
Compressive strength	Curing in water-baths at 5, 20, 35 and 50 ºC, various ages up to 3 months	10 cm cubes

The initial ambition of work package 2 was to also perform measurements in the areas of sorption and transport at other temperatures than 20 ºC. This was intended in order to enable

modeling in non-isothermal conditions. For chemically bounded water, there was an intention to use samples that had been cured in more combinations between different temperatures and moisture conditions. The work package did not manage to perform these measurements, which affected the scope of research described later in this thesis and the validation basis for the proposed models.

1.7.4 Initial decisions

Below a few necessary initial decisions are given and motivated. These mainly affect the necessary generalization level of the problem and the understanding of the requirements regarding modeling on the sub-problem level. Modeling can be performed at many levels, with various aims and enabling various types of use, *van Breugel 2015*. The purpose of the initial decisions is to simplify identification of a suitable level of modeling within this research.

1.7.4.1 The differential equations

The main choice regarding the differential equations in question is how generalized version of the mass flow to apply. After the discovery how important the temperature and its history is on one hand for all the parameters directly connected to hydration results, such as heat or chemical binding of water, as well as later for hysteresis in both sorption and transport properties, the non-isothermal version of the mass-balance is chosen.

1.7.4.2 The material types

Materials with significant storage capabilities for heat and/or moisture has to be simulated as computational objects taking up geometrical space and modeling the storage capabilities. In this class of materials there are two sub-classes identified. There are materials undergoing significant changes during the first period of time, i.e. concrete, due to hydration. In this case the various aspects of hydration such as generated heat and consumed water has to be modeled. For these materials there shall also be some kind of modeling of change in other parameters, such as sorption and transport, due to age. There are also materials that can be simulated as having constant sorption and transport properties and not contributing to generation of heat nor chemical binding of water. For these materials, such as old concrete, there shall be no simulation of hydration.

Regarding screed, both mentioned material modeling approaches may be actual. Some products have a very rapid hydration process and regarding desiccation rely mainly on diffusive exchange of moisture with surrounding air. In such a case, sorption and transport does not have to vary with age. Modeling of chemical binding of water, due to short hydration, can be simply expressed as a starting humidity or water contents, lower than saturation. In other cases, some kind of modeling of chemical binding with respect to age and temperature might be necessary to describe the behavior of the screed accurate enough for the application. Such cases are considered outside scope of this thesis.

Materials with insignificant storage capabilities for heat and/or moisture are typically simulated as objects occupying no space, i.e. infinitely thin layers, possessing resistance to transfer of heat and/or moisture. Regarding moisture, it is important to remember that the

resistance is not necessarily constant but can be dependent on the temperature and/or vapor contents of the layer.

1.7.4.3 The boundary conditions

The main key to flexibility in simulation of various boundary conditions is convective flow in combination with support for multiple layers of resistance and modeling of wind impact as additional layers. This method will be complemented with zero boundary flow. The latter case is important when sealed conditions occur in the case of moisture as well as when cross-section boundaries are used for limiting the computation area due to symmetries.

When it comes to the condition of fixed value, the only identified case of possible interest is capillary suction of condensed water from surface, e.g. during and after rain. However, this case can also be simulated using convective flow and selecting a large enough transfer coefficient. It is left for the later implementation of the simulation to select a specific method for this purpose.

1.7.4.4 Selection of calculation potential for moisture

As mentioned earlier, the selection of the computation potential for the mass balance equation can be done in various ways. The reasoning given in section 1.7.1.1 is still applicable. No new aspects of this question have been found during the analysis of the other aspects of the applied problem. The three key issues are:

- Potential continuity over material boundaries
- Formulation of the convective flow on the boundaries
- Formulation of the transport term in non-isothermal conditions

Regarding the first two, the vapor content is the preferable choice. The transport formulation in the non-isothermal case is not a trivial task and it needs further investigation into the transport phenomenology and the driving mechanisms. However, assuming as in equ. (1.6) use of a combination of gradients of both vapor content and temperature will ensure a possibility of using gradients of various moisture potentials as well as temperature and translating them to the used, double-gradient form in the equation.

1.7.4.5 Computation method

As stated in the beginning of section 1.7, a computation method for the problem was requested, that allowed a more flexible handling of moisture sorption and transport, compared to the Kirchoff's potential formulation used with finite differences in previous modeling, *Arfvidsson et al 1998–2012*. The approach chosen here is based on the Finite Element Method (FEM), *Zienkiewicz et al 2013*, for the spatial dependency of the partial differential equations involved in combination with a finite difference scheme for the time dependency. The FEM approach allows for simple and flexible treatment of various geometries:

- For 1D two-node elements with linear shape and weight functions can be seen a standard approach to all geometries. A flexible choice of integration points for Gauss Quadrature approach to evaluation of integrals of non-linear element properties allows for adjustment of computational stability's spatial dependencies.

- For 2D three-node triangular elements with linear shape and weight functions can be seen a standard approach to all polygonal geometries and allowing for good approximation of other geometries. A flexible choice of integration points for Gauss Quadrature approach to evaluation of integrals of non-linear element properties allows here also for adjustment of computational stability's spatial dependencies.

The used of finite differences in time, more specifically a weighted sum of forward and backward differences, gives a base for computational stability. Further the selection of time steps can easily be adapted to various combinations of storage and transport capacity for each element so that the requirement for the shortest time step is respected during the computation.

Another advantage of this approach is the possibility of use of a multiple iteration approach for each time step. This is done in order to deal with the non-linearities in the hydration modeling as well as non-linearities and hysteresis effects in the transport and sorption properties of moisture.

The final remark regarding computation method considers the fact that two partial differential equations shall be solved on the same domain and under the same circumstances. As clearly seen in the analysis above, there is a cross-dependency between the equations. The mass-flow of moisture is connected to the temperature of the structure as well as to the hydration and its chemical binding of water. The heat equation is connected to the moisture state through its dependency on hydration, which in turn is dependent on available water. However these two dependencies are not computationally equal in strength. There is a significant difference in speed for the dependencies where moisture phenomenology is clearly the slower one compared to heat. This allows for handling of both equations with separate FEM-formulations, coordinated in space by the same element decompositions and in time by the same time steps, where for each time step the heat problem is solved first and the moisture problem is solved thereafter. In this way solving of combined system of linear equations for two fundamentally different types of variables can be avoided without introducing computation errors due to the cross-dependencies.

1.8 Research problems

As a result of the input and analysis given in this chapter, based on the application need and by the pry-study expressed requirements, research problems are formulated for three different, however as the literature study will show, connected areas. The research problems are formulated below.

1.8.1 Hydration and chemical binding of water

The key goal of the research problem regarding hydration and chemical binding of water is to propose a model for calculation of the amount of chemically bounded water per amount of cement (kg/kg):

$$w_{Ch} = function\ of(T, v, Hist[T], Hist[v]) \qquad (1.21)$$

Also allowing for evaluation of it derivative $\frac{\partial w_{Ch}}{\partial t}$.

The following dependencies were to be addressed:

- Temperature
  - The influence on rate of reaction
  - The influence on how much water is actually bounded per kg binder and the end level of self-desiccation
- Moisture
  - The limiting influence on the rate of reaction and end of hydration

The following additional requests were also to be taken into account:

- The model for chemical binding should be preferable based on a model of hydration.
- The model of hydration should have a level of generality allowing for using it as a base for further formulation of connected models heat of hydration and development of compressive strength. The modeling of heat shall not cover the initial dissolution peak, but start in the dormant period, i.e. correspond more closely to heat generated at and after casting and not during blending.

These requests were not considered as a primary goal of the research problem, but as a secondary and optional outcome of the research.

1.8.2 Sorption of moisture

The key goal of the research problem regarding sorption of water is to propose a model for calculation of the amount of physically bounded water per amount of cement (kg/kg), i.e. the moisture contents:

$$w_{Ph} = function\ of(T, \upsilon, Hist[T], Hist[\upsilon]) \qquad (1.22)$$

allowing also for computation of partial derivatives $\frac{\partial w_{Ph}}{\partial \upsilon}$ and $\frac{\partial w_{Ph}}{\partial T}$.

The key dependencies to be addressed were relative humidity (or any other vapor potential) and temperature under the circumstances of desorption, absorption and scanning. The dependency on temperature was initially intended to be handled as a key dependency. Due to lack of measurement data regarding this influence, that limited the validation base for a proposed model, this requirement was limited to optional with an ambition to build in some temperature dependency based on theory.

1.8.3 Transport of moisture

The key goal of the research problem regarding transport of water is to propose a model for calculation of the transport term in the temperature dependent version of the mass balance equation:

$$\frac{\partial w_{Ph}}{\partial \upsilon}\frac{\partial \upsilon}{\partial t} + \frac{\partial w_{Ph}}{\partial T}\frac{\partial T}{\partial t} = -\nabla \cdot (\delta_\upsilon \nabla \upsilon + \delta_T \nabla T) - \frac{\partial w_{Ch}}{\partial t} \qquad (1.23)$$

expressing it by use of gradients of vapor contents and temperature and corresponding transport coefficients:

$$\delta_v = function\ of(T, v, Hist[T], Hist[v]) \quad (1.24)$$

$$\delta_T = function\ of(T, v, Hist[T], Hist[v]) \quad (1.25)$$

The key dependencies for the transport coefficients to be addressed were relative humidity (or any other vapor potential) and temperature under the circumstances of desorption, absorption and scanning. The dependency on temperature was initially intended to be handled as a key dependency. Due to lack of measurement data regarding this influence, that limited the validation base for a proposed model, this requirement was limited to optional with an ambition to build in some temperature dependency based on theory.

2. Literature study

The goal of this literature study is to provide an understanding of the scientific background of the research problems formulated in section 1.8, in order to facilitate formulation of their solutions. The study contains therefore both an overview of the phenomenology involved as well as earlier modeling attempts. However, these are limited regarding the level of information. As mentioned, the purpose of the study is to facilitate a specific problem solving. Hydration of concrete and moisture behavior in it are large and deep scientific areas that has been and are studied both in large and in a great detail. It is not a purpose of this chapter to provide an, in any way, complete picture of all underlaying phenomenology or of all scientific work regarding various levels of modeling of it.

The use of terms “cement”/ “binder” and “water-cement-ratio (w/c)”/“water-binder-ratio (w/b)” requires a clarification. In this document both will refer to the total amount of binders used in a specific concrete. In construction industry, attention is given to whether a supplementary cementitious material (SCM), being part of a concrete mixture, is added to the mix by the cement manufacturer as a part of cement or binder production or by a concrete manufacturer exchanging cement for an SCM as a part of concrete production. This is strongly connected to the governing standards for cement and concrete. For this work however, the question who added the SCM and what product testing according to which industrial standard did the binder mixture pass simply makes no difference, because it doesn’t affect the properties of the end product.

2.1 Hydration and its effects

The use of cementitious materials in construction as mortar and/or concrete has been practices for millennia. Various materials has been used as binders. Research and development regarding new binders is an ongoing process. The purpose of this chapter is to focus on a selection of materials, that can be used as binders, and their behavior. First the composition of binders, chemical reactions and the resulting reaction products are presented for Ordinary Portland Cement (OPC) and some supplementary cementitious materials (SCM). Later a selection of knowledge regarding reaction kinetics is presented. The last step of the literature study focuses on modeling of the hydration and some of the resulting concrete characteristics.

There has been a large amount of scientific work presented on the area of hydration of OPC and SCMs, from the more pioneering works of Powers and Brownyard, *Brouwers 2004 & 2005*, to more recent of Scrivener and Lothenbach among many others, e.g. *Scrivener & Nonat 2001*, *Scrivener et al 2015* and *Lothenbach et al 2011*. Majority of the results are available as textbooks. The overview in the first two sections of this chapter is mainly based on such a comprehensive material as *Hewlett & Liska 2019*, *Taylor 1997* and *Kurdowski 2014*. Specific references will be used occasionally to emphasize specific details in these two sections.

2.1.1 Hydration reactions, reactants and products

2.1.1.1 Clinker materials – Ordinary Portland Cement

OPC, with its binding clinker materials, containing a dominating amount of alite, has been produced since early 19th century. This is connected to development of technique got heating of cement kilns to a process temperature exceeding 1400 °C, which is necessary for the formation of alite. The production process today uses limestone as a main source of calcium and materials containing clay as complementary source of aluminosilicate. The burning process is typically divided into two stages, a calcination at a temperature of above 600 °C and later sintering at about 1450 °C. After a cooling stage the resulting material goes through grinding in order to reach desired grain size distribution and specific surface. The composition of the clinker materials may vary regarding the proportions between the components and content of small amount of additional material from the production process. However, it is based on the 4 main clinker components described below.

2.1.1.1.1 Components

Alite is one of the two calcium silicate components of OPC. It is the impure version of tri-calcium-silicate, with chemical formula $(CaO)_3 \cdot SiO_2$, and in cement chemist notation C_3S. Although C_3S is in general not thermodynamically stable under the temperature of 1250 °C, its decomposition is typically restricted by fast cooling, resulting in polymorphic transitions to phases stabilized by presence of impurities, e.g. MgO. Due to its relatively high CaO content, alite is the most reactive of the calcium silicates.

Belite is the other of the two calcium silicate components. It is the impure version of di-calcium-silicate, with chemical formula $(CaO)_2 \cdot SiO_2$, and in cement chemist notation C_2S. It forms more easily than alite but it's also dependent on quenching and impurities for stabilization of its hydraulically important polymorph. It is not as reactive as alite.

Calcium aluminate is one of the two aluminum compounds present in the OPC. Its chemical formula is $(CaO)_3 \cdot Al_2O_3$, and in cement chemist notation C_3A. It's also stabilized by impurities, about 6% Na_2O. This component is very reactive with water and alone gives an early increase in strength of concrete. This can result in too fast setting of the concrete and is normally controlled by addition of gypsum, $CaSO_4 \cdot H_2O$, that changes the reaction and slows down the kinetics, see further the next section.

Calcium aluminoferrite is the other aluminum compound present in clinker. Its chemical formula is commonly noted in cement chemist notation C_4AF. In practice the composition is varying, and a better description is given by $Ca_2(Al_xFe_{1-x})_2O_5$, where x varies around 0.5 (different limits given by different sources). This is close in composition to the commonly used C_4AF.

2.1.1.2 Composition

Typical composition of cement clinker is given in Table 2.1. Beside the main components and gypsum lower amounts of other compounds are also present.

Table 2.1. Typical composition of clinker components in OPC

Clinker component	Formula	Typical mass (%)
Alite	C_3S	45-75%
Belite	C_2S	7-32%
Calcium aluminate	C_3A	0-13%
Calcium aluminoferrite	C_4AF	0-18%
Gypsum	$C\bar{S}H_2$	2-10%

2.1.1.1.3 Reactions

Due to the fact that the clinker components are not pure versions of the key chemical compounds and both impurities and varying polymorphs are parts of the hydration, the full picture of the chemical reactions is complex and may vary between different clinkers. Below the dominating, key reactions are discussed.

Both calcium silicates react in similar way with water resulting in portlandite and so called C-S-H-gel, see equ. (2.1) and (2.2).

$$C_3S + (3 - x + y)H \rightarrow C_x - S - H_y + (3 - x)CH \quad (2.1)$$

$$C_2S + (2 - x + y)H \rightarrow C_x - S - H_y + (2 - x)CH \quad (2.2)$$

As the proportions between components in the C-S-H-gel and the structure of the gel are varying, the reaction formulae are using parameters instead of numerical values.

The main reaction pattern of the aluminate phase is more complex, and it depends on the presence of other molecules. In OPC, the main reaction takes place in presence of gypsum and results in formation of ettringite, see equ. (2.3). When the gypsum is consumed, the aluminate continues to react with ettringite and water to form the monosulphate phase, see equ. (2.4) . When ettringite is consumed the reaction can continue further, however the two first steps are normally considered most important.

$$C_3A + 3C\bar{S}H_2 + 26H \rightarrow C_6A\bar{S}_3H_{32} \quad (2.3)$$

$$2C_3A + C_6A\bar{S}_3H_{32} + 4H \rightarrow 3C_4A\bar{S}H_{12} \quad (2.4)$$

The reaction pattern of the ferrite is analogue to the aluminate, forming products with not only aluminum oxide in the structure but also iron oxide, see further discussion regarding clinker reaction products in section 2.1.1.1.4.

2.1.1.1.4 Products

The main product of the calcium silicate reactions is the C-S-H phase or C-S-H gel. It is an amorphous or nearly amorphous hydrate with the general formula $(CaO)_x \cdot SiO_2 \cdot (H_2O)_y$, where x and y can vary significantly. The structure of the phase can be characterized by

identification of SiO_4 tetrahedra, and their connections to between 0 and 4 neighboring tetrahedra through Si-O-Si bonds. This enables both amorphous structuring of the phase as well as some degree of polymerization and crystalline structures such as 1.4nm tobermorite and jennite, see Figure 2.1, and explains the large variability in proportions between the constituents of the phase.

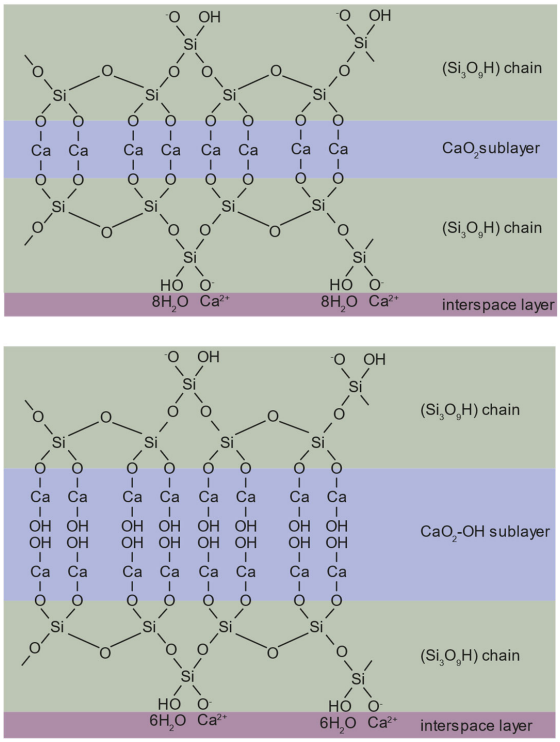

Figure 2.1, Schematical structure of 1.4nm tobermorite and jennite.

The gel is the dominating hydration product and typically responsible for the majority of properties of the cement paste and the concrete, such as strength and chemical binding of water. Due to its intrinsic porosity, it also contributes to the physical binding of water in gel pores, see further discussion about pores in section 2.2 in general and section 2.2.3.2 more specifically.

Many has studied the properties of the gel. Authors has identified different kinds of this phase depending on whether it's formed inside or outside the cement grain, inner or outer product, *Taylor 1997* and *Scrivener et al 2015*. Other has identified variation in density and adopted nomenclature of subdivision into low and high density, *Tennis & Jennings 2000*. There are also findings of differences in the gel formed at various temperatures, *Gallucci et al 2013*. The gel can also form as a result of other reactions in concrete, see further discussion on SCMs in this chapter.

From the moisture perspective, one remarkable property of the gel is the capability of chemical binding of varying amounts of water. Variation of this, together with other properties of the gel, as a result of the temperature during formation of the gel, has been studied by a variety of methods in *Gallucci et al 2013*. It has been found that the water content, in proportion to the SiO_2, has an almost linear correlation to the temperature in the interval between 5 and 60 °C, see Figure 2.2.

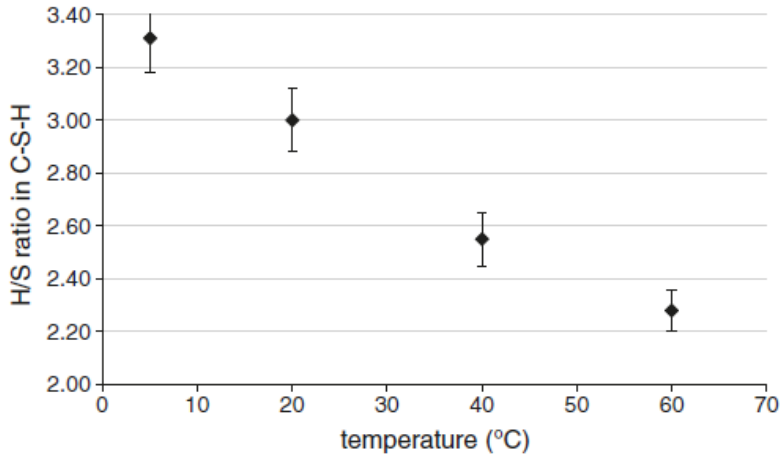

Figure 2.2, H/S ratio as function of hydration temperature, measured by TG and RD at 90 days of hydration, from Gallucci et al 2013.

The other product of the calcium silicate hydration is portlandite, or in its pure form calcium hydroxide $Ca(OH)_2$. It is a crystalline phase forming in concrete a plate-like crystals. Its contribution to the majority of properties of the paste and concrete is not as large as for C-S-H gel. There is mainly one exception to this rule. Due to its solubility in water, portlandite is the main phase responsible for the high pH of concrete and through this for corrosion protection of concrete reinforcement.

The product phases of the aluminates and ferrites are similar in structure, and in concrete chemistry are described by the same formulae: AFm and AFt. The letters A and F indicate if aluminum oxide or iron oxide is the basis of the structure and the letters m (mono) and t (tri) indicate the number of sulphates attached – one for monosulphate and three for ettringite. Both of them form rather different, crystalline structures. Due to the small amount in which they are present, their contribution to the physical properties of the cement paste is normally small. One exception to this may is late ettringite formation that may occur as a consequence of hydration at high temperatures (> 70 ºC) in its initial stages.

2.1.1.2 Supplementary Cementitious Materials

There is a whole range of materials that can be used in addition to OPC to facilitate binding of aggregate in concrete. These materials are commonly referred to as supplementary cementitious materials (SCM). Despite the fact that many of them can be used as binders

without OPC, e.g. by use of other activators, the most common use of them today is as replacement for OPC when a lower carbon dioxide footprint of concrete is desired.

2.1.1.2.1 Glasses and the pozzolanic reaction

A large variety of supplementary cementitious materials fall under the category of pozzolans or half-pozzolans. The common denominator for these materials is significant content of reactive glass phase, mainly based on amorphous silica but possibly also containing other materials such as aluminum oxide and iron oxide. These materials are used as binders in mortar and concrete. The nature of their reaction is different from the reactions of typical clinker components. The very simplified idea of the pozzolanic reaction is given in equ. (2.5).

$$S + xCH + yH \rightarrow C_x - S - H_z + (x + y - z)H \qquad (2.5)$$

A few principles for this reaction can be observed here:

- Reactive silica is needed.
- The reaction is activated by hydroxides, OH^-, and not water.
- Additional calcium has to be supported to form C-S-H-.gel.
- Additional water can be bounded but it can also be released by this reaction, see further section on silica fume.

Although portlandite is a good source of both hydroxide ions for activation and calcium, both can be supplied by other sources.

It shall also be mentioned that the presence of other metal oxides, e.g. aluminum and/or iron, in vicinity of calcium, silica and water enables, as well, formation of ettringite, monosulphate and possibly other aluminate or ferrite hydrates depending on availability of sulfates.

The true nature of reactions of a specific pozzolanic or half-pozzolanic SCM will be highly dependent on the mixture of its constituents and the nature of its activation. The possible spectrum of various content is wide. There are many natural pozzolans based on pyroclastic rocks or naturally burnt clays, with a significant historical use. There are also many artificial pozzolans such as fly ash, silica fume or burnt shales and clays. The resulting products will be mainly same or similar to the reactions of clinker components. The sections below present three artificial SCM, their properties and reaction characteristics when mixed with clinker.

2.1.1.2.2 Fly ash

Fly ash is a waste product from burning of pulverized coal in power plants. Due to high temperature of burning and sudden cooling, spherical glass particles are formed. Their composition depends strongly on the mineral composition of the coal and can vary significantly even between two different batches of coal from the same mine. Normally a larger amount of silica and significant amounts of aluminum and iron oxide are present, but oxides of calcium, magnesium, potassium, sodium as well as other constituents can also be present.

Fly ashes are classified into two classes F and C, *ASTM C618-15*, with increasing contents of calcium. Here siliceous class F is considered further. The content of glassy silica is used for a

pozzolanic reaction. Activation of this is dependent on clinker reactions to first produce portlandite that can later be used as source of hydroxide ions for activation as well as calcium. Fly ashes containing aluminum and iron contribute to additional forming of other phases than C-S-H. Fly ash is not regarded as a highly reactive pozzolan and its reaction is beside the necessity to wait for the portlandite to form, relatively slow as such and results seldom in higher degrees of reaction, i.e. not all fly ash is consumed in blended cements. A fraction of small particles of fly ash can on the other hand have an accelerating impact on the clinker reaction by acting as nucleation kernels for the clinker reaction products. Fly ash reaction result in chemical binding of relatively small amounts of water.

2.1.1.2.3 Silica fume

Silica fume is a biproduct from manufacturing of silicon metal and ferrosilicon alloys. Fumes from furnaces used for this purpose contain very small particles of amorphous silica, that are later cooled and condensed. Even names such as micro-silica and condensed silica fume are used. This SCM has a high content of amorphous silica and due to its very small particle size a very high specific surface area enabling a very high reactivity.

The reaction patter is the typical pozzolanic, however without the contributions from other metal oxides, as found for fly ash. Silica fume consumes considerable amount of portlandite and results in a negative net binding of water, i.e. parts of water bounded earlier in portlandite are released to its original state, *Helsing 1993* and *Mjörnell 1997*.

2.1.1.2.4 Slag

Blastfurnace slag is a biproduct from iron manufacturing. It contains pozzolanic material in form of silica, solidified into glass by a fast cooling process. However, a significant amount of calcium oxide is also present in slag, making it partially hydraulic. The combination of those potential reaction patterns causes slag to be classified as a half-pozzolan.

Composition of slag varies. The main constituents are calcium oxide and silica. Some presence of aluminum and magnesium oxides is also common. The reaction patter differs from the pure pozzolanic. The presence of calcium oxide enables the hydraulic reaction forming portlandite, see equ. (2.6).

$$CaO + 2H_2O \rightarrow Ca(OH)_2 \qquad (2.6)$$

In reality a combination of the hydraulic and the pozzolanic reactions occur with contributions from the other metal oxides present in the slag. Although in theory slag can activate itself, by the hydraulic reaction first followed by the pozzolanic, it is normally activated by an earlier clinker reaction. The calcium content of slag significantly decreases the amount of portlandite consumed, which makes it possible for much higher amounts of slag to be blended with clinker, compared with fly ash. It also increases the net chemical binding of water to a moderate level – higher than fly ask but lower than clinker. Slag is more reactive than fly ash but much less than silica fume. It can interfere with clinker reaction depending on its contents. An observed effect is of slowing down or temporarily inhibiting of belite reaction.

2.1.1.2.5 Limestone filler

Earlier presented SCM:s contribute significantly to the chemically activity in the binding reaction of concrete. In contrast to that, there is at least one commonly used material that in most of its use in OPC-based concrete is often regarded as "almost" chemically inert. It is limestone filler. The material typically is added during grinding. Due to its softness, compared to the clinker materials, limestone gets grinded to a very high specific surface, i.e. very small size. Being chemically inert is not truth. There is evidence that the presence of the SCM affects composition of the main reaction products, *Lothenbach et al 2008*. It is or can be chemically active both as a source of calcium oxide as well as carbonates. On the other hand is seems not to add any new reaction patterns on its own. Even if these particles are not taking a major chemical role in the binding reaction, they participate on a large scale physically by acting nucleation sites for the precipitation of the hydration products. The typical use of it today consists of routine replacement of approx. 4% of OPC for limestone filler. There are also cements where the replacement is considerably higher.

2.1.1.3 Chemical binding of water

As previously described, considerable amounts of water are chemically bounded in the products of binder reactions. Water molecules are part of almost all involved reactions. Some examples of their binding in the C-S-H-gel has been shown earlier in Figure 2.1. The structure of the reaction products has been an area for research for some time now with many contributions. Various models for the structure has been proposed and refined, e.g. *Jennings 2000*, *Tennis & Jennings 2000* and *Jennings 2008*. It is not the intention of this study to present deeper results of this work. From intended level of applied research, it is however important to realize that all water molecules are not bounded equally strong. Two typical examples of this are:

- Hydroxide ions, embedded in the structure of e.g. C-S-H-gel or as a part of portlandite crystals
- So called interlayer water or crystal water, consisting of water molecules sitting between layers or sheets of the reaction products, typically attached stronger that adsorbed molecules on the pore walls but considerably weaker than the previous example.

This results in a somehow ambiguous border between what is considered as chemically versus physically bounded water. Measurement methods regarding these two types of water in concrete can tell various stories. Chemically bounded water is sometimes interpreted as non-evaporable water. This is typically measured by drying concrete to remove evaporable water at approx. 105 ºC and then performing a themo-gravimetric analysis (TGA), e.g. *Helsing 1993*. Sometimes the TGA is performed from lower temperatures in combination with various water removal methods used to arrest hydration before the analysis, e.g. *De Weerdt et al 2011*. A typical analysis of physical water contents in various conditions consists of finding weight of a sample under specific relative humidity and temperature, *Baroghel-Bouny 2007a*. Even if isotherms are typically measured at room temperature, lower levels of relative humidity may be enough to remove not only capillary water and adsorbed molecules but also some molecules from the reaction products, e.g. *Feldman & Ramachandran 1971* and *Baquerizo et*

al 2016. This poses some challenge is comparing various research results. A more important observation in the framework of this work is that a clear border between what is considered as chemically versus physically bounded water has to be adopted. This boundary definition has to work for measurement methods used in both areas and has to be taken into account while modeling.

2.1.2 Reaction Kinetics

2.1.2.1 Relative Reactivity of Different Clinker Components

As mentioned earlier the reactivity of the four clinker materials differ. Figure 2.3 shows development of degree of hydration for the pure materials as a paste at room temperature. The first 10 hours are clearly dominated by the aluminates and ferrites, if not moderated by gypsum. This is the reason why gypsum is added to slow down these reactions, which is shown in Figure 2.3 only for the aluminate phase. This adjustment brings down the intensity at start and enables the concrete to keep its fluid consistency for a few hours. The main intensity increase is observed later mostly due to the reaction of the alite followed by the aluminate. The slowest relative kinetics are show by the belite.

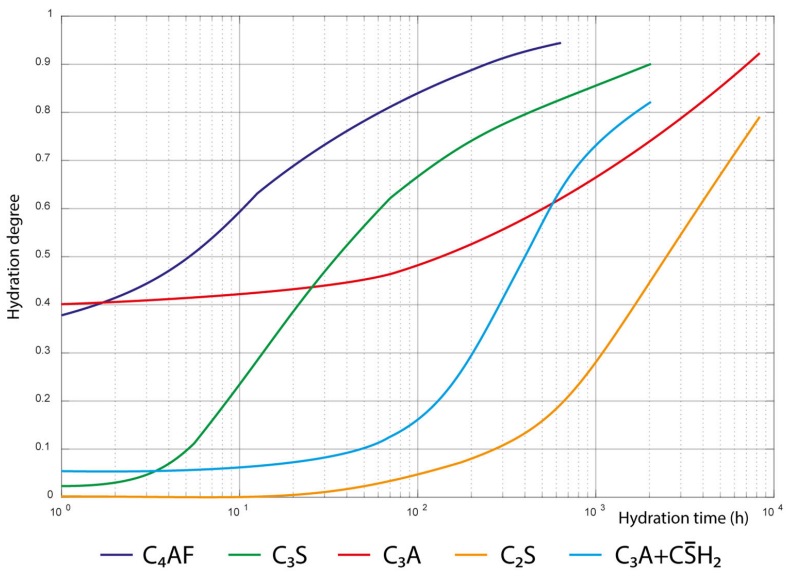

Figure 2.3. Typical hydration kinetics of pure clinker materials (calcium aluminate with and without gypsum) in paste at ambient temperature, after Hewlett & Liska 2019.

2.1.2.2 Main Phases of Clinker Reactions

In the beginning, the clinker materials come in contact with blending water and start to dissolve. The initial peak in heat intensity, shown in Figure 2.4, is the corresponding dissolution heat. After dissolution slows down, a dormant period, also called induction period, of various length takes place. There is almost no precipitation of solid reaction products during this period of time, which prevents concrete from stiffening. There have been multiple explanations to this phenomenon, e.g. buildup of thin layers of reaction products on the

cement grains, inhibiting temporarily the reaction has been proposed, e.g. *Gartner & Jennings 1987* and *Bullard et al 2011*. Another explanation is a temporary lack of nucleation sites for precipitation of C-S-H and ettringite causing the slowdown of dissolution due to saturation. The dissolution however doesn't stop which eventually causes the solution to go to a supersaturation state and further causes creation of enough of nucleation sites to transfer the entire reaction process into acceleration, e.g. *Juilland et al 2010* and *Bullard et al 2011*.

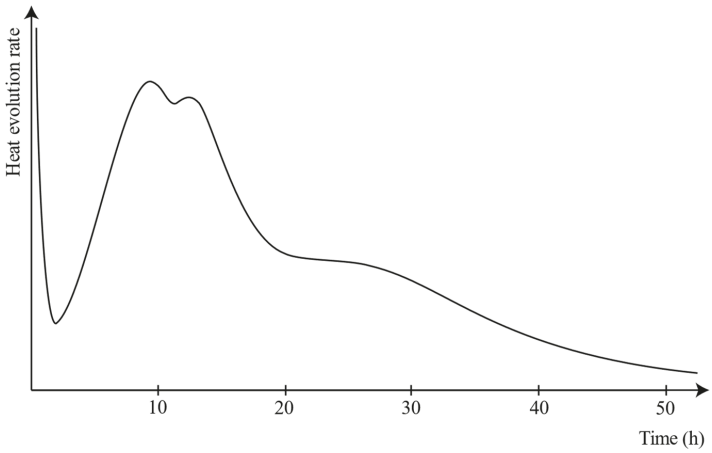

Figure 2.4, Overview of typical evolution of hydration heat rate for OPC, after various authors.

After the dormant period, the acceleration of the hydration takes place leading to the main reaction intensity peak, shown in Figure 2.4. The clinker material mainly responsible for this is alite, due to its high reactivity and large amount present. During this period the concrete sets and starts to grow significantly in strength. This is also accompanied by chemical binding of significant amount of water and the first part of the development of the pore system.

Sometimes there is visible a second intensity peak just after the main one. The cause of the intensity peak is a secondary dissolution of calcium aluminate, *Bullard et al 2011*. Initially the dissolution rate of calcium aluminate in presence of sulfate ions is decreased after some time. When all the sulfate ions from gypsum are consumed, the dissolution increases again which corresponds to the secondary peak. Various explanations to the delay has been proposed involving formation of layers on the aluminate grains that slow down the dissolution, e.g. by temporary adsorption of sulfate ions. Depending on the hydration temperature as well as the composition of the clinker this peak may sometimes be too low to be noticed against the intensity of silicate reactions.

After the main hydration peak a general decline in the total intensity of the clinker reactions takes place. Here the intense reaction of alite is successively replaced by the slower reaction of belite. The decline is also caused by decline in availability of clinker, water and possible precipitation surface, due to consumption of these in the hydration reactions.

Regarding simulation of temperature development from casting, the heat generated during dissolution is normally not of modeling interest. Before the concrete is casted on site it will be

subject to internal heat development as well as heat exchange with surroundings during transport. This is difficult to describe adequately for a general simulation. A more stable and practical starting point for a simulation is casting temperature, i.e. the temperature of the concrete immediately after being poured into formwork. This temperature is usually also measured on site.

During the decline of the main reactions another small and not especially distinctive peak in intensity of heat generation may be observed. This corresponds to transition of ettringite to monosulphate phase and the second stage of the reaction pattern of aluminates and ferrites in the presence of gypsum.

2.1.2.3 Addition of Supplementary Cementitious Materials

Supplementary cementitious materials exhibit a behavior different from OPC and depending on which SCM is considered, *Lothenbach et al 2011*. Summarizing the key aspects of their behavior, SCMs alter the total hydration reaction mainly in three ways:

- Diluting the clinker concentration and reaction
- Adding own reactions
- Interfering with or affecting clinker reaction

Effect 1 in Figure 2.5 concerns changes to the dormant period. The dilution of the clinker, caused by all SCMs, tends to prolong this period – the more dilution the longer the period. Addition of small particles that can act as nucleation sites helps to shorten it.

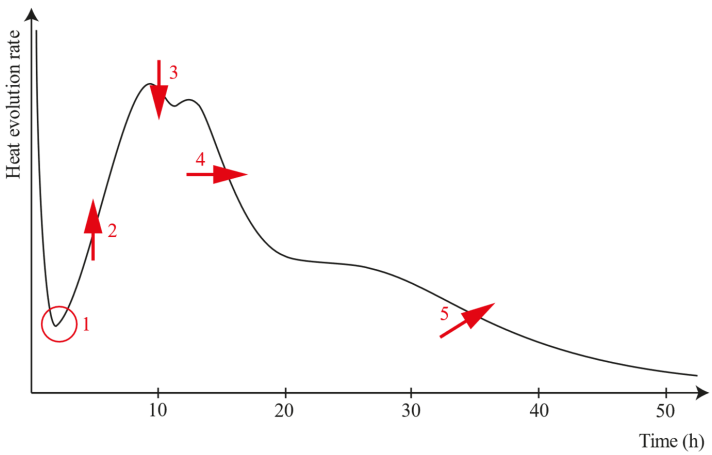

Figure 2.5, Examples of influence of SCM:s on the hydration of OPC. For details, see text.

Effect 2 in Figure 2.5 is a possible further acceleration of the acceleration period. Presence of more nucleation sites contributes to this as well as interference from fast reacting silica fume.

Effect 3 in Figure 2.5 is a general lowering of the overall intensity of reaction. This is the most common effect due to dilution of clinker and the fact that all SCM:s more or less relay on the clinker reaction or are less reactive themselves.

Effect 4 in Figure 2.5 is common for slag. The presence of hydraulic CaO interfere with silicate reactions of clinker and tend to prolong the lowered main peak area in time.

Effect 5 in Figure 2.5 is the late pozzolanic reaction. This can go on for long time and result in late generation of heat, chemical binding of water and growth of strength after the clinker reaction has basically stopped. This is very typical for fly ash.

2.1.2.3.1 Comparison of SCM Reaction Kinetics

As mentioned earlier, the SCMs have varying reactivity. This difference is clearly seen also when studied as a part of concrete with clinker as the dominating binder. In Figure 2.6 a comparison is given for the degree of pozzolanic reaction for three different blends. As clearly seen, silica fume is the most reactive and fly ash the least.

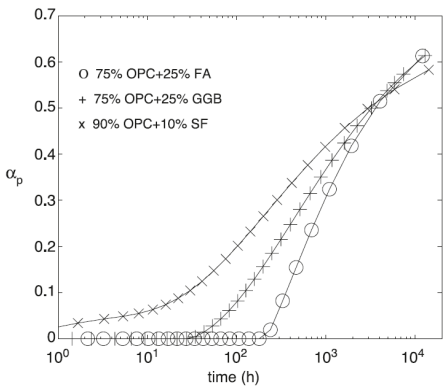

Figure 2.6, Degree of pozzolan reaction for three blends of OPC and SCM:s, from Pane & Hansen 2005.

How a specific blend between clinker and a SCM behaves is not only dependent on the choice of SCM, the amount of it and the chemical composition of both clinker and the SCM. A common practice in industry is to compensate for the lost total reactivity, due to dilution of OPC, by finer grinding. This applies to OPC and possible to the manufacturing process of the slag. Silica fume has already a very large specific surface and grinding of fly ash would destroy the spherical shape of the particles, contributing to workability of the final concrete. Increasing the specific surface of the cement will speed up the initial reaction, as it's a common technique in production of fast hardening cements.

2.1.2.4 Availability of the reactants

Availability of the reactants is a key factor in the kinetics of hydration. As mentioned earlier, the formation of hydration products has been shown to take place both inside (inner product) and outside (outer product) the cement grains. Formation of the outer product is based on dissolution of cement in water and precipitation in the space between the cement grains, e.g. on the surface of a cement or aggregate grain. Formation of the inner product assumes transport of water into and chemical binding of it inside a partially dissolved cement grain. At the start of hydration both can occur easily due to immediate contact between cement and water. As the reaction proceeds, a layer of reaction products builds up around the unhydrated

part of cement grains and continuation of the reaction is based on transport of unhydrated cement and water through that layer. The reaction in its later stage becomes affected by mobility of the reactants.

Whether the cement or the water becomes a limiting factor depends on their proportions. For OPC-dominated binder combinations, it is generally accepted that there is a limit around water-cement-ratios 0.38-0.4. For w/c-ration above that limit the cement is the limiting factor. Below the limit, water acts as a limiting factor. When availability of water limits hydration, all blending water doesn't become chemically bounded, *Mjörnell 1994*. There will still be both moisture and water left in the pore system of the concrete. Depending on the structure of the pore system, there will be pores without condensed water – typically larger pores with larger openings. Presence of water as vapor or as few molecules adsorbed to the surface of the inside of the pore is not enough to support further hydration.

Another scenario proposed by *Bullard et al 2011* is the availability of space for formation of reaction products. If a pore is simply not large enough, the reaction will not occur despite presence of condensed water.

2.1.2.5 Temperature dependency of reaction speed

Another important aspect contributing to the kinetics of hydration is its temperature dependency. In the case of an exothermal reaction, there is an energy barrier to be overcome before reactants can form products, see Figure 2.7.

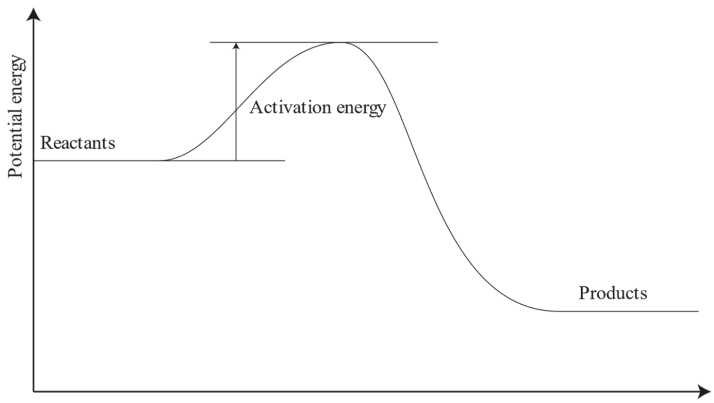

Figure 2.7, Activation energy barrier for an exothermic reaction.

Through use of the Boltzmann distribution to describe the temperature dependency of the distribution of energies among molecules of the reactants, one arrives at the Arrhenius equation expressing the basic temperature dependency of the rate constant for the reaction in question, see equ. (2.7).

$$k_r = Ae^{-E_a/RT} \tag{2.7}$$

where

k_r – is the rate constant

A – is an adaptation parameter

E_a – is the activation energy [J/mol]

R – is the gas constant [J/K mol]

T – is the absolute temperature, [K]

Hydration of cement is exothermic and has activation barriers, however it consists of not one but many reactions with different characteristics and different activation energies. This complexity of temperature dependency requires a more complicated description, which has been successfully done by use of Arrhenius equation with an activation energy that changes with temperature, see further section 2.1.3.6.

2.1.3 Earlier models of maturity, hydration and connected properties

Modeling of hydration and its results starts with an interest in strength growth. The earliest attempt to take the hydration temperature as a factor can be found in *McDaniel 1915* with results presented as diagrams. The first model explicitly taking time and temperature into consideration was presented in *McIntosh 1949*. Further research *Nurse 1949* and model development *Saul 1951* resulted in the Nurse-Saul maturity function. A more detailed history of the modeling development can be found in *Fjällström 2013*.

In general one can subdivide modeling of hydration in concrete into two groups. The first tries to describe the state of the concrete by preferably only one variable or at most a very few. Here, the earlier maturity functions or some general degree of hydration come typically to use, see further sections. Due to the complexity of chemical reactions involved and their various sensitivities, this level of modeling has a limited capacity to cover all known phenomenology in the area.

As a result of development in both measurement methods as well as in computers and simulation capability, greater insight into chemistry of hydration has been achieved together with more detailed models of various aspects of hydration, *Lothenbach & Winnefeld 2006*. This forms the second group of models, where thermodynamics and kinetics on molecular level are a key part in modeling and allow simulations taking into account various details not possible to model in the first group, e.g. specifics of binder compositions.

There are applicational advantages and disadvantages with models of both groups. The more detailed modeling is applied, the more information can be simulated, which is positive. On the other hand, this requires more detailed input, i.e. more measurements of material properties, and more computation power simulations. Due to the level of modeling identified in the formulated research problems in section 1.8.1, the second group of modeling is considered to be too detailed for the purpose of this work. The following section will focus on the first group, i.e. the macro-scale models used today.

2.1.3.1 Temperature equivalent time of maturity

The maturity measure that is most commonly used today in industry is the temperature equivalent time of maturity, initially proposed by *Freiesleben Hansen & Pedersen 1977*. Its definition is given below, see equ. (2.8).

$$t_e(t) = \Delta t_{e,0} + \int_0^t \beta_T \beta_\Delta d\tau \quad (2.8)$$

where

$t_e(t)$ – is the equivalent time of maturity [h]

$\Delta t_{e,0}$ – is the equivalent time of maturity at start, [h]

β_T – is the temperature factor [-]

β_Δ – is a general constant speed factor [h]

Defined this way time of maturity is a maturity measure that is different from the degree of hydration. However, it is used as a "working replacement" and many other properties of the young and old concrete are connected to it by used models. In order how it works, a closer look is needed at its constituents. The definition of the temperature factor was proposed by *Freiesleben Hansen & Pedersen 1977* and is given in equ. (2.9).

$$\beta_T = exp\left[\frac{E_a}{R}\left(\frac{1}{T_{ref}+273} - \frac{1}{T+273}\right)\right] \quad (2.9)$$

where

T_{ref} – is a reference temperature normally chosen to 20 [°C]

T – is temperature [°C]

By this definition, the factor is an Arrhenius type of temperature dependency for kinetics of the reaction, related to a reference temperature, i.e. by definition 1 at 20 °C. The activation energy is as earlier mentioned, temperature dependent, which was proposed by *Jonasson 1984* and is given by equ. (2.10).

$$\frac{E_a}{R} = \Theta = \Theta_{ref}\left(\frac{30}{T+10}\right)^{\kappa_3} \quad (2.10)$$

where

Θ_{ref} – is an adaptation parameter that can be interpreted as an activation temperature [K]

κ_3 – is an adaptation parameter [-]

The factor β_Δ together with the starting value $\Delta t_{e,0}$ are normally set to 1 resp. 0 but sometimes are used to shift the kinetics of the reaction to model the effects of accelerating or retarding admixtures.

This form is frequently used as a description of the maturity development during hydration and a lot of other parameters, as shown in subsections later, base their modeling on it. It can be assumed to work well during the early phase of hydration, when the temperature seems to be the main controlling factor for the kinetics, i.e. during the acceleration period. The induction period can be modelled to a certain degree by use of the starting value. However, the main problem with this definition is that the equivalent time of maturity continues to

growth infinitely with time. It is simply a clock with a temperature dependent speed. Thus, it is not a property that can be regarded as equivalent in some general sense to the degree of hydration or describing hydration other than partially. As it can be seen from the definitions of some hydration dependent properties in the later sections, all models based on temperature equivalent time of maturity have to deal with the problem of infinite growth of it with time and provide their own mechanism for stopping of growth of their own values.

2.1.3.2 Degree of hydration

2.1.3.2.1 Definitions of degree of hydration

The fundamental definition of the degree of hydration is related to the amount of cement that has hydrated, see equ. (2.11).

$$\alpha_C(t) = 1 - \frac{C(t)}{C(0)} \tag{2.11}$$

where

$\alpha_C(t)$ – is the degree of hydration, as a function of time, based on consumed cement, [-]

$C(t)$ – is the cement content, as a function of time, [kg/m^3]

As measuring the true cement contents is not as simple as measuring generated heat or chemically bounded water, two more definitions has been and are used, see equ. (2.12) and equ. (2.13), based on ratios between generated heat and generated heat when all cement is hydrated and similar for chemically bounded water.

$$\alpha_{C,W}(t) = 1 - \frac{w_{Ch}(t)}{w_{Ch}(t:C(t)=0)} \tag{2.12}$$

$$\alpha_{C,H}(t) = 1 - \frac{Q_H(t)}{Q_H(t:C(t)=0)} \tag{2.13}$$

where

$\alpha_{C,W}(t)$ – is the degree of hydration, as a function of time, based on chemically bounded water, [-]

$\alpha_{C,H}(t)$ – is the degree of hydration, as a function of time, based on generated heat, [-]

As findings in *Gallucci et al 2013* imply the amount of chemically bounded water for the same degree of hydration can vary significantly. This puts in question both measurements based on this assumption as well as models. It is also reasonable to raise the same question for the heat based definition. Varying amount of water molecules being bounded in the C-S-H phase, i.e. entering a different, more stable and lower energy state than as condensed water, will most probably affect the enthalpy of the reaction and make it temperature dependent.

2.1.3.2.2 Modeling of degree of hydration

The modeling of the degree of hydration has been connected to the equivalent time of maturity. One way was proposed by *Byfors 1980* and adjusted by *Jonasson 1984*, see equ. (2.14).

$$\alpha_C = exp\left[-\lambda_1 \left(ln\left(1+\frac{t_e}{t_1}\right)\right)^{-\kappa_1}\right] \tag{2.14}$$

where

λ_1 – is an adaptation parameter, [-]

t_1 – is an adaptation parameter, [h]

κ_1 – is an adaptation parameter, [-]

Another one is found in *Freiesleben Hansen 1978* and *Freiesleben Hansen and Pedersen 1984*, see equ. (2.15).

$$\alpha_C = exp\left[-\left(\frac{t_2}{t_e}\right)^{\kappa_2}\right] \tag{2.15}$$

where

t_2 – is an adaptation parameter, [h]

κ_2 – is an adaptation parameter, [-]

It should be observed that both models simply propose curves that fit experimental data without further interpretation of the involved parameters. They also make use of exponential functions with negative arguments approaching zero as the time of maturity grows. This is the beforementioned necessity of implementing a stopping mechanism when temperature equivalent time of maturity is used as a variable.

2.1.3.3 Compressive strength

There has been a number of models trying to express the strength development in concrete. The mostly used approach is based on time or equivalent time of maturity, e.g. *Byfors 1980* and *Carino 1982*. The currently used model in Eurocode is given by equ. (2.16).

$$f_{cc} = f_{cc,28d} exp\left\{s\left[1-\left(\frac{28}{t}\right)^{1/2}\right]\right\} \tag{2.16}$$

where

f_{cc} – is the compressive strength, [MPa]

$f_{cc,28d}$ – is the 28 days compressive strength, [MPa]

s – is an adaptation parameter, [-]

t – is the age of concrete having an average temperature of 20 ºC, [days]

The more generalized version of the same formula, used currently in Sweden, is given in *Fjällström 2013*, where time has been replaces by the temperature equivalent time of maturity and a small modification has been introduced for ages before final setting in order to be able to model the early strength more precisely for calculation of surface treatment times.

The common property of all these is that they are based on a simple expression of the state of concrete without taking under consideration which temperature history that brought the concrete in question to the specific value of equivalent time of maturity or degree of hydration. However, it has been observed that high curing temperatures may cause a sometime considerable degradation in strength. The earliest observations date to the time of planning of the Hooved dam, *Davis et al 1933*, followed by other partial observations *Saul 1951* and *McIntosh 1956*. The so called cross-over effect in strength was fully demonstrated for temperature between -4 and 49 °C by *Klieger 1958*. Since late 1980-ies there has been a development of various models reducing the strength based on the temperature. The model used currently for concrete hardening simulation in Sweden was developed by Jan-Erik Jonasson and is described in Fjällström 2013:

$$f_{cc} = f_{cc,ref} - \gamma_{drop}\, \Delta^{max}_{drop,28d}\, f_{cc,28d} \tag{2.17}$$

where

$f_{\mathrm{cc,ref}}$ – is the reference strength calculated as above without any reduction, [MPa]

$\Delta^{max}_{drop,28d}$ – is an adaptation parameter giving maximum reduction factor at 28d, [-]

γ_{drop} – is a current relative reduction factor (0-1), [-] given by:

$$\gamma_{drop} = \frac{\delta_{drop}}{\delta_{ref}} \tag{2.18}$$

where δ_{drop} and δ_{ref} are current and maximum reduction respectively:

$$\delta_{drop} = \int_0^{t_e} \gamma_{Temp}\gamma_{Time}\, \frac{d\alpha}{dt'_e}\, dt'_e \tag{2.19}$$

$$\delta_{ref} = \int_0^{672h} \gamma_{Time}\, \frac{d\alpha}{dt'_e}\, dt'_e \tag{2.20}$$

based on reduction functions of temperature and age:

$$\gamma_{Temp} = exp\left[-\left(\frac{T}{Temp_D}\right)^{-\kappa_{Temp}}\right] \tag{2.21}$$

$$\gamma_{Time} = exp\left[-\left(\frac{t_e}{time_D}\right)^{-\kappa_{Time}}\right] \tag{2.22}$$

where

$Temp_D$ – is an adaptation parameter, [ºC]

κ_{Temp} – is an adaptation parameter, [-]

$time_D$ – is an adaptation parameter, [h]

κ_{Time} – is an adaptation parameter, [-]

The strength reduction model above is clearly an empirical construct. It is based on an idea of accumulation of strength loss due to temperature over the duration of the hydration process. It has also the possibility to adjust to some degree how strong the temperature impact will be depending at which age of concrete it occurs. It is intended to fit the measurement data.

2.1.3.4 Heat of hydration

Modeling of heat of hydration is generally based on the assumption of proportionality to the degree of hydration, compare with equ. (2.13). By use of this and some of the models of the degree of hydration results in equ. (2.23).

$$Q_H = \alpha_C Q_{H,max} C \tag{2.23}$$

where

$Q_{H,max}$ – is the heat generated at full hydration per amount of cement, [J/kg]

α_C – is the degree of hydration, calculated by use of equ. (2.14) or equ. (2.15), [-]

C – is the cement content [kg/m^3]

There is discussion about the correspondence between the maximum value of the heat of hydration adapted to measurements of specific heat developments, its material based final value and the fact that the maximum degree of hydration not always reaches the value of 1, *Mills 1966* and *Jonasson 1994*.

2.1.3.5 Chemically bounded water

The general modeling of chemically bounded water is also based on the degree of hydration and the assumption of equ. (2.12). This was initially stated in *Powers & Brownyard 1948* and is expressed by the equ. (2.24).

$$w_{Ch} = \zeta \alpha_C C \tag{2.24}$$

where

ζ – is a proportion factor describing how much water get bounded per kg of hydrated cement, [-]

Typical values for ς in literature vary between 0,19 and 0,25 and the variation is assumed to reflect the varying properties of the cement. There is in general no indication of a temperature dependency despite findings in *Gallucci et al 2013*.

2.1.3.6 More general equivalent time of maturity

Attempts have been made to extend the dependencies of the maturity measure beyond temperature. One example is given in *Liao et al 2008*, where a moisture dependency is

introduced and calibrated to measurements of strength. However, a more interesting and wider generalized approach is given in *Mjörnell 1997*. A model for time of maturity and degree of reaction for two binders, OPC and silica fumes, in parallel is formulated. Below, a version of this model for only one binder will be presented and discussed. The key idea is that two additional factors governing the growth of the time of maturity are introduced, see equ. (2.25).

$$t_e(t) = \Delta t_{e,0} + \int_0^t \beta_T \beta_\varphi \beta_\alpha \beta_\Delta d\tau \qquad (2.25)$$

where

β_φ – is the moisture content factor [h]

β_α – is the factor dependent on degree of hydration [h]

The moisture factor is a limiting factor between 0 and 1. Its definition is further given as:

$$\beta_\varphi = d^x \qquad (2.26)$$

where

d – proportion of capillary pores filled with water, [0-1] [-]

x – is an adaptation parameter [-]

A formula for calculation of d is also proposed. It's based on an isotherm and assumptions that the isotherm and the proportional amount of water in the gel pores are not temperature dependent and that the chemically bounded water is only a function of the degree of hydration. These assumptions, as mentioned earlier, can be questioned on base of findings in *Gallucci et al 2013*, however the idea of dependence on the availability of the condensed water in the pore system seems definitely reasonable.

The degree of hydration factor is meant to limit the growth of the time of maturity due to phenomena such as lower amount of cement available, larger mobility challenge for cement and water to penetrate the layers of reaction products around the unhydrated cement and smaller amount of space available, where only the last phenomenon is mentioned in *Mjörnell 1997*. The following formula for the factor is proposed.

$$\beta_\alpha = \left(\frac{\alpha_{C,max} - \alpha_C}{\alpha_{C,max}}\right)^a \qquad (2.27)$$

where

$\alpha_{C,max}$ – the maximum degree of hydration, [-]

a – is an adaptation parameter [-]

Use of the maximum degree of hydration as a limiting parameter allows capturing by the model that not all cement in some mixtures will hydrate. This formula makes use of the degree of hydration that is calculated by use of equ. (2.14).

In the opinion of the author of this thesis, there are two main problems with the proposed model and the proposed adaptation of parameters. The first problem is connected to multiple stopping mechanisms. The proposed factors β_φ and β_α will act limiting on the growth of the time of maturity and have the capacity to stop it completely. This is a conscious intention in order to capture the phenomenology behind. At the same time, the used formula for the degree of hydration assumes an infinitely growing time of maturity as input. It also implements its own stopping by used of exponential function with negative argument approaching zero as the time of maturity grow, as mentioned in section 2.1.3.2.2, without mathematically separating causes for the hydration to slow down and stop. This implies that the proposed model runs two mechanisms on separate levels, both intended to model the same phenomenon in some sense.

This overlapping of responsibility for modeling causes a challenge in adaptation of data. In *Mjörnell 1997* it is stated that the parameters for the equation describing the degree of hydration are "obtained by fitting the Equations 2.5 and 2.6 to probable development of degrees of reactions of cement and silica fume of a hypothetical composition in which all cement becomes hydrated and all silica fume reacts", equation references pointing to equivalents of equ. (2.14) for respective binder. No further details on this adaptation nor its results, i.e. the values of the adapted parameters, are presented in the work. This incompleteness in description of the method makes it impossible to use or verify as it is described.

The second problem of the proposed model and adaptation method is more of a structural or mathematical character. As seen, this model of the equivalent time of maturity builds on the idea that the influences of these factors are separable, i.e. the rate of change can be modeled as a product. This assumption is clearly stated in on page 6 in *Mjörnell 1997*. It is then further used in order to capture the dependency of the modeled hydration on temperature, moisture and space/binder-related phenomenology separately. The temperature dependency for cement reaction is referred to parameters that can be found in literature, where there were adapted to measurements without taking the other dependencies into consideration. Measurements and adaptation of parameters for the other two dependencies are performed separately. However, the definition of β_α as a function of the degree of hydration, having at the same time the degree of hydration defined as a function of the time of maturity that depends on $\beta_\alpha$is a clear circular dependency. This makes the assumption that β_α will be independent of the two other limiting factors invalid. As consequence of this the assumption about the independence between the factors will be invalid. It cannot be used to claim validity of the combined adapted results, where the dependencies were captured by measurements and parameter adapted independently of each other.

2.2 Sorption of moisture

Various mechanisms can be used to store water molecules in a porous solid. Strong chemical bonds, as in form of OH^-, as well as slightly looser, so called interlayer water are normally associated with chemically bounded water and were already described preceding sections. Here, the two remaining, adsorption and capillary condensation will be discussed together with the properties of the pore system in which they take place.

2.2.1 Adsorption

Adsorption is the phenomenon of loose attachment of gas or vapor molecules on a surface of a solid. It occurs due to lack of thermodynamic equilibrium between the empty surface and the gas or vapor. There is a dynamic process of molecules attaching to the surface and of molecules detaching and leaving it. The equilibrium is achieved by balancing these two changes, resulting in a constant average amount of gas or vapor adsorbed on a surface under specific conditions, partial pressure of gas or vapor and temperature.

A typical way of describing the effect of adsorption at constant temperature is by an isotherm. It is a curve describing the relation between the gas/vapor potential, e.g. partial pressure or content, and the amount of attached gas/vapor, e.g. volume or weight. *Brunauer 1945* identifies five principal types of isotherms, based on their shapes.

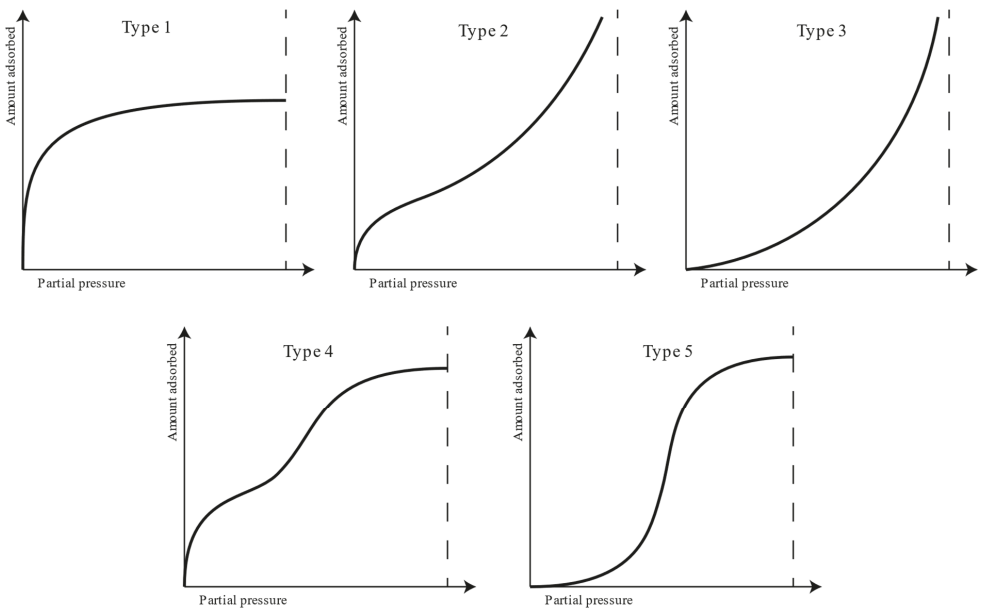

Figure 2.8, Brunauer's five types of adsorption isotherms, after Brunauer 1945.

2.2.1.1 Models

2.2.1.1.1 Langmuir

The simplest model for an adsorption isotherm was initially given by *Langmuir 1918*. It describes adsorption of molecules in only on layer on a surface – monolayer adsorption, see Figure 2.9.

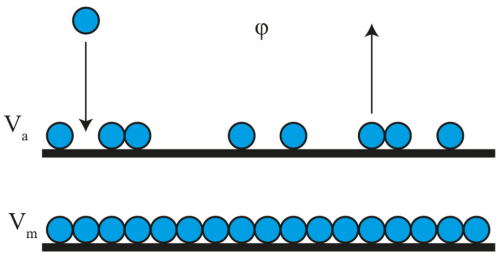

Figure 2.9, Monolayer adsorption.

It is based on the general idea of thermodynamic balance between the attaching and detaching molecules and relates their relative amounts to the partial pressure of the gas/vapor. The model equation is given in equ. (2.28).

$$V_a = \frac{b\varphi}{1+b\varphi} V_m \qquad (2.28)$$

where

V_a – is the amount of adsorbed gas/vapor, [m^3] or [kg] same as V_m

V_m – is the total possible amount of adsorbed gas/vapor adsorbed in the monolayer, [m^3] or [kg] same as V_a

b – is an adaptation parameter [-]

The Langmuir isotherm is of the type 1 according to the Figure 2.8. Its applications are limited due to the fact that in most practical cases the adsorption takes place in more than only one layer, as it does in concrete. It is however used in the lower regions of the relative gas/vapor potential in order to calculate the monolayer capacity from sorption measurements.

2.2.1.1.2 BET

A considerable extension of the Langmuir isotherm is the BET isotherm, presented in *Brunauer, Emmett & Teller 1938*. It is based on similar assumptions as the Langmuir. However it describes adsorption in not just one but multiple layers, see Figure 2.10.

The first layer is strongly bound. The higher layers assume bonding equivalent to condensed phase. The model equation of this isotherm is given by equ. (2.29).

$$V_a = \frac{b\varphi}{(1-\varphi)(1+b\varphi-\varphi)} V_m \qquad (2.29)$$

This isotherm is capable of describing of both type 2 and 3 from Figure 2.8 and is used more frequently than Langmuir.

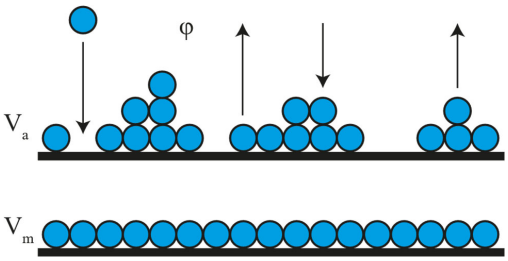

Figure 2.10, Multilayer adsorption.

2.2.1.1.3 Dent

Another important and useful isotherm for the multilayer case was proposed by *Dent 1977*. Here two different bonding energies are assumed for the first and the higher layers, but presence of two adaptation parameters in the equation allows for explicit control of both. The model is described by equ. (2.30).

$$V_a = \frac{b_0\varphi}{(1-b\varphi)(1-b\varphi+b_0\varphi)}V_m \qquad (2.30)$$

where

b_0 – is an adaptation parameter [-]

There is a larger range of applications for the Dent isotherm, which was initially developed by to the poor fitting to experimental data by Langmuir and BET isotherms.

2.2.1.2 Temperature dependency

Due the thermodynamic base of the equations in Langmuir, BET and Dent isotherms, there is a possible interpretation of the adaptation parameters involving a temperature dependency. Due to the limited use of Langmuir, the temperature interpretation for this isotherm is skipped. For BET the adaptation parameter can be interpreted according to equ. (2.31).

$$b = ce^{(E_1-E_l)/RT} \qquad (2.31)$$

where

E_1 – is the heat of adsorption for the first layer [J/mol]

E_l – is the heat of liquefaction [J/mol]

c – is an adaptation parameter[-]

For Dent the adaptation parameters can be interpreted according to equ. (2.32) and equ. (2.33).

$$b_0 = e^{-\Delta G_0/RT} \qquad (2.32)$$

$$b = e^{-\Delta G/RT} \qquad (2.33)$$

where

ΔG_0 – is the free energy of the primary adsorbed molecules [J/mol]

ΔG – is the free energy of the secondary adsorbed molecules [J/mol]

This enables further interpretation of the dependency by equ. (2.34) and equ. (2.35).

$$ln\, b_0 = \left(\frac{\Delta S_0}{R}\right) - \left(\frac{\Delta E_0}{R}\right)\left(\frac{1}{T}\right) \quad (2.34)$$

$$ln\, b = \left(\frac{\Delta S}{R}\right) - \left(\frac{\Delta E}{R}\right)\left(\frac{1}{T}\right) \quad (2.35)$$

where

ΔS_0 – is the entropy difference from the condensed liquid for the primary sites [J/mol K]

ΔS – is the entropy difference from the condensed liquid for the secondary sites [J/mol K]

ΔE_0 – is the heat of sorption difference from the condensed liquid for the primary sites [J/mol]

ΔE – is the heat of sorption difference from the condensed liquid for the secondary sites [J/mol]

This enables a possible adaptation of these isotherm models to measurements where not only the vapor potential is varied but temperature as well, giving adsorption models that can be used in non-isothermal conditions.

2.2.1.3 Geometric constraints

One disadvantage on the existing adsorption models is the fact that they assume a flat adsorption surface as a geometry. This implies that the maximum size of the layers is the same for all the layers. This will not be the case of the adsorption surface is curved. Depending on the curvature the layers can increase or decrease in size, see Figure 2.11.

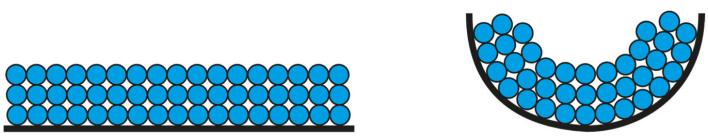

Figure 2.11, Comparison of adsorption layers on flat surface and a surface curved inward.

In concrete, as discussed later in section 2.2.3.2, there is a considerable volume of gel pores with sizes comparable to a few water molecules. This implies presence of significant curvature that will affect the layer capacity. Due to the geometrical fact that the curvature has to form closed cross-sections, the capacity of each higher layer will be smaller than for the layer closer to the surface. Only in large pores, the effect of the surface curvature will be small. Unfortunately, this property of small pores is not accounted for in the isotherm models.

2.2.2 Capillary condensation

Beside adsorption, capillary condensation is responsible for physical storage of water in the pore system of concrete and other cement-based materials. This section gives a brief explanation of the phenomena and its dependencies. It also presents an investigation of a few situations that can occur in a pore system and draws some practical conclusions.

2.2.2.1 Thermodynamic basis

Capillarity is based on a combination of two types of interaction. The first one concerns a liquid, in this case water, and a solid, in this case concrete, in contact with each other. The type of contact is characterized by the solids resistance to wetting by the liquid – in case of water and cement how hydrophilic or hydrophobic concrete is. This is governed by a balance of cohesive forces, holding a substance together with itself, and adhesive forces, holding the liquid and solid to each other. A variety of cases illustrating this is shown in Figure 2.12.

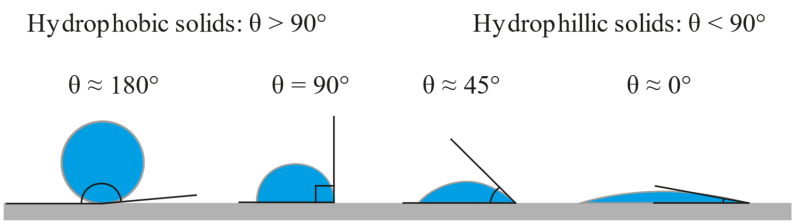

Figure 2.12, Various angles of contacts between a liquid and a solid.

The angle of contact is usually taken as a measure of how hydrophilic ($\theta < 90°$) or hydrophobic ($\theta > 90°$) a material is. Cement-based materials are considered very hydrophilic, so that the angle of contact in calculation is most often assumed to be zero.

The other key interaction behind capillarity is between the liquid and the gas/vapor. The molecules inside of the condensed phase have other molecules in close vicinity from all sides attracting each other. Molecules on the surface of the liquid lack neighbors on the gas/vapor side of the surface, experiencing a net force pulling them into the liquid, i.e. away from the surface. This force is commonly referred to as surface tension and is typically dependent on the type and the temperature of the liquid.

Putting these two phenomena together gives raise to capillarity. This is illustrated in Figure 2.13.

The surface tension will cause a force on the meniscus from the walls of the tube, depending on the contact angle. In order to keep the meniscus in mechanical balance, a negative capillary pressure, i.e. suction, will form and deliver a counteracting force on the meniscus. The balance of these two, assuming zero angle of contact, gives the famous Young-Laplace equation covering different meniscus shapes, as shown in Figure 2.14.

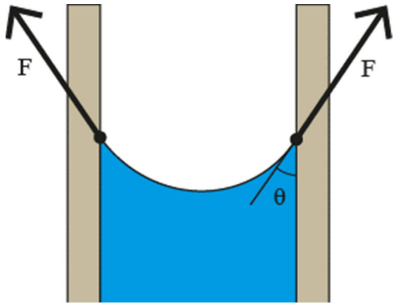

Figure 2.13, Capillarity illustrated by a water meniscus in a tube.

$$-p_c = \frac{2\sigma}{r_c} = \sigma\left(\frac{1}{r_1} + \frac{1}{r_2}\right) \tag{2.36}$$

where

p_c – is the capillary pressure [Pa]

σ – is the surface tension [N/m]

r – are the meniscus radii according to Figure 2.14 [m]

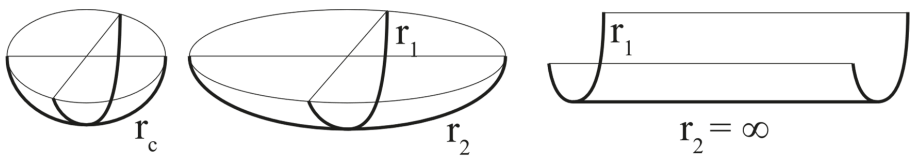

Figure 2.14, Radii for different shapes of a meniscus

This further combined with the Kelvin equation, see equ. (2.37),

$$p_c = \varrho_w R_v T \, ln(\varphi) \tag{2.37}$$

results in an equation sometimes referred to as YL-K equation, describing a relation between the relative humidity, temperature and the pore radius, see equ. (2.38) or equ. (2.39).

$$ln(\varphi) = -\frac{2\sigma}{r_c \varrho_w R_v T} \tag{2.38}$$

$$r_c = \frac{2\sigma}{-\varrho_w R_v T \, ln(\varphi)} \tag{2.39}$$

For water this relation is visualized in Figure 2.15,

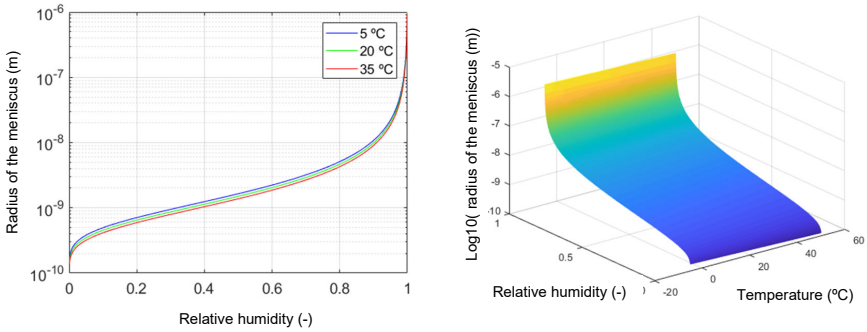

Figure 2.15, Relation between the meniscus radius of capillarity and relative humidity and temperature, left – curves of radius as a function of relative humidity for different temperatures, right – surface plot of 10-logarithm of the radius as a function of both relative humidity and temperature.

In a pore system, the meniscus radius is normally connected to a certain pore size and defines which part of the pore system is filled under which conditions, characterized by temperature and relative humidity. The characterization of the state by a momentaneous value of temperature and relative humidity is not sufficient to describe what part of the pore system is filled due to hysteresis, which is described further in section 2.2.2.2. However, let's for now put aside the hysteresis in order to visualize a more fundamental way how the relation in equ. (2.39) works in practice in a pore system in concrete.

Assuming a balance between the three variables, a certain part of the pore system is filled with water under certain temperature and humidity conditions. Given this there are three fundamental change scenarios, one for each variable in the relation:

- **A uniform change in temperature** will result in some water molecules changing phase in order to keep the meniscus forces in balance. This is partially due to the direct temperature dependence in equ. (2.39) but also to indirect dependence through surface tension and the vapor conditions at saturation. Thus, there will be a shift in relative humidity. On the other hand, the amount of water changing phase is negligible from the condensed phase point of view, which means that the change in the meniscus radius will most probably not be noticeable.
- **A change in the amount of condensed water**, resulting in change of the radius, can be supported by transport through capillary suction. In such a case a significant amount of water molecules is transported due to the fact that the transport involves the condensed phase. Assuming that there is no large temperature difference between the store and the newly transported water, i.e. no convective transport of heat, the temperature will not change significantly. The amount of heat stored in the solid part of concrete is much larger than the amount needed for smaller phase changes to correct relative humidity into balance. On the other hand, the relative humidity will have to change in order to keep the meniscus forces in balance.
- **A change in relative humidity**, can be caused by vapor diffusion in the unfilled pores. In such a case, a change in temperature will be insignificant by the same

reasoning as for the previous change case. In order to keep the meniscus in balance some water molecules will change state, i.e. condense or evaporate, causing a secondary counterchange in relative humidity and adjusting the condensed water in the pore a little. However, the amount of change in the radius will be very small compared to the secondary change in relative humidity and if the vapor transport does not continue, a transient change in relative humidity will be “swallowed” by the condensed water. In order to achieve a significant change in the amount of condensed water, the vapor transport has to continue. That may in turn result in a local temperature change due to the phase change heat of water.

2.2.2.2 Pore models and hysteresis

There are pore shapes that have the same behavior during drying and wetting, but there are also many pore shapes that have not, resulting in a hysteresis in behavior. Below some of the most commonly used pore shapes in modeling are shown and their behavior is presented together with a more general picture of the hysteretic behavior.

2.2.2.2.1 Ink-bottle pore

One of the popular pore models is the ink-bottle pore. The idealized version of this pore is a cylindrical pipe section with constant radius, closed in one end and having an opening in the other with a bottleneck and a radius of its own, see Figure 2.16.

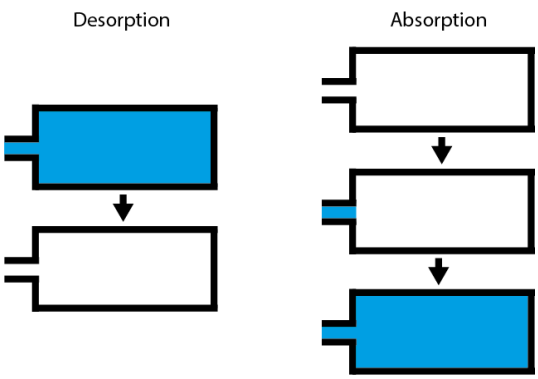

Figure 2.16, Desorption and absorption in an ink-bottle pore.

During desorption, the pore and the bottleneck are initially filled. In order to empty the pore, the bottleneck has to be emptied first. This will require a low relative humidity because the radius of the bottleneck is small. When the bottleneck is emptied the rest of the pore will be emptied as well, because if the relative humidity is too low to support a meniscus with the radius of the bottleneck it will certainly not support a meniscus with a radius of the larger pore body.

During absorption, the situation looks different. When relative humidity rises, it will first cone up to a level supporting the meniscus in the bottleneck. At that time the small volume of the bottleneck will fill, but nothing more. Due to the fact that the pore body is empty, filling of it will require formation of a meniscus with a radius of the entire pore body and at that point the relative humidity is not high enough to support it. So the rest of the pore volume remains

empty until relative humidity reaches a level supporting a meniscus with a radius of the pore body and then the entire pore is filled.

Summarizing the behavior of the ink-bottle pore, two different meniscus radii are controlling emptying and filling of the main volume of the pore. Desorption is controlled by the smaller radius of the bottleneck. Absorption is controlled by the larger radius of the pore body. This causes a hysteresis in behavior requiring at constant temperature a lower relative humidity for desorption and a higher for absorption.

One should observe that the special case of both radii being equal to each other or the opening being larger than the body will result in a behavior without hysteresis, that can also be present in a pore system.

2.2.2.2.2 Open vs closed pipe section

Presence of ink-bottle pores is not a necessity for hysteresis, which can be caused in simpler ways in cylindrical pores as well. Comparing the sorption phenomenology of a closed and an open pipe section of the same radius will give the necessary insight. The behavior of the close pipe will be the same as an ink-bottle pore with equal radii of opening and pore body, i.e. no hysteresis. The desorption behavior of the open section will also be similar with two menisci of the same radius as the pipe section. The difference here is in the absorption. When the open pipe section is empty the meniscus will have to start forming from the walls. This will result in a meniscus with the rightmost shape from Figure 2.14, where one radius is the pipe radius and the other radius is infinite. This will give a behavior for the open pipe section where the desorption is controlled by the radius of the pipe but absorption is controlled by the double radius of the pipe, compare with equ (2.36).

2.2.2.2.3 Special cases of isotherms

Hysteresis results in different behavior during wetting and drying. Trying to plot the relation between the moisture content of the material and relative humidity in isothermal conditions, i.e. drawing the isotherm, will not result in one curve see Figure 2.17.

Assuming uninterrupted drying from complete saturation to completely empty material a desorption isotherm will be obtained. Assuming uninterrupted wetting from completely empty material to complete saturation, an absorption isotherm will be obtained. Changing between desorption and absorption will put the material into so called scanning and results in a scanning isotherm.

Two additional observations regarding hysteresis are important to be made:

- As a consequence of hysteresis all moisture states between the desorption and the absorption isotherm can be possessed by the material, depending on the history of wetting/drying.
- Due to the dependency of the meniscus radius on the temperature, a change in temperature can also drive drying or wetting and put the material into scanning.

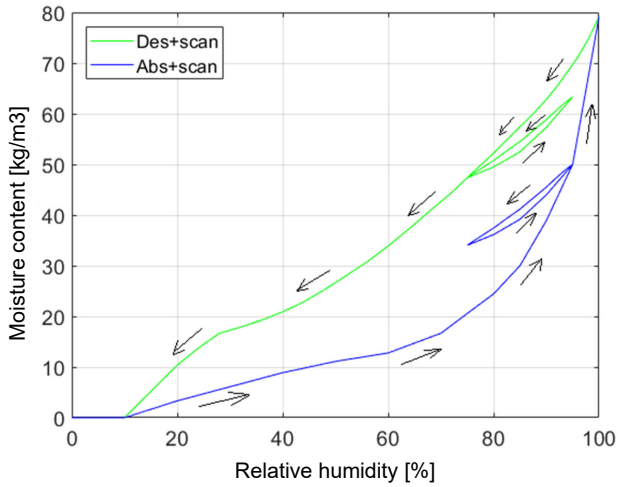

Figure 2.17, Example of isotherms for desorption (green) and absorption (blue) with scanning loops.

2.2.3 Pore structures

2.2.3.1 Porous materials

Porous materials can be found in nature, e.g. porous rocks, as well as constructed artificially, e.g. bricks and concrete. The complexity of the pore system in them can be virtually unlimited, with a large variety of unregular pores and connections in between them. Figure 2.18 gives an example of a 2-dimensional cross-section through a porous material. The present pores are not regular in shapes. The interpretation of pore body and neck and their sizes is difficult and mainly based on the principle that all bottlenecks can be interpreted as opening to pores on both sides, depending on from where the drying or filling is proceeding in the system.

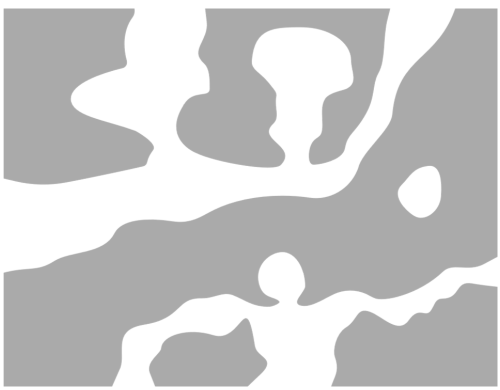

Figure 2.18, Example of an irregular pore system.

Some regularity in the pore system can be arranged in artificially constructed materials, e.g. by regular packing of same size particles, but this is more of an exception that the rule. The ideal situation with well-defined pores, unambiguous sizes and clear connections is seldom found.

An example in how such pore system can be filled with water is shown in Figure 2.19. There are adsorbed water on the walls. Some smaller pores or neck are filled with water. Some larger are empty. Some larger pores are held filled by menisci at their small necks. There is also a possibility of unconnected pores, containing a constant amount of water and not participating in changes of water content.

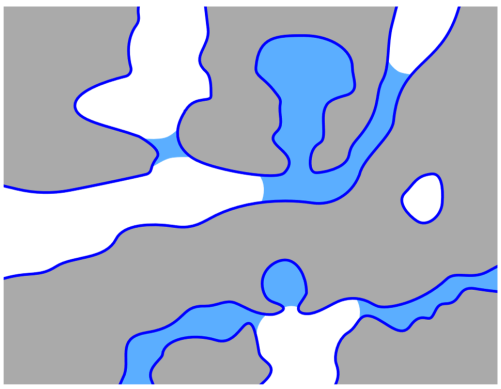

Figure 2.19, Example of water filling of an irregular pore system, with both adsorbed water on boundaries as well as capillary condensed water.

2.2.3.2 Concrete

The pore system in concrete is definitely one of the more difficult to characterize. It is formed by the walls of hydration products and aggregate. Some of the hydration products are crystalline with needle or plate-like structure resulting in significant complexity for the pores they enclose, see Figure 2.20 for example.

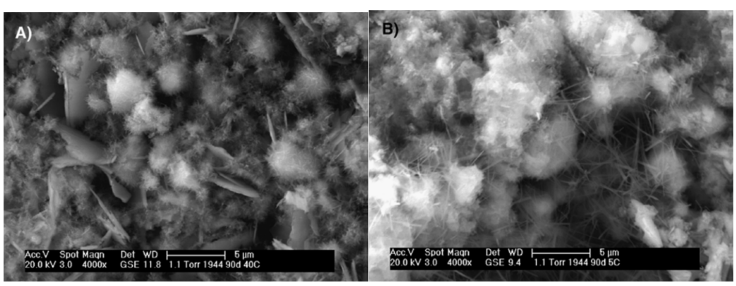

Figure 2.20, Microstructure (ESEM, fractured surfaces) of Portland-Limestone cement mortar samples hydrated for 91 days at A) 40 °C and B) 5 °C, from Lothenbach et al 2007, showing various structures (bulk, hexagonal, needle) of hydration products such as C-S-H, calcite, and ettringite.

The structure of concrete in general and especially the hydration products with main focus on the C-S-H phase is under continuous research since Powers pioneering work in the 1940-ies. There has been a number of interpretations, especially regarding C-S-H proposed lately, e.g.

Feldman & Sereda 1970, Tennis & Jennings 2000, Jennings 2008 and *Espinosa & Franke 2006*. It is not a purpose of this work to investigate these details. The necessary conclusions regarding water storage mechanisms connected to these structures are the following:

- The most strongly bounded water is present in the products as OH^- and is clearly regarded as chemically bounded.
- Many crystalline and sub-crystalline structures are formed in adjacent layers with more loosely bounded water molecules in between the layers, so called interlayer water or crystal water. This water can be removed by drying to levels < 11 % relative humidity. This water is sometimes regarded as chemically bounded because it is a direct result of the hydration reactions. It is sometime regarded as physically bounded because it can be removed by drying.
- There are pores in and between the hydration products, as well as larger voids, in which water can be adsorbed to walls as well as capillary condensed if conditions are appropriate for the size of the pore in question. All this water is considered to be physically bounded.

Investigating the pore system of concrete, the focus is on the last mechanism of water storage, i.e. the clear physical binding in the pores without the interlayer water.

In general, there is a distinction made between a few types of pores, however with ambiguous subdivision in size – varying data from varying authors. Inside the hydration products, mainly the C-S-H- gel, so called gel pores are found. These are the smallest pores in the concrete, that are considered from the moisture perspective and are normally < 5nm in size. The space between the hydration product grouped around cement grains of aggregate pieces is up to a size of around 100 nm called capillary pores. This name is a little misleading in the sense that not only capillary pores can by a place of capillary action. Large gel pores can that as well. On the other hand, the capillary action weakens considerably in larger voids and can be neglected. Growing further in size one finds air voids, that are commonly present in concrete and even larger compaction voids, i.e. places that the concrete didn't fill during compaction. Table 2.2 summarizes the pore types in concrete, the rough subdivision in sizes, possible storage mechanisms for water and connected active interval of relative humidity regarding desorption and absorption.

2.2.3.3 Bi-variate pore size distributions

Pore systems are difficult to describe. One way of doing it is the bi-variate pore size distribution, e.g. *Dullien & Dhawan 1975* and *Dullien 1992*. In its simplest form it is a matrix with different sizes of pore entries for each row and different sizes of pore bodies for each column. The matrix elements describe the pore volume for each combination of entry and body sizes. One such example is shown in Figure 2.21.

Table 2.2, Characterization of various types of pores from the point of view of physical binding of water.

Type of pore/storage	Size (approx..)	Active RH-interval (approx.)
Compacting voids	Several mm	Adsorption, almost never condensed water
Air voids	10µm-1mm	Adsorption, almost never condensed water
Capillary pores	5-100 nm	Adsorption + condensed water > 80% RF
Gel pores	< 5nm	Adsorption + condensed water 30-80% RF
(Crystal water)		E.g. 0-11% C-S-H gel, 0-30% ettringite

Such a description is probably not a perfect picture of the real pore system. However, it is useful from a functional perspective. If the sizes are interpreted as Kelvin radii, see equ. (2.39), for absorption and desorption, such a matrix gives a good description of the hydraulic properties of a pore system for calculation of water contents for any wetting/drying history.

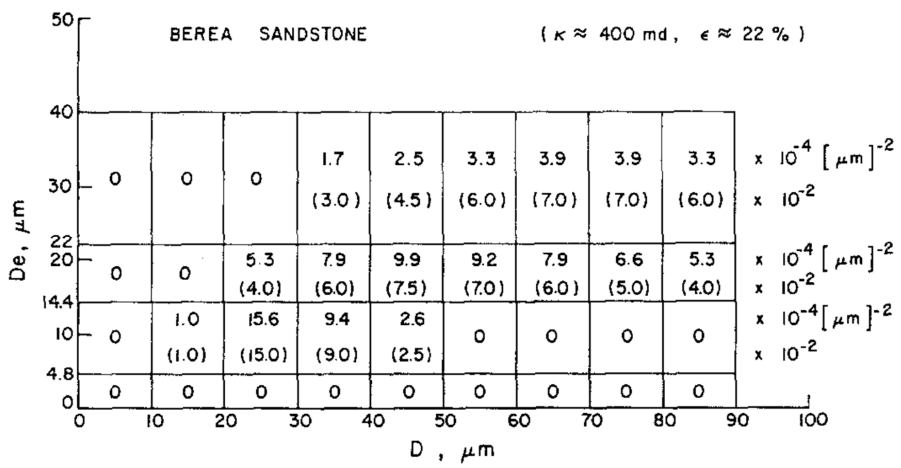

Figure 2.21, Example of a bi-variate pore-size distribution, volume density and fractional volume density in parenthesis as functions of pore diameter D and pore entry diameter De, from Dullien & Dhawan 1975.

2.2.4 Modeling

In order to describe physical binding of water in a pore system, both adsorption and capillary condensation has to be considered. Adsorption will take place on the walls of the empty pores.

This can result in filling of pores that are small enough. Otherwise, capillary condensation can fill some of the larger pores and leave some empty. Depending on the state variables and their history, there will be a combination of both phenomena defining the momentary moisture content of the pore system.

2.2.4.1 Isotherms

The simplest modeling of sorption is done by mathematically describing an isotherm. More fundamental mathematic approaches such as interpolation between measurement point, splines or curve fitting based on the shape of measured data or adaptation of one of the common adsorption isotherm models from section 0 can be used. Various attempts to base the curve form on some material reasoning has also been made, e.g. for concrete *Jonasson 1994*. The main characteristic of this approach is that the model describes only one isotherm and doesn't consider hysteresis nor temperature dependency.

2.2.4.2 Models with hysteresis

Hysteresis is a phenomenon observed in many fields and attempts to model sorption with hysteresis goes back to 1930-ies, when the first description of it was published by Haines. Even here there are empirical models, designed to fit experimental data, e.g. *Li 2005*, *Wei & Dewoolkar 2006* and *Nyman et al. 2006*. There are also conceptual models, based on assumptions of material characteristics. These are mainly adopting a domain-based approach, where sorption sites, so called domains, are the base of reasoning. These correspond normally to groups of pores. They can be dependent or independent in their behavior. Pioneering work was initially done for the independent domain modeling by *Everett 1954a*, *1954b* and *1955* and others. Due to discrepancies with experimental data further development occurred with other proposed models, e.g. *Mualem 1974* and *Derluyn et al 2012*.

The main concept of the domain based modeling is well illustrated by the model proposed by *Mualem 1974*. Here sorption sites are described by a water distribution function $f(\bar{r},\bar{\rho})$ where the variables are normalized neck and body radii of the pores. Calculation of water content is based on integration over feasible parts of the total domain. It further assumes that the distribution is separable in each variable, enabling separability during integration, see equ. (2.40).

$$w_{Ph} = \iint f(\bar{r},\bar{\rho})d\bar{r}d\bar{\rho} = \int l(\bar{\rho})d\bar{\rho}\int h(\bar{r})d\bar{r} \qquad (2.40)$$

Based on how the entire domain is filled and emptied during the history of wetting and drying, see Figure 2.22, and by use of integration and a calculation scheme, the model derives a way to calculate the moisture content by use of data from desorption and adsorption isotherms only.

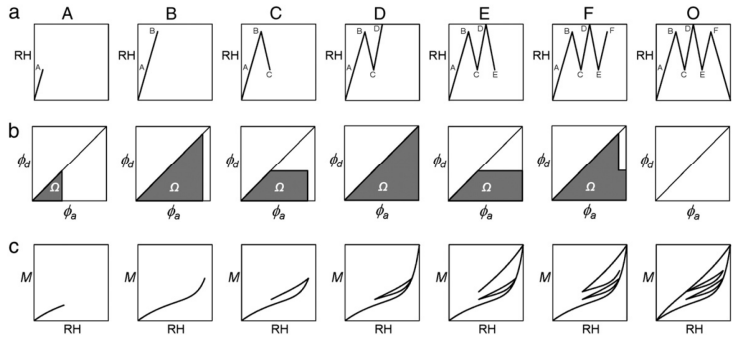

Figure 2.22, Illustration of successive domain coverage by steps in a drying and wetting process; top row: changes in RH; middle row: changes in the 2D domain (potential during absorption vs. desorption); bottom row: sorption curve RH vs. mass content; from Derluyn et al 2012.

There has been further refinement of this model by *Mualem and Dagan 1975* by introducing of weighting function into the main integral in equ. (2.40) to deal with discrepancies from experimental data.

Derluyn et al 2012 adopts a similar approach. However, the domain is not allowing pore necks with radii larger than pore bodies, corresponding to setting the distribution function to zero on half of the main domain. There are no direct assumptions made about the distribution function as such. By integration and a similar calculation scheme a more fundamental representation of the necessary model information is formulated and a mathematical representation for curve fitting is proposed. 7 parameters are adapted and necessary to describe the entire model with full capacity to calculate desorption, absorption and scanning.

Other approaches to modeling of sorption are also available. One mathematically based model is presented in *Deeb et al 2023*, using axisymmetric and homotopic properties of curve transformation to construct sorption and scanning curves from measured absorption and/or desorption curve. Also attempts to take in effects of varying temperature has been made, e.g. by developing water retention models, *Cai et al 2921*, or/and adapting models for adsorption isotherms to hysteresis and temperature effects, *Hefti & Mazzotti 2014*.

The value of modeling of hysteresis and/or temperature effects on sorption is of course dependent on the situation and conditions simulated. When cycles of wetting/drying and or non-isothermal conditions are implied, the importance of modeling of these phenomena is in general recognized, e.g. *Busser et al 2019* and *Bashir et al 2009*.

2.3 Transport of moisture

2.3.1 Different phases

The physically bounded water is present in concrete in condensed and adsorbed form as well as vapor. Transport of water in concrete is mainly involving only two of them. The adsorbed molecules can contribute with a surface flow, *Cunningham & Williams 1980*, but it is considered negligible compared with the flow of the other phases. The remaining two phases do not follow the same laws of transport and are not affected in the same way by temperature.

The net transport is a combination of their contributions, according to the filling state of the pore system discussed earlier in chapter 2.2.

The next two sections present transport phenomenology and modeling for each of the two phases. The last section of this chapter focuses on the combined transport.

2.3.2 Condensed water transport

2.3.2.1 Navier – Stokes

The most general transport formulation for an incompressible fluid is the Navier-Stokes equation, with one of its forms given in equ. (2.41).

$$\frac{\partial \boldsymbol{v}}{\partial t} = \boldsymbol{F_g} - \frac{1}{\rho}\nabla p + \mu_K \nabla^2 \boldsymbol{v} - (\boldsymbol{v} \cdot \nabla)\boldsymbol{v} \qquad (2.41)$$

where

v – is the velocity field of the fluid [m/s]

$\boldsymbol{F_g}$ – is the gravity field [m/s^2]

μ_K – is the kinematic viscosity of the fluid [m^2/s]

This formulation is capable of capturing both laminar and turbulent flow but requires a detailed information about the shape of the pore system, in order to specify the correct boundary conditions. *Johannesson 2000a* proposes an even more advanced approach taking into account not only interaction between the fluid and the solid but also displacement and stress of the solid. By using various thermodynamical and material-related arguments the equations are simplified to a level when one-dimensional percolation of water into mortar by capillary suction is simulated. However, even in a problem such heavily simplified *Johannesson 2002a* concludes difficulties with finding appropriate boundary conditions.

2.3.2.2 Hagen – Poiseuille / Darcy

For a laminar flow in a straight tube, see Figure 2.23, a simplified flow law is known as Hagen-Poiseuille, see equ. (2.42).

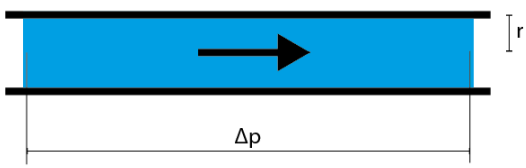

Figure 2.23. Laminar flow in a straight tube.

$$Q = \frac{\pi r^4}{8\mu_D L}\Delta p \qquad (2.42)$$

where

Q – is the volumetric flow rate [m^3/s]

r – is the tube radius [m]

L – is the tube length [m]

Δp – is the pressure drop over the tube length [Pa]

The field version of the fluid flow through an isotropic medium is the generalized version of the Darcy's law given by equ. (2.43), e.g. *Bear 1972*.

$$\boldsymbol{q} = -\frac{k}{\mu_D}\nabla\left(p + F_{g,z}\varrho_w z\right) \qquad (2.43)$$

where

q – is the flux field of the fluid [m/s]

k – is the intrinsic permeability of the medium [m^2]

μ_D – is the dynamic viscosity of the fluid [Pa s]

$F_{g,z}$ – is the gravitational force z-component [N/kg]

z – is the height coordinate [m]

2.3.2.3 Deviations from Darcy

Validity of Darcy's las requires flow slow enough not to become turbulent. This is controlled by the Reynold's number, given in equ. (2.44).

$$Re = \frac{\rho v L}{\mu_D} \qquad (2.44)$$

where

v – is the velocity of the fluid with respect to the medium [m/s]

L – is a characteristic linear dimension [m]

The region of laminar flow is considered to end for Re somewhere between 1 and 10, *Bear 1972*.

Validity of Darcy's las is also limited from below by the so called minimum gradient. Various explanations have been proposed for this effect, see discussion in *Bear 1972*. The effect is that below a certain gradient there is simply no net flow and in the vicinity of the threshold, the flow is not considered linear.

The flow in concrete that is not a result of external pressure is normally not considered to be fast enough to result in turbulence. The effect of minimum gradient only very small flows and this deviation is considered also to have insignificant effect on the overall moisture flow in concrete.

2.3.2.4 Temperature Dependency

Due to the dependency of sorption conditions on the temperature, a thermic change will have an impact on the transport conditions. The thermodynamic balance in capillary forces can

cause the capillary pressure to change due to a change in temperature, which in turn will imply a different pressure gradient and change the driving force of the Darcy flow.

However, if the pressure gradient is assumed to be constant, the only change in Darcy's law is the temperature dependent viscosity of the water.

2.3.3 Vapor transport

Vapor transport follow partially different laws. This section presents two main mechanisms, diffusion and convection, as well as some special cases of deviations from the general rules.

2.3.3.1 Diffusion

Diffusion is the process of molecular transport, driven by differences in concentration. An illustration is given in Figure 2.24.

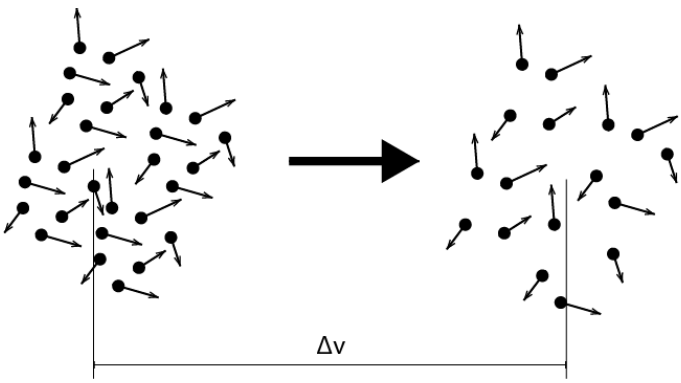

Figure 2.24. Diffusion of gas/vapor molecules

On the left side there is a higher concentration of the molecules and they collide more frequently with each other. On the right side the concentration is lower and the collisions are fewer. The net force originating from the difference in colliding will push molecules from the higher concentration to the lower. This principle is described mathematically by Fick's law and shown in equ. (2.45).

$$\boldsymbol{g} = -D_v \nabla v_v \tag{2.45}$$

where

$\boldsymbol{g}$ – is the field of moisture flow [kg/m^2 s]

D_v – is the diffusivity [m^2/s]

Combined with the ideal gas law, the flux can also be expressed as driven by gradients of partial pressure and temperature, see equ. (2.46).

$$\boldsymbol{g} = -\frac{D_v}{R_v T} \nabla p_v + \frac{D_v p_v}{R_v T^2} \nabla T \tag{2.46}$$

2.3.3.2 Convection

Convection is another possible transport mechanism for vapor. In such a case the air containing vapor is moving, driven by a gradient in total pressure and the containing vapor is travelling along. The movement of air and the contained vapor follows typically Navier-Stokes equation, but for compressible media instead of incompressible, as the case was in section 2.3.2 with condensed water. Possible simplification to Darcy's law may apply if the flow isn't turbulent. However, it has been found that the pressure differences in in pore system of concrete under normal conditions for moisture transport are small enough to neglect this transport mechanism for vapor, *Zhang 2014*.

2.3.3.3 Deviations

Molecular motion in vapor due to diffusion in vicinity of a water surface is governed by the evaporation of water. A transport of vapor causes a back transport of air due to the constant total pressure. However, the air is not absorbed by the water surface, which causes a small convective flow transporting the mixture of vapor and air from the water surface. This phenomenon is sometimes referred to as Stefan flow, Fuchs 1959. Its importance in the pore system is small due to its local effect around the water surfaces only and the limited amount of contact surfaces between condensed water and air.

Knudsen diffusion, also referred to as Klinkenberg effect or slip phenomenon, occurs when the diameter of the pores approaches the same size as the mean free path of the water molecules. Collisions with the walls of the pores will simply start to have a significant effect on the net forces from the collisions, that will no longer be random and dependent only/mainly on the vapor content. This results in some increase in the diffusive flow in the pore system. In concrete this effect takes place in both gel pore and smaller capillary pores *Zhang 2014*.

Due to molecular interactions in gas mixtures, various effects can occur for the molecules of the different gases. The diffusion in a binary gas mixture does not only occur due to the difference in concentration. Pressure diffusion caused gases with heavy and light molecules to move to the regions of high and low pressure respectively. Forced diffusion occurs when there is a force per unit mass that acts differently on the molecules of the two gases. Thermal diffusion causes the heavier molecules to migrate towards the cooler regions of the flow and act in the opposite direction to pressure diffusion during an expansion, *Bird 1994*.

2.3.4 Combined transport

The pore system in concrete can be filled, partially filled or empty, depending on the conditions and their history. These three situations interpreted locally in just one pore may result in three types of moisture flow, see Figure 2.25.

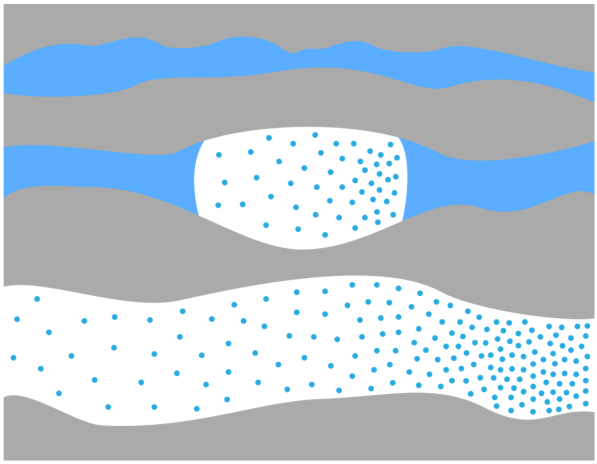

Figure 2.25. Three types of moisture flow in a tube pore, depending on geometry and filling state, enabling simple flow, combined flow in series and combined flow in parallel.

The two extreme cases are flow of condensed water in a filled pore and flow of vapor in an empty pore. These are easily described by Darcy's las and Fick's law with possible adjustments to some of the deviations. The third alternative in the partially filled pore gives a mixture of the two flows, connected in series.

In order not to model what happens in each single pore one can adopt a continuous approach to the moisture flow in concrete. This implies looking at a control volume of concrete of a size large by an order of magnitude or two compared to the typical capillary pore sizes, i.e. around 10-100 µm. In such a case, pore sections shown in Figure 2.25 will be facilitating a potential flow in parallel. One has also to take into account that many pore are interconnected with each other so that connections in series and in parallel mix.

2.3.4.1 Geometry of the pore system

The geometry of the pore system is a challenge in understanding and modeling of the moisture flow through it. One aspect that differ from idealized picture of the straight piece of tube is what is called tortuosity, see Figure 2.26.

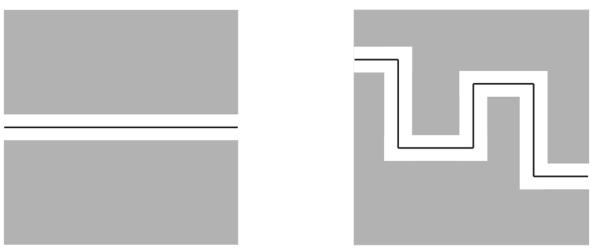

Figure 2.26. Examples of two bodies allowing molecules to pass through, however with significantly different path length for the same body thickness.

In mathematical sense it is a property of a curve, describing how curvy it is from the transport efficiency point of view. Normally it is defined as a ratio between the curve length and the

distance between its end points. In a pore system, the tortuosity factor is defined as a mean length of path of fluid molecules passing through, divided by the thickness of the porous material in the direction of the pressure gradient.

Another geometrical aspect of the complexity of the pore systems is the fact that the pores seldom have constant radius, see example of idealized tubes with varying radii in Figure 2.27.

Figure 2.27. Two examples of parallel tubes with varying radii.

Attempt has been made to describe the transport and permeability in idealized versions of radius variation as well as by constructing cells with tube bundles in all three dimensions and investigating the flow in various direction through such a system *Dullien 1975a* and *Dullien 1992*.

Further challenge originates in the connectivity of the pores. Here attempts have been done, e.g. *Koplik 1982* to investigate the transport with respects to various networks, as examples of regular connectivity, see Figure 2.28. Experimental investigations of permeability of porous networks in concrete have shown dependencies on various aspects of the porous system, e.g. *Ye 2004*. It is in general recognized that different types of pore networks have impact on transport and drying of porous media, *Surasani et al 2010*.

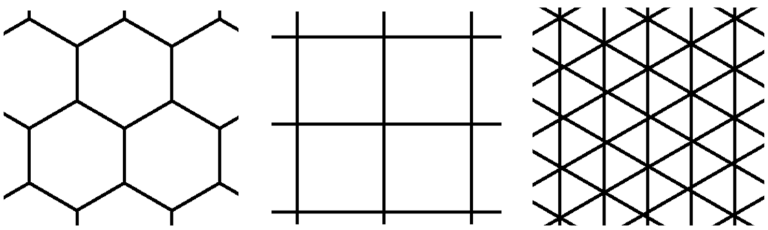

Figure 2.28. Examples of 2D network models, hexagonal, square and trigonal.

2.3.4.2 Dependency on the state of the pore system

The most fundamental aspect of the dependency of the moisture transport on the state of the pore system is based on the subdivision by condensation, i.e. in filled and empty pores. This controls whether vapor transport by Fick's law or liquid transport by Darcy's law are applicable.

2.3.4.2.1 Moisture potential and temperature

The two different flow laws will result in different dependencies and flow characteristics. Expressing Darcy's law, equ. (2.43), with translating the capillary pressure into vapor contents and temperature, by use of equ. (1.2), and neglecting the gravitational effects gives:

$$-\frac{k}{\mu_D}\nabla(p_c) = -\frac{k\varrho_w R_v}{\mu_D}\nabla(T\,ln\,\varphi) = -\frac{k\varrho_w R_v}{\mu_D}[ln\,\varphi\,\nabla T + T\nabla(ln\,\varphi)]$$

$$= -\frac{k\varrho_w R_v}{\mu_D}\left[ln\,\varphi\,\nabla T + \frac{T}{\varphi}\nabla\varphi\right] = -\frac{k\varrho_w R_v}{\mu_D}\left[ln\,\varphi\,\nabla T + \frac{T(v_s\nabla v - v\nabla v_s)}{\varphi {v_s}^2}\right]$$

$$= -\frac{k\varrho_w R_v}{\mu_D}\left[ln\,\varphi\,\nabla T + \frac{T}{v}\nabla v - \frac{Tv}{\varphi {v_s}^2}\frac{dv_s}{dT}\nabla T\right] = -\frac{k\varrho_w R_v}{\mu_D}\left[\frac{T}{v}\nabla v + \left(ln\left(\frac{v}{v_s}\right) - \frac{T}{v_s}\frac{dv_s}{dT}\right)\nabla T\right]$$

Multiplying by density, in order to get the rate of mass flow per area, and by exchanging dynamic viscosity divided by density for kinematic viscosity, this results finally in equ. (2.47).

$$\boldsymbol{g} = \varrho_w \boldsymbol{q} = -\frac{k\varrho_w R_v T}{\mu_K v}\nabla v - \frac{k\varrho_w R_v}{\mu_K}\left(ln\left(\frac{v}{v_s}\right) - \frac{T}{v_s}\frac{dv_s}{dT}\right)\nabla T \qquad (2.47)$$

Comparing it further to Fick's law in equ. (2.48), clearly identifies significant differences.

$$\boldsymbol{g} = -D_v\nabla v \qquad (2.48)$$

One major difference is between the transport coefficients for the gradient in vapor contents. Another large difference is the presence of the temperature gradient in the Darcy's law as a complement to the driving vapor content gradient with a coefficient dependent on both vapor contents and temperature.

To this adds the temperature dependency of properties such as vapor diffusivity in air and dynamic viscosity of water. There is also a possibility of dependency on either or both potentials through deviations from the ordinary transport mechanisms, described in section 2.3.2.3 and 2.3.3.3.

2.3.4.2.2 State history and hysteresis

The hysteresis of sorption, described earlier in 2.2.2.2 and 2.2.4.2, has also an impact of the transport. This is natural, because the basic impact on the filling state of the pore system affects which pores are filled and which are not. Thus, the subdivision of the moisture transport between the different mechanisms and how they interconnect and cooperate to produce a total transport effect is affected.

An empirical example of this is given in *Saeidpour & Wadsö 2016*, where different transport coefficients were measured during desorption and absorption conditions in the concrete samples, see Figure 2.29.

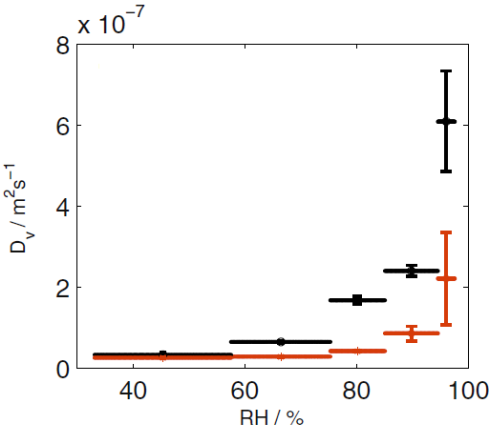

Figure 2.29, Transport coefficients for vapor contents as function of relative humidity during desorption (black) and absorption (red) for OPC mortar w/b=0.4 from Saeidpour & Wadsö 2016.

The position of the coefficients in the Figure 2.29 clearly resembles the form of typical desorption and adsorption isotherms. It is reasonable to expect scanning effects on the transport properties similar to the scanning in sorption, making the transport coefficients in reality dependent on the entire moisture and temperature history of the concrete.

2.3.5 Modeling

Depending on the application and involved conditions and requirements, different models for moisture transport in porous media have been used. On pore level there are examples of capillary-dominated transport, exploring different angles of contact for various fluids and porous media, *Singh et al 2019*. A more fundamental approach using chemical potential for vapor transport in partially saturated pores is another example of pore level modeling, *Addassi et al 2016*. Connecting of pore-level phenomenology with macro-scale modeling can be done by using of cell on the micro-level and, by periodic repetition, connecting its properties with the macro-scale modeling of transport, *Bennai et al 2016*.An example of microstructure-based modeling of permeability in cementitious materials is given by Zhang et al 2013

An approach, more typical for concrete, is to handle the medium on macro-scale. This involves a selection of driving potential for the moisture flow and can result in either one potential or a combination of two or more, with transport coefficients being typically non-linear functions of the state of the medium, such as moisture contents and temperature. Examples of these approaches are given by *Pesavento et al 2016*, *Vu & Tsotsas 2018, Vasil'ev et al 2015, Seredyński et al 2020* and *Johannesson 2000b*.

3. Modeling

3.1 Scope and limits of models

This section specifies some early decisions regarding scope and limits of models proposed later. This is done in order to not model unnecessary conditions as well as to make sure that models in different areas are compatible and can be used with each other.

3.1.1 Start of hydration

As described in sec. 2.1.2.2, hydration start when water comes in contact with cement during blending of the concrete mix, which results immediately in dissolution of some part of the cement and generates an initial peak in the heat intensity. At this stage of the process very little if any compressive strength is gained and there is almost no precipitation, thus almost no chemical binding of water. All of this happens during blending and is not of modeling interest to someone interested in simulating concrete behavior after the concrete is put into formwork, i.e. from casting.

That first stage of hydration is followed by a dormant period with a time span regulated by addition of admixtures in order to get the concrete to the building site and into the formwork before setting. During the dormant phase casting takes place, i.e. the concrete is poured into the framework. This moment is considered as the start of the simulation, that the hydration model in this research is intended to be used in. In order to cope with these requirements, following decisions are made:

- Modeling of hydration shall start in the dormant phase. The intensity of the reaction, i.e. the time derivative of the degree of hydration, shall at casting be close to zero and allow for a very slow start.
- The initial heat peak due to mainly dissolution heat during blending will not be covered by the total heat modeling.
- All chemical binding of water must be modeled from the initial water contents in the blend.
- Strength development before casting will not be modeled here.

3.1.2 Chemically vs. physically bounded water

Water can be bounded in concrete in many ways. The chemical reaction with cement will result in incorporating water into the solid products of the reactions. This can result in quite strong bonds like for OH^-. Weak bonds are also possible and are mostly found in the area of physical binding such as adsorption of water molecules to the surface of the air filled pores. There are various ways of subdividing these phenomena. The previously mentioned. i.e. chemically vs. physically, used type of bond as a criterium. Subdivision into evaporable vs. non-evaporable water is more oriented after measurement methods and uses drying at 105 ºC as separation.

In the area of simulation of drying and interaction with other materials in a typical construction site application, the main purpose of such a subdivision is to separate water that

will be stored irreversibly from water that can be moved in and out of the material. This has to take into account typical conditions that concrete can be subjected to. Strong chemical bonds are reversible, but only when the reaction products are heated to considerable temperature levels (e.g. thermos-gravimetric analysis) that typically do not occur in construction application of concrete. Such bonds has to be treated as irreversible in this application. On the other hand, storage in form of capillary condensed and adsorbed water is reversible and directly connected to the relative humidity and temperature of the material in ranges occurring in the application.

A perfect drying technique, preserving the microstructure of concrete does not exist according to *Snoeck et al 2014*. The same seems to be valid for the subdivision between chemically and physically bounded water. The challenge in this subdivision is to find a reasonable definition of the border between the reversible and irreversible storage that describes the phenomenology of the material close enough and is also practical from the measurement perspective. Some of the water bounded due to the hydration of binders can be removed without use of high temperatures. The so called crystal water or the C-S-H-gel is one example, where lowering relative humidity below 11 % at 20 ºC can result in removal that will not be replaced by new water molecules if the relative humidity is increased, *Feldman & Ramachandran 1971* and *Collier et al 2008*. Also ettringite, binding 32 water molecules per molecule, give away some of its water easily, already at about 30 % RH, *Baquerizo et al 2016*.

In order to describe such a border between the two types of water for one reaction product, a curve in the space spanned by relative humidity and temperature would be necessary. This gets even more complicated when various reaction products are involved. This situation calls for some kind of practical compromise where:

- reversible storage conditions are really giving reversible storage, without change in the irreversibly stored water that could result in a shift between desorption isotherms
- subdivision does cover all water, i.e. same criterium is used as a limit in measurements of both type of storage
- there is no overlap in modeling, i.e. same water does not appear in measurements of the two types of water.

Such a border criterium is proposed by *Feldman & Ramachandran 1971*, by discovering that drying to 11 % RH at 20 ºC does not change the desorption isotherms, i.e. does not affect significantly chemically bounded water of the reaction products. Relative humidities below 11 % do typically not occur at construction sites or during use of a concrete structure. Thus this criterium is acceptable from the application point of view and will be used during the rest of this thesis. The consequences for the measurements of so called chemically and physically bounded water become:

- Chemically bounded water, or irreversibly stored water, is water that is measured by a thermos-gravimetric analysis (TGA) on a sample that has been previously dried in an environment of 11 % RH and 20 ºC to a stable weight. There is no lower temperature

limit for the TGA in this measurement but care has to be taken to separate weight loss of water from carbon dioxide.

- Physically bounded water, or reversible stored water, is water that is measured by a sorption scale between saturation of a material sample and 11 % RH as the driest condition at 20 ºC.

3.1.3 Saturation Limit

Concrete at saturation has neither 100 % RH nor the entire pore system filled with water. The presence of dissolved binders and/or end products of hydration in the pore water (e.g. OH^-, Ca^{2+}, K^+, Na^+) decreases the water activity and the corresponding RH to somewhere between 95 and 98 %, *Hedenblad 1987*, depending on the binder composition, water-binder-ratio and temperature. At the same time there are pores, e.g. compaction and air pores, that the capillary forces are too week to fill.

There are various mechanisms that can be applied to limit the relative humidity at saturation in concrete in a simulation. One way of dealing with this is to simply move the saturation conditions to 100 % RH and accept the errors this will imply in modeling of sorption and transport in the moisture range close to saturation. In the targeted area of application, such conditions are not a large part of the simulation. In order to dry concrete effectively, an effort is normally made to protect it from high surrounding relative humidities and/or direct contact with water. Another approach to the problem is setting the moisture capacity, i.e. the slope of sorption curves, to a very low value between the real saturation and 100% RH. Letting the moisture capacity vanish completely is numerically inconvenient. A low value will on one hand allow relative humidity in concrete to rise beyond its real saturation limit but the extra amount of stored water will be very low. Regarding transport properties, the maximum value is then used both at saturation and 100 % RH, giving a constant section on the curve of transport coefficient as a function of relative humidity.

The models proposed in this thesis for transport and sorption shall support both methods described above.

3.1.4 Sorption and Transport During Early Hydration

During hydration the pore system of concrete is changing. Water penetrates and form gel pores in the inner product areas or former binder grains. In outer product areas the porosity between the binder and aggregate grains decreases and pores change shape, volume, opening sizes and connections. This has of course an impact on sorption and transport properties. Measuring these is however a large challenge. Sorption and transport measurements require significant time for the water to interact with the pore system. During that time, the properties of the pore system change if the hydration is ongoing.

Arresting hydration may be a tempting option to handle this challenge. Most such methods require removal of water from concrete, *Zhang & Scherer 2011* and *Collier et al 2008*. This gives a nice and controlled stop of hydration at various times or ages. However, these methods cannot be used in measuring water sorption and transport because the later measurement requires interaction between water and the pore system of concrete, which will immediately restart the earlier arrested hydration.

Partial replacement of cement by similarly sized, chemically inert material is another way to arrest hydration at various stages, *Termkhajornkit et al 2015*. A certain fraction of total amount of cement is replaced by inert material. The mixed concrete is given time enough to reach full hydration. The result is assumed to be equivalent to concrete without replacement, reaching only degree of hydration corresponding to the fraction of the cement replaced. This method allows for presence of water in the pore system of concrete, which will enable measurements of sorption and transport. There are however other considerations complicating this approach. Whether the formed pore system is significantly close to the concrete without cement replacement but at a certain degree of hydration, can be questioned. In one case all cement grains will be partially hydrated. In the other case some will be fully hydrated and some not at all due to the replacement. The amount of hydrated cement and chemically bounded water will possibly be the same. This enables the total porosity to be equivalent in both cases. However, the geometrical distribution of the hydration products will definitely differ, probably affecting the distribution of the total porosity into single pores and the connections between them. Another complication with this method is current use of more than one binder in modern cements and concretes. Various binders typically react in different time scales and a partial replacement corresponding after full hydration to a real case with hydration arrested at a specific age becomes very difficult to perform reliably.

As age dependency for sorption and transport was not considered as primary goal of this work, this area will be left for future research. The proposed models shall address sorption and transport properties constant with regard to age.

3.1.5 Low Temperature Domain

As modelled in the currently applied temperature equivalent time of maturity, see equ. 3.8-3.10 or *Freiesleben Hansen & Pedersen 1977* and *Jonasson 1984*, the water in pore system of concrete does not freeze at 0 ºC due to the impact of dissolved ions and capillary forces. Instead it takes part in hydration. Currently, as described in section 2.1.3, the temperature equivalent time of maturity grows at temperatures above -10 ºC. This modeling decision is based on previously acquired measured data. Different binder combinations used today may have an impact on this through different chemistry and/or different pore system formed. However, at the time of writing this thesis, reliable data regarding hydration performance at temperatures below 0 ºC is not available to any larger extent. Due to these circumstances, it is assumed that the current hydration limit in the low temperature range shall be reused in the proposed models.

3.2 Modeling of hydration and connected properties

The general strategy behind the proposed model is to eliminate the currently used mid-variable – the temperature-equivalent time of maturity. This variable serves as a maturity measure, grown out of earlier summations of temperature-weighted hydration time. It is not physically interpretable, thus not measurable even in theory. Instead the proposed model uses as core variable a degree of reaction for the cement, also called cement-oriented degree of hydration. The theoretical advantages of this choice are:

- This variable is easy to interpret. It goes from 0 to 1. 0 means that no cement has reacted. 1 means that all cement has reacted.
- This variable does not continue to grow infinitely, which means that any variable based upon this works with a direct reaction measure and does not have to invent its own stopping mechanism.
- This variable can be measured, even if with larger effort that chemically bounded water or compressive strength.
- If more than one binder with significantly different reaction characteristics are used, this model can easily be extended to cover the situation.

Connected properties such as chemically bounded water will be based on the cement-oriented degree of hydration.

3.2.1 Degree of hydration (cement oriented)

The complexity of kinetics of the cement hydration has already been presented in the earlier literature study, see section 2.1.2. Proposing a model adequately taking into account all involved mechanisms during different phases is beyond the level of this work, nor necessary to solve the current research problem. The starting point of this model is a general reaction kinetics formulation, connecting rate of change in concentration of one component to a product of powers of concentrations of other components and a parameter, typically dependent on temperature, see equ. (3.1).

$$\frac{dc_j}{dt} = k \prod_i c_i^{\alpha_i} \qquad (3.1)$$

where

c_i – are the relative concentrations of reactants and/or products [-]

α_i – are the orders of dependency [-]

k – is the parameter, typically dependent on temperature [1/s]

$\frac{dc_j}{dt}$ – is the rate of change of concentration j [1/s]

This model works according to the following principles:

- The parameter k gives the basis for the rate of reaction
- The concentrations on the right side of the equation work as controlling factors, conceptually independent of each other but in practice dependent on reaction itself and possible transport processes etc.
    - Reactant concentrations go from higher to lower values and by use of positive exponents imply successive change from enabling to inhibiting the reaction
    - Product concentrations, if present, go from lower to higher values and by use of negative exponents imply successive change from enabling to inhibiting the reaction
- The parameter k is typically not a constant but varies with temperature, thus describing the temperature dependency of the reaction.

The structure of this equation is used to propose below a similar equation for the cement-oriented degree of hydration:

$$\frac{d\alpha_C}{dt} = \prod_i \beta_i \qquad (3.2)$$

where

α_c – are the degree of hydration for the cement [-]

β_i – are factors influencing the rate of change of the degree of hydration of the cement [-]

The differential formulation above requires of course integration to evaluate the degree of hydration, as shown below together with the specific influencing factors defined and presented in the following sections:

$$\alpha_C(t) = \int_0^t \prod_i \beta_i(t')\, dt' = \int_0^t \beta_T \beta_w \beta_\alpha \beta_{start} dt' \qquad (3.3)$$

At this stage it is of value to observe some similarities and differences between the formula above and both the temperature-equivalent time of maturity and the generalized time of maturity proposed by *Mjörnell 1997*:

- All models build on a differential formulation and require numerical integration (time step summation) to evaluate their values.
- All models use a product of factors as the integrand, thus insinuating an apparent separability of factors both as a concept and in adaptation. The conceptual interpretation here is that the factors represent controlling mechanisms that work independently of each other. One typical approach for construction of such model is to:
    - Let one factor give some base
    - Let other control it by
        - inhibiting it (factor range 0-1)
        - regulating it versus some reference conditions (factor 1 for reference conditions and variation around it).
- Only the proposed model delivers degree of hydration. The other two require a further calculation by a function with adapted parameters to calculate the degree of hydration.
- The true separability is valid only for the temperature-equivalent time of maturity being dependent on temperature, i.e. no cross-dependencies by default.
- The generalized time of maturity uses a factor dependent on the degree of hydration, which is itself modeled as a function of the equivalent time of maturity. This introduces a direct circular dependency and destroys the separability between the factors, see reasoning in the literature study, sec. 2.1.3.6.
- The same lack of mathematical separability is valid for the proposed model above, thus to the use of degree of cement hydration in one of the factors. The apparent separability can only be considered on a conceptual level in the interpretation of the model. It cannot be used as a simplification in measurements or adaptation of parameters.

3.2.1.1 Availability of cement

This factor is one of the two factors corresponding to the concentration of reactants and is selected to be the basic rate factor for the model and its formula is given by equ. (3.4).

$$\beta_\alpha = b_c \left(\frac{\alpha_{C,max} - \alpha_C}{\alpha_{C,max}} \right)^{\kappa_c} \tag{3.4}$$

where

b_c – is a rate adaptation parameter [-]

κ_c – is an order of dependency, adaptation parameter [-]

$\alpha_{c,max}$ – is the maximum value for the hydration degree [-]

This factor gives the basic rate of reaction and it goes from b_c to 0 as the degree of hydration goes from 0 to its maximum value. How fast the factor changes with the degree of hydration is regulated by the order of dependency κ_c. The maximum value for the hydration degree $\alpha_{c,max}$ is implemented to allow for modeling of situations where there is knowledge that all the cement will not react and no other mechanisms are used to model the stop of hydration. For closer discussion on how to use the factors together see sec. 3.2.1.5.

An observation shall be made in comparison to the use of a similar parameter construct in *Mjörnell 1997*, which states that the factor describes the successive decrease of space for the products to precipitate. Author of this thesis wishes to challenge this interpretation. First and forward this factor is a typical measure of concentration of a reactant and directly expresses the reactants availability for the reaction. Precipitation can take place on any chemically compatible surface, which in practice will by beside cement grains also possible aggregate surfaces and reaction product surfaces. The total area of this surface varies during the precipitation, typically increases in the acceleration period and decreases later. Such a variation is not described by the proposed control factor. One could argue that there is some limited correlation between the control factor and the later part of development of the size of the precipitation surface. What is possibly more interesting to express in some way beside the precipitation area is the volumetric interpretation of the “space for precipitation”, which takes place indirectly in the next control term, describing primarily the availability of water for the reaction.

3.2.1.2 Availability of water

This is the other factor describing the influence of concentration of reactants, in this case the water. The idea is the same as earlier proposed for the water corresponding term in the externed model of time of maturity in *Mjörnell 1997*. Beside the fact that the term here is used in modeling of the degree of hydration of the cement and not in calculation of a time of maturity, there is also another difference. The earlier construct uses, as a measure for concentration of water available for the reaction, the relative amount of water available in capillary pores. The formula below proposes a slightly more generalized formulation where the relative amount of water in the part of the pore system corresponding to an upper section of the desorption curve is used, with the region limit to be adapted as a parameter.

$$\beta_w = \left(\frac{w_{Ph} - w_{Ph,stop}}{w_{Ph,max} - w_{Ph,stop}}\right)^{\kappa_w} \quad (3.5)$$

where

w_{Ph} – is the amount of physically bounded water in the system [kg/m³], a function of the relative humidity history as well as temperature history

$w_{Ph,max}$ – is the amount of physically bounded water in the system at saturation [kg/m³]

$w_{Ph,stop}$ – is the amount of physically bounded water in the system [kg/m³] below the limit when water does not longer take part in the reaction.

κ_w – is an adaptation parameter [-]

Definition and calculation of these terms is connected to the sorption model presented in sec. 3.3, where the amount of physically bounded water is modeled as a function of history in RH and temperature:

$$w_{Ph}(t) = w_{Ph}([1, \varphi_1, \dots, \varphi_t], [T_0, T_1, \dots, T_t]) \quad (3.6)$$

where

$[1, \varphi_1, \dots, \varphi_t]$ – is the history of changes in relative humidity from saturation to the current value [-]

$[T_0, T_1, \dots, T_t]$ – is the history of changes in temperature from casting to the current value [ºC]

The limit for the amount of water that doesn't take part in the reaction is defined as:

$$w_{Ph,stop} = w_{Ph}([1, \varphi_{stop}], 20\ °C) \quad (3.7)$$

where

φ_{stop} – is an adaptation parameter [-]

As a consequence of this, the water that is available for the reaction is the water that is desiccated during pure desorption from saturation to φ_{stop} at a temperature of 20 ºC. The concept behind this definition is the same as in the earlier model proposal, however the limit is not connected to water in capillary pore only or a specific model of capillary porosity.

This term is intended to start at 1 and decrease asymptotically towards 0 as available water is consumed by the reaction. Whether it reaches 0 or not is dependent on if water or cement is the limiting factor in hydration. A practical problem may occur in evaluation of the term at early ages. If the sorption model behind the function of physically bounded water, used above, is based on measured sorption data, i.e. desorption/absorption/scanning curve, these cannot usually be measured at early ages, see the discussion in sec 3.3.13, which gives a sorption model with validity that does not cover early hydration. This may result in the fact that the maximum amount of physically bounded water at saturation that the model can handle may be smaller than the amount of blending water decreased by chemically bounded water. In such a

situation a practical solution is adopted where the control term is set to 1 due to the fact that the water contents has not yet become a limiting factor for the reaction.

$$\beta_w = 1 \; if \; w_{Ph,max} < w_b - w_{Ch} \tag{3.8}$$

where

w_b – is the amount of blending water [kg/m³]

w_{Ch} – is the amount of chemically bounded water [kg/m³]

The obvious interpretation of this term is of course expressing the availability of water. However, due to the recognized fact that all capillary condensed water is not available for the reaction, *Mjörnell 1994*, this term indirectly also expresses the limiting condition regarding volumetric space available for precipitation of reaction products. Not all water contents contributes to this term – only water in a part of the pore system with the largest pores/pore openings. This observation completes the comparison with the space limitation expression in the model proposed earlier in *Mjörnell 1997*, started in the end of section 3.2.1.1.

3.2.1.3 Temperature dependency of reaction velocity

The temperature dependency of the reaction rate is modeled in the same way as in the case of the temperature equivanet time of maturity. It describes a temperature dependency of Arrhenius type with an activation energy that is dependent on the temperature, see previously described in sec. 2.1.3.1. It is simply a reuse of a model that has worked well for many years. The formulae are given by the equ. (3.9) and equ. (3.10).

$$\beta_T = exp\left[\Theta\left(\frac{1}{T_{ref}+273} - \frac{1}{T+273}\right)\right] \tag{3.9}$$

$$\Theta = \Theta_{ref}\left(\frac{30}{T+10}\right)^{\kappa_3} \tag{3.10}$$

where

Θ_{ref} – is an adaptation parameter [K]

κ_3 – is an adaptation parameter [-]

T_{ref} – is a reference temperature chosen to 20 [°C]

3.2.1.4 Dormant phase delay

This factor is a pure mathematical construct for inhibiting the growth of the degree of hydration from the beginning of the simulation. As stared earlier, see 3.1.1, the modeling shall start in the dormant period with low intensity of the reaction and a certain delay. When that is over a smooth transition to high growth of reaction rate is desirable. This is achieved by using the term given by equ. (3.11).

$$\beta_{start} = 1 - b_{start} exp(-\tau_{start}\alpha_C) \tag{3.11}$$

where

b_{start} – is an adaptation parameter [-]

τ_{start} – is an adaptation parameter [-]

A diagram of β_{start} as a function of the degree of hydration for a typical choice of the adaptation parameters is shown in Figure 3.1.

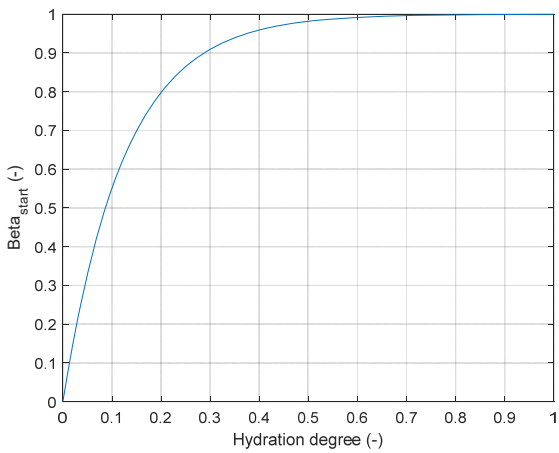

Figure 3.1. The delay factor β_{start} as a function of the degree of hydration for an example choice of parameters $b_{start} = 0.99999$ and $\tau_{start} = 8$ in a typical range of adaptation.

3.2.1.5 How the factors work together

The general roles in this model are:

- β_α is the basic rate factor (value between 0 and b_c)
- β_{start} and β_w are limiting factors (values between 0 and 1)
- β_T is a regulating factor (reference value of 1 and variation around)

As stated earlier in the formulation of the research problem, this model is intended to start modeling of the hydration process in the dormant period and not from the initial dissolving of the cement. This is achieved by a combination of β_α as the general speed factor at its maximum value from the beginning and β_{start} at very low values at the beginning of the hydration, later growing rapidly to 1.

The general temperature dependency is implemented by β_T and is affecting all stages of reaction in the same way. It uses 20 °C as a reference (factor value 1) with decreasing below and increasing above. This factor can temporarily stop the growth of degree of hydration if the temperature drops low enough, which corresponds to freezing the capillary water.

Limiting and permanent stopping of the reaction can be caused by one of two factors, β_α and/or β_w, depending on which is the limiting component in reality, i.e. the initial water-to-binder-ratio of the concrete.

There are two ways of running and adapting the model, depending on if information on the moisture conditions is present. If it is, β_w is used in its full definition to model limitations by water availability and the maximum degree of hydration $\alpha_{c,max}$ is set to 1 in β_α. If the water does not become limiting then all the cement will eventually hydrate and the hydration degree will grow to 1, limited by β_α. If the water will become limiting then β_w will inhibit the growth of the degree of hydration and it will reach whatever its maximum value will be, somewhere below 1.

If there is no moisture information available, the model can still be run by setting β_w to 1 and using $\alpha_{c,max}$ as a control parameter for stopping the reaction. If it is set to 1 then the cement availability will be the limiting factor in reality and all cement will be eventually hydrated. If it is set lower than 1 then other factors will limit and stop the reaction in reality not allowing the hydration degree to raise all the way to 1. This situation corresponds to water being the limiting factor without explicitly modeling the moisture conditions.

3.2.2 Adjusted degree of hydration (water oriented)

In order to capture that the amount of water chemically bounded per amount of cement varies with temperature, *Gallucci et al 2013*, a new value is introduced in the model. This value is calculated in parallel with the hydration degree of the cement and can be interpreted as a water oriented equivalent or degree of hydration. However, this value is not an absolute measure of consumed water. It is defined by its time derivative in a fashion relative to the time derivative of the hydration degree of the cement, see equ. (3.12).

$$\frac{d\alpha_W}{dt} = \beta_{adj}\frac{d\alpha_C}{dt} \tag{3.12}$$

where

a_W – is the adjusted or water oriented degree of hydration [-]

β_{adj} – is the temperature dependent adjustment factor given by

$$\beta_{adj} = \left[1 - b_{adj}(T - 20°C)\right] \tag{3.13}$$

where

b_{adj} – is an adaptation parameter [-]

T – is the hydration temperature [ºC]

The consequence of these definitions is that a_w is a measure relative to a_c. At 20 ºC these two values will increase at the same rate. If the temperature is higher, the increase rate of a_w will be lower than a_c and the opposite will be valid if the temperature is lower. The adjustment factor is linear with temperature, precisely as the results from *Gallucci et al 2013* indicate. In order to evaluate the full value of a_w an integration has to be performed:

$$\alpha_W(t) = \int_0^t \beta_{adj}\frac{d\alpha_c}{dt}dt' = \int_0^t \beta_{adj}\beta_T\beta_w\beta_\alpha\beta_{start}dt' \tag{3.14}$$

Due to lack of data outside the temperature range of 5-60 ºC, the variation of β_{adj} cannot be assumed to follow the same linear characteristics as within the range, examined in *Gallucci et al 2013*. In order not to overestimate the effects of temperature on the amount of chemically bounded water, the values of β_{adj} outside the mentioned temperature range are limited by use of constant extrapolation instead of equ. (3.13).

3.2.3 Connected properties

3.2.3.1 Chemically bounded water

Connecting the amount of chemically bounded water to the model already defined is straight forward by the use of equ. (3.15).

$$w_{Ch} = w_{Ch,ref}\alpha_W \tag{3.15}$$

where

w_{Ch} – is the amount of chemically bounded water [kg/m³]

$w_{Ch,ref}$ – is an adaptation parameter [kg/m³]

It shall be noted that the adaptation parameter $w_{Ch,ref}$ is the amount of water chemically bounded per amount of cement at full hydration at a temperature of 20 ºC.

3.2.3.2 Compressive strength

Although the main goal of this work is not to propose a model for the compressive strength, is has been required that the hydration model has a generality that allows for construction of such a connection later. The argument that is does centers around the two values α_c and α_w that together possess both:

- much stronger correlation to the state of hydration than the temperature equivalent time of maturity, on which today's model for strength is build
- a measure of how temperature has influenced not only the rate of reaction but also is some sense the quality of it, while it is known that such an influence is clearly present for compressive strength

Having in mind observations of an almost linear correlation between development of the degree of hydration and compressive strength at constant temperature, it should be possible to successfully propose a model for strength based either on a direct connection:

$$f_{cc} = g(\alpha_C) + h(\alpha_W) \tag{3.16}$$

or a differential one

$$\frac{df_{cc}}{dt} = g\left(\frac{d\alpha_C}{dt}\right) + h\left(\frac{d\alpha_W}{dt}\right) \tag{3.17}$$

where

$g(x)$ and $h(x)$ – are two functions, not deviating especially much from linearity at least in the differential case.

3.2.3.3 Hydration heat

In case of the heat of hydration, a very similar approach, as for compressive strength, is adopted. Although the evidence for temperature variation of the average heat of hydration per increase in the degree of hydration of the binder is yet to be presented, it can be argued that this should be the case due to different amount of water per increase in the degree of hydration of the binder changing state during the reaction resulting is different enthalpy release. This implies a reasonable probability of successful model development for this variable in the same manner as proposed above for the compressive strength.

3.2.4 Adaptation to measured data

Due to the circular dependency on the degree of hydration in the model, separation of dependencies cannot be applied during adaptation of the parameters. This together with the non-linearities in the proposed functions for the various influencing factors eliminate possibilities for applying linear regression. Instead an error function for the adaptation is formed, based on the measured data:

$$Error(\overline{p}) = \sum_i \left[w_{Ch,m}(\overline{x}_i) - w_{Ch}(\overline{p}, \overline{x}_i) \right]^2 \qquad (3.18)$$

where

$\overline{\mathrm{x}}_\mathrm{i}$ – is a full set of environmental conditions defining one measurement point

$w_{Ch,\mathrm{m}}(\overline{\mathrm{x}}_\mathrm{i})$ – is the amount of water chemically bounded [kg/m³], measured at the environmental conditions specified by $\overline{\mathrm{x}}_\mathrm{i}$

$\overline{\mathrm{p}}$ – is a full set of model parameters being adapted

$w_{Ch}(\overline{\mathrm{p}}, \overline{\mathrm{x}}_\mathrm{i})$ – is the amount of water chemically bounded [kg/m³], calculated using the model and the set of parameters $\overline{\mathrm{p}}$ for the environmental conditions specified by $\overline{\mathrm{x}}_\mathrm{i}$

$\mathrm{E}(\overline{\mathrm{p}})$– is the adaptation error for the set of parameters $\overline{\mathrm{p}}$

The adaptation becomes then an optimization problem, in this case minimizing the sum of squares of errors in each measured point:

$$\min_{\overline{p}} Error(\overline{p}) \qquad (3.19)$$

If measurements of various variables are used during the adaptation, e.g. chemically bounded water, heat of hydration and compressive strength, the squares of errors of the various variables are typically normalized per variable or weighted with some different strategy before summed. There are also constraints to this problem. All parameters introduced so far are required to be positive. The requirements may be stricter than that. The parameter $w_{Ch,ref}$ is due to earlier measurements by various sources, see e.g. *Powers & Brownyard 1948* or *Helsing 1993* expected to be somewhere in the area of 0.19 to 0.25.

In order to find a feasible minimum to the error function, numerical methods for non-linear optimization problems have to be used. It is not the intention of this thesis to go in deep into this area of mathematics, however a few word on how to practically deal with this challenge

are given in this section. In order to get a more complete and deeper picture of mathematical optimization theory in general and the connected numerical methods in particular see for instance *Nocedal & Wright 2006*.

Numerical methods for non-linear problems consists of algorithms starting at a selected parameter value and executing a search for a better point, lower value of the error function, in the parameter space. Some of them are guaranteed to deliver a local minimum, but there are no methods that for sure deliver a global minimum. What is delivered is typically dependent on the selection of the starting point for the search. The methods make different assumptions about information available regarding the error function. Simplest assumption is only evaluation of the error function at any given point in the parameter space, resulting in a class of methods referred to as Derivative-Free Optimization (DFO). One easily available example is the implementation of *fminsearch* function in Matlab (R2021b), using a DFO simplex search method, which unfortunately is not guaranteed to deliver a local minimum.

More advanced approaches are typically combinations of a method for selection of a search direction in the parameter space with a method of performing the search by some structured stepping along the selected direction with, in this case, control of the parameter constraints – a so called Line Search. Selection of the search direction uses typically more information about the error function. Conjugated Gradient methods use typically the gradient of the error function, i.e. its first order derivatives with respect to the adaptation parameters. Newton's method uses second order derivatives in the form of a Hessian matrix, which is the inverse of the matrix of the second order derivatives, i.e. the Jacobian. In this work a middle approach between the two has been used. There is a class of methods called Quasi-Newton Methods, where the idea is to only use the gradient information in each point when choosing the search direction, but at the same using an approximation of the Hessian to select better directions and speed up the search. In this work one of the original methods in this class, Davidon-Fletcher-Powell, is used.

3.2.5 Model validation

Adaptations to measured chemically bounded water for three mortars are presented below. For each one a comparison is made to what is considered the current reference model on this level of applied modeling. Due to the facts that the proposed model can be run with or without moisture information from a sorption model and that the reference model does not model any moisture influence, the comparison is done for two cases:

- one with measurements on only sealed samples and without modeling of moisture influence in the proposed model ($\beta_w = 0$)
- one with measurements on both sealed and saturated samples, including explicit modeling of moisture influence in the proposed model

Data used for model validation and comparison are taken from *Stelmarczyk et al 2019*. Due to the fact that the referenced report is in Swedish, a brief summary of the used material and methods will be given below.

The measurements were done on samples consisting of mortar based on a commercial CEM II-A/V. Three different water-binder ratios were used: 0.32, 0.40 and 0.55. The mixes were based on commercial style concrete mixes with crushed aggregate only, a consistency class S4 and a D-max of 16mm. However, for the mortar only aggregate fractions up to 1 mm were used. The specimens were cured in temperature-controlled and seal or saturated conditions. Drying in 11% RF at 20 ºC was later used to remove the physically bounded water according to the earlier decision for how to interpret the border between the chemically and physically bounded water, see sec. 3.1.2. Finally the chemically bounded water was determined with a TGA-analysis.

3.2.5.1 Reference model for comparison

An obvious candidate for model comparison at this level of applied modeling is the hydration model mentioned earlier in the literature study sec. 2.1.3.6 with its connection to chemically bounded water according to sec. 2.1.3.5, proposed in *Mjörnell 1997*. The faulty assumption regarding separability of the influencing factors, proposed in the adaptation for the old model can easily be overcome by use of same non-linear adaptation methodology as described above for the proposed model. However, as pointed out in detail in earlier discussion in section 2.1.3.6, there are still two problems with this adaptation. The lack of explanation for how to subdivide the responsibility for double stopping mechanisms in the total model as well as the incomplete description of how to handle parameter adaptation for the hydration degree function would simply require too much of guessing how to perform the adaptation. Due to the above, the model proposed in *Mjörnell 1994* was abandoned in this comparison.

The second best option is to fall back on the ordinary model för the temperature-equivalent time of maturity according to section 2.1.3.1, being a base for the degree of hydration according to section 2.1.3.2.2 and its connection to chemically bounded water according to section 2.1.3.5. This adaptation is typically done in two steps. First an adaptation of the maturity function is traditionally done against strength data, using the model connection according to section 2.1.3.3. Later an adaptation of all parameters for the degree of hydration and chemically bounded water is done simultaneously by use of the non-linear adaptation described above.

3.2.5.2 Modeling with moisture variation

The diagrams in Figure 3.3 and Figure 3.4 compare adaptation of the proposed (new) and the reference (old) model to measured chemically bounded water at different times after casting for both sealed and saturated samples of concrete with w/c=0.32, hydrated at various temperatures, with R^2-values for the adaptations.

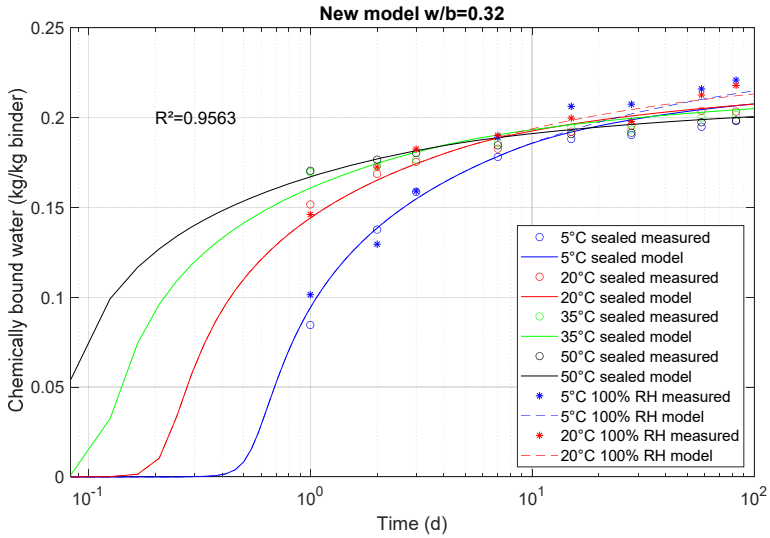

Figure 3.2. Adaptation of the proposed model with explicit modeling of moisture to measurements at different times after casting, on sealed and saturated samples, cured at different temperatures. Water-binder ratio 0.32. Amount of chemically bounded water per amount of binder as a function of time after casting.

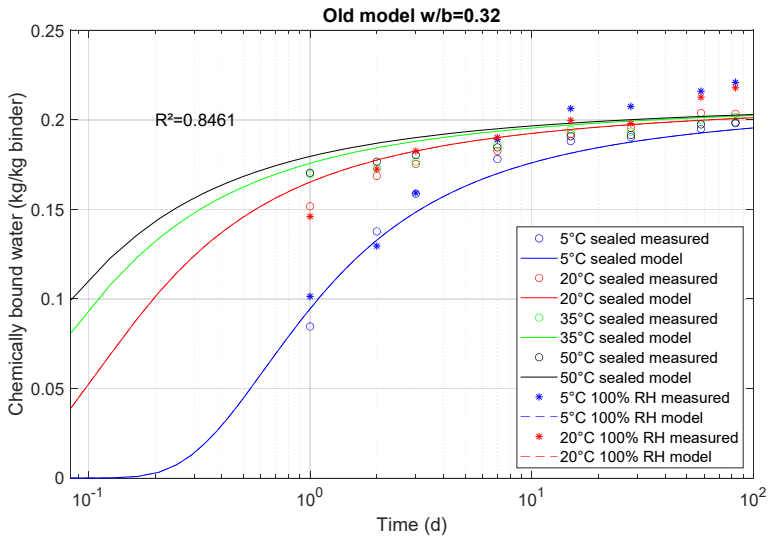

Figure 3.3. Adaptation of the reference model to measurements at different times after casting, on sealed and saturated samples, cured at different temperatures. Water-binder ratio 0.32. Amount of chemically bounded water per amount of binder as a function of time after casting.

The diagrams in Figure 3.5 and Figure 3.6 compare adaptation of the proposed (new) and the reference (old) model to measured chemically bounded water at different times after casting for both sealed and saturated samples of concrete with w/c=0.40, hydrated at various temperatures, with R^2-values for the adaptations.

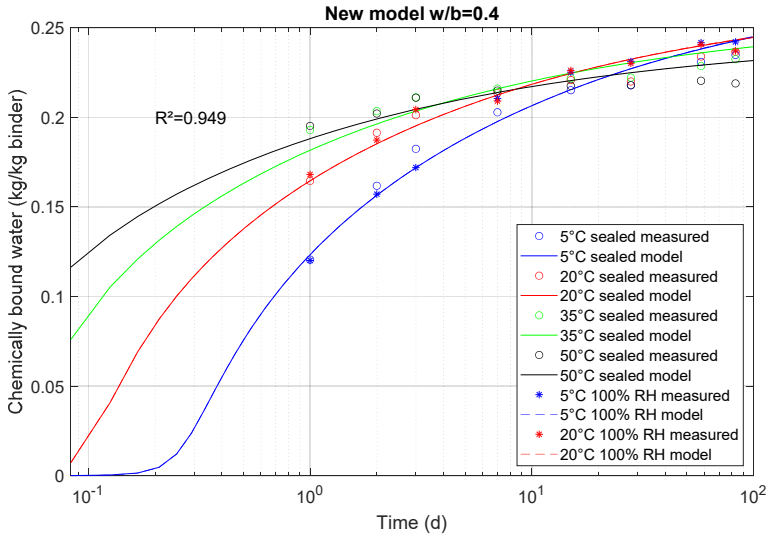

Figure 3.4. Adaptation of the proposed model with explicit modeling of moisture to measurements at different times after casting, on sealed and saturated samples, cured at different temperatures. Water-binder ratio 0.40. Amount of chemically bounded water per amount of binder as a function of time after casting.

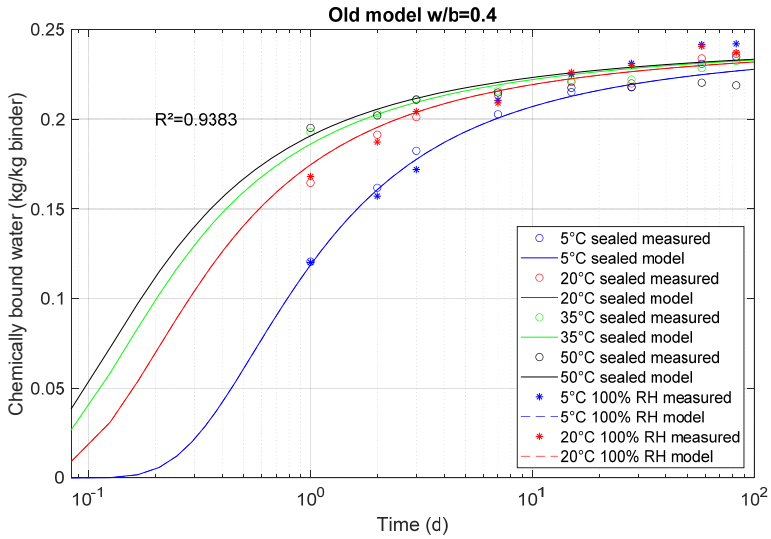

Figure 3.5. Adaptation of the reference model to measurements at different times after casting, on sealed and saturated samples, cured at different temperatures. Water-binder ratio 0.40. Amount of chemically bounded water per amount of binder as a function of time after casting.

The diagrams in Figure 3.6 and Figure 3.7 compare adaptation of the proposed (new) and the reference (old) model to measured chemically bounded water at different times after casting for both sealed and saturated samples of concrete with w/c=0.55, hydrated at various temperatures, with R^2-values for the adaptations.

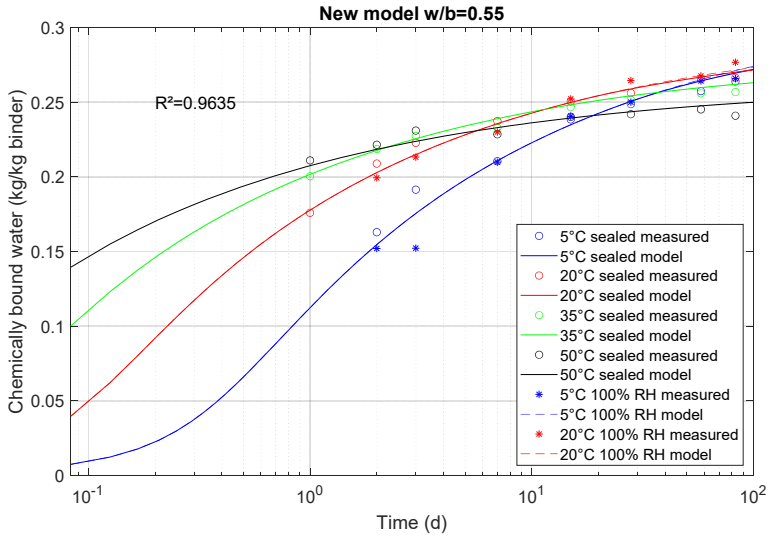

Figure 3.6. Adaptation of the proposed model with explicit modeling of moisture to measurements at different times after casting, on sealed and saturated samples, cured at different temperatures. Water-binder ratio 0.55. Amount of chemically bounded water per amount of binder as a function of time after casting.

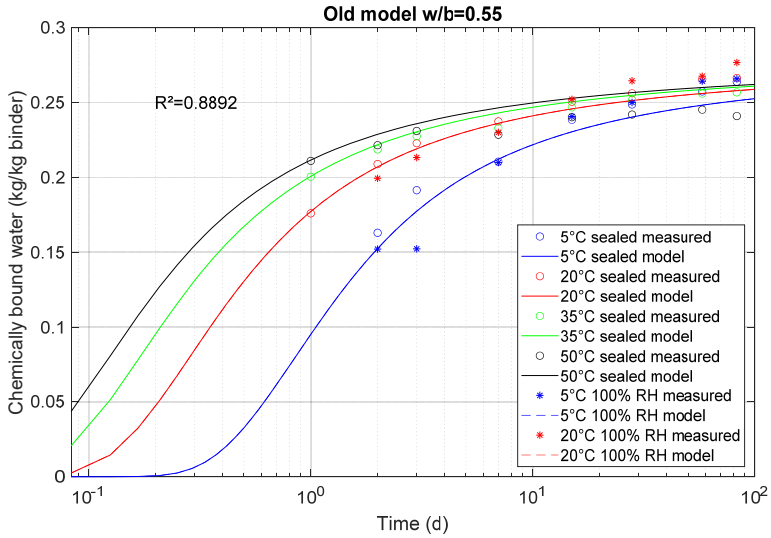

Figure 3.7. Adaptation of the reference model to measurements at different times after casting, on sealed and saturated samples, cured at different temperatures. Water-binder ratio 0.55. Amount of chemically bounded water per amount of binder as a function of time after casting.

3.2.5.3 Modeling without moisture variation

The diagrams in Figure 3.8 and Figure 3.9 compare adaptation of the proposed (new) and the reference (old) model to measured chemically bounded water at different times after casting

for sealed samples of concrete with w/c=0.32, hydrated at various temperatures, with R^2-values for the adaptations.

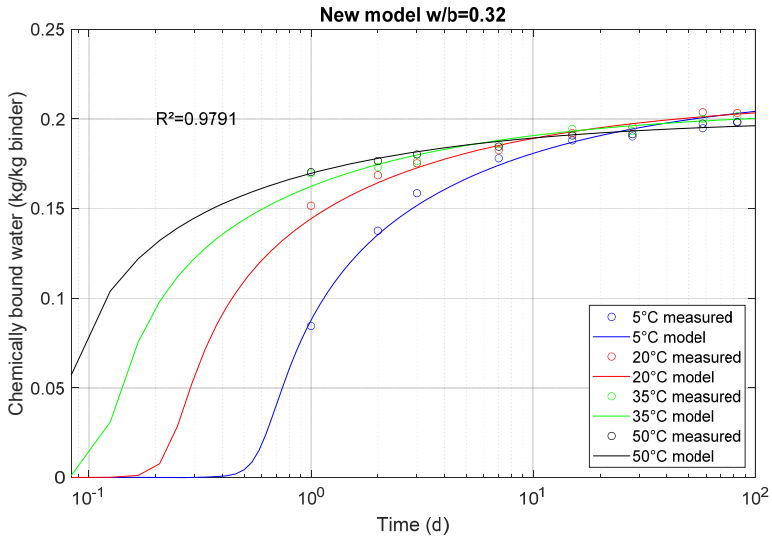

Figure 3.8. Adaptation of the proposed model without modeling of moisture to measurements at different times after casting, on sealed and saturated samples, cured at different temperatures. Water-binder ratio 0.32. Amount of chemically bounded water per amount of binder as a function of time after casting.

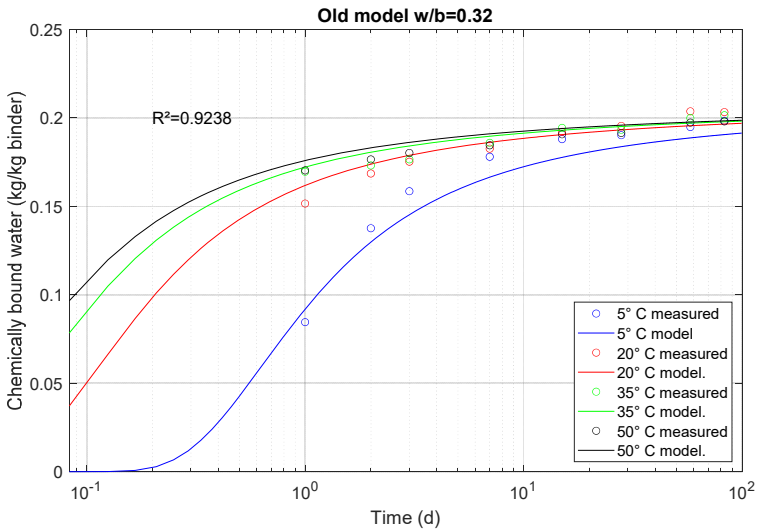

Figure 3.9. Adaptation of the reference model to measurements at different times after casting, on sealed and saturated samples, cured at different temperatures. Water-binder ratio 0.32. Amount of chemically bounded water per amount of binder as a function of time after casting.

The diagrams in Figure 3.10Figure 3.3 and Figure 3.11 compare adaptation of the proposed (new) and the reference (old) model to measured chemically bounded water at different times

after casting for sealed samples of concrete with w/c=0.40, hydrated at various temperatures, with R^2-values for the adaptations.

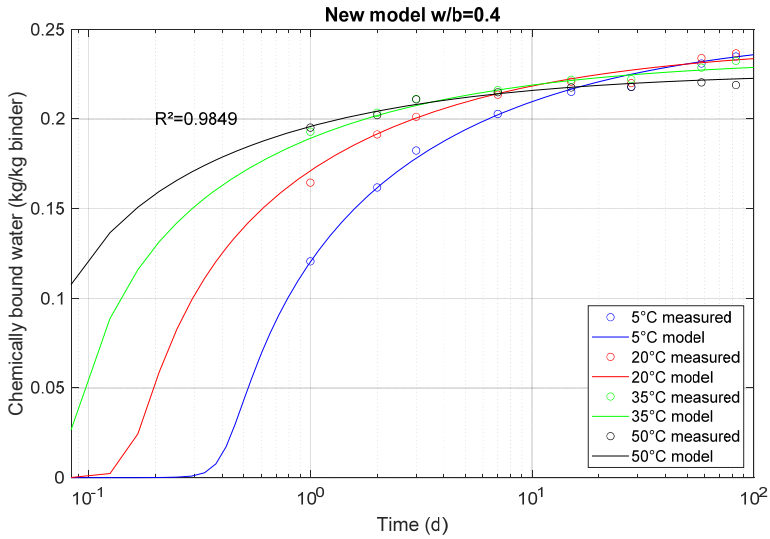

Figure 3.10. Adaptation of the proposed model without modeling of moisture to measurements at different times after casting, on sealed and saturated samples, cured at different temperatures. Water-binder ratio 0.40. Amount of chemically bounded water per amount of binder as a function of time after casting.

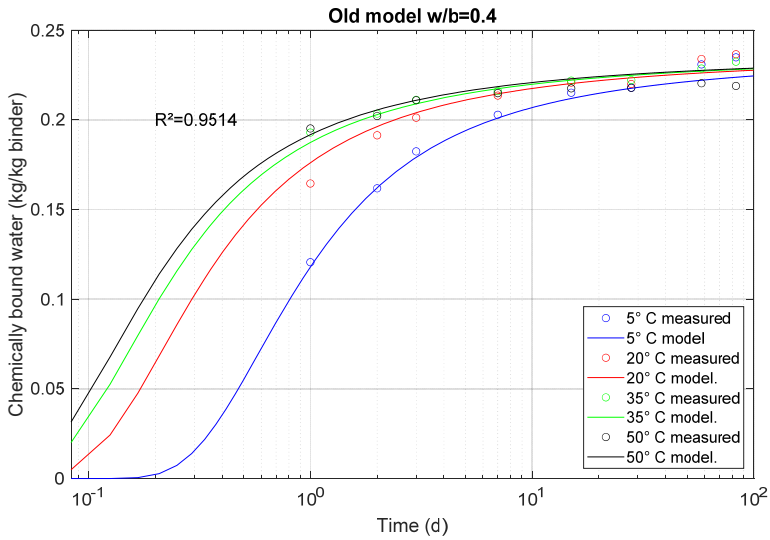

Figure 3.11. Adaptation of the reference model to measurements at different times after casting, on sealed and saturated samples, cured at different temperatures. Water-binder ratio 0.40. Amount of chemically bounded water per amount of binder as a function of time after casting.

The diagrams in Figure 3.12 and Figure 3.13 compare adaptation of the proposed (new) and the reference (old) model to measured chemically bounded water at different times after

casting for sealed samples of concrete with w/c=0.55, hydrated at various temperatures, with R^2-values for the adaptations.

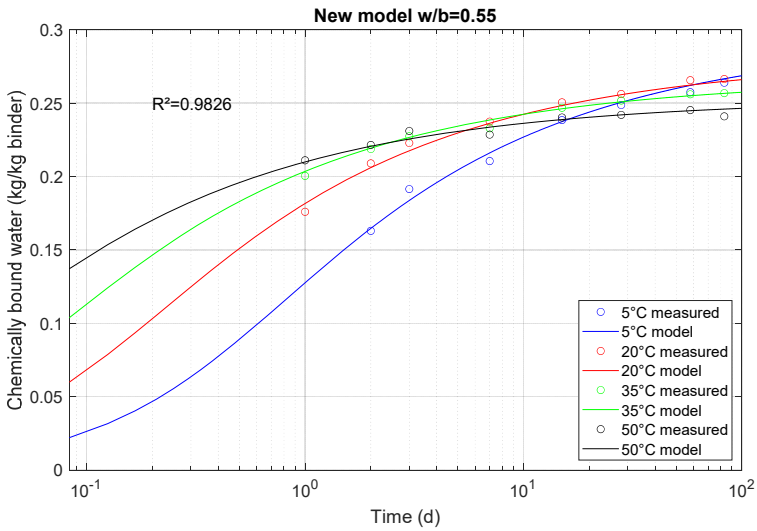

Figure 3.12. Adaptation of the proposed model without modeling of moisture to measurements at different times after casting, on sealed and saturated samples, cured at different temperatures. Water-binder ratio 0.55. Amount of chemically bounded water per amount of binder as a function of time after casting.

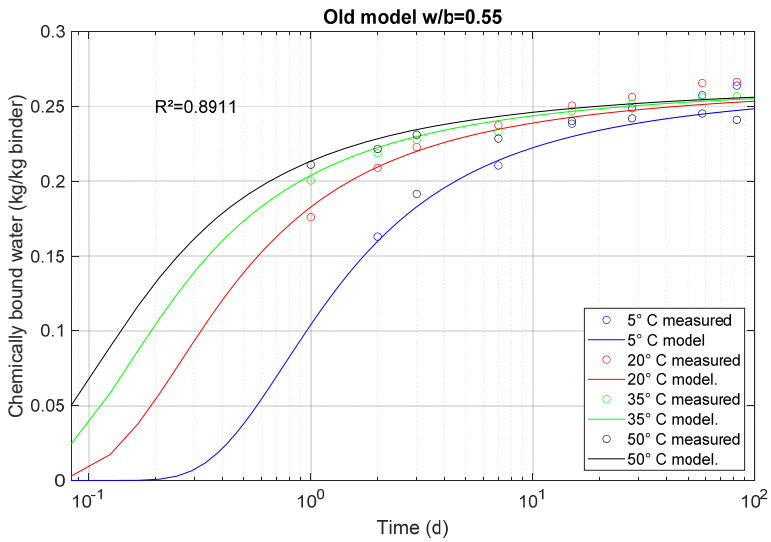

Figure 3.13. Adaptation of the reference model to measurements at different times after casting, on sealed and saturated samples, cured at different temperatures. Water-binder ratio 0.55. Amount of chemically bounded water per amount of binder as a function of time after casting.

3.2.5.4 Result summary

The coefficients of determination for all adaptations are summarized in Table 3.1.

Table 3.1. Coefficients of determination for all adaptations in this chapter.

Water-binder ratio	With moisture data and modeling in proposed model	Coefficient of determination R^2	
		Proposed model	Reference model (see section 3.2.5.1)
0.32	Yes	0.9563	0.8461
0.40	Yes	0.9490	0.9383
0.55	Yes	0.9635	0.8892
0.32	No	0.9791	0.9238
0.40	No	0.9849	0.9514
0.55	No	0.9826	0.8911

Based on the result diagrams, the proposed model seems to work as intended. The following observations summarize a few more specific aspects of the adaptations and the model comparison:

- **Temperature crossover** – the phenomenon of low temperature leading to low reaction rate but high end value of amount of chemical bounded water and high temperature to the opposite is well modeled for all water-binder ratios as well as for both the case with and without moisture control. This phenomenon is not modeled at all by the reference model.
- **Moisture control** – here the clear difference between the models is visible for water-binder ratio of 0.32. This is understandable due to the fact that this is the only case where water is clearly the limiting factor for the reaction.
- **Coefficients of determination** – the differences show clearly that the proposed model offers a better adaptation to the measured data. It shall also be observed that the higher levels of R2 for the non-moisture case are a result of a smaller data set, where only sealed samples were taken into the adaptation comparison.

3.3 Modeling of sorption

As earlier stated in sec. 1.8.2, the key goals of the desired sorption model are modeling of desorption, absorption and scanning with a primary dependency on a moisture potential and a secondary dependency on temperature not assuming access to measurements under different temperatures but only being based on theory. Construction of the proposed model fulfilling this requirements is based on the following steps:

1. Use of domain-based approach to sorption modeling.

2. Use of a matrix formulation of a bi-variate sorption site distribution with a flexible approach to number of adaptable parameters instead of a mathematical function with just a few.
3. Choice of a control variable, for description of wetting and drying history, connected directly to the properties/size of menisci defining the border between capillary condensed water and air in the pore system instead of a moisture potential.
4. Continuous formulation of the entire model utilizing integration over domains corresponding to the submatrices of the bi-variate sorption site distribution in order to evaluate the contents of physically bounded water for isothermal conditions
5. Extending the isothermal model to cover non-isothermal conditions

The following sections will describe in detail each step of the model building. Further some key computation and adaptation aspects will be presented as well as model validation based on a few sets of data.

3.3.1 Domain-based approach

The proposed model adopts a so called domain-based approach, a technique mentioned earlier in sec. 2.2.4.2. It uses a description of a concentration of sorption sites ordered in two dimensions according to two variables describing a desorption and an absorption condition, see equ. (3.20).

$$f(\varphi_d, \varphi_a) \tag{3.20}$$

where

$f(\varphi_d, \varphi_a)$ – is the concentration of sorption sites [kg/m³]

Administrating a history of state changes gives a possibility for integration of contributions from the sorption sites in various parts of the entire domain, corresponding to the specific state changes, as indicated in equ. (3.21).

$$w_{Ph} = \int_{History(\varphi_d, \varphi_a, \dots)} f(\varphi_d, \varphi_a) d\varphi_d \varphi_a \tag{3.21}$$

This enables full-scale modeling of desorption, absorption and scanning. Typical application of this approach uses relative humidity or some other moisture potential as the type of controlling variable for administration of desorption and absorption conditions. This does not take temperature into account. The proposed approach is different, in order to enable modeling of temperature dependency, which will be explained in section 3.3.3.

3.3.2 Bi-variate distribution

Two classes of proposed descriptions of the population of sorption sites have been proposed in literature, as already mentioned in the literature study in sections 2.2.3.3 and 2.2.4.2. One can build a model by proposing a specific mathematical function describing the sorption density for integration. Another approach is exemplified by the bi-variate pore size distribution, *Dullien & Dhawan 1975*, making use of a table or matrix, explicitly specifying volumes/masses of water involved for various combinations of pore sizes and pore entry sizes or, in a more generalized way, desorption and absorption conditions. The later variant is

chosen as a base for the proposed sorption model, mainly due to the larger amount of flexibility. In a matrix formulation, the number of rows/columns can be adapted to the resolution of the sorption curve measurements and give a large number of possible degrees of freedom in the model, as shown in Figure 3.14.

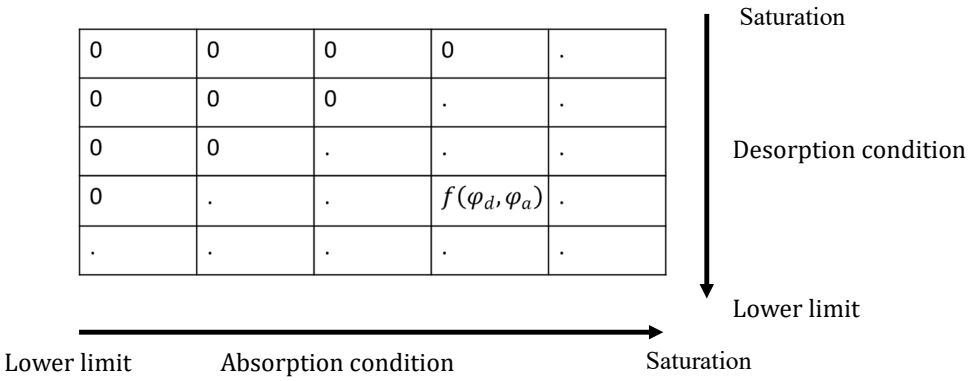

Figure 3.14. Matrix layout of the sorption site distribution with indicated interpretation of desorption and absorption conditions as well as the zero elements preventing mathematical reversing of hysteresis. Arrows are indicating the change of control variables during absorption and desorption.

One restriction that is adopted is that all matrix elements with a corresponding hydraulic pore radius smaller than the hydraulic entry radius are by definition zero. This is done to prevent modeling of absorption taking place at a lower humidity that at desorption, i.e. mathematical reversing of the hysteresis. Such a situation would imply that a sorption site, e.g. a pore, is both empty and filled at the same time, due to contradicting conditions for desorption and absorption.

3.3.3 Choosing meniscus property as dependency variable

In a domain based model, there is a need to administrate changes in drying/wetting of the concrete, in order to be able to evaluate the modeled value, see equ. (3.21). In isothermal conditions the typical choice of the variable to administrate the state changes of desorption and absorption is relative humidity. It is easy to handle during measurements and is mathematically well defined and easy to model. This results in a wetting/drying history being described as a set of steps in desorption and absorption, e.g. $History(\varphi_d, \varphi_a, \dots)$. In general, any variable being a monotonous function of any vapor potential, i.e. unambiguously describing wetting/drying change of state, will do. Because the goal of modeling is to in a later stage allow for taking temperature variation in account, a different choice of control variable is done.

As earlier mentioned in section 2.2.2, the physical border between the empty and water filled parts of the pore system is defined by menisci holding the capillary condensed water in place. The size of meniscus that is supported by the conditions is by equ. (2.36) dependent on capillary pressure, a function of temperature and relative humidity, and surface tension of water, a function of temperature. This makes the size of meniscus a good expression of

wetting/drying condition in non-isothermal conditions. It captures the underlying thermodynamical dependencies by being an unambiguous function of both involved potentials, i.e. relative humidity and temperature, and each pore has meniscus radii corresponding to filling and emptying of the pore.

To later allow for accurate modeling of hydraulic condition for capillary condensation and thus separating influence of adsorption and capillary condensation, some size property of the hydraulic radius corresponding to the temperature and relative humidity or any other vapor potential is favorable to be selected as control variable. A sorption site will typically have a desorption value and an absorption value for the selected radius property. The exact geometrical interpretation will of course depend on the pore shape/type behind, but that doesn't have to be known by the model as long as there is site density connected to the desorption and absorption criteria expressed in radii. In such a case, the criteria will automatically become a function of both relative humidity and temperature, according to the earlier equation (2.39) given also below as equ. (3.22). One should observe that the surface tension of water σ in the equation above also has a dependency on the temperature.

$$r_h(\varphi, T) = \frac{2\sigma}{-\varrho_w R_v T \ln \varphi} \tag{3.22}$$

However, the direct choice of the hydraulic radius is not problem free from the point of view of mathematical modeling. The hydraulic radius of the condensed water at a relative humidity of 100% is by definition infinite and infinities are not well suited for numerical calculations. In order to avoid this situation but still work with a value describing the same criterion, some other property of the meniscus, connected to the radius has to be used.

In mathematics, while describing geometrical properties of plane curves, two measures are used to express how much the curve tends to bend. One is curvature and the other is radius of curvature, see e.g. *Råde & Westergren 2004*. Beside the fact that curvature has a sign and indicate both in which direction and how much the curve bends but the radius is only a positive value indicating in a different way how much the curve bends, they are inverses of each other. This relation will be used to select a mathematically convenient control variable in the domain based model in this thesis.

In order to avoid handling infinite meniscus radii, the inverse of the radius is chosen as a control variable for administrating wetting/drying history. Inspired by the mathematical relation for plane curves, the variable will be referred to as *hydraulic curvature of the meniscus*, or simplified *meniscus curvature*, and is given by equ. (3.23).

$$c(\varphi, T) = \frac{1}{r_h} = \frac{-\varrho_w R_v T \ln \varphi}{2\sigma} \tag{3.23}$$

$c(\varphi, T)$ – hydraulic curvature of meniscus [1/m], a function of relative humidity and temperature

The value of the meniscus curvature at the endpoint at 100% RH becomes zero and the modeling of the other end of the RH scale, i.e. 0% RH that would result in an infinity, is not

of interest in the intended application. Some principles, regarding how this new variable works in reality, are summarized below:

- Saturation is equivalent to no meniscus curvature at all, i.e. $c = 0$.
- The driest condition modeled has to be chosen. Here, the border condition between chemically and physically bounded water is used $c_{max} = c(11\%\ RH,\ 20\ °C)$.
- The spanning interval for c, on which absorption and desorption will be described by the matrix entries becomes $[0;\ c_{max}]$.
- Desorption implies increase of c, i.e. $c_x \rightarrow c_{x+1}$ where $c_x < c_{x+1}$
- Absorption implies decrease of c, i.e. $c_x \rightarrow c_{x+1}$ where $c_x > c_{x+1}$

For the isothermal case, this will just be an unusual choice of a control variable reflecting only changes in relative humidity. For the non-isothermal case, modeling of a border between parts of pore system that are filled with condensed water resp. empty with adsorbed water on the walls, will be enabled as shown further in section 3.3.13.

3.3.4 Continuous formulation for isothermal conditions

To ensure a smooth result in evaluation of the physically bounded water with respect to continuity of both its value and derivatives, a continuous formulation is adapted. The matrix representation of the bi-variate sorption site distribution does not represent amount of physically bounded water, but a second order mixed derivative of the amount of physically bounded water with respect to both sorption conditions modeled as the dimensions of the matrix, see Figure 3.15.

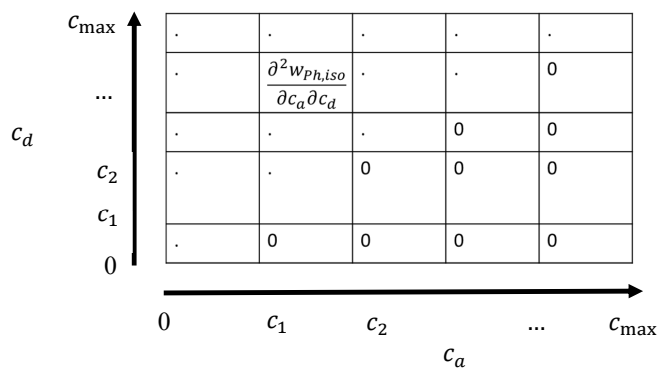

Figure 3.15. Proposed matrix layout of the sorption site distribution as a function of desorption and absorption conditions described with meniscus curvature of capillary condensed water. Observe that the dimensions have new direction and the zero elements new positions in the matrix, compared to Figure 3.14.

In this matrix layout, each column corresponds to an interval between two absorption conditions, i.e. two meniscus curvature values, and each row to an interval between two desorption conditions. The entire matrix spans from meniscus curvature of 0, corresponding to saturation, to a maximum meniscus curvature of c_{max}, corresponding to 11% relative humidity at 20 ºC as defined in section 3.3.3. The borders between the rows and columns are

given by the selection of meniscus curvature values $[\,0, c_1, c_2, \ldots c_{\max}]$. Each entry in the matrix defines the constant value of $\frac{\partial^2 w_{Ph}}{\partial c_a \partial c_d}$ for the domain corresponding to the combination of absorption and desorption meniscus curvature intervals for the entry's row and column borders.

This arrangement allows for integration in two dimensions over the matrix as a domain in order to evaluate the amount of physically bounded water for any sorption history, as indicated in equ. (3.24).

$$w_{Ph,iso} = \int_{History(c_d,c_a,\ldots)} \frac{\partial^2 w_{Ph,iso}}{\partial c_a \partial c_d} dc_a dc_d \qquad (3.24)$$

where

$w_{Ph,iso}$ – is physically bounded water in isothermal modeling conditions [kg/m^3]

The evaluation procedure is based on *Derluyn et al 2012*. Here it is adapted to the new definition of sorption coordinate and the fact that modeling always start from saturation for drying concrete. In the next section a step by step approach to an example drying and wetting history is given, in order to visualize how the procedure works. Further sections formalize the procedure into an algorithm for administrating and updating the state history as well as for integral evaluation of a generalized state history.

3.3.5 Evaluation from a simple history

The starting step of an evaluation is always saturation. This state corresponds to the integral of all sorption sites, i.e. over the entire domain except for $c_a > c_d$, which prevents inverted hysteresis. The situation is shown in Figure 3.16.

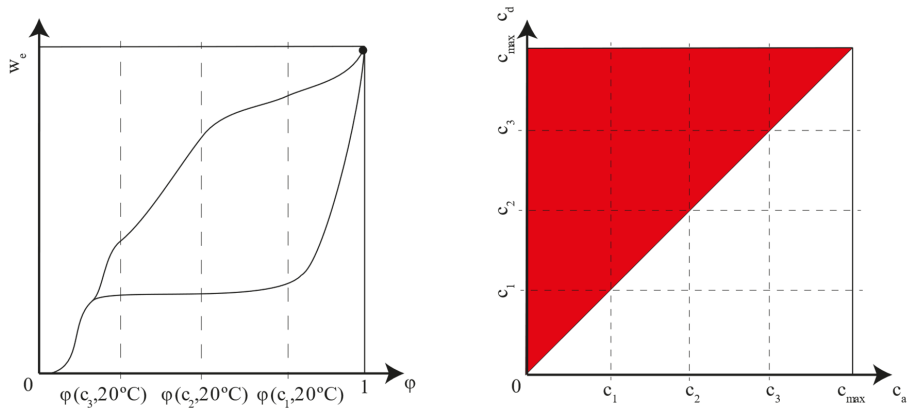

Figure 3.16. State of full saturation. Sorption isotherms at 20 ºC to the left and integration domain to the right. Black dot marks the state in the isotherm diagram and the red area in the domain diagram.

The state history has by this received its starting step, absorption to meniscus curvature 0.

$$History = [Abs \rightarrow 0] \qquad (3.25)$$

The corresponding total amount of physically bounded water consists of one integral term and is given by equ. (3.26).

$$w_{Ph,iso} = \int_0^{c_{max}} \int_{c_a}^{c_{max}} \frac{\partial^2 w_{Ph,iso}}{\partial c_a \partial c_d} dc_d \, dc_a \tag{3.26}$$

The second step is the start of desorption and it takes the meniscus curvature down to c_1, see Figure 3.17.

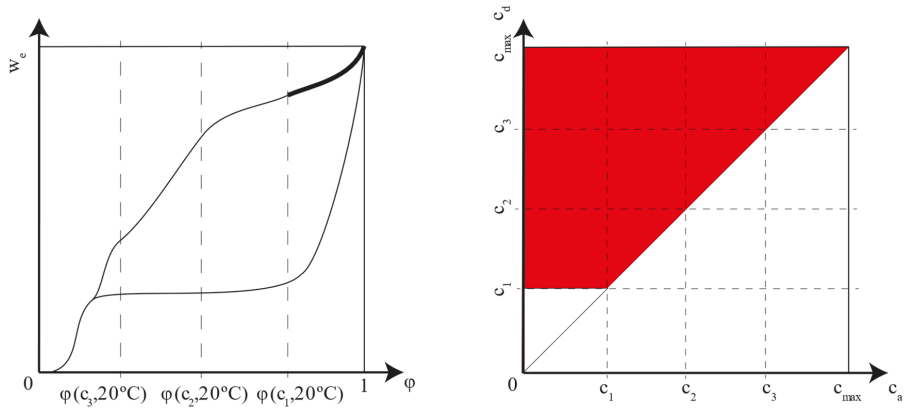

Figure 3.17. First desorption step to c_1. Sorption isotherms at 20 ºC to the left and integration domain to the right. Thick part of the isotherms marks the history in the isotherm diagram and the red area the corresponding domain in the domain diagram. Observe that the integration domain is now reduced by a triangle from 0 to c_1.

The updated state history has now two steps, as seen below.

$$History = [Abs \rightarrow 0, Des \rightarrow c_1] \tag{3.27}$$

The corresponding total amount of physically bounded water has now two terms, each corresponding to the two steps in the history:

$$w_{Ph,iso} = \int_0^{c_{max}} \int_{c_a}^{c_{max}} \frac{\partial^2 w_{Ph,iso}}{\partial c_a \partial c_d} dc_d \, dc_a - \int_0^{c_1} \int_{c_a}^{c_1} \frac{\partial^2 w_{Ph,iso}}{\partial c_a \partial c_d} dc_d \, dc_a \tag{3.28}$$

In the third step, the desorption continues further down to a meniscus curvature of c_3. This does not imply a new step in the history or the integration. The last step describing desorption is simply enlarged from the earlier limit of c_1 to the new limit of c_3, as seen in Figure 3.18.

The updated state history reflects this change:

$$History = [Abs \rightarrow 0, Des \rightarrow c_3] \tag{3.29}$$

as well as the total amount of physically bounded water:

$$w_{Ph,iso} = \int_0^{c_{max}} \int_{c_a}^{c_{max}} \frac{\partial^2 w_{Ph,iso}}{\partial c_a \partial c_d} dc_d \, dc_a - \int_0^{c_3} \int_{c_a}^{c_3} \frac{\partial^2 w_{Ph,iso}}{\partial c_a \partial c_d} dc_d \, dc_a \tag{3.30}$$

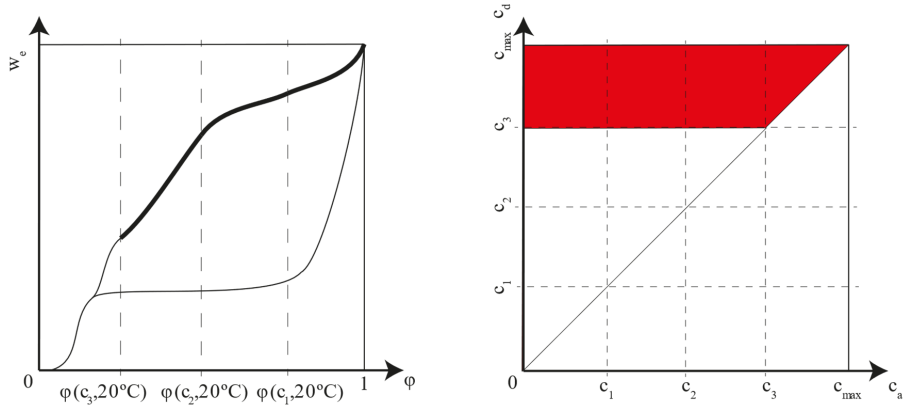

Figure 3.18. Second desorption step to c_3. Sorption isotherms at 20 ºC to the left and integration domain to the right. Thick part of the isotherms marks the history in the isotherm diagram and the red area the corresponding domain in the domain diagram. Observe that previous triangle that reduced the integration domain is now enlarged to a triangle from 0 to c_3.

In the fourth step, absorption up to c_1 is performed. This takes the system into scanning along a scanning isotherm, as clearly seen in Figure 3.19. A corresponding triangular region between c_3 and c_1 is added to the integration domain to reflect this change.

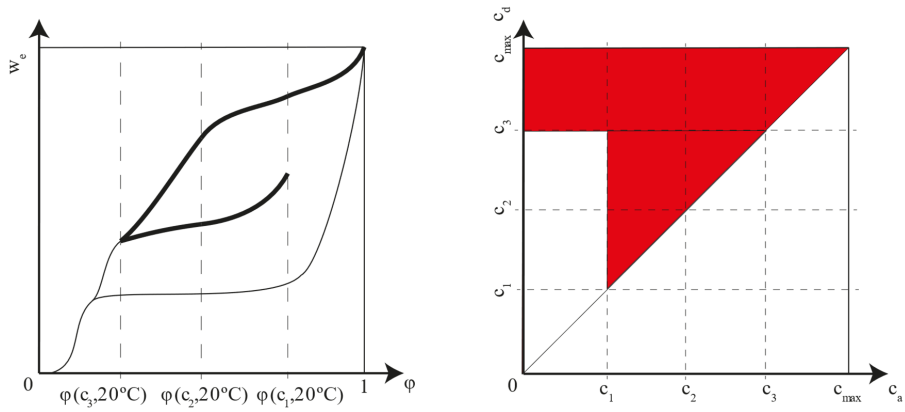

Figure 3.19. Absorption step to c_1, taking the system into scanning. Sorption isotherms at 20 ºC to the left and integration domain to the right. Thick part of the isotherms marks the history in the isotherm diagram and the red area the corresponding domain in the domain diagram. Now a red triangle from c_1 to c_3 is added to the previous integration domain.

The state history receives a new step to describe the change of direction in sorption:

$$History = [Abs \rightarrow 0, Des \rightarrow c_3, Abs \rightarrow c_1] \qquad (3.31)$$

The total amount of physically bounded water consists now of three integrals, one for each step in the history:

$$w_{Ph,iso} = \int_0^{c_{max}} \int_{c_a}^{c_{max}} \frac{\partial^2 w_{Ph,iso}}{\partial c_a \partial c_d} dc_d\, dc_a - \int_0^{c_3} \int_{c_a}^{c_3} \frac{\partial^2 w_{Ph,iso}}{\partial c_a \partial c_d} dc_d\, dc_a +$$

$$\int_{c_1}^{c_3}\int_{c_a}^{c_3}\frac{\partial^2 w_{Ph,iso}}{\partial c_a \partial c_d}dc_d\,dc_a \tag{3.32}$$

The fifth step consists of a desorption to a meniscus curvature of c_2. The system is still in scanning, but now drying, see Figure 3.20. The corresponding triangle between c_1 and c_2 is now removed from the integration domain.

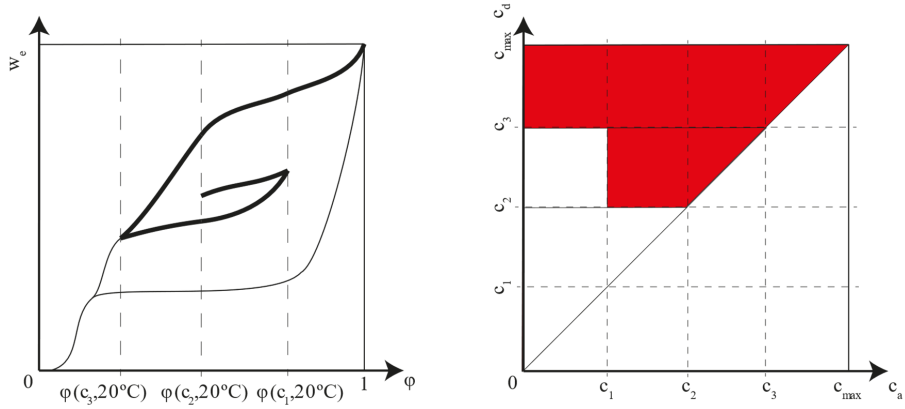

Figure 3.20. Desorption scanning step to c_2. Sorption isotherms at 20 ºC to the left and integration domain to the right. Thick part of the isotherms marks the history in the isotherm diagram and the red area the corresponding domain in the domain diagram. A new triangle from c_1 to c_2 is removed from the previous integration domain.

The state history receives a new desorption entry and consists now of four steps:

$$History = [Abs \rightarrow 0, Des \rightarrow c_3, Abs \rightarrow c_1, Des \rightarrow c_2] \tag{3.33}$$

The total amount of physically bounded water has consequently four corresponding integral terms:

$$w_{Ph,iso} = \int_0^{c_{max}}\int_{c_a}^{c_{max}}\frac{\partial^2 w_{Ph,iso}}{\partial c_a \partial c_d}dc_d\,dc_a - \int_0^{c_3}\int_{c_a}^{c_3}\frac{\partial^2 w_{Ph,iso}}{\partial c_a \partial c_d}dc_d\,dc_a +$$

$$\int_{c_1}^{c_3}\int_{c_a}^{c_3}\frac{\partial^2 w_{Ph,iso}}{\partial c_a \partial c_d}dc_d\,dc_a - \int_{c_1}^{c_2}\int_{c_a}^{c_2}\frac{\partial^2 w_{Ph,iso}}{\partial c_a \partial c_d}dc_d\,dc_a \tag{3.34}$$

The sixth step, last in this example, continues the desorption all the way to c_3. This closes the scanning loop and brings the system back to the desorption isotherm. Accordingly, the integration domain is restored to the same as for the initial desorption to c_3, see Figure 3.21.

The last desorption step in the previous state history is enlarged all the way down to c_3. But there is already a preceding desorption step to this meniscus curvature, which means that the history can be simplified by removing the steps after the first desorption to c_3, i.e. eliminating the scanning loop:

$$History = [Abs \rightarrow 0, \boldsymbol{Des \rightarrow c_3}, Abs \rightarrow c_1, \boldsymbol{Des \rightarrow c_3}] = [Abs \rightarrow 0, Des \rightarrow c_3] \tag{3.35}$$

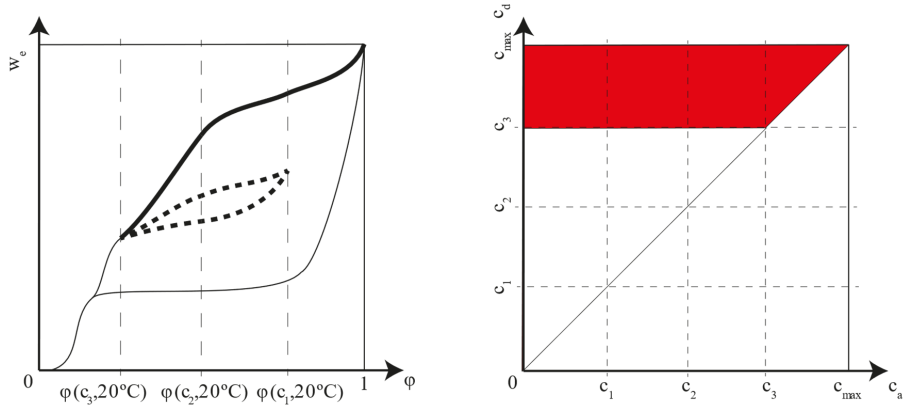

Figure 3.21. Further desorption step to c_3, returning to the desorption isotherm and effectively removing the scanning loop. Sorption isotherms at 20 ºC to the left and integration domain to the right. Thick part of the isotherms marks the history in the isotherm diagram and the red area the corresponding domain in the domain diagram. The earlier integration domain corresponding to desorption to c_3 is now restored.

The corresponding total amount of physically bounded water is after the simplification of the state history by elimination of the scanning loop, again given by two integral terms:

$$w_{Ph,iso} = \int_0^{c_{max}} \int_{c_a}^{c_{max}} \frac{\partial^2 w_{Ph,iso}}{\partial c_a \partial c_d} dc_d\, dc_a - \int_0^{c_3} \int_{c_a}^{c_3} \frac{\partial^2 w_{Ph,iso}}{\partial c_a \partial c_d} dc_d\, dc_a \qquad (3.36)$$

It is important at this stage to notice that the model above lack some possibility to direct physical interpretation. The history of the control variable will correctly describe on the integration domain the functional border between the part of the pore system that is filled will capillary condensed water and the part that is not. This however does not imply that the sorption site concentration, that is integrated in order to evaluate the amount of water, corresponds to capillary condensed water only. The integral expresses the total amount of physically bounded water, i.e. both capillary condensed water on one side of the functional border as well as adsorbed water on the other. In the isothermal case, this model is simply a convenient way of flexible modeling of variation of active sorption sites as a function of wetting/drying history due to both physical phenomena involved at the same time. This will however change in the non-isothermal case, as later shown in section 3.3.13.

3.3.6 Administrating state change

In practice the state changes are normally described as changes in the moisture potential Δφ and in the non-isothermal case also the temperature ΔT. As both these values contribute to the change in meniscus curvature, a new meniscus curvature value has to be calculated and the total change in the meniscus curvature value decides if the state change is absorption or desorption.

$$\Delta c = c(\varphi + \Delta\varphi, T + \Delta T) - c(\varphi, T) \qquad (3.37)$$

Administrating the state change follows a few basic principles. It starts at saturation. If there is a change between wetting and drying, a new step is added. If drying or wetting continues, the last step is simply adjusted to a new meniscus curvature. After all changes, an attempt to

simplify the history is done in order to try to eliminate possible closed loops, i.e. scanning or a full absorption to saturation again. The formal algorithm is given below:

- Start
  - Starting state of the history is always saturation History= $[Abs \rightarrow 0]$
- Desorption $c_x \rightarrow c_{x+1}$ where $c_x < c_{x+1}$
  - If the preceding step is desorption, i.e. History= $[\dots, Des \rightarrow c_x]$
    - Enlarge the last desorption step by changing c_x to c_{x+1}.
    - No new step.
    - Try to simplify.
  - If the preceding step is absorption, i.e. History= $[\dots, Abs \rightarrow c_x]$
    - Add a new desorption step, i.e. History= $[\dots, Abs \rightarrow c_x, Des \rightarrow c_{x+1}]$.
    - Try to simplify.
- Absorption $c_x \rightarrow c_{x+1}$ where $c_x > c_{x+1}$
  - If the preceding step is absorption, i.e. History= $[\dots, Abs \rightarrow c_x]$
    - Enlarge the last absorption step by changing c_x to c_{x+1}.
    - No new step.
    - Try to simplify.
  - If the preceding step is desorption, i.e. History= $[\dots, Des \rightarrow c_x]$
    - Add a new absorption step, i.e. History= $[\dots, Des \rightarrow c_x, Abs \rightarrow c_{x+1}]$.
    - Try to simplify.
- Simplification
  - If the last step is desorption and there is a previous desorption step with a meniscus curvature equal to or smaller than the last step, i.e. History= $[\dots, Des \rightarrow c_x, \dots, Des \rightarrow c_y]$ where $c_y \geq c_x$
    - Remove all steps after the older desorption step $Des \rightarrow c_x$, adjusting its meniscus curvature to c_y if $c_y > c_x$, i.e. History= $[\dots, Des \rightarrow c_x = c_y, \sout{\dots, Des \rightarrow c_y}] = [\dots, Des \rightarrow c_y]$
    - Try to simplify again.
  - If the last step is absorption and there is a previous absorption step with a meniscus curvature equal to or larger than the last step, i.e. History= $[\dots, Abs \rightarrow c_x, \dots, Abs \rightarrow c_y]$ where $c_y \leq c_x$
    - Remove all steps after the older absorption step $Abs \rightarrow c_x$, adjusting its meniscus curvature to c_y if $c_y < c_x$, i.e. History= $[\dots, Abs \rightarrow c_x = c_y, \sout{\dots, Abs \rightarrow c_y}] = [\dots, Abs \rightarrow c_y]$
    - Try to simplify again.

3.3.7 Evaluation from a general history

As seen in the earlier example in sec. 3.3.5, each step in the state history results in an integral over a triangular domain and the sum of all contributions gives the total amount of physically bounded water. Generalization of this approach to any given history is given as a summation formula in equ. (3.38).

$$w_{Ph,iso} = \int_{History(c_d,c_a,\dots)} \frac{\partial^2 w_{Ph,iso}}{\partial c_a \partial c_d} dc_a dc_d = \sum_{History(c_d,c_a,\dots)} \Delta w_{Ph,iso}(Step_x) \quad (3.38)$$

The contribution for the starting step of absorption to saturation is:

$$\Delta w_{Ph,iso}(Abs: 0) = \int_0^{c_{max}} \int_{c_a}^{c_{max}} \frac{\partial^2 w_{Ph,iso}}{\partial c_a \partial c_d} dc_d \, dc_a \quad (3.39)$$

The contribution for a desorption step is:

$$\Delta w_{Ph,iso}(Des: c_x) = -\int_{c_{x-1}}^{c_x} \int_{c_a}^{c_x} \frac{\partial^2 w_{Ph,iso}}{\partial c_a \partial c_d} dc_d \, dc_a \quad (3.40)$$

The contribution for an absorption step is:

$$\Delta w_{Ph,iso}(Abs: c_x) = \int_{c_x}^{c_{x-1}} \int_{c_a}^{c_{x-1}} \frac{\partial^2 w_{Ph,iso}}{\partial c_a \partial c_d} dc_d \, dc_a \quad (3.41)$$

3.3.8 Adaptation to measured data – initial considerations

The presented model allows mathematically for a significant number of degrees of freedom. All diagonal elements and all elements on one side of the diagonal of the matrix can be adapted. For a matrix of dimension n this gives $(n+1)n/2$ elements. Another element of choice in the adaptation is the sequence of meniscus curvature values, used as a base for the matrix interpretation and defining the dimension of the matrix. The situation can be summarized as a potentially undetermined mathematical problem –with more degrees of freedom than a typical amount of constraints from sorption measurements. This opens up for a multitude of adaptation methods. It is not the ambition of this work to take a, in any sense, complete look at this adaptation problem. Below, some observations about some aspects of the matrix are done. These are further used to propose two adaptation methods for two specific situations regarding availability of measurement data, see section 3.3.9 and 3.3.10. Later, a flexible manipulation operation on an existing matrix is defined that can be further adapted to adjust the matrix elements to scanning measurements, see section 3.3.11. Finally, a generalized approach to adaptation in isothermal conditions is investigated, see section 3.3.12, and some considerations regarding necessary model extensions to fully cover non-isothermal conditions from phenomenological perspective are discussed, see 3.3.13.

Two observations are fundamental, to easily populate the matrix elements with values based on the probably most common sorption measurements – desorption and absorption curves. There is a structural correspondence between these two curves and the matrix of the proposed model. Assuming the same set of meniscus curvature steps for both curves

$$[0, c_1, \dots, c_{max}]$$

let the corresponding water contents for the desorption curve be given by

$$[\, w_d(0), w_d(c_1), \dots, w_d(c_{max})]$$

and for the absorption curve by

$$[\, w_a(0), w_a(c_1), \dots, w_a(c_{max})]$$

The structural connection to the model matrix is that the integration of the water contents over each row of the matrix gives the water contents difference between the corresponding desorption steps and the integration of the water contents over each column of the matrix gives the water contents difference between the corresponding absorption steps.

In order to visualize this, five desorption steps and their corresponding domains of integration are shown in Figure 3.22, starting at saturation and ending at an empty pore system at the chosen meniscus curvature c_{max}. The integrals over the matrix giving the water contents at the desorption steps are:

$$w_d(0) = \int_0^{c_{max}} \int_{c_a}^{c_{max}} \frac{\partial^2 w_{Ph,iso}}{\partial c_a \partial c_d} dc_d\, dc_a - \int_0^{0} \int_{c_a}^{0} \frac{\partial^2 w_{Ph,iso}}{\partial c_a \partial c_d} dc_d\, dc_a$$

$$= \int_0^{c_{max}} \int_{c_a}^{c_{max}} \frac{\partial^2 w_{Ph,iso}}{\partial c_a \partial c_d} dc_d\, dc_a$$

$$w_d(c_1) = \int_0^{c_{max}} \int_{c_a}^{c_{max}} \frac{\partial^2 w_{Ph,iso}}{\partial c_a \partial c_d} dc_d\, dc_a - \int_0^{c_1} \int_{c_a}^{c_1} \frac{\partial^2 w_{Ph,iso}}{\partial c_a \partial c_d} dc_d\, dc_a$$

$$w_d(c_2) = \int_0^{c_{max}} \int_{c_a}^{c_{max}} \frac{\partial^2 w_{Ph,iso}}{\partial c_a \partial c_d} dc_d\, dc_a - \int_0^{c_2} \int_{c_a}^{c_2} \frac{\partial^2 w_{Ph,iso}}{\partial c_a \partial c_d} dc_d\, dc_a$$

$$w_d(c_3) = \int_0^{c_{max}} \int_{c_a}^{c_{max}} \frac{\partial^2 w_{Ph,iso}}{\partial c_a \partial c_d} dc_d\, dc_a - \int_0^{c_3} \int_{c_a}^{c_3} \frac{\partial^2 w_{Ph,iso}}{\partial c_a \partial c_d} dc_d\, dc_a$$

$$w_d(c_{max}) = \int_0^{c_{max}} \int_{c_a}^{c_{max}} \frac{\partial^2 w_{Ph,iso}}{\partial c_a \partial c_d} dc_d\, dc_a - \int_0^{c_{max}} \int_{c_a}^{c_{max}} \frac{\partial^2 w_{Ph,iso}}{\partial c_a \partial c_d} dc_d\, dc_a = 0$$

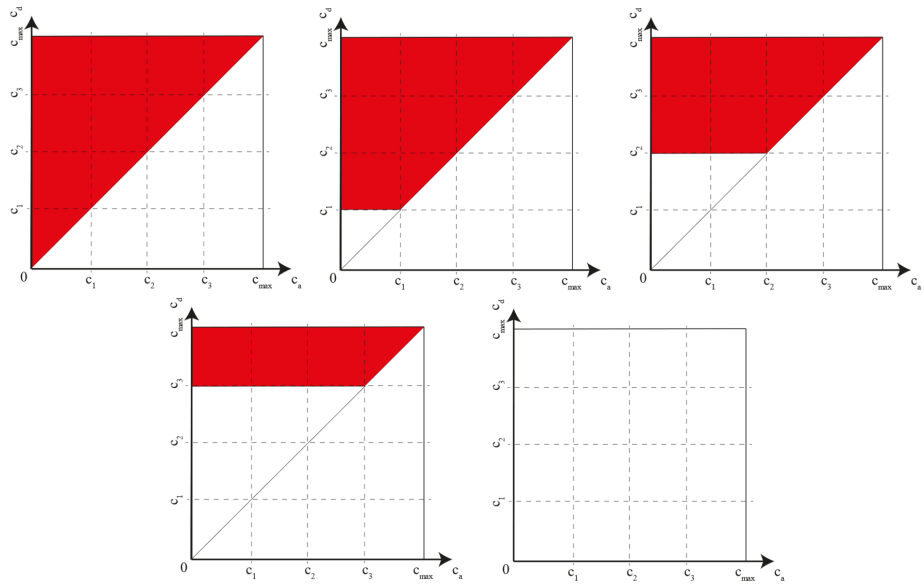

Figure 3.22. Integration domains corresponding to the desorption steps $w_d(0)$, $w_d(c_1)$, $w_d(c_2)$, $w_d(c_3)$ and $w_d(c_{max})$.

Taking the differences between these equations gives:

$$w_d(0) - w_d(c_1) = \int_0^{c_1} \int_{c_a}^{c_1} \frac{\partial^2 w_{Ph,iso}}{\partial c_a \partial c_d} dc_d\, dc_a$$

$$w_d(c_1) - w_d(c_2) = -\int_0^{c_1} \int_{c_a}^{c_1} \frac{\partial^2 w_{Ph,iso}}{\partial c_a \partial c_d} dc_d\, dc_a + \int_0^{c_2} \int_{c_a}^{c_2} \frac{\partial^2 w_{Ph,iso}}{\partial c_a \partial c_d} dc_d\, dc_a$$

$$w_d(c_2) - w_d(c_3) = -\int_0^{c_2} \int_{c_a}^{c_2} \frac{\partial^2 w_{Ph,iso}}{\partial c_a \partial c_d} dc_d\, dc_a + \int_0^{c_3} \int_{c_a}^{c_3} \frac{\partial^2 w_{Ph,iso}}{\partial c_a \partial c_d} dc_d\, dc_a$$

$$w_d(c_3) - w_d(c_{max}) = -\int_0^{c_3} \int_{c_a}^{c_3} \frac{\partial^2 w_{Ph,iso}}{\partial c_a \partial c_d} dc_d\, dc_a + \int_0^{c_{max}} \int_{c_a}^{c_{max}} \frac{\partial^2 w_{Ph,iso}}{\partial c_a \partial c_d} dc_d\, dc_a$$

which is the explicit connection between the desorption steps and the contents integrals over each row of the matrix, as visualized by the integration domains in Figure 3.23.

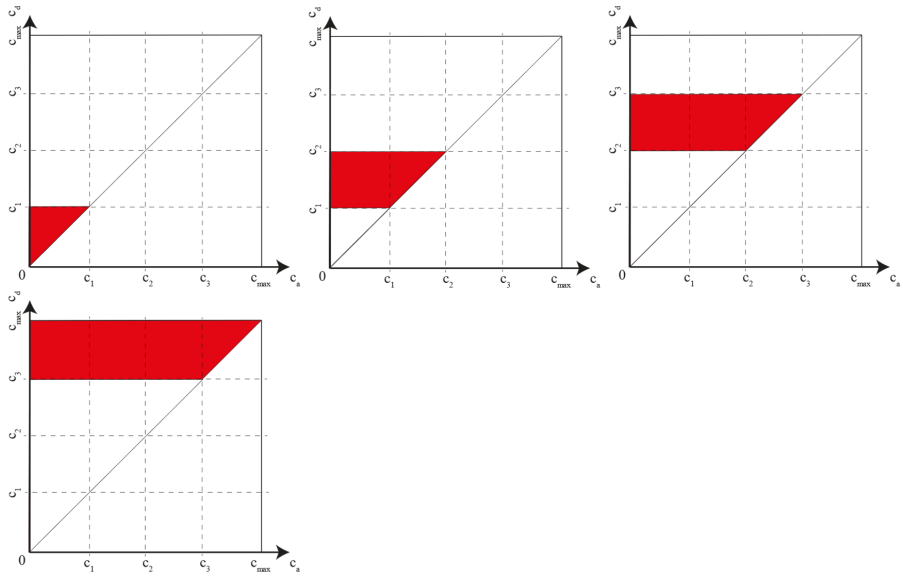

Figure 3.23. Integration domains corresponding to the differences between the desorption steps $w_d(0) - w_d(c_1)$, $w_d(c_1) - w_d(c_2)$, $w_d(c_2) - w_d(c_3)$ *and* $w_d(c_3) - w_d(c_{max})$.

A similar explanation can be given for the absorption case, with five steps shown in Figure 3.24. The integrals over the matrix giving the water contents at the absorption steps are:

$$w_a(c_{max}) = \int_{c_{max}}^{c_{max}} \int_{c_a}^{c_{max}} \frac{\partial^2 w_{Ph,iso}}{\partial c_a \partial c_d} dc_d\, dc_a = 0$$

$$w_a(c_3) = \int_{c_3}^{c_{max}} \int_{c_a}^{c_{max}} \frac{\partial^2 w_{Ph,iso}}{\partial c_a \partial c_d} dc_d\, dc_a$$

$$w_a(c_2) = \int_{c_2}^{c_{max}} \int_{c_a}^{c_{max}} \frac{\partial^2 w_{Ph,iso}}{\partial c_a \partial c_d} dc_d\, dc_a$$

$$w_a(c_1) = \int_{c_1}^{c_{max}} \int_{c_a}^{c_{max}} \frac{\partial^2 w_{Ph,iso}}{\partial c_a \partial c_d} dc_d\, dc_a$$

$$w_a(0) = \int_{0}^{c_{max}} \int_{c_a}^{c_{max}} \frac{\partial^2 w_{Ph,iso}}{\partial c_a \partial c_d} dc_d\, dc_a$$

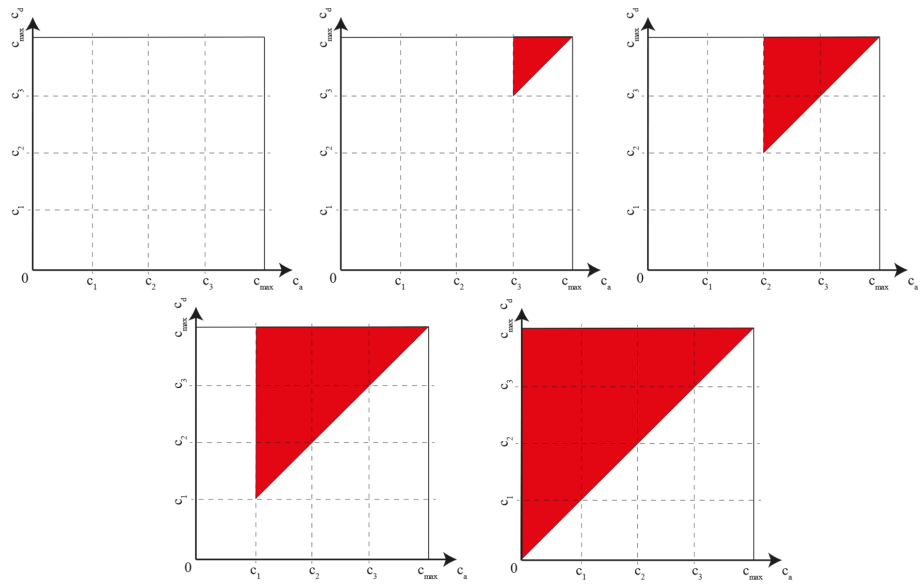

Figure 3.24. Integration domains corresponding to the absorption steps $w_a(c_{max})$, $w_a(c_3)$, $w_a(c_2)$, $w_a(c_1)$ and $w_a(0)$.

Taking the differences between these equations gives:

$$w_a(0) - w_a(c_1) = \int_0^{c_{max}} \int_{c_a}^{c_{max}} \frac{\partial^2 w_{Ph,iso}}{\partial c_a \partial c_d} dc_d\, dc_a - \int_{c_1}^{c_{max}} \int_{c_a}^{c_{max}} \frac{\partial^2 w_{Ph,iso}}{\partial c_a \partial c_d} dc_d\, dc_a$$

$$w_a(c_1) - w_a(c_2) = \int_{c_1}^{c_{max}} \int_{c_a}^{c_{max}} \frac{\partial^2 w_{Ph,iso}}{\partial c_a \partial c_d} dc_d\, dc_a - \int_{c_2}^{c_{max}} \int_{c_a}^{c_{max}} \frac{\partial^2 w_{Ph,iso}}{\partial c_a \partial c_d} dc_d\, dc_a$$

$$w_a(c_2) - w_a(c_3) = \int_{c_2}^{c_{max}} \int_{c_a}^{c_{max}} \frac{\partial^2 w_{Ph,iso}}{\partial c_a \partial c_d} dc_d\, dc_a - \int_{c_3}^{c_{max}} \int_{c_a}^{c_{max}} \frac{\partial^2 w_{Ph,iso}}{\partial c_a \partial c_d} dc_d\, dc_a$$

$$w_a(c_3) - w_a(c_{max}) = \int_{c_3}^{c_{max}} \int_{c_a}^{c_{max}} \frac{\partial^2 w_{Ph,iso}}{\partial c_a \partial c_d} dc_d\, dc_a$$

which is the explicit connection between the desorption steps and the contents integrals over each row of the matrix, as visualized by the integration domains in Figure 3.25.

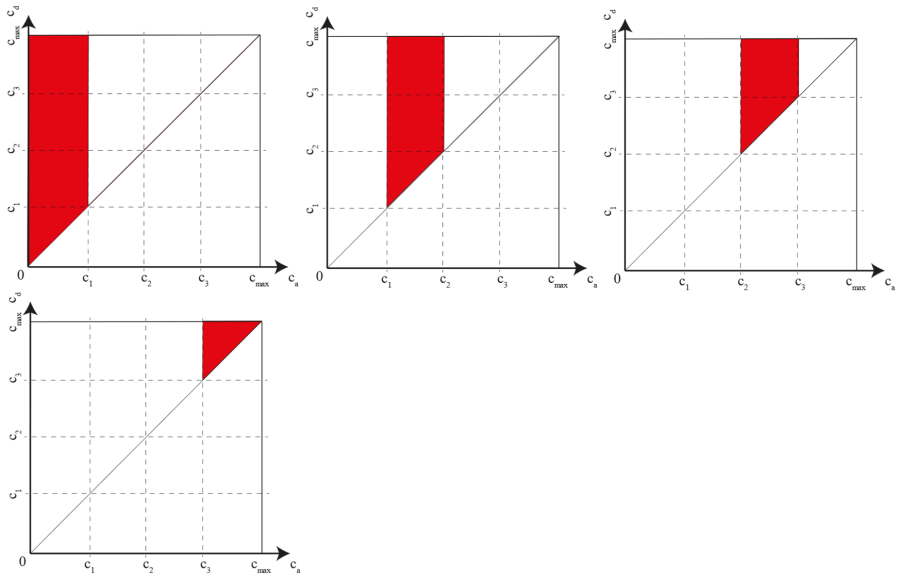

Figure 3.25. Integration domains corresponding to the differences between the absorption steps $w_a(0) - w_a(c_1)$, $w_a(c_1) - w_a(c_2)$, $w_a(c_2) - w_a(c_3)$ *and* $w_a(c_3) - w_a(c_{max})$.

Summarizing the reasoning above gives the following conclusions:

- Each cell of the matrix corresponds to a rectangular integration domain in the space spanned by c_a and c_d.
- Only elements on one side of the diagonal are used to prevent mathematically reversing the hysteresis.
- Integration domains for the diagonal elements are thus only half compared to the ordinary non-zero cells, i.e. are corresponding to only one side of the diagonal.
- Integrating the sorption density (constant in each cell) over the domain of the cell gives the corresponding water amount.
- Summing up water amount over an entire row gives the difference between water amounts for the corresponding desorption steps.
- Summing up water amount over an entire column gives the difference between water amounts for the corresponding absorption steps.

These conclusions shall be used below in construction of algorithms for selection of matrix elements and adapting the model to measured data.

3.3.9 Adaptation to one sorption isotherm

A typical, simple set of sorption data is only one sorption isotherm, used as both desorption and absorption. In such a case there is no data supporting hysteresis and a reasonable conclusion of that is that the model should not produce any scanning effects. As will be shown below, this is not possible with the proposed model. The model will, due to its mathematics, always produce some hysteresis and scanning, at least between the measurement

data. This is simplest to visualize by a short illustration of a test set of data given based on only two meniscus curvatures $[0, c_{max}]$ having the water contents $[\, w(0), w(c_{max}) = 0\,]$, assuming equality between desorption and absorption measurements. i.e. $w_a(c) = w_d(c) = w(c)$. For this situation, let's use the simplest model representation by a matrix of only one element, where the column and row borders correspond to the only two meniscus curvature values from the measured data $[0, c_{max}]$. This situation is illustrated in Figure 3.26, where the corresponding integration domains for successive absorption and desorption steps are shown.

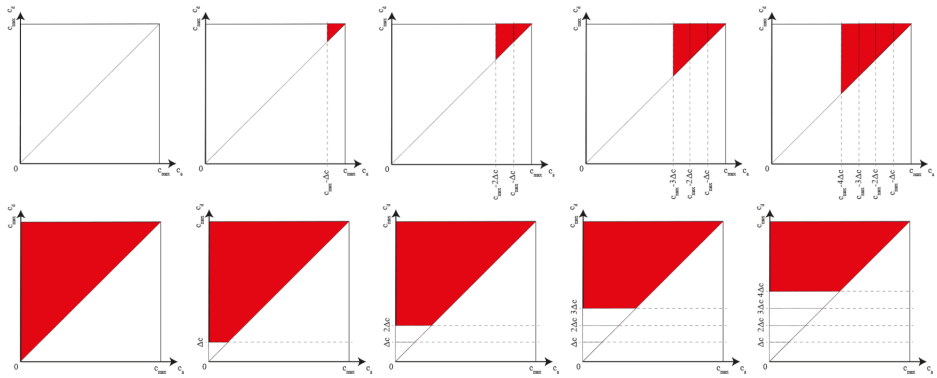

Figure 3.26. Successive decrease of integration domain during desorption (lower row) and increase during absorption (upper row) for a model with one element sorption site matrix. Observe that the integration domain increases or decreases with the area of a triangle with both base and height equal to the change in the control variable (meniscus curvature), which implies quadratic dependency of the constant integral over the region on the control variable.

The matrix is containing only one element. In order to get the measured water contents at full saturation, i.e. for the integration over the entire triangular region between 0 and c_{max} to give $w(0)$, the only one matrix element representing the concentration of the sorption sites $\frac{\partial^2 w_{Ph,iso}}{\partial c_a \partial c_d}$ will obviously have to be $\frac{2w(0)}{c_{max}^2}$. As shown in the visualization in the integration domains in Figure 3.26, there is a quadratic relation between the area of the integration domain and the control variable which together with constant sorption site concentration give the result value the same dependency. During desorption this results in small changes of water contents close to saturation end of the meniscus curvature interval and large in the empty end. The opposite is true for the absorption stepping. This will result in different absorption and desorption curves in the middle of a meniscus curvature interval, even if both curves meet at the end points – a numerical hysteresis.

In practice, more than two points are typically used as measured data. While given a larger set of measurements of water content as a function of relative humidity, the typical approach will be to use the meniscus curvatures of the measurement points as the borders for the matrix rows and columns. In order to minimize the effect of the hysteresis from the integration, the obvious idea is to set all non-diagonal elements of the matrix to zero. This will reduce the dependency of how the integration domain evolves during wetting or drying. The entire water contents will then have to be represented by the diagonal elements of the matrix. This is easily

done by extending the approach above to each step in sorption data, giving for column/row corresponding to change in meniscus curvature between c_x and c_{x+1} a matrix element with value of $\frac{2(w(c_x)-w(c_{x+1}))}{(c_x-c_{x+1})^2}$. This approach result in a fully determined problem and results in exact representation of all measured data, however with some hysteresis in between.

Figure 3.27 visualizes an example of how this works in practice for measurement input of only one sorption curve, measured at 20 ºC, showing the resulting desorption and absorption curves from the adapted model in the corresponding sorption plane $[\varphi(c, T = 20℃), w(c)]$. The sorption data are taken from *Olsson et al 2018*. It should be noted that the materials in the reference most probably had hysteresis in their sorption behavior, but the measurements were done only during desorption conditions. The use of this data as an example is intended to show how the proposed model behaves with only one sorption curve as input data and does not reflect the full behavior of the materials used in *Olsson et al 2018*.

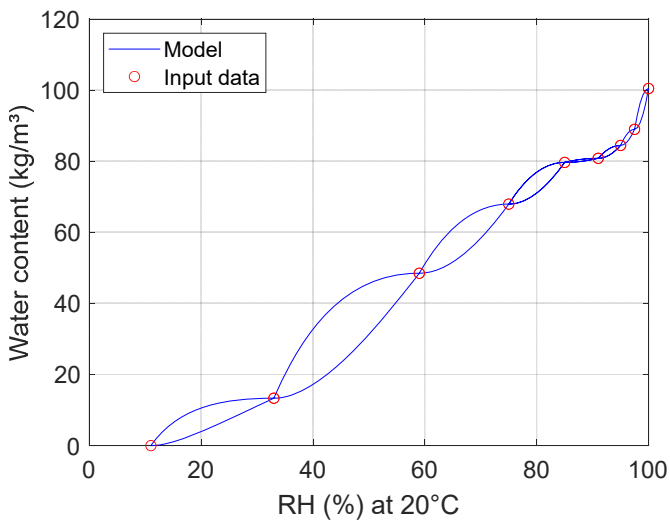

Figure 3.27. Example of adaptation to only one sorption curve at constant temperature. Data taken from Olsson et al 2018 for desorption of OPC, w/c=0.38 at the age of 8 months.

As expected, model curves for absorption and desorption respect exactly all the measured data. This gives a coefficients of determination equal by definition to 1. In between the measured data, there is, as expected, some hysteretic behavior. As also clearly seen, the hysteretic behavior decreases in strength with decreasing distance between the input data – compare small hysteresis in the high relative humidity region (85-100%) with the low-mid humidity region (11-75%).

This is however only an example of a simplified use of the proposed model. The model is not developed intentionally for modeling of non-hysteretic behavior. The only reason for presenting this example is to understand some of the properties of the proposed model and the methods for selection of the matrix elements.

3.3.10 Adaptation to absorption and desorption isotherms without scanning data

Adapting exactly to desorption and absorption data by use of correspondence between amount summing over row and columns of the model matrix can be used in a more general situation. Assuming desorption and absorption isotherms for the same set of n conditions gives for a model matrix of n rows/columns a mathematical problem of adapting $(n+1)n/2$ potentially non-zero elements to $2n$ measured values. Combining these two numbers into an inequality and solving for n gives that the adaptation problem is:

- overdetermined for $n < 3$
- determined for $n = 3$
- underdetermined for $n > 3$

This means that in most cases there will be more than one way of choosing the matrix elements so that the desorption and absorption measurements are fitted exactly. One simple way of achieving such an adaptation is distributing equally water amount contributions between the elements. This can be done in two steps:

- For each row distribute the water amount of corresponding desorption step equally between all non-zero elements of the row.
- For each column except last one, starting at the column with only one non-zero element
    - Calculate the water amount of the column, which will most probably differ from the corresponding absorption step
    - Calculate multiplicative factor to correct the water amount to be equal to the corresponding absorption step. Multiplicative factor is used to not disturb proportions of elements within the column.
    - Correct the column by use of the calculated factor.
    - Distribute the difference between the uncorrected, i.e. old, and the corrected column values equally to remaining uncorrected columns so that the water amounts corresponding to rows remain unchanged by the column correction
- The last column will not require any correction. Its corresponding water contents will be equal to the last absorption step after correction all the preceding columns.

Validity of this algorithm is proved by simple reasoning. The subdivision for each row results in filling the matrix with parameters in such a way that each row corresponds to a connected desorption step and the entire matrix corresponds to the total amount of stored water at saturation. Successive adjusting columns makes sure that the amount of water for each column but the last one, is made to correspond to the connected absorption step. Two facts shall now be observed:

- The column adjustments are performed in such a way that the water corresponding to the rows is not changed, i.e. the rows still correspond to the connected desorption steps and no water is neither added nor removed from the matrix.

- The sum of all desorption steps and the sum of all absorption steps is equal. It corresponds to the total amount of water at saturation.

These two facts imply that after correcting all columns but one, the last column must represent the difference between the total amount of water at saturation and the sum of all water represented by all the other columns, i.e. the last absorption step, and does not need any correction.

An example of such an adaptation is shown in Figure 3.28. As expected, the curves fit exactly all the measured values. The figure also shows two examples of scanning loops from the desorption curve. By choosing another way of distributing the water amounts between the matrix elements, one can change the scanning performance. As long as the water amount of the matrix rows and columns continue to correspond to the desorption and absorption steps, the two sorption curves will not be affected, i.e. such changes will adjust scanning performance only.

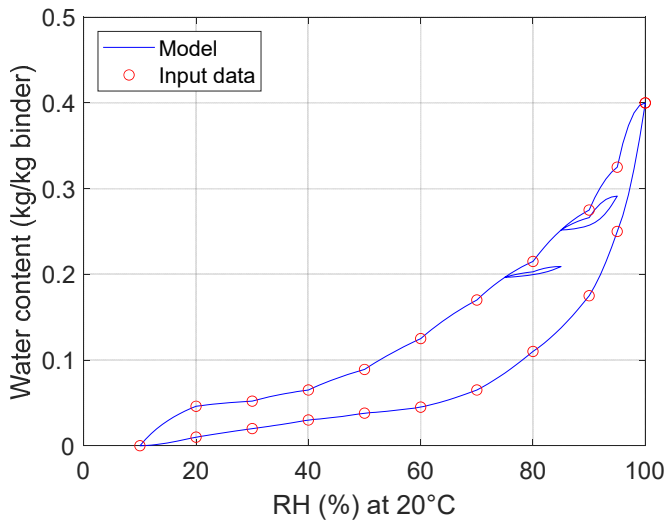

Figure 3.28. Example of adaptation to both desorption and absorption data at constant temperature. Data from Nilsson 2021 for w/c=0.6. Adjustment of data performed due to selection of 10% RH as empty conditions.

3.3.11 Adaptation to absorption and desorption isotherms with scanning data

One way of handling the situation when desorption, absorption and scanning data are available is to use the previously presented algorithm to adapt precisely to desorption and absorption curves without use of the scanning data and simply compare how well the model approximates the scanning measurements. The result will of course be dependent on how the water amounts from the sorption steps are subdivided between the elements of the model matrix. One example of this is given in Figure 3.29, where the algorithm from section 3.3.10 was used to adapt to only desorption and absorption data. The figure shows the adaptation including how it simulates two scanning loops, for which there are measured data. As a comparison, similar use of another method is shown in Figure 3.30, where algorithm from

Mualem 1974 is used as model. For more explicit definition of algorithm see *Zhang 2014*, algorithm referred to as Mualem Model II. The presented coefficients of determination are based on all measured data covering desorption, absorption and scanning.

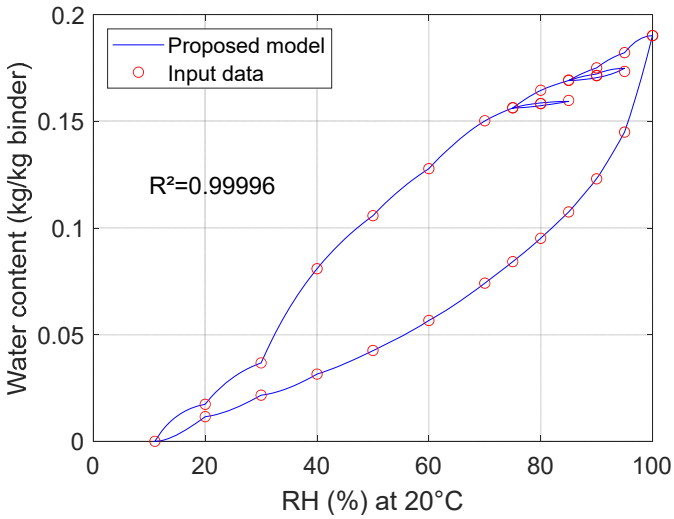

Figure 3.29. Example of adaptation according to section 3.3.10 to both desorption and absorption data at constant temperature and comparison of model performance with scanning data as well. Data from Stelmarczyk et al 2019 for w/c=0.40 at an age of 6 months. Value at 100% RH corresponds to saturation.

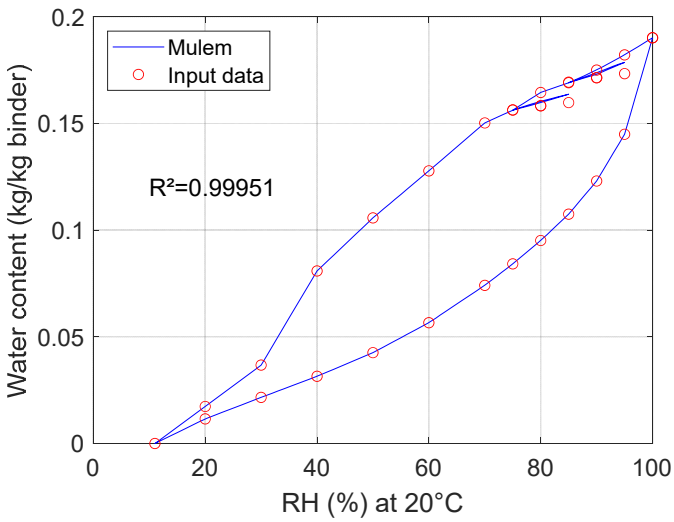

Figure 3.30. Example of adaptation model in Zhang 2014 referred to as Mualem Model II to both desorption and absorption data at constant temperature and comparison of model performance with scanning data as well. Data from Stelmarczyk et al 2019 for w/c=0.40 at an age of 6 months. Value at 100% RH corresponds to saturation

One way to take the scanning data into account when adapting the matrix elements is to use an adjustment cell. This concept is based on the earlier observation that if meniscus curvature boundaries of the rows and columns correspond to the data points in the desorption and absorption curves and a change of element value does not affect the amounts corresponding to whole rows and columns, the desorption and absorption performance remains unchanged. Such an adjustment is typically applied to four elements forming an intersection of two rows and two columns. That pattern forms what is referred to as the adjustment cell. The proposed adjustment is shown in Figure 3.31.

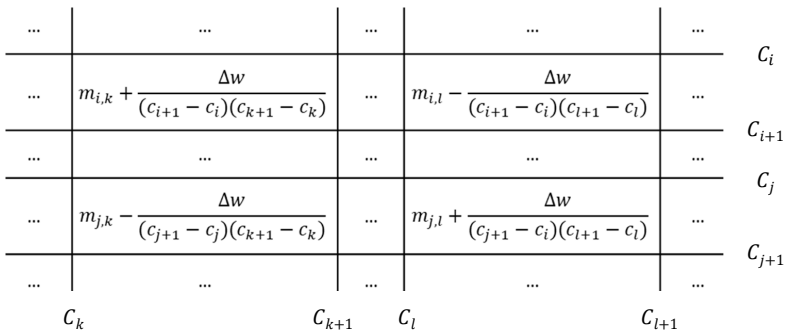

Figure 3.31. General adjustment cell in the model matrix $\mathbf{m}$ *for rows i and j and columns k and l, where any choice of* Δw*, not making any element negative, will not affect total column or row amounts.*

The idea is to adjust the sorption concentrations with an amount change $\pm\Delta w$ divided by the area of each cell in such a way the net change for each column and/or row remains zero. This is achieved by using the positive sign of change along one diagonal of the cell and a negative along the other. As long a history of meniscus curvature consists only of desorption or absorption steps, the corresponding amount of water will not be affected by the change due to the uniform movement of the integration border, a straight line, in either one or the other dimension. On the other hand, when a change from wetting to drying or vice versa occurs, i.e. scanning, a corner will be formed on the border of the integration area, e.g. see Figure 3.19 and Figure 3.20. In that situation it will be possible to choose an adjustment cell with a corresponding total area that intersects the corner in question, which will allow the adjustment Δw to affect both sides of the integration area differently and thus change the scanning performance. This concept assumes of course that the adjustment Δw is chosen in such a way that neither of the affected elements becomes negative.

Based on this idea one can construct a method of adaptation containing two steps:

- Exact adaptation to the desorption and absorption data.
- Successive adjustment by use of various choices of the adjustment cell above, until some satisfaction criteria is fulfilled.

This work does not present such a method. This remains as a topic for future research.

3.3.12 General approach to adaptation in isothermal conditions

There is a more holistic approach to the entire adaptation problem in isothermal conditions. This is based on the insight that using a piece-wise constant sorption site concentration, described by a matrix of elements, will result in an amount of water for any meniscus curvature history, dependent linearly on the matrix elements. This can be shown by investigation of equ. 3.38:

$$w_{Ph,iso} = \int_{History(c_d,c_a,\dots)} \frac{\partial^2 w_{Ph,iso}}{\partial c_a \partial c_d} dc_a dc_d = \sum_{History(c_d,c_a,\dots)} \Delta w_{Ph,iso}(Step_x) \quad (3.42)$$

Reusing the fact that $\frac{\partial^2 w_{Ph}}{\partial c_a \partial c_d}$ is a piece-wise constant function, described by the elements of the model matrix m, the amount of water from each step becomes a weighted sum of the elements of the model matrix

$$\Delta w_{Ph,iso}(Step_x) = \sum_{i,j} A_{i,j}(Step_x) m_{i,j} \quad (3.43)$$

where $A_{i,j}(Step_x)$ is the area of the cross-section between the domain corresponding to the matrix element $m_{i,j}$ and the integration domain for step x, with a sign indicating wetting or drying. Summarizing over all steps of the meniscus curvature history, the total amount of water is clearly linearly dependent on the coefficients of the model matrix:

$$w_{Ph,iso} = \sum_{i,j} \left[m_{i,j} \sum_{History(c_d,c_a,\dots)} A_{i,j}(Step_x) \right] = \sum_{i,j} m_{i,j} B_{i,j} \quad (3.44)$$

with the coefficient of linearity given by

$$B_{i,j} = \sum_{History(c_d,c_a,\dots)} A_{i,j}(Step_x) \quad (3.45)$$

Before continuing with the general approach to adaptation let's change and simplify the nomenclature of the problem by replacing the two dimensional indexing by a one dimensional. Let adaptation parameters p_k, where $k = 1..s = \frac{n(n+1)}{2}$, replace the elements $m_{i,j}$ of the model matrix that are by definition none-zero and n is the number of columns/rows of the model matrix. Let further coefficients b_k, where $k = 1..s$, replace the corresponding coefficients $B_{i,j}$ for a given meniscus curvature history. This transform equ. 3.44 into

$$w_{Ph,iso}(H_j) = \sum_{i=1}^{s} p_i b_{i,j} \quad (3.46)$$

where H_j is a history of meniscus curvature and $b_{i,j}$ is the set of corresponding linear coefficients of the adapted parameters.

Now, assuming that there is a set of measured amounts of water $w_{m,j}$ with corresponding meniscus curvature histories H_j, where $j = 1..q$, it is possible to formulate a measure of an adaptation error by calculating the sum of squares of differences for each measured value.

$$Error = \sum_{j=1}^{q} \left[w_{Ph,iso}(H_j) - w_{m,j} \right]^2 \quad (3.47)$$

For this function to reach a global minimum, all its partial derivatives with respect to all parameters p_k have to vanish:

$$\frac{\partial}{\partial p_k} Error = \frac{\partial}{\partial p_k}\left(\sum_{j=1}^{q}\left[w_{Ph,iso}(H_j) - w_{m,j}\right]^2\right) = 0,\ k = 1..s \qquad (3.48)$$

Calculating further with use of equ. 3.46 gives

$$\frac{\partial}{\partial p_k} Error = 2\sum_{1}^{q}\left[w_{Ph,iso}(H_j) - w_{m,j}\right]b_{k,j} = 2\sum_{j=1}^{q}\left[\sum_{i=1}^{s} p_i b_{i,j} - w_{m,j}\right]b_{k,j} = 0 \qquad (3.49)$$

This gives a system of *s* equations linear in the parameters *p*:

$$\sum_{i=1}^{s} p_i \sum_{j=1}^{q} b_{i,j} b_{k,j} = \sum_{j=1}^{q} w_{m,j} b_{k,j},\ k = 1..s \qquad (3.50)$$

or in matrix notation

$$\begin{bmatrix} \sum_{j=1}^{q} b_{1,j} b_{1,j} & \cdots & \sum_{j=1}^{q} b_{s,j} b_{1,j} \\ \vdots & \ddots & \vdots \\ \sum_{j=1}^{q} b_{1,j} b_{s,j} & \cdots & \sum_{j=1}^{q} b_{s,j} b_{s,j} \end{bmatrix} \begin{bmatrix} p_1 \\ \vdots \\ p_s \end{bmatrix} = \begin{bmatrix} \sum_{j=1}^{q} w_{m,j} b_{1,j} \\ \vdots \\ \sum_{j=1}^{q} w_{m,j} b_{s,j} \end{bmatrix} \qquad (3.51)$$

The set of parameters, solving this system of equations, gives the minimum for the error in the adaptation and can be chosen as the elements of the model matrix *m*. In theory, this makes the approach above a general method of adaptation of model matrix elements for a given set of meniscus curvature boundaries and any type of measured data.

It is however not guaranteed that such a solution exists. *s* linear equations and *s* unknowns implies existence of a solution only and only if the equations are linearly independent. Recalling earlier adaptations to desorption and absorption curves, it is obvious that undetermined situations exist and these will result in lack of linear independency between all the equation in the system, i.e. the corresponding main matrix of equ. 3.51 not being of full rank. Fixing this problem can be done by:

- Reducing the size of the matrix and the amount of parameters to be adapted
- Selecting different meniscus curvature boundaries for the matrix columns/rows
- Increasing the number of measured data
- Selecting different meniscus curvature histories behind the measured data
- A combination of all above

Due to the fact that the main matrix of the equ. 3.51 is not dependent on measured values, i.e. water amounts, but only on the meniscus curvature boundaries for the matrix columns/rows and meniscus curvature histories to be used as measuring conditions, the main matrix can be calculated before measurements are executed. This allows for adjustment of the model and/or measurement plan in order to avoid underdetermination of the entire adaptation problem.

Another possible complication in this approach is the possibility of receiving a set of adapted parameters p_k with at least one parameter negative. Although mathematically possible, such set of parameters lacks appropriate physical interpretation, indicating a negative concentration

of sorption sites under some conditions. In the authors opinion, such a solution shall be interpreted as an inappropriate choice of matrix size and meniscus curvature boundaries versus the number of and meniscus curvature histories behind the measured data and not used. Adjustments proposed for solving the problem of linear dependence in the adaptation equation above may be used to solve this problem as well, at least regarding changes in the matrix size and meniscus curvature boundaries. Any changes to the measurement conditions are unfortunately impractical, due to the fact that the adapted parameters are dependent on the measured data and such an adjustment would require execution of new measurements to reflect the changes in measurement conditions. It is also possible to take the constraint $p_k \geq 0$ into account from the beginning by use of optimization methods for constrained problems. For the constrained approach, the reader is referred to textbooks in optimization theory, e.g. *Nocedal & Wright 2006*.

3.3.13 Formulation for the non-isothermal case

As earlier mentioned, the history of the control variable is directly describing the functional border between the part of the pore system that is filled will capillary condensed water and the part that is not, on the integration domain. However, working with only one site concentration, as in the isothermal version of the model above, will imply the same dependency on the moisture potential and temperature for all the physically bounded water. This will introduce an error in the non-isothermal case due to phenomenological differences between the behavior of capillary condensed and adsorbed water in the pore system. In order to handle this challenge, a split in modeling of the total amount of water into the two contributions is introduced in the non-isothermal case.

$$w_{Ph,ni} = w_{cc} + w_{ad} \tag{3.52}$$

where

$w_{Ph,\mathrm{ni}}$ – is physically bounded water in non-isothermal modeling conditions [kg/m^3]

w_{cc} – is capillary condensed water, i.e. water in the filled part of the pore system [kg/m^3]

w_{ad} – is adsorbed water, i.e. water molecules of the walls of the empty part of the pore system [kg/m^3]

Modeling of capillary condensed water is done in exactly the same way as earlier modeling of physically bounded water in isothermal conditions with the exception that the sorption site concentration now describes only capillary water and not all water as a function of the absorption and desorption conditions. The corresponding model matrix is shown in Figure 3.32 and the equations defining the evaluation of the value is given below:

$$w_{cc} = \int_{History(c_d,c_a,\dots)} \frac{\partial^2 w_{cc}}{\partial c_a \partial c_d} dc_a dc_d = \sum_{History(c_d,c_a,\dots)} \Delta w_{cc}(Step_x) \tag{3.53}$$

where

$\Delta w_{\mathrm{cc}}(Step_x)$ – is a contribution from each step in the history of meniscus curvature [kg/m^3]

The administration of the meniscus curvature changes, now including the varying temperature, is done as described in section 3.3.6 and evaluation of the step changes and the summation is done as described in section 3.3.7, using the matrix with $\frac{\partial^2 w_{cc}}{\partial c_a \partial c_d}$ as site concentrations.

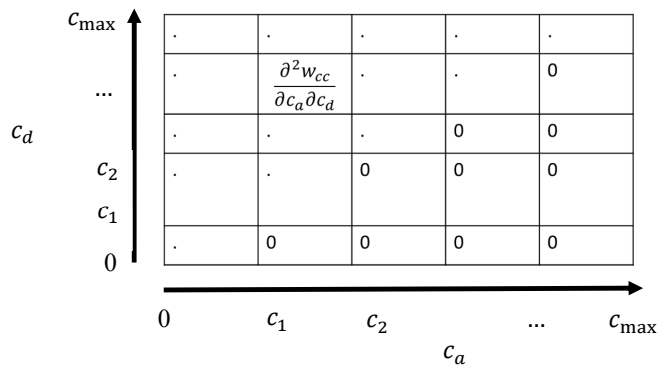

Figure 3.32. Proposed matrix layout of the sorption site distribution for capillary condensed water as a function of desorption and absorption conditions described with meniscus curvature.

Modeling of adsorbed water is in general described by the formula:

$$w_{ad} = f_{ad}(\varphi, T) w_{ad,1} \tag{3.54}$$

where

$w_{ad,1}$ – is water adsorbed in the monolayer of the empty part of the pore system [kg/m^3]

$f_{ad}(\varphi, T)$ – is a suitable modeling function dependent on which basic adsorption model from section 0 is used [-]

If one prefers to use BET, using equations 3.29 and 3.30, the modeling function will be:

$$f_{ad}(\varphi, T) = \frac{b\varphi}{(1-\varphi)(1+b\varphi-\varphi)} \tag{3.55}$$

where

$$b = ce^{(E_1 - E_l)/RT} \tag{3.56}$$

If Dent is preferred, the modeling function will be

$$f_{ad}(\varphi, T) = \frac{b_0 \varphi}{(1-b\varphi)(1-b\varphi+b_0\varphi)} \tag{3.57}$$

where

$$b_0 = e^{-\Delta G_0/RT} \tag{3.58}$$

$$b = e^{-\Delta G/RT} \tag{3.59}$$

The size of the monolayer will of course vary due to the variation of which part of the pore system is filled with capillary condensed water and which is not. Here, the administrated history of meniscus curvature comes to use because it describes the border between these two parts of the pore system on the domain of desorption and absorption control variables. A new model matrix is used with the site concentration describing only the water adsorbed in the monolayer of an empty pore system is used, see Figure 3.33. The difference from previous uses of this model idea is that the integration shall be performed over the empty part of the domain is stead of, as earlier, the filled one. This is easily done by taking the difference between the integral over the entire domain and the integral performed as earlier.

$$w_{ad,1} = \int_{Entire\ domain} \frac{\partial^2 w_{ad,1}}{\partial c_a \partial c_d} dc_a dc_d - \int_{History(c_d,c_a,\dots)} \frac{\partial^2 w_{ad,1}}{\partial c_a \partial c_d} dc_a dc_d \tag{3.60}$$

$$w_{ad,1} = \Delta w_{ad,1}(Abs: 0) - \sum_{History(c_d,c_a,\dots)} \Delta w_{ad,1}(Step_x) \tag{3.61}$$

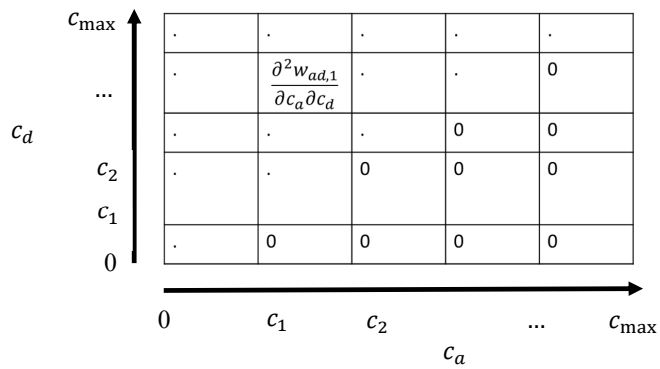

Figure 3.33. Proposed matrix layout of the sorption site distribution for the monolayer of adsorbed water as a function of desorption and absorption conditions described with meniscus curvature.

This model enables a physical interpretation of the contributions of the physically bounded water. The history of the meniscus curvature describes a border between the filled and the empty part of the pore system. Integration on each side of this border of the model matrices, with respective sorption site concentration, gives contributions from capillary condensed water and adsorbed water based on thermodynamically interpretable models of each phenomenon.

It shall also be mentioned that the matrices expressing the site concentration for capillary condensed water and the monolayer of adsorbed water does not need to be of the same size nor use the same border subdivision of meniscus curvature between rows/columns. The common part of the modeling is the use of the history of meniscus curvature, which is independent of how the matrices approximate the modeled site concentrations, as long as they cover the same total span of interest of the meniscus curvature $[0;\ c_{max}]$.

3.3.14 Adaptation to data in non-isothermal conditions

The cost of a structurally flexible model, that is interpretable in phenomenological terms, is often it's complexity, especially when it comes to adaptation to measured data. This statement is definitely valid for the proposed model for non-isothermal conditions. Introduction of the second model matrix for the adsorption monolayer capacity increases the number of parameters to adapt. This is however not the worst problem. The adsorption model function $f_{ad}(\varphi, T)$ destroys the linearity between the resulting water amount and the adaptation parameters, that was present in the isothermal case. From a general point of view, the adaptation can still be performed by searching for a minimum of an adaptation error:

$$Error = \sum_{j=1}^{q} \left[w_{Ph,ni}(H_j) - w_{m,j} \right]^2 \qquad (3.62)$$

With the difference that methods for non-linear problems from optimization theory have to be used due to lack of linearity in dependencies. There are however some observations that can simplify the adaptation problem.

A closer look at the adsorption part of the model reveals that the matrix based modeling of the monolayer capacity describes the structural aspects of the pore system while the model function describes the physical properties of the adsorbent and the surface to which it attaches. In a situation when already having the parameters for the model function for one material and assuming that another material differs mainly in structural properties of the pore system, the model function can be reused. This will transform the problem back to the linear version, as in the isothermal case, but with more parameters from two matrixes to adapt. In such a case the adaptation method from section 3.3.12 can be used.

Another simplification, this time reducing size of the problem, can be based on assumption that the functions describing sorption site concentrations, for capillary condensed water and for the adsorbed monolayer, are not independent of each other. This would enable a description of one as a function of the other, e.g.:

$$\frac{\partial^2 w_{ad,1}}{\partial c_a \partial c_d}(c_a, c_d) = f\left[\frac{\partial^2 w_{cc}}{\partial c_a \partial c_d}(c_a, c_d) \right] \qquad (3.63)$$

Such an assumption will eliminate an entire matrix of adaptation parameters to the cost of adding a few for the function *f*. This approach has however to be investigated further and the validity of the assumption and a suitable choice of the transfer function has to be shown.

3.3.15 Variation in time/age/degree of hydration

The pore system is a result of the hydration of cement and forming of products of cements reaction with water. Thus a development of the pore system takes time during hydration. This implies that the pore system does not in general have a constant distribution of sorption sites with respect to absorption and desorption conditions. In order to describe this variation a variable matrix or a sequence of constant matrices with some kind of interpolation between are necessary. Due to the fact that this variation is not a primary goal of the research problem and practical limitations, the scope of this work does not cover such a solution. It will form a part of the proposed future research.

3.3.16 Calculation of computational parameters

For the computation not only the amount of physically bounded water is needed but also its partial derivatives with respect to vapor content $\frac{\partial w_{Ph}}{\partial \upsilon}$ and temperature $\frac{\partial w_{Ph}}{\partial T}$. These are approximated by finite differences, i.e. by $\frac{\Delta w_{Ph}}{\Delta \upsilon}$ and $\frac{\Delta w_{Ph}}{\Delta T}$, based on a suitable choice of $\Delta\upsilon$ and ΔT with respect to how fast the state changes during a simulation.

A complication shall also be mentioned to any evaluation of the partial derivatives, not only approximated by finite differences, in a model allowing scanning and not only following one isotherm. The values of the partial derivatives are direction dependent. They are not the same for an absorption change and a desorption change, even if infinitesimal. This is due to different slopes of base and scanning isotherms. When the direction of the change is known, this is not a problem. During a simulation however, this is not the case and a choice has to be made without this knowledge. A statistically recommended approach is to use the same change direction as in the preceding computational step or iteration for the section of material in question. A typical simulation of concrete after casting with some interaction with surroundings contains a limited number of changes between drying and wetting if any. With reasonably small time steps the chances are simply much larger that the material will continue with what is does in the next step or iteration in the computation.

3.3.17 Model validation

Previous sections covering model formulation and adaptation of model parameters have already presented multiple contributions to the validation of the proposed model in various situations. The contributions has mainly been of three kinds:

- Mathematical, i.e. model performance has been mathematically derived or proven.
- Physical, i.e. parts of model are directly based on underlying physical models of relevant phenomena.
- Shown in adaptation to measured data and/or comparison with other model.

The presented material is summarized in Table 3.2.

Table 3.2. Summary of proposed models and adaptation methods for sorption and their validation status.

Case / measured data	Model/method properties	Validation
Isothermal, measured data forming one sorption curve, section 3.3.9	Passing exactly through measured points and some scanning in between Handles underdetermined situation with fewer measurements than adaptation parameters	Derived/proven mathematically and shown in adaptation

Case / measured data	Model/method properties	Validation
Isothermal, measured data forming desorption and absorption curves, section 3.3.10	Passing exactly through measured points and scanning in between Handles underdetermined situation with fewer measurements than adaptation parameters	Derived/proven mathematically for a family of method for adaptation of parameters. One specific method proposed and shown in adaptation.
Isothermal, measured data forming desorption, absorption and scanning curves, section 3.3.11	Passing exactly through measured points, scanning in between, no specific adaptation to scanning data Handles underdetermined situation with fewer measurements than adaptation parameters	Derived/proven mathematically for a family of method for adaptation of parameters. One specific method proposed, shown in adaptation and compared to other relevant model.
	Adjustment cell that can be used to adjust scanning performance without changing exact passing through measured desorption and absorption points	Adjustment cell effect derived/proven mathematically.
Isothermal, generalized case, section 3.3.12	General adaptation for determined and overdetermined situations, giving possibility to test determination status for a measurement layout	Derived/proven mathematically.
Non-isothermal, generalized case, section 3.3.14	General adaptation for determined and overdetermined situations	Based directly on physical modeling of underlying phenomena.

3.4 Modeling of transport

3.4.1 Formulation for the isothermal case

A number of facts shall be observed for the isothermal case, as already stated in the literature study, see section 2.3. When the temperature is constant, the translation between the different

moisture potentials, except water content, becomes simplified. This implies that as long the transport coefficient is allowed to vary non-linearly with the moisture state, it doesn't matter which potential is chosen to drive the transport. In most cases, the measurements of transport properties are expressed as coefficients for vapor transport according to Fick's law. This harmonizes with the requirements from section 1.8.3 on the desired transport model so the intention here is to use that approach.

Further observation of typical measurements of this coefficient, e.g. *Hedenblad 1993*, *Olsson et al 2018 or Saeidpour & Wadsö 2016*, shows a monotonously growing dependency on the relative humidity at constant temperature. *Saeidpour & Wadsö 2016* and Stelmarczyk et al 2019 shows hysteretic properties by measurements of the transport coefficient in both desorption and absorption. This indicates a dependency on the filling state of the pore system, somehow similar as for the total water contents.

Based on these observation, the proposed model for the transport coefficient for moisture transport in the isothermal case follows the transport formulation of Fick's law:

$$\boldsymbol{g} = -\delta_{v,iso}\nabla v \qquad (3.64)$$

and reuses the same mathematical model as for sorption in the isothermal case, see sections 3.3.4-3.3.7. This means that the matrix elements for the transport model contain the contributions to the transport properties divided by both sorption state variables $\frac{\partial^2 \delta_{v,\mathrm{iso}}}{\partial c_a \partial c_d}$ instead of sorption site concentration contribution to water amount $\frac{\partial^2 w_{Ph,iso}}{\partial c_a \partial c_d}$.

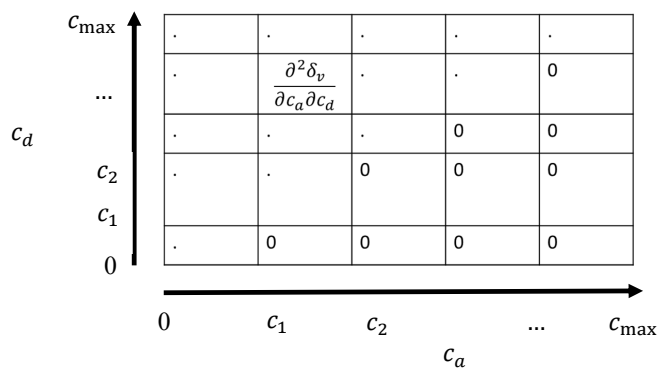

Figure 3.34. Proposed matrix layout of the transport coefficient contributions as a function of desorption and absorption conditions described with meniscus curvature .

The meniscus curvature history, describing the wetting and drying of the material is reused as it is. The evaluation of the total value of the transport coefficient is done in the same way as for the water amount:

$$\delta_{v,\mathrm{iso}} = \delta_{v,\mathrm{iso,offset}} + \int_{History(c_d,c_a,\ldots)} \frac{\partial^2 \delta_{v,\mathrm{iso}}}{\partial c_a \partial c_d} dc_a dc_d \qquad (3.65)$$

$$\delta_{v,\mathrm{iso}} = \delta_{v,\mathrm{iso,offset}} + \sum_{History(c_d,c_a,\ldots)} \Delta\delta_{v,\mathrm{iso}}(Step_x) \quad (3.66)$$

where $\delta_{v,\mathrm{iso,offset}}$ is the starting value for the transport coefficient at c_{max}, which does not have to vanish as it did in the sorption case.

3.4.2 Adaptation to data forming one transport curve

Dealing with transport data measured in one set of moisture conditions only, normally desorption, the adaptation procedure for a similar case in sorption modeling from section 3.3.9 is used. Here a similar result is obtained with exact representation of the measured values and some hysteresis effects in between. Figure 3.35 shown an adaptation of such kind to transport coefficients from *Hedenblad 1993* concrete with OPC only for w/b = 0.60. Figure 3.36 shows another such adaptation to transport coefficients from *Olsson et at 2018* for concrete with OPC + 5% silica fume and w/b = 0.53.

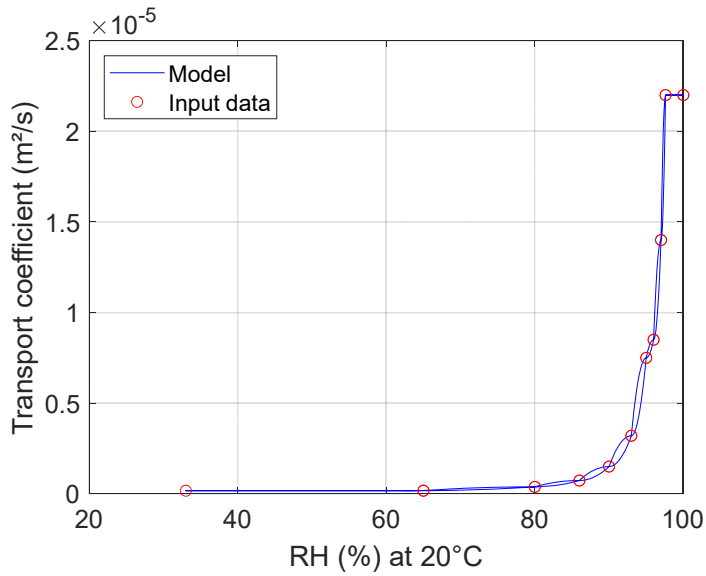

Figure 3.35. Adaptation of isothermal transport model to transport coefficients measured under one set of conditions (desorption) from Hedenblad 1993, water-binder ratio 0,6, last value at 97.6 % RH used also as value at saturation.

3.4.3 Adaptation to transport data in desorption and absorption

In the situation of having measured coefficients in both desorption and absorption, the adaptation procedure for a similar case in sorption modeling from section 3.3.10 is used. Here a similar result is obtained with exact representation of the measured values (input data in figures) and modeling of scanning effects based on the distribution method for the contributions to the transport coefficient in the row and columns of the matrix. Figure 3.37 shows an adaptation to transport coefficients from *Saeidpour & Wadsö 2016*, for concrete with OPC and w/b = 0.5. Figure 3.38 shows an adaptation to transport coefficients from Stelmarczyk et al 2019, concrete with CEM II-A/V w/b=0.55. Both figures show two scanning loops from the desorption curve. These scanning curves do not correspond to any

values measured in scanning. They are shown to visualize the performance in scanning of the model adapted to values measured only in absorption and desorption.

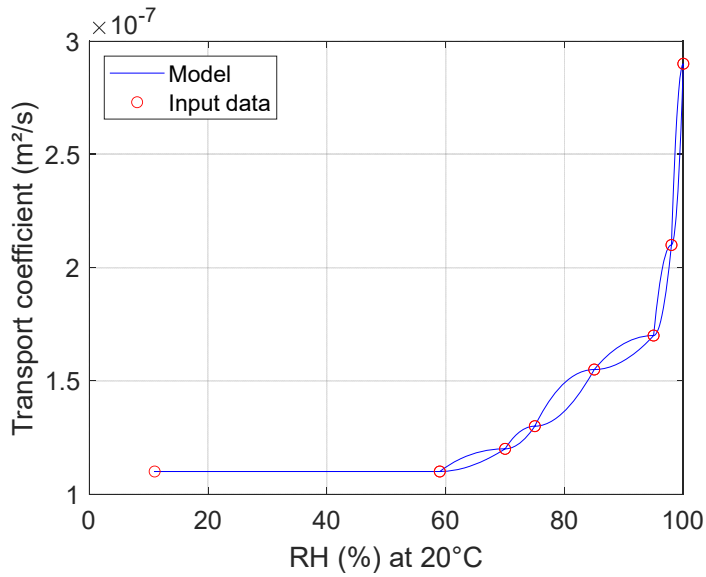

Figure 3.36. Adaptation of isothermal transport model to transport coefficients measured under one set of conditions (desorption) from Olsson et al 2018, OPC with 5% SF water-binder ratio 0.53, values from figure 3a.

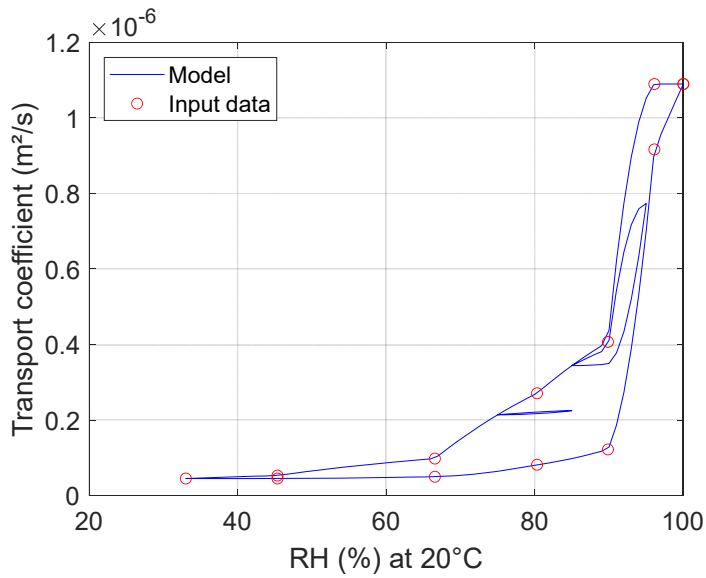

Figure 3.37. Adaptation of isothermal transport model to transport coefficients measured under desorption and absorption from Saeidpour & Wadsö 2016, OPC water-binder ratio 0.5, values from figure 5a at the middle of resp. RH-interval, desorption value of highest RH-interval used as common value at saturation, absorption value of lowest RH-interval used as common value at lower border of lowest RH-interval. Two scanning loops (85%-95% and 75%-85%) for model performance from desorption curve shown.

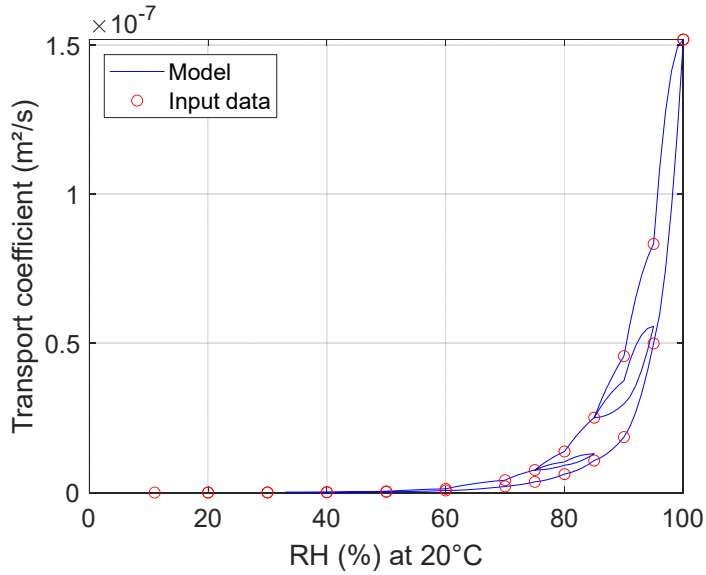

Figure 3.38. Adaptation of isothermal transport model to transport coefficients measured under desorption and absorption from Stelmarczyk et al 2019, water-binder ratio 0.55. Two scanning loops (85%-95% and 75%-85%) for model performance from desorption curve shown.

3.4.4 Adaptation to transport data in desorption, absorption and scanning

In the situation of having measured coefficients in desorption, absorption and scanning, the adaptation procedures from similar cases in isothermal sorption modeling can be adapted. For closed details see sections 3.3.11 and 3.3.12.

3.4.5 Simplified formulation for the non-isothermal case

Simplified formulation for the non-isothermal case builds on the idea of choosing a dominating phenomenology to approximate the full behavior. As stated in section 1.6, the purpose of the models proposed in this thesis is to enable simulation of drying in concrete and moisture exchange with other material while drying. This implies that the state of concrete will, during simulation, be in the part of the moisture spectra close to the saturation end. Taking into account that many desorption curves for moder concrete indicate quite high water contents at relative humidities as low as 75-80%, the capillary suction will probably dominate the transport behavior due to the fact that the majority of the transport ways in the pore system will be filled with water. This implies to choose capillary suction as the dominating phenomenology for transport modeling in the simplified non-isothermal case. Reusing the translation of the transport term for capillary suction into gradients of vapor content and temperature from equ. 3.47 and rearranging gives:

$$\boldsymbol{g} = -\frac{k\varrho_w R_v T}{\mu_K v}\nabla v - \frac{k\varrho_w R_v}{\mu_K}\left(ln\left(\frac{v}{v_s}\right) - \frac{T}{v_s}\frac{dv_s}{dT}\right)\nabla T \qquad (3.67)$$

$$\boldsymbol{g} = -k\varrho_w R_v\left[\frac{T}{\mu_K v}\nabla v - \frac{1}{\mu_K}\left(ln\left(\frac{v}{v_s}\right) - \frac{T}{v_s}\frac{dv_s}{dT}\right)\nabla T\right] \qquad (3.68)$$

In the last equation, the terms forming the transport coefficients for the driving potential gradients has been separated into three multiplicative parts:

- Green – permeability
- Turquoise – constants or approximated as constants
- Pink – state variables or functions of state variables

Of these, the green permeability is the only one directly connected to which parts of the pore system are filled with water. This make it a logical choice to model by reuse of the sorption model for the isothermal situation, see sections 3.3.4-3.3.7, or as for the entire transport coefficient in the isothermal case in section 3.4.1. This means that the matrix elements for the transport model contain the contributions to the permeability term divided by both sorption state variables $\frac{\partial^2 k}{\partial c_a \partial c_d}$ instead of sorption site concentration contribution to water amount $\frac{\partial^2 w_{Ph,iso}}{\partial c_a \partial c_d}$.

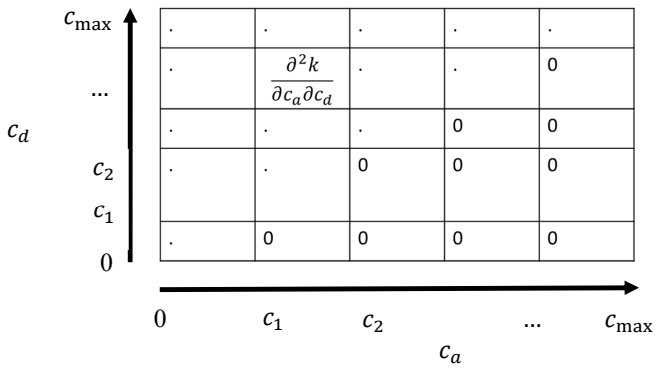

Figure 3.39. Proposed matrix layout of the permeability contributions as a function of desorption and absorption conditions described with meniscus curvature .

The meniscus curvature history, describing the wetting and drying of the material is reused as it is. The evaluation of the total value of the permeability is done in the same way as for the water amount, with the correction for a non-vanishing starting value of k_{offset}:

$$k = k_{\text{offset}} + \int_{History(c_d,c_a,\dots)} \frac{\partial^2 k}{\partial c_a \partial c_d} dc_a dc_d = \sum_{History(c_d,c_a,\dots)} \Delta k(Step_x) \qquad (3.69)$$

In this way calculated permeability is then used together with the remaining terms from the equ. 3.67 to calculate the transport coefficients for both potential gradients:

$$\delta_v = \frac{k \varrho_w R_v T}{\mu_K v} \qquad (3.70)$$

$$\delta_T = \frac{k \varrho_w R_v}{\mu_K} \left(ln\left(\frac{v}{v_s}\right) - \frac{T}{v_s} \frac{dv_s}{dT} \right) \qquad (3.71)$$

3.4.6 Adaptation of the simplified formulation to isothermal data

The adaptation problem is for this model formulation limited only to the matrix adaptation of the permeability. The rest of the terms in the transport coefficient are either constants, approximated as constants, state variables of function of state variables. While using transport data measured in isothermal conditions, the adaptation problem is simplified further by vanishing of the temperature gradient term. The measured transport coefficients have to be recalculated to corresponding permeabilities:

$$\delta_{v,m} = \frac{k_m \varrho_w R_v T}{\mu_K \upsilon} \tag{3.72}$$

$$k_m = \frac{\delta_{v,m} \mu_K \upsilon}{\varrho_w R_v T} \tag{3.73}$$

The permeabilities from the measurements are then used for the adaptation of the matrix elements. In the situation of having measured coefficients in both desorption and absorption, the adaptation procedure for a similar case in sorption modeling from section 3.3.10 is used. Here a similar result is obtained with exact representation of the measured values and modeling of scanning effects based on the distribution method for the contributions to the transport coefficient in the row and columns of the matrix, as seen in Figure 3.40 and Figure 3.41.

As seen in Figure 3.40, there is a possibility of a strange interpolation effect, where small temporary decrease can be seen in the adapted transport coefficient for vapor contents gradient, when relative humidity is increased. In order to understand this phenomenon, one has to compare the mathematical interpolation in this model with the isothermal model. In the isothermal case the model matrix represents contributions to δ_v directly and with positive matrix elements there is no mathematical possibility for the interpolated value to decrease with decreasing meniscus curvature , i.e. increasing relative humidity at constant temperature. In the simplified non-isothermal case, the matrix elements represents contributions to permeability. Looking closer at the equ. 3.70 reveals that the connection between δ_v and k at constant temperature involves linear scaling with vapor contents as factor. The interpolation result on the matrix model, with contributions to the permeability, is linear in meniscus curvature , i.e. non-linear in relative humidity or vapor contents at constant temperature. This combination of linear pre-scaling and non-linear interpolation with respect to vapor contents and relative humidity is the searched explanation. The observed effect is purely mathematical. It is most easily observed when there are large distances between the measured values and on isotherm sections with low slope. As shown in another adaptation in Figure 3.41, when number of measured points is increased, this effect disappears.

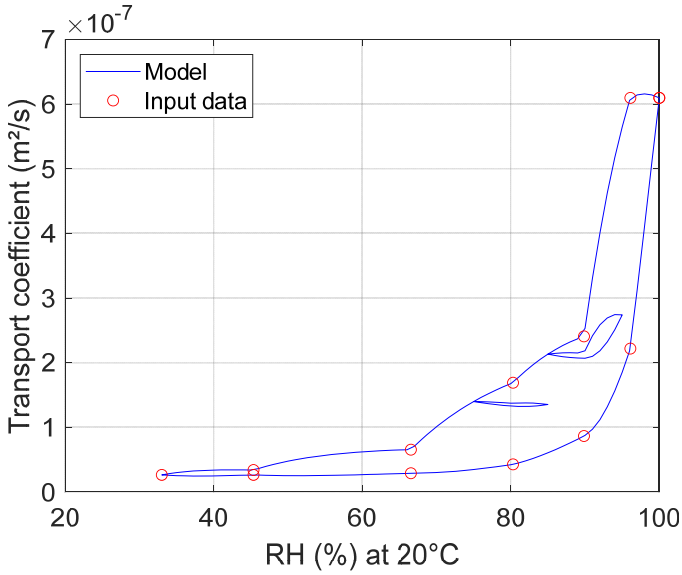

Figure 3.40. Transport coefficient for vapor contents gradient, adaptation of simplified non-isothermal transport model to transport coefficients measured under desorption and absorption from Saeidpour & Wadsö 2016, OPC water-binder ratio 0.5, values from figure 5a at the middle of resp. RH-interval, desorption value of highest RH-interval used as common value at saturation, absorption value of lowest RH-interval used as common value at lower border of lowest RH-interval. Two scanning loops (85%-95% and 75%-85%) for model performance from desorption curve shown.

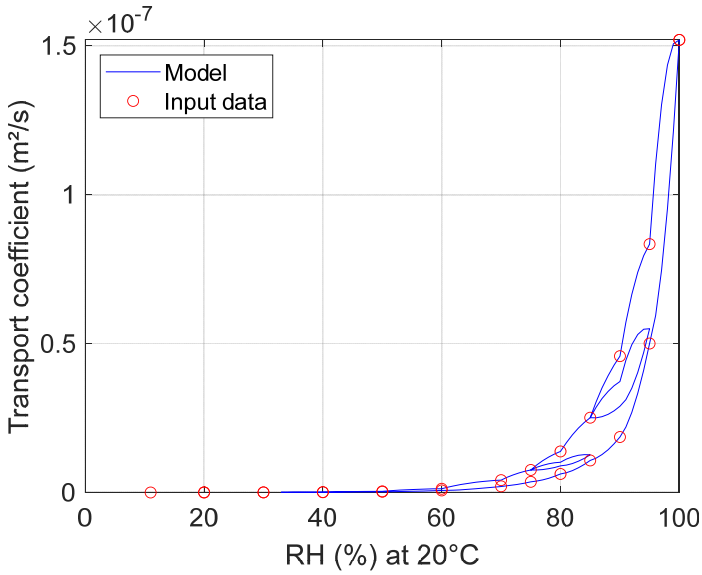

Figure 3.41. Transport coefficient for vapor contents gradient, adaptation of simplified non-isothermal transport model to transport coefficients measured under desorption and absorption from Stelmarczyk et al 2019, water-binder ratio 0.55. Two scanning loops (85%-95% and 75%-85%) for model performance from desorption curve shown.

The simplified non-isothermal model supports not only modeling of the transport coefficient for vapor contents gradient but also for the temperature gradient and the temperature and temperature history variation of both. Figure 3.42 and Figure 3.43 shows the same combination of isotherms for desorption with scanning loops and absorption for both transport coefficients at three different temperatures.

One should remember here to not interpret transport contributions from these two terms separately. They are together a result of using capillary suction model as basis for the transport simplification in this model variant and they together represent the transport driven by the gradient of capillary pressure.

If measured transport coefficients during scanning are available as well, the methodology for adaptation of the matrix elements from sections 3.3.11 and 3.3.12 can be used.

If measured transport coefficients are available only for desorption conditions, the methodology for adaptation of matrix elements from section 3.3.9 can be used.

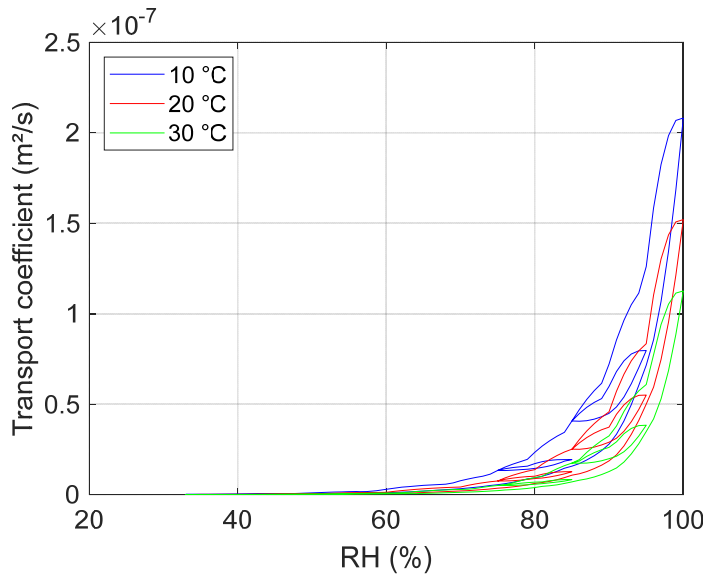

Figure 3.42. Transport coefficient for vapor contents gradient at different temperatures, adaptation of simplified non-isothermal transport model to transport coefficients measured under desorption and absorption from Stelmarczyk et al 2019, water-binder ratio 0.55. Two scanning loops (85%-95% and 75%-85%) for model performance from desorption curve shown.

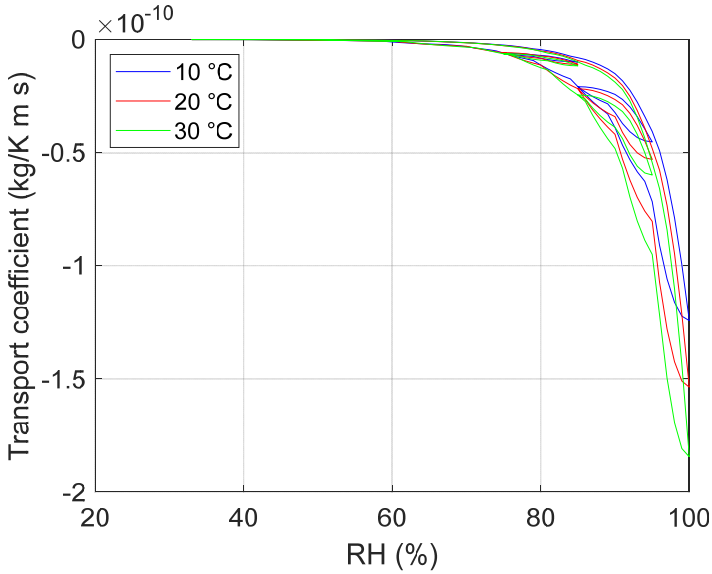

Figure 3.43. Transport coefficient for temperature gradient at different temperatures, adaptation of simplified non-isothermal transport model to transport coefficients measured under desorption and absorption from Stelmarczyk et al 2019, water-binder ratio 0.55. Two scanning loops (85%-95% and 75%-85%) for model performance from desorption curve shown.

3.4.7 Generalized formulation for the non-isothermal case

Using parallel models for capillary suction and vapor diffusion and summing up the result transport has earlier been proposed and shown in e.g. *Johannesson 2002*. This approach seems more general and it can be applied with the flexibility of the newly proposed models. The capillary suction part can be taken directly from section 3.4.5. The vapor term should follow the basic vapor transport model, i.e. Fick:

$$\boldsymbol{g} = -D_v \nabla v \qquad (3.74)$$

where

D_v – is the vapor diffusivity in air, a function of temperature [m^2/s]

What is missing in this term is the reflection of the fact that the space in general is restricted by concrete and only a small fraction of it, i.e. the pore system, is available for vapor diffusion. Assuming some level of homogeneity of the structure of the pore system, the details of its size distribution and connectivity do not have to be modeled, but can be replaced by a continuous formulation for the entire volume of the concrete by introducing a factor γ_v that gives the fraction of the entire cross-section through the volume of concrete that is available for vapor diffusion:

$$\boldsymbol{g} = -\gamma_v D_v \nabla v \qquad (3.75)$$

This factor, γ_v [-], is typically a function of how large part of the pore system is filled with air and not condensed water that will stop the diffusion of vapor. For modeling of such a property

with a direct dependence on the wetting/drying history the matrix formulation in the proposed model for adsorption monolayer size from section 3.3.13 can be used, with a correction for a non-vanishing stating value of $\gamma_{v,\text{offset}}$.

$$\gamma_v = \gamma_{v,offset} + \int_{Entire\ domain} \frac{\partial^2 \gamma_v}{\partial c_a \partial c_d} dc_a dc_d - \int_{History(c_d,c_a,\dots)} \frac{\partial^2 \gamma_v}{\partial c_a \partial c_d} dc_a dc_d \quad (3.76)$$

$$\gamma_v = \gamma_{v,offset} + \Delta\gamma_v(Abs{:}\,0) - \sum_{History(c_d,c_a,\dots)} \Delta\gamma_v(Step_x) \quad (3.77)$$

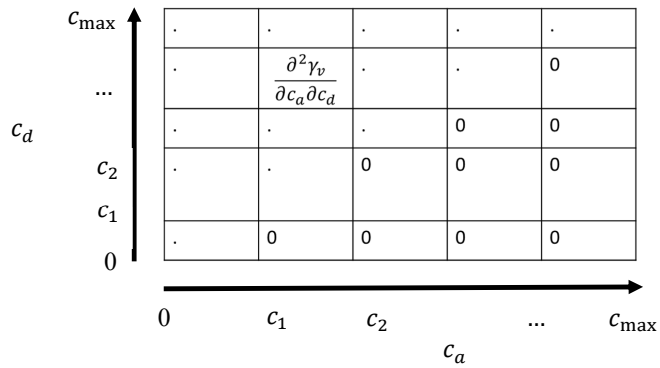

Figure 3.44. Proposed matrix layout of the cross-section contributions to the vapor diffusion as a function of desorption and absorption conditions described with meniscus curvature .

This will after summarizing with the transport term for the capillary suction give:

$$\boldsymbol{g} = -\left[\frac{k\varrho_w R_v T}{\mu_K \upsilon} + \gamma_v D_v\right] \nabla\upsilon - \frac{k\varrho_w R_v}{\mu_K}\left(ln\left(\frac{\upsilon}{\upsilon_s}\right) - \frac{T}{\upsilon_s}\frac{d\upsilon_s}{dT}\right) \nabla T \quad (3.78)$$

where the capillary suction permeability k and the diffusion cross-section γ_v are modeled by one matrix each and the other terms are direct functions of the state variables. The transport coefficients for the respective gradient become:

$$\delta_v = \frac{k\varrho_w R_v T}{\mu_K \upsilon} + \gamma_v D_v \quad (3.79)$$

$$\delta_T = \frac{k\varrho_w R_v}{\mu_K}\left(ln\left(\frac{\upsilon}{\upsilon_s}\right) - \frac{T}{\upsilon_s}\frac{d\upsilon_s}{dT}\right) \quad (3.80)$$

3.4.8 Adaptation of the generalized formulation

Adaptation of a transport model for gradients in both vapor content and temperature in non-isothermal contains the task of subdividing of the total transport into two parts, driven by respective potential. In the section 3.4.5 a simplified model was used, where the adaptation parameters didn't require transport measurements with a temperature gradient. The transport coefficient for the temperature gradient could by the model simplification be calculated from data adapted to isothermal transport, see section 3.4.6. This is not the case in the general approach. Subdivision of the total transport into driven by respective potential gradient has to be a part of the adaptation procedure. This implies that the measured data do not consist of

transport coefficients measured in various conditions but total transport terms measured in various conditions regarding both potential values, their history or more specifically the history of the meniscus curvature and potential gradients $\boldsymbol{g}_m(v, T, Hist(c), \nabla v, \nabla T)$, or simplified into just a one-dimensional case $g_{x,m}(v, T, Hist(c), \frac{\partial v}{\partial x}, \frac{\partial T}{\partial x})$. The equation for the adaptation becomes:

$$g_{x,m} = -\left[\frac{k\varrho_w R_v T}{\mu_K v} + \gamma_v D_v\right]\frac{\partial v}{\partial x} - \frac{k\varrho_w R_v}{\mu_K}\left(ln\left(\frac{v}{v_s}\right) - \frac{T}{v_s}\frac{dv_s}{dT}\right)\frac{\partial T}{\partial x} \tag{3.81}$$

and after some rearrangement:

$$g_{x,m} = f^k k\big(Hist(c)\big) + f^\gamma \gamma_v\big(Hist(c)\big) \tag{3.82}$$

where

$$f^k = -\frac{\varrho_w R_v}{\mu_K}\left[\frac{T}{v}\frac{\partial v}{\partial x} - \left(ln\left(\frac{v}{v_s}\right) - \frac{T}{v_s}\frac{dv_s}{dT}\right)\frac{\partial T}{\partial x}\right] \tag{3.83}$$

$$f^\gamma = -D_v\frac{\partial v}{\partial x} \tag{3.84}$$

are functions of state variables or their gradients and are known constants for each measured transport value. As already shown in section 3.3.12, a value evaluated from a matrix in the proposed model for any given history of the meniscus curvature is a linear combination of the matrix elements. Assuming some feasible selection of meniscus curvature boundaries for the matrix structure (row/columns), this results in the adaptation equation 3.82 being linear. This can be shown by use of derivation of equ. 3.42 – 3.45 from section 3.3.12 together with equations giving $k\big(Hist(c)\big)$ and $\gamma_v\big(Hist(c)\big)$, i.e. 3.69 and 3.77. These together result in:

$$k\big(Hist(c)\big) = k_{offset} + \sum_{i,j} m_{i,j}^k B_{i,j}^k \tag{3.85}$$

$$\gamma_v\big(Hist(c)\big) = \gamma_{v,offset} + \sum_{i,j} m_{i,j}^\gamma B_{i,j}^\gamma \tag{3.86}$$

with the coefficients of linearity are given by

$$B_{i,j}^k = \sum_{History(c_d, c_a, \dots)} A_{i,j}^k(Step_x) \tag{3.87}$$

$$B_{i,j}^\gamma = \sum_{History(c_d, c_a, \dots)} A_{i,j}^\gamma(Step_x) \tag{3.88}$$

For permeability calculation based on model matrix m^k, $\mathrm{A}_{\mathrm{i,j}}^{\mathrm{k}}(Step_x)$ is the area of the cross-section between the domain corresponding to the matrix element $m_{i,j}^k$ and the integration domain for step x in the history of meniscus curvature , with a sign indicating wetting or drying. For calculation of γ_v based on model matrix m^γ, $\mathrm{A}_{\mathrm{i,j}}^{\gamma}(Step_x)$ is the area of the cross-section between the domain corresponding to the matrix element $m_{i,j}^\gamma$ and the integration domain for step x, with a sign indicating wetting or drying. Observe that here the integration domain corresponds to the empty part of the pore system instead of the part filled with capillary condensed water, as was the case for permeability calculation.

Now, let's change and simplify the nomenclature of the problem by a substitution replacing the two dimensional indexing by a one dimensional and putting all adaptation parameters and their coefficients into two indexed variables.

Let:

- adaptation parameter $p_1 = k_{\text{offset}}$
- adaptation parameters p_k, where $k = 2..r+1$, replace the elements $m_{i,j}^k$ of the model matrix for permeability, that are by definition none-zero, where r is their number
- adaptation parameter $p_{r+2} = \gamma_{v,\text{offset}}$
- adaptation parameters p_k, where $k = r+3..s+r+2$, replace the elements $m_{i,j}^\gamma$ of the model matrix for γ_v, that are by definition none-zero, where s is their number

Let further:

- coefficient $b_1 = 1$
- coefficients b_k, where $k = 2..r+1$, replace the coefficients $\mathrm{B}_{\mathrm{i,j}}^{\mathrm{k}}$ for the non-zero elements $m_{i,j}^k$ from the equ. 3.85
- coefficient $b_{r+2} = 1$
- coefficients b_k, where $k = r+3..s+r+2$, replace the coefficients $\mathrm{B}_{\mathrm{i,j}}^{\gamma}$ for the non-zero elements $\mathrm{m}_{\mathrm{i,j}}^{\gamma}$ from the equ. 3.86

Let finally:

- coefficient $c_{i,j} = f_j^k b_i$, where $i = 1..r+1$ and f_j^k is a function of state variables according to equ. 3.83 corresponding to state and meniscus curvature history H_j
- coefficient $c_{i,j} = f_j^\gamma b_i$, where $i = r+2..s+r+2$ and f_j^γ is a function of state variables according to equ. 3.84 corresponding to state and meniscus curvature history H_j

This transform equ. 3.82 into

$$g_{x,m,j} = \sum_{i=1}^{s+r+2} p_i c_{i,j} \qquad (3.89)$$

for any measured total transport coefficient $g_{x,m,\mathrm{j}}$ corresponding to state and meniscus curvature history H_j. Calculating the adaptation error for an entire set of measurements $g_{x,m,j}$ with corresponding state and meniscus curvature histories H_j, where $j = 1..q$, gives:

$$Error = \sum_{j=1}^{q} \left[\sum_{i=1}^{s+r+2} p_i c_{i,j} - g_{x,m,j}\right]^2 \qquad (3.90)$$

For this function to reach a global minimum, all its partial derivatives with respect to all parameters p_k have to vanish:

$$\frac{\partial}{\partial p_k} Error = \frac{\partial}{\partial p_k}\left(\sum_{j=1}^{q} \left[\sum_{i=1}^{s+r+2} p_i c_{i,j} - g_{x,m,j}\right]^2\right) = 0,\ k = 1..s+r+2 \qquad (3.91)$$

Calculating further gives

$$\frac{\partial}{\partial p_k} Error = 2\sum_{j=1}^{q}\left[\sum_{i=1}^{s+r+2} p_i c_{i,j} - g_{x,m,j}\right] c_{k,j} = 0 \qquad (3.92)$$

This gives a system of *s+r+2* equations, linear in the parameters *p*:

$$\sum_{i=1}^{s+r+2} p_i \sum_{j=1}^{q} c_{i,j} c_{k,j} = \sum_{j=1}^{q} g_{x,m,j} c_{k,j}\,,\ k = 1..s+r+2 \qquad (3.93)$$

or in matrix notation

$$\begin{bmatrix} \sum_{j=1}^{q} c_{1,j}c_{1,j} & \cdots & \sum_{j=1}^{q} c_{s+r+2,j}c_{1,j} \\ \vdots & \ddots & \vdots \\ \sum_{j=1}^{q} c_{1,j}c_{s+r+2,j} & \cdots & \sum_{j=1}^{q} c_{s+r+2,j}c_{s+r+2,j} \end{bmatrix} \begin{bmatrix} p_1 \\ \vdots \\ p_{s+r+2} \end{bmatrix} = \begin{bmatrix} \sum_{j=1}^{q} g_{x,m,j}c_{1,j} \\ \vdots \\ \sum_{j=1}^{q} g_{x,m,j}c_{s+r+2,j} \end{bmatrix} \qquad (3.94)$$

The set of parameters, solving this system of equations, gives the minimum for the error in the adaptation and can be chosen as the corresponding values for k_{offset}, $\gamma_{v,\text{offset}}$ and elements of the model matrices $m_{i,j}^{k}$ and $m_{i,j}^{\gamma}$ according to the substitution above.

Summarizing, this linear regression method, previously given in section 3.3.12 can be adapted and applied to this problem, with the differences that:

- the adaptation will occur for the elements in two matrices and their offset values simultaneously
- the basic evaluation formulae for these two will differ in the sense that one matrix will use contributions on one side of the boundary, defined by the meniscus curvature history, and the other matrix on the other side
- calculation of the elements of the final matrix equation 3.94 contains pre-scaling of coefficient contributions by functions of state variables for each measurement condition used, according to the final step in the substitution given above

All conclusions from section 3.3.12 regarding determination of the adaptation problem and existence of a solution are valid in this case as well, when corrected for the differences above, due to their dependence on the linearity of the problem.

3.4.9 Model validation

Previous sections covering model formulation and adaptation of model parameters have already presented multiple contributions to the validation of the proposed model in various situations. The contributions has mainly been of three kinds:

- Mathematical, i.e. model performance has been mathematically derived or proven.
- Physical, i.e. parts of model are directly based on underlying physical models of relevant phenomena.
- Shown in adaptation to measured data and/or comparison with other model.

Due to basing large parts of the transport modeling on the matrix-based, abstract model underlying proposed sorption model, parts of the validation were already presented in section 3.3. The presented material is summarized in Table 3.3.

Table 3.3. Summary of proposed models and adaptation methods for transport and their validation status.

Case / measured data	Model/method properties	Validation
Isothermal, measured data forming one curve with transport coefficients, section 3.4.2	Passing exactly through measured points and some scanning in between Handles underdetermined situation with fewer measurements than adaptation parameters	Basic validation see 3.3.9. Application to transport shown in adaptation.
Isothermal, measured data forming curves with transport coefficients for desorption and absorption, section 3.4.3	Passing exactly through measured points and scanning in between Handles underdetermined situation with fewer measurements than adaptation parameters	Basic validation see 3.3.10. Application to transport shown in adaptation.
Isothermal, measured data forming curves with transport coefficients for desorption and scanning, section 3.4.4	Passing exactly through measured points, scanning in between, no specific adaptation to scanning data Handles underdetermined situation with fewer measurements than adaptation parameters	Basic validation see 3.3.11
	Adjustment cell that can be used to adjust scanning performance without changing exact passing through measured desorption and absorption points	Basic validation see 3.3.11.
Isothermal, generalized case, section 3.4.4	General adaptation for determined and overdetermined situations, giving possibility to test determination status for a measurement layout	Basic validation see 3.3.12.

Case / measured data	Model/method properties	Validation
Simplified non-isothermal, measured data in isothermal conditions forming one curve with transport coefficients, section 3.4.6	Passing exactly through measured points and some scanning in between Domination of transport by capillary suction assumed Handles underdetermined situation with fewer measurements than adaptation parameters	Basic validation see 3.3.9.
Simplified non-isothermal, measured data in isothermal conditions forming curves with transport coefficients for desorption and absorption, section 3.4.6	Passing exactly through measured points and scanning in between Domination of transport by capillary suction assumed Handles underdetermined situation with fewer measurements than adaptation parameters	Basic validation see 3.3.10. Application to transport partially shown in adaptation.
Simplified non-isothermal, measured data in isothermal conditions forming curves with transport coefficients for desorption and scanning, section 3.4.6	Passing exactly through measured points, scanning in between, no specific adaptation to scanning data Domination of transport by capillary suction assumed Handles underdetermined situation with fewer measurements than adaptation parameters	Basic validation see 3.3.11
	Adjustment cell that can be used to adjust scanning performance without changing exact passing through measured desorption and absorption points	Basic validation see 3.3.11.

Case / measured data	Model/method properties	Validation
Simplified non-isothermal, measured data in isothermal conditions, generalized case, section 3.4.6	General adaptation for determined and overdetermined situations, giving possibility to test determination status for a measurement layout Domination of transport by capillary suction assumed	Basic validation see 3.3.12.
Non-isothermal, measurements of transport in non-isothermal conditions with temperature gradient, generalized case, section 3.4.8	General adaptation for determined and overdetermined situations	Basic validation see 3.3.12.

4. Discussion and conclusions

4.1 Hydration and connected properties

The proposed model of hydration offers the possibility to model the degree of hydration of the binder directly, without the middle-step of temperature-equivalent time of hydration. The differential modeling follows in structure a well-known basic model of kinetics and uses separate influencing factors that are natural to interpret from the phenomenological point of view. Most of the adapted parameters have physical interpretations with exception of the factor for the initial slow start of the hydration, which is a pure mathematical construct. This interpretation possibility is not given for an important part of the reference model, where all parameters of equ. (2.14), translating temperature-equivalent time of maturity to the degree of hydration, have purely mathematical meaning.

Further, the proposed hydration model and its direct application to calculation of chemically bounded water forms a modeling platform that can be used to connect further values. As mentioned before, the immediate candidates are heat of hydration and compressive strength. This can result after further research in one model structure for all hydration-dependent properties of interest.

Together with the outline of non-linear methodology for parameter adaptation, the model offers a variety of ways to adapt the parameters. An adaptation to chemically bounded water measurements is shown in section 3.2.5, where the degree of hydration of the binder is not measured but handled as a variable internal to the model. This adaptation is presented in two versions, one with and one without explicit modeling of moisture influence. Another approach would be to adapt the parameters more directly to measured degree of hydration, possibly also in combination with chemically bounded water. In such a scenario the amount of measurements could be more balanced between the two measured variables.

A more direct quality difference between the proposed and the reference model is seen in the capability to model the dependency on temperature of the formed reaction products, in the presented case in amount of chemically bounded water per amount of hydrated binder. Measurements presented in section 3.2.5 clearly show a cross-over effect of temperature, where low temperature gives initially slow rate of growth but high final value and high temperature gives the opposite. The reference mode lacks the mathematical capability to model that phenomenon, which is clearly seen in the diagrams. The proposed model captures the phenomenon much better, which is clearly seen in both diagrams and in the comparison of coefficients of determination in section in section 3.2.5. This advantage is present both in the case of modeling with explicit influence of moisture and adaptation to values from both sealed and saturated samples, as well as in the case of modeling without moisture influence and adaptation to value from sealed samples only.

The implemented moisture control is based on a domain-based sorption model and as assumption that the amount of physically bounded water from saturation down to a certain level of desorption is available for hydration. This is implemented by using a limit expressed

as relative humidity under desorption at room temperature. This may not be the most optimal way of formulating the limiting criterion. For ink-bottle pores, a desorption condition correspond to the hydraulic radii of openings of the pores and not the pore sizes. If the volumetric space availability is the most limiting factor for the availability of condensed water for hydration, then the hydraulic radii of corresponding to the pore sizes could prove to give a more adequate limit of availability. On the other hand, if other forms of pores are dominating, this may not necessarily be true. This area is probably worth further investigation.

The proposed model is limited to deal with one binder. However, it can easily be extended to explicitly model hydration for more than one binder in a mix. This can be done by modeling one degree of hydration for each binder, e.g. α_{b1}, α_{b2}, etc. Use of separate equations defining the rate of change of the degrees of hydration allows for extending these by influencing factors describing how the presence of one binder or its reaction products affect the reactions of the other binders. This approach has already been used in *Mjörnell 1997* to model a combination of OPC and silica fumes by use of two times of maturity and two degrees of hydration, however with the disadvantages earlier pointed out in section 2.1.3.6.

One more observation regarding the proposed model has to be made. Despite of all its flexibilities, at the time of writing this model has a very limited validation base. The reason for this is simply availability of measurements of chemically bounded water in varying curing conditions, according to the adopted definition of the border between chemically and physically bounded water. Older, more extensive measurements of chemically bounded water for Swedish binders are available in *Mjörnell 1997* as well as *Helsing 1993*. However, these are based on an initial drying at 100-105 ºC to remove what is defined as evaporable water, which makes them incompatible with the adopted definitions in this work. In order to gain more confidence in the applicability of this model, a further validation using other concrete mixes should be performed.

The conclusion from the discussion above can be summarized by following:

- The proposed hydration model is based on classical kinetics modeling, directly giving the degree of hydration of the cement, without using equivalent time of maturity as a middle step.
- The proposed model uses influence of availability of cement, availability of water and Arrhenius type of temperature dependency of the reaction rate.
- The proposed model starts modeling in the dormant phase of hydration and allows for adaptation of a feasible mathematically delayed start of the main reaction.
- A further connection to chemically bounded water is proposed utilizing a temperature dependent amount of water being bounded per amount of cement.
- The proposed model is shown to perform better that the reference model on a measured set of values for chemically bounded water in various moisture and temperature conditions for a set or w/b-ratios and one binder combination. The proposed model's capacity to capture a cross-over effect in temperature for chemically bounded water is demonstrated, as well as its capacity to capture the influence of either cement or water as the limiting factor for the reaction.

4.2 Sorption

The proposed sorption model can be used to model desorption, absorption and scanning. It can be adapted to various sets of measured data. The proposed model differs from classical models for sorption in its structure. Classical models work typically with a fixed number of parameters, that describe water sorption in the porous structure in a fixed way, similar to a specific mathematical function, e.g. linear, logarithmic or quadratic, approximating a complex curve. The proposed model offers a possibility of selecting freely the size of the involved matrix or matrices and the meniscus curvature limits corresponding to their columns and rows. This is comparable to use of splines, where a complex curve is approximated by used of multiple segments of simpler curves or lines. This offers a flexibility that can be used to describe the variations in the structure of the underlying pore system more adequately than with a fixed set of parameters.

This flexibility comes to a price of a potential challenge in adaptation of parameters. For instance, it is easy to end up with an underdetermined problem, i.e. having more parameters to adapt than what is supported by the amount of measurements. This opens up for a variety of possible methods to select the parameters, resulting in models with various behavior. The example method in the isothermal case, giving exact representation of measured absorption and desorption data with the proposed distribution of sorption site contributions, is just one way of solving the adaptation problem, while other are also possible. By these methods one can simulate sorption behavior based only on absorption and desorption measurements and assumptions underlying the chosen method to calculate the matrix elements.

The general adaptation for the isothermal case uses mathematical minimization of a quadratic error in adaptation and linear dependency of water amount on the model parameters. This gives a possibility for checking the determination of the adaptation problem and possible correction of conditions selected for the intended measurements before execution of these. Checking the determination of the adaptation problem can thus be used as a planning tool for the intended measurements if the general adaptation methodology is to be used afterwards.

In the non-isothermal case, non-linear optimization methods has to be used to find the parameters. This is a complication resulting from the mathematical complexity of the model. This price is paid for the possibility of direct physical interpretation of the contributing phenomena of capillary condensation and surface adsorption of water in the filled respectively non-filled part of the pore system. Again, both utilize matrices for flexible, spline-like modeling of the structural aspects of the pore system: total mount for the capillary condensed water and monolayer amount for the adsorbed water.

The conclusion from the discussion above can be summarized by following:

- The proposed model covers desorption, absorption and scanning
- The proposed model can be adapted to various sets of measured data – one sorption curve, desorption and absorption etc.
- The proposed model offers significant flexibility in functional description of the structural impact of the pore system

- The model is proposed in versions for both isothermal and non-isothermal conditions.
- In the non-isothermal case, the model offers direct interpretation of model parts as underlying physical phenomena.
- A wide range of methods to adapt parameters is introduced, covering underdetermined, determined and overdetermined situations regarding support by measured data for isothermal conditions and determined/overdetermined for non-isothermal.

4.3 Transport

Modeling of moisture transport in concrete for application in predicting of drying has typically focused on isothermal conditions and assumed no hysteresis. These two fact have implied no need to develop a specific model for the transport properties. It was briefly considered to be enough with measuring the transport coefficient for a selected potential gradient, as a function of relative humidity or some other suitable moisture potential, and use simple interpolation in between the values, e.g. linear.

Acknowledging the dependency of moisture transport on how and to which extent the pore system is filled with capillary condensed water, in a similar fashion as for sorption, changes fundamentally this situation and forms the first reason for proposing of a specific model for the transport properties to deal with the hysteresis. The proposed transport model takes this phenomenology into account in all three presented variants: isothermal, simplified non-isothermal and generalized non-isothermal. The model utilizes the same underlying matrix-based integration over various parts of a domain of sites contributing to transport, depending on the wetting/drying history as for the proposed sorption model. It inherits thus similar characteristics regarding flexibility in modeling as well as potential challenge in adaptation of parameters, as discussed in section 4.2.

The desire to model situations where the temperature is not constant is the other requirement behind the presented modeling. Here there are two types of variations to take into account:

- Variation in time, i.e. transport at different temperatures but without any temperature gradient
- Variation in time and space, i.e. transport at different temperatures and under a temperature gradient

The first situation requires taking into account how temperature variation affects the transport properties. The second one also adds the impact of a temperature gradient as a driving potential to the moisture transport. Both presented models for non-isothermal conditions try to deal with both situations, but in a different way.

The simplified version of the model assumes phenomenological domination of capillary suction over vapor diffusion. It models the total moisture transport and is adapted to measured data for total moisture transport. However, it interprets the total moisture transport as an effect of capillary suction only to simplify the phenomenological temperature influence on it. Translating the physical model for capillary suction from being driven by gradient of capillary

pressure to gradient of vapor contents results in an additional dependency on the temperature gradient. This gives a possibility to adapt the model parameters to data measured either in isothermal conditions (shown), or to data at different temperatures with or without a gradient (not shown). The resulting model and its parameters take the temperature gradient into account beside the gradient in vapor contents, but this is mainly a result of translating of the basic transport formulation, from capillary pressure driven to vapor contents and temperature driven. How well it approximates the reality remains to be seen. The model is theoretically correct in two situations:

- If adapted to measurements in isothermal conditions, the model is correct at the same isothermal conditions, interpolating slightly differently between the adapted measurement points that the fully isothermal version of the model.
- If capillary suction is the only transport taking place in reality.

The first situation occurs obviously at a constant temperature being the same as during the measurements. The second situation does not really occur. Event at saturation, the compaction and air pores are normally empty, allowing for vapor transport to influence the total moisture transport to at least some extent. The further the simulation conditions deviate from the measurement temperature and full saturation the larger the difference between the simulated and the real transport can be expected. From the applicational perspective, the interesting question is which is more correct – the isothermal model or the simplified non-isothermal – and for how large domain of deviation from the conditions optimal for the simplified non-isothermal model.

Comparing this simplified non-isothermal model to findings in literature is not an easy task. Complexity of both measurement arrangements and interpretation, calculation and validation of the measurement results is challenging in cases with transport driven by both moisture and temperature gradients. The effect of temperature gradient in this model is clearly decreasing for the total transport. *Trabelsi et al 2012* shows findings where temperature gradient has increasing effect at low moisture levels, where vapor diffusion should be dominating, and decreasing effect at higher moisture levels, where capillary suction should be dominating. This is in line with the model behavior above. On the other hand, different effects of temperature gradient can be found in *Qin et al 2008* and *Wang & Xi 2017*.

The generalized version of the non-isothermal model takes the phenomenology of both capillary suction and vapor diffusion into account. However, this cannot be assumed to be a correct representation of the reality. The total flow is modeled as a sum of flows resulting from both phenomena. This would be correct if the flows would take place truly in parallel, which they don't. As mentioned in section 2.3.4, the combined transport is much more complex due to the complexity of the pore system and how the pores are filled with water. The model summarizing transport contributions from both phenomena has to be seen mainly as a mathematical device for adaptation of parameters combining both types of influences and not as a direct model of the underlying physics. The advantage of the proposed model still covers modeling of hysteresis and a significant flexibility of description of the influence of the geometry of the pore system. The remaining question is of course how well it works in

reality and how much better it performs than the simplified version at various levels of saturation and in various temperature conditions.

The conclusion from the discussion above can be summarized by following:

- The proposed model covers modeling of transport coefficients in conditions of desorption, absorption and scanning
- The proposed model can be adapted to various sets of measured data – one transport curve, two curves in desorption and absorption etc.
- The proposed model offers significant flexibility in functional description of the structural impact of the pore system
- The model is proposed in versions for isothermal conditions, non-isothermal conditions assuming dominance of capillary suction and general non-isothermal conditions.
- In the non-isothermal case, the model offers direct interpretation of model parts as underlying physical phenomena and utilizes use of temperature gradient beside vapor contents gradient to express the transport term.
- A wide range of methods to adapt parameters is introduced, covering underdetermined, determined and overdetermined situations regarding support by measured data for isothermal conditions and determined/overdetermined for non-isothermal.

4.4 Domain based modeling with hydraulic curvature of meniscus

The presented models for sorption and transport make use of a domain based model, utilizing a matrix of site concentration values. In the case of sorption the values are interpreted as sorption sites and in the case of transport as contributions to the total transport coefficient. However, the model as such can be used to express any value, whose contributions are spread out over the pore system and are dependent on its filling status. One candidate can be transport coefficients for ions, depending on availability of capillary condensed water to use as a medium for transport.

The presented domain based model utilizes the hydraulic curvature of the meniscus as control variables for administration of filling/emptying history. This approach gives a physically correct modeling of the border between the capillary condensed water and the empty part of the pore system in non-isothermal conditions. It enables to correctly evaluate integrals over the concentration site, expressed by the matrix, for desorption, absorption and scanning caused by changes in moisture and temperature conditions.

The possibility of changing the size of the model matrix and the control variable borders corresponding to columns/rows enables adjustment of the model resolution in a spline-like fashion, depending on the set of measured data available. Finally, the presented set of adaptation procedures for various cases in sorption and transport models contributes further to the flexibility of the model family.

The conclusion from the discussion above can be summarized by following:

- The presented sorption and transport models utilize an underlying abstract domain based model, using a matrix representation of site concentration and hydraulic curvature of meniscus as a control variable for filling/emptying history.
- The abstract domain based model can be used to express any value, whose contributions can be assumed to be distributed over the pore system and dependent on its filling status.
- The use of hydraulic curvature of the meniscus gives physically correct control over filling/emptying history under any change of moisture and temperature conditions.
- The model offers flexibility in both resolution of modeling and adaptation procedures.

5. Future research

5.1 Hydration and connected properties

The probably most obvious need of further research is to widen the validation base for the proposed model to cover more concrete mixes with other binders. Another type of widening that can be of research interest is to adapt the model to measured degree of hydration of the binder directly and to also combine adaptations to both the degree of hydration and the chemically bounded water.

Another area directly connected to the proposed model that is in need of further investigation is how to optimally express the influencing moisture contents, i.e. which part of the physically bounded water that really is available for the reaction. The accuracy of the proposed model may be improved in that way for simulations of concrete where the water is the limiting factor for the reaction.

Connecting compressive strength and hydration heat to the presented hydration model, as mentioned in sec. 3.2.3.2 and 3.2.3.3 is also considered as an area of immediate future research. There are at least two major ways in which compressive strength and heat of hydration could be modeled that could be investigated. This step would make the proposed model more complete regarding modeling of properties connected to hydration.

Regarding heat of hydration, a clearer picture whether the amount of heat generated per amount of hydrated binder varies with temperature would be also of interest. If different amount of water is bounded per amount of hydrated binder depending on the temperature, then it is reasonable to suspect that the enthalpy of the reaction per amount of hydrated binder will also differ. At the time of writing there is only evidence that the temperature dependency of both rate of growth/rection and also of the quality of end products affects compressive strength and chemically bounded water. If this is true also for the generated heat, the proposed model should make it possible to take that variation into account while modeling heat of hydration in a similar way as for chemically bounded water.

Extending the proposed model to explicitly model hydration for more than one binder is also of interest for further research. Today's efforts to lower the CO_2-footprint of concrete make extensive use of exchanging OPC for SCM:s with sometimes significantly different reaction kinetics. Such a scenario may be difficult to model adequately by treating the used binder combination as one binder in the model.

5.2 Sorption

The presented model opens up large possibilities for interesting further research. The probably most obvious area is extending the practical validation basis through testing the model performance versus measured data. This is especially relevant to the non-isothermal case of the model, where any practical testing was not possible in the scope of this. The fact that the proposed model does not assume any properties of the pore system specific to concrete or cementitious material in general make it also interesting to see how it performs in modeling

sorption in other cases than water in concrete. Thus, the validation basis could be extended to any medium under phenomenology of capillary condensation and adsorption in any pore system.

The introduced idea of adjusting scanning performance by the adjustment cell without altering key absorption and desorption performance requires further work before it can be used. Here, proposal of a methodology to identify appropriate cells for adjusting specific scanning performance would be welcome together with a formulation of a structured method to adjust a model to a set of scanning data.

Another area for further research in adaptation methodology is the non-isothermal case. The need of simplification of the full-scale non-linear approach is already identified. Any methodology for smaller amount of measured data, i.e. the underdetermined case, as proposed for the isothermal case, would also of interest.

Finally, the dynamics of the pore system in time, age, degree of hydration or any other suitable variable describing how concrete changes due to hydration needs to be addressed. The presented model might play a role in such an approach. In such a case an interpolation method between models for different ages has to be formulated, taking into account both interpolation between model matrices as well as the administration of the history of meniscus curvature while changes in the structure and water contents of the pore system occur simultaneously.

5.3 Transport

One obvious area for further research is widening the validation basis for the presented model variants. This would imply performing measurement of moisture transport under conditions covering variations of interest in relative humidity, temperature, as well as history and gradients of these. From the phenomenological point of view, the recent findings of differences in transport coefficient in isothermal conditions measured during desorption and absorption, indicating presence of the same kind of hysteresis as in moisture sorption open up a new area for investigation of transport of moisture in concrete. The proposed model and its capability to deal with hysteresis, with the flexibility of the same level as for the proposed sorption model would clearly benefit from wider validation than what is presented. This applies to both isothermal and non-isothermal conditions and potentially to all three versions of the proposed transport model.

Transport in non-isothermal conditions is another area where further research would be of value. One question is how well the simplified version will perform under varying temperature with and without a temperature gradient. Because of the significant phenomenological simplification behind this model variant, it is also of interest to investigate the performance of the model versus the temperature and saturation domain and its deviation from optimal conditions for the underlying simplification.

The performance of the generalized transport model for non-isothermal conditions also offers possibilities for validation testing, especially in conditions with a temperature gradient. As already mentioned in section 2.3.5, there has been some research in this area however without

a comparable level of flexibility in modeling and mostly without taking the hysteresis into account.

The underlying construct of matrices administrating contributions to the total transport coefficients from various parts of the pore system, depending on their filling status offers similar areas for further research as for sorption. Further proposals of methods for adaptation of the model parameters are of interest, especially for the underdetermined cases enabling a reasonable practical limitations of the amount of measurements. A more general investigation of how well the model performs versus the necessary amount of measurements it requires is also an area where research of testing character would be of value.

The last general remark regarding transport in non-isothermal conditions is obviously a request for further research in other model formulations. The proposed generalized model is not an adequate description of the underlying phenomenology, due to its parallel modeling of contributions from capillary suction and vapor diffusion. The complexity of the pore system in cement-based materials offers here significant possibilities for other attempts to describe and model the moisture transport in non-isothermal conditions.

5.4 Domain based modeling with hydraulic curvature of meniscus

As mentioned in the discussion in section 4.4, the abstract domain based model underlying the presented sorption and transport models, can be used to express any value, whose contributions are spread out over the pore system and are dependent on its filling status. It would be of value to see how well this model can be applied to express other values than sorption and transport coefficients for water, possibly also for other materials than concrete.

Bibliography

Addassi et al 2016 - Addassi M., Schreyer L., Johannesson B., Lin H., *Pore-scale modeling of vapor transport in partially saturated capillary tube with variable area using chemical potential*, Water Resources Research 2016

Alexanderson 2000 – J. Alexanderson, *Secondary emissions from alkali attack on adhesives and PVC floorings*, AMA-nytt 1/2000

Anderberg & Wadsö 2007 – Anderberg A., Wadsö L., *A computer-based programme that simulates the drying of selflevelling flooring compounds*, TVBM-7191, Div. of Building Materials LTH Lund 2007

Arfvidsson 1998 - Arfvidsson J., *Moisture Transport in Porous Media, Modelling Based on Kirchhoff Potentials*. Dep. Of Building Materials, LTH, Lund 1998. Report TVBH-1010

Arfvidsson et al 1998–2012 – Arfvidsson J., Hedenblad G., Nilsson L.-O., *Datorprogrammet TorkaS 3, som prognosverktyg vid val av ekonomisk betongkvalitet från uttorkningssynpunkt,* (title in English: *TorkaS 3, predicting tool for choice of economical concrete quality from the desiccation point of view*), software, www.fuktcentrum.lth.se

Arfvidsson et al 2017 – Arfvidsson J., Harderup L.-E., Samuelson I., *Fukthandbok, Praktik och teori*, (title in English: *Moisture Handbook, Practice and Theory*), AB Svensk Byggtjänst 2017

ASTM C618-15 – American Society for Testing and Materials, *ASTM C618 Standard specification for coal fly ash and raw or calcinated natural pozzolan for use in concrete*, ASTM 2015

Baquerizo et al 2016 - Baquerizo L. G., Matschei T., Scrivener K. L., *Impact of water activity on the stability of ettringite*, Cement and Concrete Research 79 (2016)

Baroghel-Bouny 2007a – Baroghel-Bouny V., *Water vapour sorption experiments on hardened cementitious materials Part I: Essential tool for analysis of hygral behaviour and its relation to pore structure*, Cement and Concrete Research 37 (2007)

Baroghel-Bouny 2007b – Baroghel-Bouny V., *Water vapour sorption experiments on hardened cementitious materials Part II: Essential tool for assessment of transport properties and for durability prediction*, Cement and Concrete Research 37 (2007)

Bashir et al 2009 – Bashir R., Smith J. E., Henry E. J., Stolle D., *On the Importance of Hysteresis in Numerical Modeling of Surfactant-Induced Unsaturated Flow*, Soil & Sediment Contamination, 2009

Bear 1972 – Bear J., *Dynamics of Fluids in Porous Media*, Dover Publications Inc., New York 1972, ISBN-13: 978-0-486-65675-5

Bennai et al 2016 - Bennai F., Abahri K., Belarbi R., Tahakourt A., *Periodic homogenization for heat, air, and moisture transfer of porous building materials*, Numerical Heat Transfer Part B-Fundamentals, 2016

Bird 1994 – Bird G. A., *Molecular Gas Dynamics and he Direct Simulation of Gas Flows*, Oxford University Press, 1994, ISBN 0-19-856195-4

Bornehag 1994 – C.-G. Bornehag, *Mönsteranalys av inomhusluft*, (title in English: *Pattern Analysis of Inhouse Air*), R23:1994 Byggforskningsrådet

Brouwers 2004 – Brouwers H. J. H., *The work of Powers and Brownyard revisited: Part 1*, Cement and Concrete Research 34 (2004)

Brouwers 2005 – Brouwers H. J. H., *The work of Powers and Brownyard revisited: Part 5*, Cement and Concrete Research 35 (2005)

Brunauer 1945 – Brunauer S., *The Adsorption of Gases and Vapors*, *Vol 1*, Princeton University Press 1945

Brunauer, Emmett & Teller 1938 – Brunauer S, Emmett P. H., Teller E., *Adsorption of Gases in Multimolecular Layers*, vol 60, 1938,

Bullard et al 2011– W. Bullard J. W., Jennings H. M., Livingston R. A., Nonat A., Scherer G. W., Schweitzer J. S., Scrivener K. L., Thomas J. J., *Mechanisms of cement hydration*, Cement and Concrete Research 41 (2011)

Busser et al 2019 - Busser T., Berger J., Piot A., Pailha M., Woloszyn M., *Comparison of model numerical predictions of heat and moisture transfer in porous media with experimental observations at material and wall scales: An analysis of recent trends*, Drying Technology 2019

Byfors 1980 – Byfors J., *Plain Concrete at Early Ages*, Swedish Cement and Concrete Research Institute, Report Fo/Research 3:80, Stockholm 1980

Byggföretagen & SBUF 2013–2023 – *Produktionsplanering betong*, (title in English: Production Planning Concrete), software, SBUF 2013-2020, Byggföretagen 2020-2023, www.byggforetagen.se/ppb

Cai et al 2022 – Cai G., Liu Y., Zhou A., Li J., Yang R., Zhao C., *Temperature-dependent water retention curve model for both adsorption and capillarity*, Acta Geotechnica (2022)

Carino 1982 – Carino N. J., *Maturity Function for Concrete*, Proceeding from International Conference on Concrete at Early Ages, TILEM, Paris 1982, Vol 1

Collier et al 2008 - Collier N. C., Sharp J.H., Milestone J.H., Hill J., Godfrey I.H., *The influence of water removal techniques on the composition and microstructure of hardened cement pastes*, Cement and Concrete Research 38 (2008)

Cunningham & Williams 1980 - Cunningham R. E., Williams R. J. J., *Diffusion in Gases and Porous Media*, Springer Science+Business Media New York 1980

Davis et al 1933 – Davis R. E., Carlson R. W., Troxell G. E., Kelly J. W., *Cement Investigations for the Hoover Dam*, Journal of the American Concrete Institute - Proceedings at the 29th annual Convention, Chicago, February 21-23 1933

Deeb et al 2023 - Deeb A., Benmahiddine F., Berger J., Belarbi R., *Development of a hysteresis model based on axisymmetric and homotopic properties to predict moisture transfer in building materials*, Journal of Building Physics, Volume 46, Issue 5, March 2023

De Weerdt et al 2011 – De Weerdt K., Ben Haha M., Le Saout G., Kjellsen K. O., Justnes H., Lothenbach B., *Hydration mechanisms of ternary Portland cements containing limestone powder and fly ash*, Cement and Concrete Research 41 (2011)

Dent 1977 – Dent R. W., *A Multilayer Theory for Gas Sorption, Part I: Sorption of a Single Gas*, Textile Research Journal 1977

Derluyn et al 2012 – Derluyn H., Derome D., Carmeliet J., Stora E., Barbarulo R., *Hysteretic moisture behavior of concrete: Modeling and analysis*, Cement and Concrete Research 42 (2012) p.1379–1388

Dullien 1975a – Dullien F. A. L., *New Network Permeability Model of Porous Media*, AIChE Journal 1975 Vol 21, No. 2

Dullien 1975b – Dullien F. A. L., *Single Phase Flow Through Porous Media and Pore Structure*, The Chemical Engineering Journal, 10 1975

Dullien & Dhawan 1975 – Dullien F. A. L., Dhawan G. K., *Bivariate Pore-Size Distributions of Some Sandstones*, Journal of Colloid and Interface Science, Vol. 52, No. I, July 1975

Dullien 1992 – Dullien F. A. L., *Porous Media, Fluid Transport and Pore Structure*, Second edition, Academic Press Inc. San Diago 1992, ISBN 0-12-223651-3

Espinosa & Franke 2006 – Espinosa R.M., Franke L., *Inkbottle Pore-Method: Prediction of hygroscopic water content in hardened cement paste at variable climatic conditions*, Cement and Concrete Research 36 (2006) p. 1954–1968

Everett 1954a – Everett D. H., *A general approach to hysteresis Part 2: Development of the domain theory*, Transactions of the Faraday Society; 1954, Vol. 50

Everett 1954b – Everett D. H., *A general approach to hysteresis Part 3 — A formal treatment of the independent domain model of hysteresis*, Transactions of the Faraday Society; 1954, Vol. 50

Everett 1955 – Everett D. H., *A general approach to hysteresis. Part 4. An alternative formulation of the domain model*, Transactions of the Faraday Society; 1955, Vol. 51

Feldman & Sereda 1970 – Feldman R. F., Sereda P. J., *A New Model for Hydrated Portland Cement and Its Practical Implications*, Engineering Journal Vol. 53 1970

Feldman & Ramachandran 1971 – Feldman R. F., Ramachandran V. S., *Differentiation of Interlayer and Adsorbed Water in Hydrated Portland Cement by Thermal Analysis*, Cement and Concrete Research Vol 1 1971,

Fjällström 2013 – Fjellström P., *Measurement and Modelling of Young Concrete Properties Test*, Licentiate Thesis, Luleå University of Technology, Luleå 2013

Freiesleben Hansen & Pedersen 1977 – Freiesleben Hansen P., Pedersen E. J., *Maturity Computer for Controlled Curing and Hardening of Concrete*, Nordisk Betong, Vol. 1, No. 19, 1977, pp. 21-25

Freiesleben Hansen 1978 – Freiesleben Hansen P., *Portland Cement, Curing Technology 1 & 2*, Portland cement, Aalborg Portland/BKF-Centralen Aalborg/Lyngby, 1978

Freiesleben Hansen & Pedersen 1984 – Freiesleben Hansen P., Pedersen E.J., *Curing of Concrete Structures*, Danish Concrete and Structural Research Institute, Report prepared for CEM – General Task Group No. 20, Durability and Service Life of Concrete structures, December 1984

Fuchs 1959 – Fuchs N. A., *Evaporation and Droplet Growth in Gaseous Media*, Pergamon Press 1959

Gallucci et al 2013 – Gallucci E., Zhang X., Scrivener K. L., *Effect of temperature on the microstructure of calcium silicate hydrate (C-S-H)*, Cement and Concrete Research 53 (2013)

Gartner & Jennings 1987 – Gartner E.M., Jennings H.M., *Thermodynamics of calcium silicate hydrates and their solutions*, Journal of the American Ceramic Society 70 (10) (1987)

Haines 1930 – Haines W. B., *Studies in the physical properties of soil. V. The hysteresis effect in capillary properties, and the modes of moisture distribution associated therewith*, Journal of Agricultural Science, Jan 1930, Vol. 20 Issue 1,

Hedenblad 1987 – Hedenblad G., *Effect of soluble salt on the sorption isotherm,* Report TVBM-3035, Division of Building Materials, LTH, Lund University 1987

Hedenblad 1993 – Hedenblad G., *Moisture Permeability of Mature Concrete, Cement Mortar and Cement Paste*. Dep. of Building Materials, LTH, Lund 1993. Report TVBM-1014.

Hefti & Mazzotti 2014 - Hefti M., Mazzotti M., *Modeling water vapor adsorption/desorption cycles*, Adsorption (2014)

Helsing 1993 – Helsing Atlassi E., *A Quantitative Thermogravimetric Study on the Nonevaporable Water in Mature Silica Fume Concrete*, Dep. Of Building Materials, CTH, Göteborg 1993, Report P-93:6

Hewlett & Liska 2019 – Hewlett P. C., Liska M., *Lea's Chemistry of Cement and Concrete*, Fifth edition, Butterworth-Heinemann, Elsevier, Oxford 2019, ISBN 978-0-08-100773-0

JEJMS Concrete AB 1999 – *ConTeSt Pro Program för temperatur- och spänningsberäkning i betong*, (title in English: *ConTeSt Pro Computer Program for Calculation of Development of Temperature and Stress in Concrete*), software, JEJMS Concrete AB 1999

Jennings 2000 – Jennings H. M., *A model for the microstructure of calcium silicate hydrate in cement paste*, Cement and Concrete Research 30 (2000)

Jennings 2008 – Jennings H. M., *Refinements to colloid model of C-S-H in cement: CM-II*, Cement and Concrete Research 38 (2008)

Jennings et al 2015 - Jennings H. M., Kumar A., *Sant G., Quantitative discrimination of the nano-pore-structure of cement paste during drying: New insights from water sorption isotherms*, Cement and Concrete Research 76 (2015)

Johannesson 2000a – Johannesson B., *Modeling of a viscous fluid percolating a porous material due to capillary forces*, Report TVBM-3095, Div. of Building Materials LTH Lund 2000

Johannesson 2000b – Johannesson B., Transport and Sorption Phenomena in Concrete and Other Porous Media, Doctoral Thesis, TVBM 1019, Div. of Building Materials LTH Lund 2000

Johannesson 2002 – Johannessson B. F., *Prestudy on diffusion and transient condensation of water vapor in cement mortar*, Cement and Concrete Research 32 (2002)

Jonasson 1984 – Jonasson J.-E., *Slipform Construction – Calculations for Assessing Protection Against Early Freezing*, Swedish Cement and Concrete Research Institute, Report Fo/Research 84:4, Stockholm 1984

Jonasson & Stelmarczyk 1991 – Jonasson J.-E., Stelmarczyk M., *Hett5 Program för beräkning av temperatur- och hållfasthetsutveckling*, (title in English: *Hett5 Computer Program for Calculation of Development of Temperature and Strength*), software, Betong Data AB 1991

Jonasson 1994 – Jonasson, J.-E., *Modelling of Temperature, Moisture and Stresses in Young Concrete*, Thesis 1994:153D, Luleå University of Technology, Luleå 1994

Juilland et al 2010 – Juilland P., Gallucci E., Flatt R., Scrivener K., *Dissolution theory applied to the induction period in alite hydration* , Cement and Concrete Research 40 (2010)

Klemczak 2011 – Klemczak B., *Prediction of Coupled Heat and Moisture Transfer in Early-Age Massive Concrete*, Numerical Heat Transfer, Part A, 60: 212–233, 2011

Klieger 1958 – Klieger P., *Effects of Mixing and Curing Temperature on Concrete Strength*, Journal of the American Concrete Institute Vol. 54, No. 12, June 1958

Koplik 1982 – Koplik J., *Creeping flow in two-dimensional networks*, Journal of Fluid Mechanics Vol. 119 1982

Kurdowski 2014 – Kurdowski W., *Cement and Concrete Chemistry*, Springer 2014, ISBN 978-94-007-7944-0

Langmuir 1918 – Langmuir I, *The Adsorption of Gases on Plane Surfaces of Glass Mica and Platinum,* 1918

Li 2005 – Li X. S., *Modelling of hysteresis response for arbitrary wetting/drying paths*, Computers and Geotechnics 32 (2005)

Liao et al 2008 – Liao W.-C., Lee B. J., Kang C. W., *A humidity-adjusted maturity function for the early age strength prediction of concrete*, Cement & Concrete Composites 20 (2008)

Lothenbach & Winnefeld 2006 - Lothenbach B., Winnefeld F., *Thermodynamic modelling of the hydration of Portland cement*, Cement and Concrete Research 36 (2006

Lothenbach et al 2007 – Lothenbach B., Winnefeld F., Alder C., Wieland E., Lunk P., *Effect of temperature on the pore solution, microstructure and hydration products of Portland cement pastes*, Cement and Concrete Research 37 (2007)

Lothenbach et al 2008 - Lothenbach B., Saout G. L., Gallucci E., Scrivener K., *Influence of limestone on the hydration of Portland cements*, Cement and Concrete Research 38 (2008)

Lothenbach et al. 2011 - Lothenbach B, Scrivener K., Hooton R. D., *Supplementary cementitious materials*, Cement and Concrete Research 41 (2011)

Luikov 1980 – Luikov A. B., *Heat and Mass Transfer*, English Translation, Revised from the Russion Edition 1978, Mir Publishers Moscow 1980

McDaniel 1915 – McDaniel A. B., *Influence of Temperature on the Strength of Concrete*, Bulletin No. 81, University of Illinoi, Engineering Experiment Station, July 1915

McIntosh 1949 – McIntosh J. D., *Electrical Curing of Concrete*, Magazine of Concrete Research, Vol. 1, No. 1, January 1949

McIntosh 1956 – McIntosh J. D., *The Effects of Low-temperature Curing on the Compressive Strength of Concrete*, Proceedings, RILEM Symposium on Winter Concreting – Theory and practice, Session BII, Danish Institute for Building Research, Copenhagen, Denmark, 1956

Mills 1966 – Mills R. H., *Factors Influencing Cessation of Hydration in Water-Cured Cement Pastes*, Special Report No. 90, Proceedings of the Symposium on the Structure of Portland Cement Paste and Concrete, Washington, DC, 1966

Mjörnell 1994 – Norling Mjörnell K., *Self-desiccation in Concrete*, Dep. of Building Materials, CTH, Göteborg 1994, Report P-94:2

Mjörnell 1997 – Norling Mjörnell K., *Moisture Conditions in High Performance Concrete - mathematical modelling and measurements,* Dep. of Building Materials, CTH, Göteborg 1997, Report P-97:6

Mualem 1974 – Mualem Y., *A Conceptual Model of Hyseresis*, Water Resourses Research Vol. 10 No. 2. 1974

Mualem & Dagan 1975 – Mualem Y., Dagan G., *Dependent domain model of capillary hysteresis*, Water Resources Research Vol. 11, Issue 3, 1975

Nilsson 1979 – Nilsson L.-O., *Fuktmätning*, (title in English: *Moisture Measurement*), Rapport TVBM-3008, LTH Lund 1979

Nilsson 2006 – Nilsson L.-O., *Modelling moisture conditions in cementitious materials – some present challenges,* Keynote paper at 2nd International Symposium on Advances in Concrete through Science and Engineering, September 11-13, 2006, Quebec City, Canada

Nilsson 2021 – Nilsson L. O., *Betonghandbok Material Del II, Kap. 17 Fukt och betong*, (title in English: *Concrete Handbook Material, Part II, Chap 17 Moisture and concrete*), AB Svensk Byggtjänst 2021

Nocedal & Wright 2006 – Nocedal J., Wright S. J., *Numerical Optimization*, Springer Science+Business Media, 2006, ISBN-10: 0-387-30303-0

Nurse 1949 – Nurse R. W., *Steam Curing of Concrete*, Magazine of Concrete Research, Vol. 1, No 2. June 1949

Nyman et al 2006 – Nyman U., Gustafsson P. J., Johannesson B., Hägglund R., A numerical method for the evaluation of non-linear transient moisture flow in cellulosic materials, International Journal for Numerical Methods in Engineering, 2006

Olsson et al 2018 – Olsson N., Nilssona L.-O., Åhs M., Baroghel-Bouny V., *Moisture transport and sorption in cement based materials containing slag or silica fume*, Cement and Concrete Research 106 (2018) p. 23–32

Pane & Hansen 2005 – Pane I., Hansen W., *Investigation of blended cement hydration by isothermal calorimetry and thermal analysis*, Cement and Concrete Research 35 (2005)

Pesavento et al 2017 – Pesavento F., Schrefler B. A., Sciume G., *Multiphase Flow in Deforming Porous Media: A Review*, Archives of Computational Methods in Engineering (2017)

Powers & Brownyard 1948 – Powers T. C., Brownyard T. L., *Studies of the Physical Properties of Hardened Portland Cement Paste*, Research Laboratories of the Portland Cement Association, Bulletin 22, Chicago 1948

Qin et al 2008 – Qin M., Belarbi R., Ait-Mokhtar A., Nilsson L.-O., *Nonisothermal moisture transport in hygroscopic building materials: modeling for the determination of moisture transport coefficients*, Transport in Porous Media 2008

RBK 2023 – *Fuktmätningsmanual – Betong & Golvavjämning*, (title in English: *Manual for Moisture Measurement – Concrete and Screed*), version 7:0, Rådet för byggkompetens (RBK) 2023

Råde & Westergren 2004 – Råde L., Westergren B., *Mathematics Handbook for Science and Engineering*, Springer-Verlag & Studentlitteratur 2004, ISBN 3-540-21141-1

Saeidpour & Wadsö 2016 – Saeidpour M.,Wadsö L., *Moisture diffusion coefficients of mortars in absorption and desorption*, Cement and Concrete Research 83 (2016) p. 179–187

Saul 1951 – Saul A. G. A., *Principals Underlying the Steam Curing of Concrete at Atmospheric Pressure*, Magazine of Concrete Research," Vol. 2, No. 6, March 1951

SBUF et al 1997 – *Hett97 Program för beräkning av temperatur- och hållfasthetsutveckling i betong*, (title in English: *Hett97 Computer Program for Calculation of Development of Temperature and Strength in Concrete*), software, SBUF, NCC AB, Cementa AB, SFF 1997

Scrivener & Nonat 2011 – Scrivener K. L., Nonat A., *Hydration of cementitious materials, present and future*, Cement and Concrete Research 41 (2011)

Scrivener et al 2015 - Scrivener K. L., Juilland P., Monteiro P. J. M., *Advances in understanding hydration of Portland cement*, Cement and Concrete Research 78 (2015)

Seredyński et al 2020 - Seredyński M., Wasik M., Łapka P., Furmański P., Cieślikiewicz .Ł, Pietrak K., Kubiś M., Wiśniewski T. S., Jaworski M., *Analysis of Non-Equilibrium and Equilibrium Models of Heat and Moisture Transfer in a Wet Porous Building Material*, Energies 2020,

Singh et al 2019 - Singh K., Jung M., Brinkmann M., Seemann R., *Capillary-Dominated Fluid Displacement in Porous Media*, Annual Review of Fluid Mechanics 2019

Sjöberg 2001 – Sjöberg A., *Secondary emissions from concrete floors with bonded flooring materials – effects of alkaline hydrolysis and stored decomposition products*, Thesis, Dep. Of Building Materials CTH, Göteborg 2001, Publication P-01:2

Snoeck et al 2014 – Snoeck D., Velasco L.F., Mignon A., Van Vlierberghe S., Dubruel P., Lodewyckx P., De Belie N., *The influence of different drying techniques on the water sorption properties of cement-based materials*, Cement and Concrete Research 2014

Stelmarczyk et al 2015 – Stelmarczyk M., Hedlund H., Johansson P., Nilsson L.-O., Åhs M., Rapp T., *Förstudie och metodutveckling för implementering av fuktberäkningsmodul i datorprogrammet Produktionsplanering Betong Slutrapport*, (title in English: *Pre-study and Method Development for Implementation of Calculation of Desiccation in the Computer Program Produktionsplanering Betong, Final Report*),SBUF 13064, 2015, www.sbuf.se

Stelmarczyk et al 2019 – Stelmarczyk M., Rapp T., Hedlund H., Carlström S., *Utveckling av beräkning av uttorkning i programmet Produktionsplanering Betong samt Inmätning av Bascement för uttorkningsberäkning i Produktionsplanering Betong Slutrapport*, (title in English: *Development of Calculation of Desiccation in the Computer Program Produktionsplanering Betong and Measurements of Properties of Bascement for Calculation of Desiccation in the Computer Program Produktionsplanering Betong, Final Report*), SBUF 13197 & 13198, 2019, www.sbuf.se

Surasani et al 2010 - Surasani V. K., Metzger T., Tsotsas E., *Drying Simulations of Various 3D Pore Structures by a Nonisothermal Pore Network Model*, Drying Technology 2010

Svensk Byggtjänst 2018 – *Allmän material- och arbetsbeskrivning för husbyggnadsarbeten* (AMA Hus 18), (title in English: *General Description of Materials and Work for Housing Construction*), Svensk Byggtjänst 2018

Svensson Tengberg 2018 – Svensson Tengberg C., *INVENTERING: UTTORKNING AV BETONGGOLV Betong med mineraliska tillsatsmaterial*, (title in English: *Inventory: Desiccation of Concrete Floors with Supplementary Cementitious Materials*), SBUF 13358, 2018, www.sbuf.se

Taylor 1997 – Taylor H. F. W., *Cement Chemistry*, Second edition, Thomas Telford Publishing, London 1997, ISBN 0 7277 2592 0

Tennis & Jennings 2000 – Tennis P. D., Jennings H. M., *A model for two types of calcium silicate hydrate in the microstructure of Portland cement pastes*, Cement and Concrete Research 30 (2000)

Termkhajornkit et al 2015 - Termkhajornkit P., Barbarulo R., Chanvillard G., *Microstructurally-designed cement pastes: A mimic strategy to determine the relationships between microstructure and properties at any hydration degree*, Cement and Concrete Research 71 (2015)

Trabelsi et al 2012 - Trabelsi A., Belarbi R., Abahri K., Qin M., *Assessment of temperature gradient effects on moisture transfer through thermogradient coefficient*, Building Simulation, 2012

van Breugel 2015 – van Breugel K., *Conceptual and numerical modeling and simulation of microstructure of cement-based materials*, Journal of Sustainable Cement-Based Materials 2015

van Breugel 2018 – van Breugel K., *How models can make a difference for a sustainable future of the building industry*, Materials and Structures (2018)

Vasil'ev et al - Vasil'ev G. P., Lichman V. A., Peskov N. V., Semendyaeva N. L., *Numerical Modeling of Heat and Moisture Diffusion in Porous Materials*, Computational Mathematics and Modeling, Vol. 26, No. 4, October, 2015

Vu & Tsotsas 2018 - Vu H. T., Tsotsas E., *Mass and Heat Transport Models for Analysis of the Drying Process in Porous Media: A Review and Numerical Implementation*, International Journal of Chemical Engineering Volume 2018

Wadsö 2016 - Wadsö L., *Construction Materials Science*, Building Materials, Lund University 2016

Wang 2013 – Wang Y., *Performance Assessment of Cement-based Materials Blended with Micronized Sand: Microstructure, Durability and Sustainability*, Doctoral Thesis, Technische Universiteit Delft 2013

Wang & Xi – Wang Y., Xi Y., *The Effect of Temperature on Moisture Transport in Concrete*, Materials 2017

Wei & Dewoolkar 2006 – Wei C., Dewoolkar M. M., Formulation of capillary hysteresis with internal state variables, Water Resources Research Vol. 42, 2006

Wengholt Johnsson 1995 – Wengholt Johnsson H., *Kemisk emission från golvsystem – effekt av olika betongkvalitet och fuktbelastning*, (title in English: *Chemical Emission from Floor Systems – Effect of Different Concrete Qualities and Moisture Levels*), Dep. of Building Materials, CTH, Göteborg 1995, Report P-95:4

Ye 2004 – Ye G., *Percolation of capillary pores in hardening cement pastes*, Cement and Concrete Research 35 (2005)

Zhang & Scherer 2011 – Zhang J., Scherer G. W., *Comparison of methods for arresting hydration of cement*, Cement and Concrete Research 41 (2011)

Zhang et al 2013 – Zhang M., Ye G., van Breugel K., *Microstructure-based modeling of permeability of cementitious materials using multiple-relaxation-time lattice Boltzmann method*, Computational Materials Science 68 (2013)

Zhang 2014 – Zhang Z., *Modeling of sorption hysteresis and its effect on moisture transport within cementitious materials*, Thesis, Université Paris-Est, 2014

Zienkiewicz et al 2013 – Zienkiewicz O. C., Taylor R. L., Zhu J. Z., *The Finite Element Method: Its Basus and Fundamentals*, 7th edition, Butterworth-Heinemann 2013

Department of SBN
Division of Building Materials

ISSN 1402-1544
ISBN 978-91-8048-428-2 (print)
ISBN 978-91-8048-429-9 (pdf)

Luleå University of Technology 2023

LULEÅ
UNIVERSITY
OF TECHNOLOGY